IDENTIFICATION AND CHARACTERISATION OF ARABIDOPSIS ER ACCESSORY PROTEINS

Alison Ferguson, BSc

Thesis submitted to the
University of Nottingham
for the degree of Doctor of Philosophy

February 2012

ABSTRACT

ER accessory proteins are a novel class of endoplasmic reticulum (ER) proteins that facilitate the exit of polytopic membrane proteins from the ER. They are important for the correct targeting of their cognate polytopic membrane proteins to the plasma membrane (PM) and their absence leads to abnormal accumulation of their target in the ER. Until recently, it was not clear if such proteins exist in plants. However, work by Dharmasiri et al (2006) and Gonzales et al (2005) suggest that such proteins exists in plants too. Polytopic membrane proteins such as nutrient transporters, hormone transporters and sugar transporters are a very important class of proteins as they regulate many important physiological and biochemical processes. Better understanding of the targeting of these proteins to the PM is of considerable agronomic interest due to the importance of efficient use of resources in sustainable agriculture.

One of the projects aims is to identify novel ER accessory proteins in Arabidopsis. Using a bioinformatics approach, 40 novel ER resident proteins were identified from a protein localisation database (LOPIT) generated by Dunkley et al (2006) as potential candidates for ER accessory proteins. Genetic, phenotypic and molecular approaches have been used to assess their role as potential ER accessory proteins. A few promising candidates have been identified, one of which AtBPL1 and related family. The AtBPL1 family has similarity to mammalian BAP31 which has been shown to function as an ER accessory protein (Ladasky et al, 2006). To determine if AtBPL1 family plays a similar role in plants a detailed molecular characterisation was carried out, this involved detailed expression analysis using reporter genes and

in situ immunolocalisation and characterisation of miRNA lines. Smart screens suggest that BPL1 family members may be involved in the targeting of a nitrate transporter, however its precise target is currently unknown.

A key focus of this present investigation have been on further characterisation of AXR4, which is required for the correct targeting of AUX1 to the plasma membrane (Dharmasiri et al, 2006). AUX1 belongs to a multi-gene family, involving three other members, LAX1, LAX2 and LAX3. Using genetic and cell biology approaches, AXR4 has been shown to be necessary for the correct localisation of at least two other members of this family LAX2 and LAX3. AXR4 mutants show defects in targeting of LAX2 and LAX3 to the plasmamembrane and show weak lax2 and lax3 phenotypes. Co-Immunoprecipitation studies revealed that AXR4 and AUX1 interact directly when co-expressed in insect cells. Finally molecular, bioinformatics and protein modelling approachs were used to probe the function of alpha beta hydrolase domain in AXR4 function. AXR4 appears to be tolerant to amino acid subsitition even at highly conserved amino acids, suggesting that the alpha beta hydrolase domain may not be important for its function.

TABLE OF CONTENTS

List of figures and tables

Abbreviations

2,4-D	2,4-Dichlorophenoxyacetic acid
AAP:	Amino acid permease
ABCB:	MULTIDRUG RESISTANCE/P-GLYCOPROTEIN
AChE:	Acetylcholinesterase
ARF:	ADP Ribosylation Factors
AUX1:	AUXIN RESISTANT 1
AXR4:	AUXIN RESISTANT 4
AxS:	AXR4 random site directed mutagenesis
B:	Boron
BAP:	Bacterial alkaline phosphatase
BPL:	BAP31-like
BSA:	Bovine serum albumin
C:	Carbon
Ca:	Calcium
catC:	Cathepson C
catZ:	Cathepson Z
CCR5:	CC chemokine receptor 5
cDNA:	Complementary DNA
Co-IP:	Co-immunoprecipitation
COPI:	Coat protein complex I
COPII:	Coat protein complex II
Cu:	Copper
DDM:	Dodecyl-β-maltoside
DEX:	Dexamethasone
DNA:	Deoxyribonucleic acid
dNTP:	Deoxyribonucleotide triphosphate
DTT:	Dithiothreitol

EDTA:	Ethylenediaminetetraacetic acid
ER:	Endoplasmic reticulum
ERAD:	Endoplasmic reticulum-associated degradation
ERES:	ER exit sites
EtOH:	Ethanol
FCS:	Foetal calf serum
Fe:	Iron
GAP1P:	General amino acid permease protein 1
GAT1:	GABA transporter-1
HA:	Hemagglutinin
HRP:	Horse radish peroxidase
IP:	Immunopreciptation
K:	Potassium
KO:	Knock out
KOH:	Potassium hydroxide
LAX:	LIKE-AUXIN RESISTANT 1
LB:	Luria-Bertani
LDL:	Low-density lipoprotein
LOPIT:	Localisation of organelle proteins by isotope tagging
M6P:	Mannose 6-phosphate
MeOH:	Methanol
Mg:	Magnesium
$MgSO_4$:	Magnesium sulphate
MLO15:	MILDEW RESISTANCE LOCUS O 15
MOI:	Multiplicity of infection
MS:	Murashige and Skoog
MVB:	Multivesicular bodies
N:	Nitrogen
Na:	Sodium
NaCl:	Sodium chloride
NASC:	Nottingham Arabidopsis Stock Centre
NLGN:	Neuroligin
NP-40:	Nonyl phenoxypolyethoxylethanol 40

NO_3-:	Nitrate
PAC:	Precursor accumulating vesicles
PBS:	Phosphate buffered saline
PCR:	Polymerase chain reaction
PHT1:	Peptide/histidine transporter 1
Pi:	Phosphate
PIN:	Pinformed
PM:	Plasma membrane
PVC:	Prevacuolar compartments
RBL5:	RHOMBOID-like protein 5
RNA:	Ribonucleic acid
RNase:	Ribonuclease
S:	Sulphur
SDS:	Sodium dodecyl sulphate
SDW:	Sterile distilled water
SDS-PAGE:	Sodium dodecyl sulphate polyacrylamide gel electrophoresis
SNARE:	Souble NSF Attachment Protein Receptor
TBS:	Tris buffered saline
TGN:	Trans-Golgi network
Wt:	Wild type
X-Gluc:	5-bromo-4-chloro-3-indolyl-beta-D-glucuronic acid cyclohexylammonium salt
Zn:	Zinc

Acknowledgements

I would like to express my gratitude and thanks to my supervisor Dr Ranjan Swarup, for all of his help, support and patience. I have learnt so many numerous skills from him over the course of my PhD, which have laid down the foundations for my future career.

I would also like to thank Dr Ian Kerr for his help and advice during my time in his lab. I must thank all the members of Malcolm Bennett's lab group, past and present, for their advice, help and laughter.

Finally a big thanks to my friends (old and new) whose support was invaluable and has seen me through to the end. With a special thanks to David Watson, whose kind words and actions, lent me strength for the completion of my thesis.

CHAPTER 1

INTRODUCTION

1. INTRODUCTION

One third of the eukaryotic proteome is passed through the secretory pathway en route to their final intra- or extra-cellular destination. Therefore highly specific sorting and trafficking is required to get proteins to their final destination (e.g. plasma membrane, lysosomes, organelles, vacuole or to be secreted from the cell) (Wiseman et al, 2007). These include soluble proteins and integral membrane proteins, collectively referred to as 'cargo proteins' (van Vilet et al, 2003). Trafficking occurs throughout the endomembrane system, as well as to final destinations such as specific organelles; chloroplast, mitochondria, nucleus, and plasma membrane (PM). The endomembrane system of eukaryotic cells alone comprises the organelles of the secretory and endocytic pathways, the endoplasmic reticulum (ER), the Golgi apparatus, the trans-Golgi network (TGN), prevacuolar compartments (PVC), lytic compartments (vacuoles or lysosomes), storage vacuoles (plants), endosomes, and the plasma membrane (Nebenführ, 2002). The localisation of these cargo proteins to specific destinations is therefore complex, involving multiple interactions, especially for polytopic membrane proteins and ligand-receptors where correct conformation is extremely important (van Vilet et al, 2003). Sorting of these cargo proteins and transportation to their final destination is controlled by vesicular transport intermediates and their interacting proteins, allowing cargo to be transported from one organelle to specific membranes where they then fuse with the cell membrane to deliver their contents (Hanton et al, 2005b; Palade, 1975). Currently 4752 polytopic membrane proteins have been discovered in Arabidopsis (approximately 17 % of the proteome) (Ward, 2001), therefore numerous proteins will be required for correct structural conformation and trafficking.

1.1. PROTEIN TRAFFICKING

Protein trafficking in eukaryotes is dependent on accurate targeting of transport vesicles between precisely defined membrane-bound compartments along the biosynthetic pathway and endocytic pathways. In the past few decades considerable progress has been made in understanding protein trafficking and the molecular

machinery that maintains and regulates membrane traffic. In general vesicular traffic seems to be operated by similar molecular machinery in all eukaryotic organisms, as evidenced by homology, many small GTPases, SNAREs, and their associating proteins are present in animal, yeast and plants (see Ueda & Nakano, 2002 for a review). However, it has also been demonstrated that plants have also developed a unique system which not only use conserved machinery but also contain modifications. For example in plant cells the trans Golgi network (TGN) not only carries out TGN functions found in other eukaryotes, but also functions as the early endosome in plants (Ueda & Nakano, 2002).

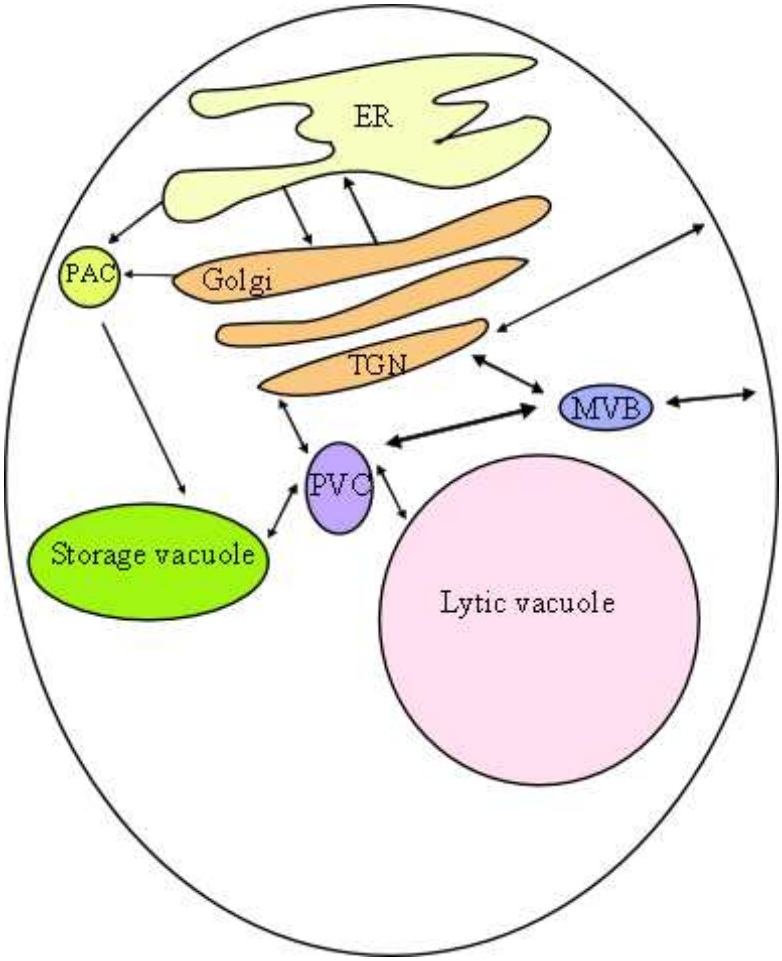

Figure 1: Model showing simplified trafficking routes in the biosynthetic and endocytic traffic

ER = Endoplasmic reticulum; TGN = trans Golgi network; PAC = precursor accumulating vesicles; PVC = prevacuolar compartment; MVB = multivesicular bodies.

Secretory and endocytic traffic allows the cell to have a high level of regulation on the abundance of plasma-membrane proteins such as receptors, transporters and ion channels, allowing the cell to have fast adaptability to its environment (reviewed by Richter et al, 2009).

1.1.1. Biosynthetic pathways

To correctly process, target and transport proteins to their final destination, a complex trafficking within the cell occurs (see figure 1). Cargo proteins are synthesised on endoplasmic reticulum (ER)-bound ribosomes, and enter or cross the ER membrane cotranslationally, within the ER they are correctly folded, assembled and processed (see van Vilet et al, 2003 for a review). Protein folding within the secretory pathway needs to process diverse protein conformations as well as being specific enough to recognise misfolded proteins that can be targeted for degradation (Buck et al, 2007). 30% of synthesised proteins are estimated to become misfolded, and these proteins are degraded by the endoplasmic reticulum-associated degradation (ERAD) which is a cytoplasmic ubiquitin-proteasome pathway (Yamamoto, 2009). After correct folding the proteins need to be transported to the Golgi and downstream compartments for further processing and sorting. Transport occurs through lipid vesicles where the cargo proteins are packaged into the vesicles, these are then transported to the correct localisation where the vesicle fuses with the cell membrane, and delivers the cargo proteins into the membrane (Palade, 1975). Vesicular trafficking has been shown to occur in both the forward (anterograde) direction (from the ER to the plasma membrane) or in reverse (retrograde) direction (Hanton et al, 2005b).

Most proteins that leave the ER are trafficked to the Golgi complex (through coat protein complex II [COPII] vesicles), although some vesicles have been shown to bypass the Golgi and head straight to the storage vacuole (Jürgens & Geldner, 2002; Levanony et al, 1992). Presumably these proteins are the ones that do not need further processing within the Golgi complex, and have been shown to bud from the ER in vesicular structures, known as precursor-accumulating (PAC) vesicles

(Levanony et al, 1992; Mitsuhashi et al, 2001). Other proteins/lipids have been shown to traffic between the ER and the plastid, allowing stromal proteins to be processed in the secretory pathway, such as glycosylation (Nanjo et al, 2006; Rouillé et al, 2000; Xu et al, 2008; reviewed by Inaba & Schnell, 2008).

Once the proteins reach the Golgi, final processing of the proteins occurs. For example glycoproteins, glycolipids and proteoglycans encounter modifications by a large number of enzymes (such as glycosyltransferases, sulfotransferases and proteases) (Prydz et al, 2008). The Golgi complex is also extremely important for correct trafficking and it is the major sorting station of the newly synthesised proteins allowing them to be transported to their final destination (Jürgens & Geldner, 2002).

Transport back to the ER occurs in the cis-cisternae of the Golgi (through COPI vesicles), and this is an essential pathway that continually recycles proteins and lipids from the Golgi to the ER in order to maintain an equilibrium between anterograde and retrograde transport pathways (Hanton et al, 2005; Neumann et al, 2003). Main protein sorting however occurs at the trans-Golgi network (TGN), which sorts proteins to their specific destinations by segregating into specific sets of membrane-enclosed carriers (Bonifacino & Rojas, 2009). Sorting at the TGN is complex especially in plants, as it does not only sort the anterograde traffic (mediated by two vesicles, clathrin-coat vesicles and dense vesicles) of newly synthesised proteins to the plasma membrane, vacuoles and the late endosomes (Vitale & Hinz, 2005). It also sorts endocytosed proteins from the plasma membrane and the late endosomes, meaning that it is also involved in retrograde traffic (also mediated by clathrin-coat and dense vesicles), cycling of plasma membrane proteins and transport of proteins to the late endosomes for their degradation in lytic vacuoles (Nebenführ, 2002).

The TGN and late endosomes are involved in the sorting of material to the vacuoles in plant cells. In plants, there are at least two kinds of vacuoles, lytic vacuoles which have an equivalent function to lysosomes in yeast, and a plant-specific protein storage vacuole (Surpin & Raikhel, 2004).

1.1.2. Endocytic pathways

In plants the endocytic pathway and the biosynthetic pathway are tightly linked as the majority of sorting for both pathways occurs at the TGN. The endocytic pathway is essential to internalise exogenous material to the endosomes (through clathrin-dependent and independent vesicles) and allow highly controlled regulation of signalling/transport at the cell surface (Geldner, 2004). In eukaryotic cells endosomes are separated into two types based on their function, the early endosome and the late endosomes (review by Otegui & Spitzer, 2008). The early endosome receives endocytosed cargo from the plasma membrane and is involved in recycling these cargos back to the plasma membrane or sorting the proteins to the late endosome. In the plant cell the TGN acts as the early endosome, rather than a separate organelle as found in other eukaryotic cells (Otegui & Spitzer, 2008). The late endosome, known as multivesicular bodies (MVBs) or prevacuolar compartments (PVC) in plant cells, are involved in the anterograde trafficking of proteins to the vacuoles and the sorting of membrane proteins for degradation, as well as retrograde trafficking of vacuolar cargo receptors (e.g. SNARES) back to the TGN (Johnannes & Popoff, 2008; Otegui & Spitzer, 2008). It is also believed that there may be a third compartment a 'recycling endosome' as ARF-GEF-GNOM (involved in the recycling of PIN proteins) does not localise to the TGN or the MVB (Geldner et al, 2003).

1.2. ENDOPLASMIC RETICULUM TRAFFICKING

Once the protein is assembled and correctly folded, it exits the ER en route to the Golgi in coat protein complex-II (COPII) vesicles (Baines & Zhang, 2007). The COPII coat is comprised of three main subunits, two heterodimeric complexes, Sec23p/24p and Sec13p/31p, and a small Ras-like GTPase Sar1 (Barlowe et al, 1993, 1994, reviewed by Lee & Miller, 2007). This COPII mechanism has been shown to be highly conserved in eukaryotic cells (reviewed by Hanton et al, 2005b), however recent evidence suggests that plants have evolved unique characteristics to serve plant specific needs. It has been shown in plant systems that the ER and Golgi are in

close contact and that the Golgi has been shown to stream over the ER (Hanton et al, 2006).

COPII vesicles are formed in response to activation of Sar1 by Sec12p-GEF, which causes Sar1p-GTP to bind to ER membranes and recruit Sec23p/24p-GAP, which in turn recruits Sec13p/31p (Bar-Peled & Raikhel, 1997; Barlowe & Schekman, 1993; Schekman & Orci, 1996, reviewed by Memon, 2004). Sec23/24-Sar1 complex is thought to select cargo for export, as well as proteins required for vesicle direction (SNAREs), before the recruitment of Sec13/31 which polymerises into an octahedral cage and deforms the membrane into a bud (Bickford et al, 2004; Fath et al, 2007; Hanton et al, 2005b). After this, hydrolysis of GTP by Sar1p (stimulated by Sec23p) causes Sar1p to dissociate from the membrane, allowing the protein coat to be released and the vesicle can then go on to fuse with its target membrane (see figure 2) (Haung et al, 2001; Yoshihisa et al, 1993).

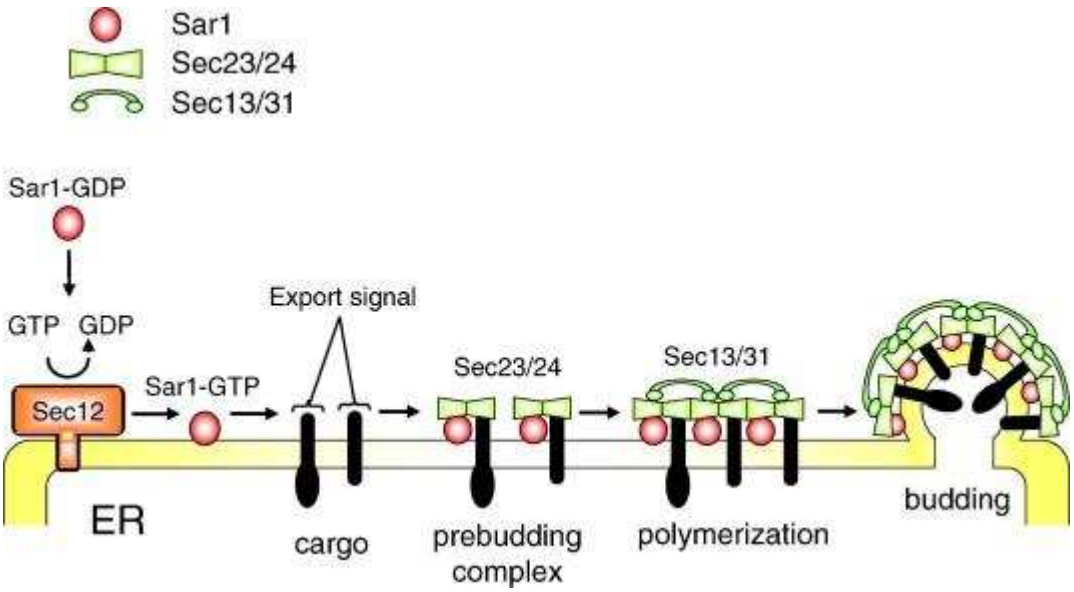

Figure 2: COPII vesicle production and selective packaging of cargo into the budding vesicle (from Sato & Nakano, 2007).

Vesicle formation is restricted to specialised ER exit sites (ERES) and the budding of the vesicle is caused by the polymerisation of the subunits causing deformation of the ER membrane (Barlowe et al, 1994; Heinzer et al, 2008). Upon budding, the

contents of COPII vesicles are delivered to the Golgi. Several models have been proposed to explain this process, taking into account the unique dynamics of the ER and the Golgi, such as the 'vacuum cleaner' (Boevink et al, 1998), 'stop-and-go' (Nebenführ et al, 1999), 'secretory unit' (daSilva et al, 2004, Stefano et al, 2006), and 'kiss-and-run' model (Yang et al, 2005). Research showed that the percentage of Golgi in contact with ERES varies from 20-80 % (Kang & Staehelin, 2008). This

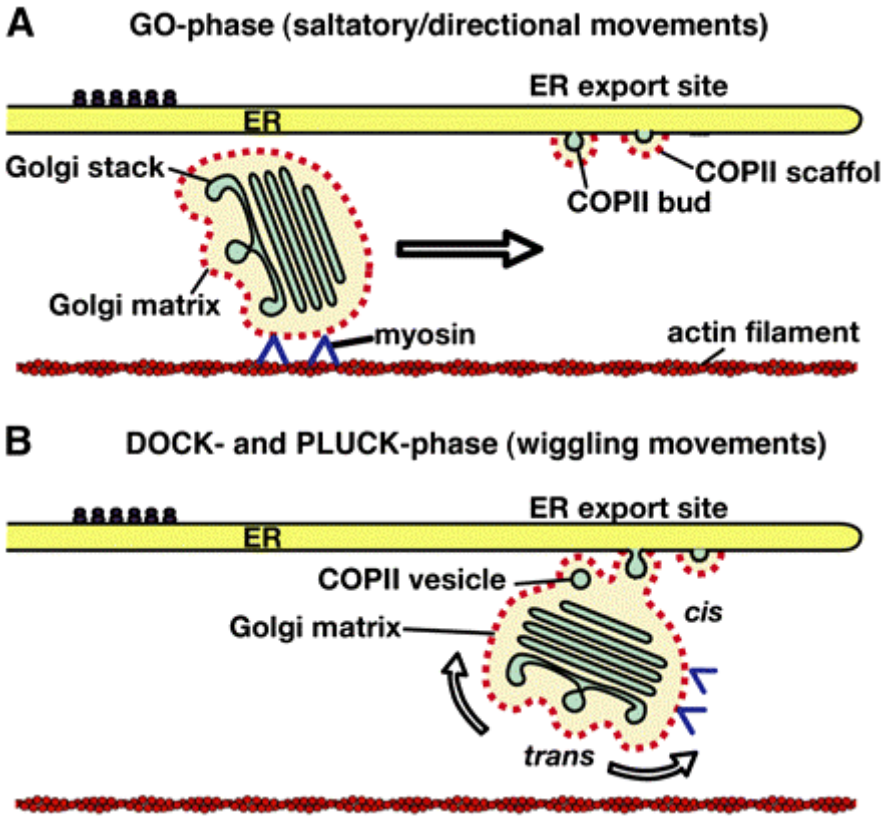

may suggest that the 'stop-and-go' or 'kiss-and-run' model is most likely to be correct.

Figure 3: 'Dock, pluck and go' model of ER-to-Golgi vesicle trafficking

A) Shows the Go-phase where the Golgi stacks travel along the ER by myosin motors along actin filaments. B) Shows the 'dock and pluck' phase where the COPII scaffold attaches to the cis-side of the Golgi matrix and pulls the passing Golgi off the actin track. Allowing the Golgi to halt its progress and the wiggling movement of the Golgi allows COPII vesicles to be plucked from the ER. After COPII vesicle harvesting is complete the Golgi can resume its Go-phase (from Staehelin & Kang, 2008).

Both these models are based on the fact that the Golgi stops at ERES sites to allow protein trafficking. Kang & Staehelin (2008) research suggested that the 'stop' signal is mediated by scaffold-type molecules that assemble on the COPII vesicles that fix the cis-side of the Golgi to the ERES allowing the two organelles to become physically coupled. Based on their research they suggested a fifth model 'dock, pluck and go' where the scaffold captures passing Golgi and the movement of the connected Golgi stacks provides the energy to pluck the budding COPII vesicles and scaffolds (see figure 3). The Golgi can then resume its translational movement when COPII vesicle harvesting is complete (Staehelin & Kang, 2008). This model is supported by the fact that randomly dispersed COPII vesicles constitute <5% of the total COPII vesicle population, supporting the model that COPII vesicles are released only when Golgi stacks are in close proximity to an ERES (Kang & Staehelin, 2008).

1.3. PROTEIN SORTING

Sorting of proteins is extremely important so that they can be transported to the correct final destination, but how is this achieved? There have been numerous reviews on this subject, showing that sorting takes places in all compartments of the secretory system, such as in the ER (Baines & Zhang, 2007; Sato & Nakano, 2007), Golgi (Beck et al, 2009; Hawes & Satiat-Jeunemaitre, 2005; Jürgens & Geldner, 2002; Neumann et al, 2003), and endosomes (Braulke & Bonifacino, 2009; Johnannes & Popoff, 2008; Vitale & Hinz, 2005).

There is belief that proteins have a default destination; with soluble proteins having a default destination to the plasma membrane (Denecke et al, 1990; Handlington & Denecke, 2000), and membrane proteins are believed to have either the tonoplast or the plasma membrane as their default pathway (Hofte & Chrispeels, 1992; Vitale & Raikhel, 1999). However it is obvious that specific sorting takes place within the secretory system, often relying on motifs within the cargo proteins that interact directly or indirectly with the transport vesicles to allow correct loading and transport to their final destination.

1.3.1. Sorting in the ER

The COPII vesicle accommodates an extraordinary variety of cargo proteins with different structures, functions and ultimate destinations; therefore sorting at the ER has to cope with this diversity (Sato & Nakano, 2007). It was believed that a bulk flow transport was the main way of transporting proteins to the Golgi through nonspecific transport, meaning that the proteins were not sorted at the ER but were all packaged together on route to the Golgi (Heinzer et al, 2008; Philipson et al, 2001). However a lot of evidence supports more specific sorting at the ER allowing for selective transport of cargo through specific sorting signals and packaging into COPII vesicles (Baines & Zhang, 2007). Bulk flow transport has been shown to be a remarkably inefficient transport method and only contributes in a minor way to protein secretion (Malkus et al, 2002). It is now quite evident that most secretory proteins are actively sorted into COPII vesicles (Sato & Nakano, 2007). Selective recruitment of cargo proteins into vesicles can be divided into two groups; (i) those that directly bind to components of the COPII coat through ER exit sequence motifs and (ii) those that require specific receptors (accessory proteins) to link them to COPII vesicles (Baines & Zhang, 2007; Herrmann et al, 1999).

Direct interaction between cytosolic tails of membrane cargo proteins and COPII vesicles, such as Sar1p and the Sec23/24p complex is thought to mediate cargo selection (Aridor et al, 2001; Kuehn et al, 1998). Studies have shown that Sec24p is primarily responsible for cargo binding, as it contains three distinct binding sites (Miller et al, 2003) and has multiple isoforms (3 in yeast and 4 in humans) allowing wide-ranging possibilities for combinatorial selection of ER export motifs (Barlowe et al, 1994; Higashio et al, 2000; Pagano et al, 1999; Roberg et al, 1999; Wendeler et al, 2007). Several classes of ER export motifs which are recognised by COPII vesicle are currently known, such as the di-hydrophobic motifs (FF, YY, LL or FY) (Contreras et al, 2004; Kappeler et al, 1997; Otte & Barlowe, 2002), dibasic Arg-Lys-Xaa-Arg-Lys motif (Antonny & Schekman, 2001; Yuasa et al, 2004), RLXD motif (Fernández-Sánchez et al, 2008), LVV motif (Zaarour et al, 2009), diacidic Asp/Glu-Xaa-Asp/Glu motif (Hanton et al, 2005a; Mikosch et al, 2006; Nishimura &

Balch, 1997; Sieben et al, 2008; Zelazny et al, 2008), YxxxNPF, LxxME and LxxLE motifs (Mossessova et al, 2003).

These specific motifs can allow specific interaction with different Sec24 proteins which may be essential for their final localisation. For example the motif RLXD motif on GLYT1 binds specifically to the Sec24D isoform (Fernández-Sánchez et al, 2008). There has been a lot of evidence that binding of these proteins to the Sec24 proteins can be highly specific to certain isoforms, for example SERT can only exit the ER by recruiting Sec24C. Whereas closely related transporter proteins DAT, NET and GAG transporter 1 relies on Sec24D for ER export, showing that even closely related proteins can have exclusive Sec24 isoforms that they require for loading into COPII vesicles (Sucic et al, 2011). It has also been discovered recently that Sec24 can be phosphorylated by kinases such as Akt, this phosphorylation/dephosphorylation of the different isoforms could allow further diversity and specificity for transport of cargo (Sharpe et al, 2011).

Recent evidence suggests that sorting at the ER is not only vital for transport to the Golgi but also to its correct final localisation. GABA transporter-1 (GAT1) is reliant on COPII trafficking, Reiterer et al (2008) looked at a mutant of the GAT1 (GAT1-RL/AS) that can no longer interact with Sec24 and therefore is not loaded into COPII vesicles. GAT1-RL/AS was shown to still passage through the Golgi (probably through bulk flow) but was unable to be localised correctly to the axon terminal of neuronal cells (Reiterer et al, 2008).

Surprisingly secretory proteins without ER export motifs are also loaded into COPII vesicles. These proteins (cargo proteins) are selectively recruited to COPII vesicles through relatively new and novel proteins called ER accessory proteins that facilitate loading into COPII vesicles by direct or indirect interaction with COPII components. Some ER accessory proteins for example carry an ER export motif which is recognised by the COPII coat as well as a domain which interacts with the secretory cargo allowing loading of the cargo protein (Wendeler et al, 2007). Cargo proteins include soluble luminal cargo, such as glycoproteins and transmembrane proteins (Sato & Nakano, 2007). In the ER it has been shown that many exported proteins

require multiple signals to be packed into COPII vesicles, such as a combination of the above ER exit motifs or associations with more than one ER accessory proteins (Sato & Nakano, 2007).

1.4. ER ACCESSORY PROTEINS

A large number of secretory proteins are dependent on specific accessory proteins for exit from the ER. These accessory proteins can be divided into three groups; outfitters, escorts and transport receptors (see figure 4). The outfitters are involved in establishing or maintaining a secretion-competent conformation of the cargo protein and include specific folding catalysts and chaperones that remain within the ER (Herrmann et al, 1999). In this case the protein itself should have an ER exit motif and requires the outfitter to make sure it is in the correct configuration allowing this ER exit motif to interact with COPII vesicles. An example of an outfitter is Shr3p in yeast, which is required for the trafficking of amino acid permeases (e.g. Gap1p) to the plasma membrane (Ljungdahl et al, 1992). In the Shr3p null mutant Gap1p is no longer folded correctly and the proteins aggregate together, preventing Gap1p from being loaded into COPII vesicles causing Gap1p accumulation in the ER. This is specific to 18 members of the amino acid permease (aap) yeast gene family, as other proteins localisation is unaffected in the Shr3p mutant (Gilstring et al, 1999; Kota & Ljungdahl, 2005). Failure of cargo proteins to associate with their specific outfitter accessory protein results in incorrect folding and/or aggregation, causing the protein to be retained in the ER and are ultimately degraded via the ERAD pathway (Kota et al, 2007). Another role of outfitters would be to ‘mark’ the cargo proteins for ER exit (e.g. phosphorylation), or active involvement in the loading of the cargo into COPII (escort contains motif which interacts with COPII but prevents escort loading) vesicle. For example Saito et al (2007) showed that TANGO1 is necessary for loading of collagen VII into COPII vesicles. Collagen VII is a bulky protein (900 kDa) and is unable to fit into the generic COPII vesicle (60-90 nm) in diameter. TANGO1 is believed to slow COPII biosynthesis by binding to Sec23/24 through the PRD domain (the same domain as Sec13/31 bind) therefore influencing the recruitment of Sec13/31. This allows the COPII vesicle to grow larger than it normally would and allow the loading of collagen VII, once the collagen VII is

loaded it becomes unbound from TANGO1 and this change in conformation may allow TANGO1 to release Sec23/24, allowing the final recruitment of Sec13/31 and budding of the vesicle. It has been shown that it does not influence the transport of a related protein collagen I and therefore is specific for collagen VII (Saito et al, 2009).

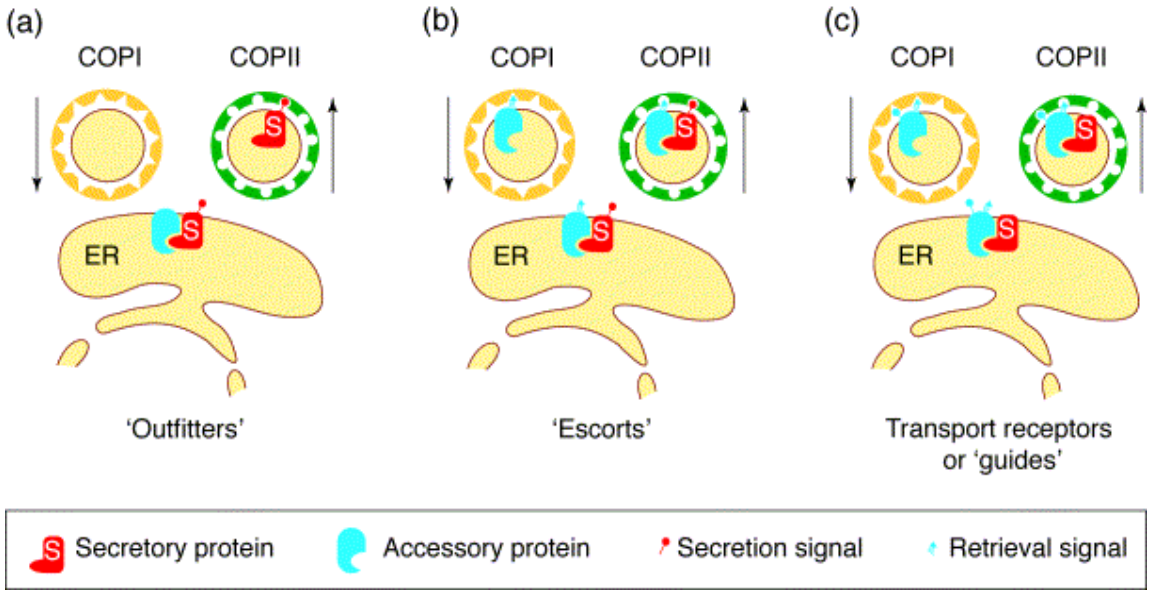

Figure 4: A model of different types of ER accessory proteins

Figure taken from Hermann et al, 1999 - ER accessory proteins can facilitate the transport of cargo proteins to the Golgi in three main ways. (a) They are involved in processing of the protein so that it is in the correct configuration for transport into COPII vesicles. (b) They travel with the secretory protein in the COPII vesicles, through indirect interaction with the COPII coat proteins (c) The third hypothesis is they might actively recruit cargo protein at the ERES into budding vesicles and transport with them by direct interaction with COPII vesicles (from Herrmann et al, 1999).

The escorts have a similar function but differ in the fact that they accompany their cargo proteins to the Golgi, they therefore include regulatory molecules needed to prevent premature activity or binding of substrates to the cargo protein (Herrmann et al, 1999). A well-studied example of a mammalian escort protein is RAP, which is involved in the correct localisation of low-density lipoprotein (LDL) receptor family (Bu et al, 1995). In the absence of RAP, LDL receptors aggregate in the ER due to

premature binding of ligands and are ultimately degraded; therefore RAP acts as an escorting accessory protein through the secretory pathway preventing premature interaction with ligands (Bu & Schwartz, 1998).

The third group, transport receptors or guides also cycle between the ER and Golgi, however they are involved in direct interaction with COPII vesicles, providing the information required for selective uptake (Herrmann et al, 1999). Well known mammalian transport receptors are LMAN1-MCFDC protein complex that are involved in the transport of factors V and VIII (F5F8D) and two lysosomal proteins cathepson C (catC) and cathepson Z (catZ) (Appenzeller et al, 1999; Cunningham et al, 2003; Zhang et al, 2005). The cytoplasmic tail of LMANI contains a FF ER exit motif that interacts with the COPII coats allowing selective cargo loading of its substrate (Baines & Zhang, 2007).

ER Accessory protein	**Function**	**Cargo**	**Species**	**References**
RanBP2	Outfitter	Opsin	Bos taurus	Ferreira et al, 1996
TANGO1	Outfitter	Collagen VII	Drosophila melanogaster	Saito et al, 2009
CALF-1 and UNC-36	Putative outfitter	CaV2 channel	Caenorhabditis elegans	Saheki & Bargemann, 2009
Calmodulin	Putative outfitter	KCNQ2 K+ channel	Homo sapiens	Alaimo et al, 2009
DRiP78	Putative outfitter	Dopamine D1 receptor	Homo sapiens	Bermak et al, 2001
NinaA	Escort	Rhodopsin	Drosophila melanogaster	Baker et al, 1994; Colley et al, 1991
RAP	Escort	LDL receptor family	Homo sapiens	Bu et al, 1995

Yif1B	Escort	Serotonin (5-HT-1A) receptor	Rattus norvegicus	Carrel et al, 2008
CD4	Putative escort	CC chemokine receptor 5 (CCR5)	Homo sapiens	Anchour et al, 2009
ODR-4	Putative escort	Odorant receptors	Caenorhabditis elegans	Dwyer et al, 1996
PX-RICS and GABARAP	Putative escort	Cadherin β-catnin complex; FGFR4 cadherin complex	Homo sapiens	Nakamura et al, 2008
RAMP1	Putative escort	Calcitonin-like receptor	Homo sapiens	McLatchie et al, 1998
Stargazin	Putative escort	AMPA receptors (GluR1)	Cercopithecus aethiops	Vandenberghe et al, 2005
ERGIC-53 (LMAN1) - MCFD2[d]	Transport receptor	FV and FVIII; catC and catZ	Mus musculus and Homo sapiens	Appenzeller et al, 1999; Cunningham et al, 2003; Nyfeler et al, 2006; Zhang et al, 2005
MRAP	Transport receptor	Melanocortin 2 receptor	Homo sapiens	Webb et al, 2009
Bap31	Putative Transport receptor	Cellubrevin, MHC class I, CD11b/CD18,	Mus musculus and Homo sapiens	Annaert et al, 1997; Ladasky et al, 2006;

		Tetraspanins (CD9 and CD81)		Paquet et al, 2004; Stojanovic et al, 2005; Zen et al, 2004
Cornichon	Putative Transport receptor	Gurken	Drosophila melanogaster	Bökel et al, 2005
Pho86	Outfitter	Pho84p	Saccharomyces cerevisiae	Kota & Ljungdahl, 2005; Lau et al, 2000
Shr3p	Outfitter	Amino acid permeases - Gap1p	Saccharomyces cerevisiae	Gilstring et al, 1999; Kota & Ljungdahl, 2005; Kuehn et al, 1996; Ljungdahl et al, 1992
Chs7	Putative outfitter	Chs3	Saccharomyces cerevisiae	Kota & Ljungdahl, 2005; Trilla et al, 1999
Gsf2	Putative outfitter	Hxt1p	Saccharomyces cerevisiae	Kota & Ljungdahl, 2005; Sherwood & Carlson, 1999
Vma12p, Vma21p and Vma22p	Putative escort	Vacuolar H^+-ATPase	Saccharomyces cerevisiae	Malkus et al, 2004
Emp24p–	Transport	Gas1p and	Saccharomyces	Muñiz et al,

Erv25p	receptor	Suc2p	cerevisiae	2000
Erv26p/Svp26p	Transport receptor	Pro-ALP and Ktr3p	Saccharomyces cerevisiae	Bue et al, 2006, 216
Erv29p	Transport receptor	Gpαf , CPY and CFTR	Saccharomyces cerevisiae	Belden & Barlowe, 2001; Suaud et al, 2011
Emp46p–Emp47p[c]	Putative Transport receptor	Glycoproteins of unknown identity	Saccharomyces cerevisiae	Sato & Nakano, 2003
Erv14p/15p	Putative Transport receptor	Axl2p and Sma2p	Saccharomyces cerevisiae	Nakanishi, 2007; Powers & Barlowe, 1998, 2002
Erv41p–Erv46p[c]	Putative Transport receptor	None identified	Saccharomyces cerevisiae and Mus musculus	Welsh et al, 2006
PHF1	Outfitter	PHT1	Arabidopsis thaliana	González et al, 2005
AXR4	Putative outfitter	AUX1	Arabidopsis thaliana	Dharmasiri et al, 2006
NAR2.1	Putative outfitter	NRT2.1	Arabidopsis thaliana	Wirth et al, 2007

Table 1: A list of potential ER accessory proteins, adapted from Baines & Zhang, (2007)

[a] Confirmed outfitters meet the following two criteria: (i) ER resident protein, (ii) evidence that deficiency selectively impairs cargo transport. Putative outfitters depend on whether it has been proven that the protein does not cycle in the secretory pathway.

[b] Confirmed escorts meet the following two criteria: (i) cycles in the secretory pathway, (ii) evidence that deficiency selective impairs cargo transport. Putative escorts depend on whether it has been proven that the protein cycles in the secretory pathway.

[c] Confirmed transport receptors meet the following three criteria: (i) contains a transmembrane component and cycles in the early secretory pathway, (ii) evidence that deficiency selectively impairs cargo transport, and (iii) evidence for a specific receptor-cargo interaction. Putative transport receptors meet two of the three criteria

[d] MCFD2 seems to be dispensable for transport of catC (cathepson C) and catZ (cathepson Z) (Nyfeler et al, 2006)

A large number and varied mechanisms of ER accessory proteins have been discovered in mammalian and yeast systems to date, and it is likely more will be discovered as we learn more about trafficking within the cell. The recent discovery of three plant ER accessory proteins AXR4, PHF1, and NAR2.1 is exciting as it shows that a similar mechanism also exists in plants. AXR4 is a putative outfitter, which selectively regulates the localisation of AUX1 (an auxin influx carrier) to the plasma membrane (Dharmasiri et al, 2006). axr4 mutant causes abnormal accumulation of AUX1 in the ER and abolishes AUX1 location, while other plasma membrane proteins remain unaffected (Dharmasiri et al, 2006). AXR4 has an ER localisation and a putative α/β hydrolase domain, AXR4 therefore may facilitate trafficking by acting as an outfitter by modifying AUX1 for correct conformation and therefore allowing it to be recognised as cargo by COPII vesicles (Dharmasiri et al, 2006).

Similar to AXR4, mutations in PHF1 led to abnormal accumulation of its target protein PHT1 (a phosphate transporter) within the ER, and loss of correct localisation (González et al, 2005). PHF1 is also believed to be an outfitter as it is also localised to the ER and has not been detected in COPII vesicles (González et al, 2005). Another possible plant ER accessory protein is NAR2.1 that possibly regulates NRT2.1 (a high-affinity nitrate uptake protein) localisation to the plasma membrane (Wirth et al, 2007). While mutants in PHF1 and AXR4 causes accumulation of their substrate in the ER, in NAR2.1 mutant NRT2.1 is absent from fractions suggesting that NAR2.1 may be needed to prevent degradation through ERAD and allowing proper folding for vesicle transport (Wirth et al, 2007). The recent discovery of these three potential ER accessory proteins suggests that other polytopic membrane proteins in plants require their own cognate ER accessory protein to facilitate folding

and/or transport. It is estimated that as many as 35% of the entire human genome enters the secretory pathway at the ER, therefore there are possibilities of numerous other ER accessory proteins to be discovered (Saito et al, 2009).

1.5. AXR4 – AN ER ACCESSORY PROTEIN?

AUXIN RESISTANT4 (AXR4) is a 473aa protein which is localised to the ER (see figure 5) (Dharmasiri et al, 2006; Dunkley et al, 2006). It was initially indentified in screens for auxin resistant root elongation (Hobbie & Estelle, 1995) and altered root gravitropism (Simmons et al, 1995). Detailed characterisation of the mutant revealed a weak aux1-like phenotype (Dharmasiri et al, 2006). It also shared a number of other characteristics with aux1 mutant such as reduced lateral root number and similar responses to applications of different types of auxin (Hobbie & Estelle, 1995; Yamamoto & Yamamoto, 1998, 1999). These results suggested that AXR4 may function in the same pathway as AUX1 (Dharmasiri et al, 2006).

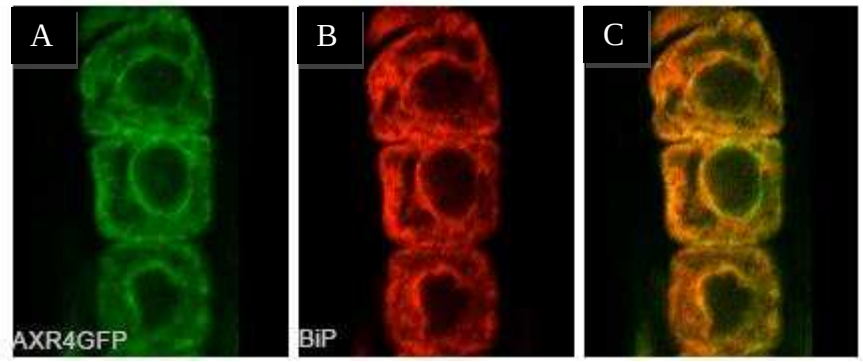

Figure 5: AXR4-GFP localisation in root cells using confocal imaging
(A) AXR4-GFP localisation in root cells using antibodies to GFP (anti-GFP). (B) Localisation of BiP (a known ER resident protein) in root cells using anti-BiP. (C) Superimposed confocal images of AXR4-GFP and BiP localisation confirming ER localisation of AXR4 (from Dharmasiri et al, 2006).

AUX1 is an auxin influx carrier which belongs to the auxin amino acid permease (AAP) family of proton-driven transporters (Bennett et al, 1996). AUX1 has been shown to be polar and non polar distributed within different cell files. In protophloem cells, AUX1 is targeted to the apical face of the cell plasma membrane

surface, whereas in epidermal cells AUX1 appears to be targeted preferentially to the upper and lower membrane surfaces (Swarup et al, 2001).

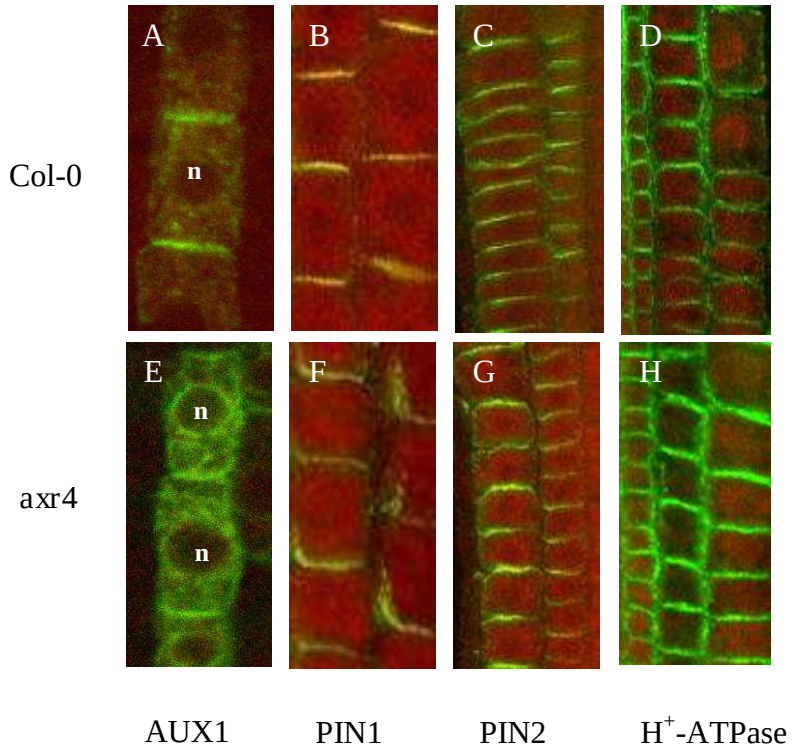

Figure 6: AUX1 trafficking is affected in the axr4 mutant
Hemagglutinin (HA)-AUX1 localisation in the protophloem of Col-0 (A) and axr4-2 (E); PIN1 localisation in Col-0 (B) and axr4-2 (F); PIN2 localisation in Col-0 (C) and axr4-2 (G); and localisation of plasma membrane H^+-ATPase in Col-0 (D) and axr4-2 (H) (from Dharmasiri et al, 2006).

Dharmasiri et al (2006) showed that in the axr4 mutant AUX1 protein accumulated in the endoplasmic reticulum (ER) instead of being localised correctly to the plasma membrane. They provided evidence that AXR4 was specific to AUX1 as the axr4 mutation had no effect on the localisation of other plasma membrane proteins such as PIN1, PIN2 and H^+-ATPase (see figure 6) (Dharmasiri et al, 2006). This mislocalization of AUX1 explains the axr4 phenotype, and the weaker phenotype may be due to the fact that small amount of AUX1 is still correctly localised to the plasma membrane in axr4 (Dharmasiri et al, 2006).

AXR4 acts as an ER accessory protein as it is necessary for the correct localisation of AUX1, however how it actually provides this targeting is unknown. Looking at the protein sequence, structure and possible domains would allow some insight into AXR4 function. AXR4 is a single copy gene which is a plant specific protein, with a single membrane spanning domain near the N-terminus and contains two loosely conserved esterase lipase domains (αβ hydrolase fold) which are found in a diverse group of hydrolytic enzymes (Dharmasiri et al, 2006; Holmquist, 2000). Tendot Abu Baker (2007) demonstrated that AXR4 C-terminal is within the ER lumen, suggesting that the C-terminal may interact with AUX1, to fold, modify or allow loading of AUX1 into COPII vesicles. Several hypotheses have been proposed for AXR4 function to allow exit of AUX1 from the ER, such as the correct folding of AUX1, post translational modification of AUX1 and regulating lipid composition of ERES.

1.6. AIMS AND OBJECTIVES

My project has two main aims

(1) Investigation of possible functions of AXR4;

- Determine if AXR4 and AUX1 interact directly using co-immunoprecipitation experiments.
- Determine if AXR4 is involved in the transport of other members of the AUX1/LAX family
- Determine if the α-β hydrolyse fold domain is important for AXR4 function

(2) Discover new ER accessory proteins in Arabidopsis;

- Identify potential ER accessory proteins using a bioinformatic and functional studies.
- Characterise any potential ER accessory protein to determine their role.

CHAPTER 2

MATERIAL AND METHODS

2. MATERIAL AND METHODS

2.1. PLANT MATERIALS

Arabidopsis thaliana seeds were obtained from the Nottingham Arabidopsis Stock Centre (NASC) or from the Bennett Laboratory seed stocks (Plant Sciences, University of Nottingham). For a full list of plant materials used during this study, see appendix 9.1.

2.2. PLANT GROWTH

2.2.1. Plant growth media

For routine plant growth Murashige and Skoog (MS) media (Sigma-Aldrich) was used at 2.15 g/L basal salts, with 1.0 % (w/v) Bacto^{TM} agar (Appleton Woods), and adjusted to pH 5.8 with 1.0 M KOH. For more detailed nutrient studies, a growth medium was made up to allow changes within the nutrient composition of the media (control solution). This had 1.0 % (w/v) Bacto^{TM} agar, and adjusted to pH 5.8 with 0.1 M HCl.

MS media	NH_4NO_3 825 mg/L, H_3BO_3 3.1 mg/L, $CaCl_2$ 166.1 mg/L, $CoCl_2.6H_2O$ 0.0125 mg/L, $CuSO_4.5H_2O$ 0.0125 mg/L, $Na_2EDTA.2H_2O$ 18.6 mg/L, $FeSO_4.7H_2O$ 13.9 mg/L, $MgSO_4$ 90.35 mg/L, $MnSO_4.H_2O$ 8.45 mg/L, $(NH_4)_6Mo_7O_{24}$ 0.125 mg/L, KI 0.415 mg/L, KNO_3 950 mg/L; KH_2PO_4 85 mg/L, and $ZnSO_4.7H_2O$ 4.3 mg/L (Murashige and Skoog, 1962).
Control solution	KH_2PO_4 34.0 mg/L, KOH 28.1 mg/L, $MgSO_4.7H_2O$ 184.8 mg/L, $CaCl_2.2H_2O$ 3.6 mg/L, FeNaEDTA 36.7 mg/L, $Ca(NO_3)_2.4H_2O$ 944.6, H_3BO_3 1.9 mg/L, $MnSO_4.4H_2O$ 2.2 mg/L, $ZnSO_4.7H_2O$ 0.3 mg/L, $CuSO_4.5H_2O$ 0.8 mg/L, $Na_2MoO_4.2H_2O$ 0.1 mg/L

Bacto™ agar	calcium 0.179 %, chloride 0.021 %, cobalt < 0.001 %, copper < 0.001 %, iron 0.002 %, lead < 0.001 %, magnesium 0.068 %, manganese < 0.001 %, nitrate < 0.005 %, phosphate < 0.005 %, potassium 0.121 %, sodium 0.837 %, sulfate 1.778 %, sulfur 0.841%, tin < 0.001%, and zinc < 0.001 %

For plant selection, antibiotics or chemicals required were added after autoclaving, at the following concentrations; 2,4-D 25 nM/ml, DEX 10 nM/ml, hygromycin 50 μg/ml, kanamycin monosulphate 50 μg/ml.

2.2.2. In vitro

Arabidopsis thaliana seeds were surface sterilised in 50 % (v/v) bleach (Sigma) for 6 minutes, then washed 4 times in sterile distilled water containing 0.15% Triton X-100. The seeds were then either washed in 70 % (v/v) ethanol and left to dry on Whatman filter paper, or sown directly onto the agar with the use of a Gilson. The seeds were vernalised in the dark at 4^{o}C for 48 hours and then germinated vertically at 20 ±2 °C under constant light conditions for two weeks.

Transformed seeds were grown with appropriate antibiotics for 2 weeks, Arabidopsis seedlings that developed dark green true leaves and an extending root system were transferred to compost.

2.2.3. In vivo

After two weeks growth on plates, the seedlings were transferred to individual 9cm pots containing Levington M3 compost (Scotts U.K. Professional, U.K.). This compost was supplemented with 50 mL L^{-1} compost of systemic insecticide "Intercept" [70% (w/w) Imidacloprid] prepared at 0.2 g L^{-1} to prevent sciarid fly infestation. The plants were then placed in disposable sleeves (Zwapak, Netherlands) to prevent cross-pollination. The glasshouse was maintained at 21-23 ^{o}C with a 16 h light and 8 h dark cycle, with a light intensity of 150 μmols $m^{-2}s^{-1}$.

2.2.4. Root cultures

Root cultures of Arabidopsis thaliana were generated according to the modified protocol of Rouse et al (1996). Seeds were surface sterilised in 70 % (v/v) ethanol for 2 minutes, followed by treatment with 20 % (v/v) sodium hypochlorite for 30 minutes. The seeds were washed four times with sterile distilled water, and 2-10 sterile seeds were placed in 250 ml Erlenmeyer flasks containing 100 ml of Gamborg B5 medium (2 % [w/v] sucrose, 0.32 % [w/v] Gamborg B5 salts [Sigma-Aldrich] and 0.05 % [w/v] MES-KOH, pH 5.8 and 1 % Gamborg B5 Vitamin Mix [Sigma-Aldrich]), and sealed with sterile cotton wool plug. Root cultures were grown for 4-5 weeks in shaking incubators in the dark at 100 rpm and temperature of 20-22 ^{o}C.

2.2.5. Nutrient screen

Nutrient smart screens were based on main nutrient solution media (see 2.2.1) with the concentration of specific nutrients adjusted. These screens included; copper (0.1, 10, 20 and 50 μM), nitrogen (0, 0.05 and 4 mM), phosphorous 0 [20 and 100 μM Fe], 0.01 [20 and 100 μM Fe], 0.05 and 25 mM), sodium (0.1, 50, 100 and 200 mM), sulphate (0, 0.1, and 1 mM) and zinc (1, 500 and 1000 μM). See appendix 9.3 for making of stock solutions for the smart screens and 6.4 for smart screen media composition. The phenotypes were characterised after 5 days growth, and again after 2 weeks growth.

2.2.6. DEX treatment

Seedlings were grown for four days and then transferred to plates containing 1 μM dexamethasone (DEX) and the phenotype was observed for one week.

2.2.7. 2,4-D assays

Seedlings were grown on various concentrations of 2,4-D (25, 50 and 100 nM), and the root length was scored after 5-7 days.

2.3. BACTERIA GROWTH

2.3.1. Bacterial growth media

Luria-Bertani (LB) broth had the following composition; 0.5% (w/v) yeast extract, 1.0% (w/v) bacto-trytone, 1.0% (w/v) NaCl, pH 7.0. For plates, 1.0% (w/v) bacto agar was added. Antibiotics were used in plates and broth at the following concentrations: ampicillin 100 μg/ml, hygromycin 50 μg/ml, kanamycin monosulphate 50 μg/ml, rifampicin 25 μg/ml, and spectinomycin 100 μg/ml.

2.4. INSECT CELL GROWTH

2.4.1. Insect cell growth media

Insect Xpress-FCS growth medium had the following composition; Insect Xpress medium [Lonza] supplemented with 10 % (v/v) heat-inactivated foetal calf serum [Biowhittaker], and 50 units/ml of penicillin and streptomycin mixture [King & Possee, 1992].

2.4.2. Insect cell growth

For all baculovirus expression experiments performed in this study, the Sf9 insect cell line (Vaughn et al, 1977) derived from ovarian tissue of Spodoptera frugiperda were used. All the insect cell manipulations were performed using standard cell culture techniques (King & Possee, 1992). Sf9 insect cells were propagated and maintained as cell monolayer cultures in T75 flasks and as a suspension culture in 50 ml conical flasks containing Insect Xpress-FCS growth medium at 28 ^{o}C in a humid atmosphere. The suspension cultures were placed in an orbital incubator maintained at 90-120 rpm, Suspension cultures were passaged thrice weekly (when they reached a cell density of ca. 8 x 10^6 cells/ml), and were seeded into fresh media at a density of 1.0 x 10^6 cells/ml. Monolayer cultures were passaged at confluency with a 1:10 dilution (typically every 3-4 days).

2.4.3. Small-scale infection of insect cells with recombinant baculovirus

Sf9 cells were seeded in 10 ml aliquots at a cell density of 1 x 10^6 cells in 50 ml conical flasks and left to grow O/N shaking at 28 ^oC until cell density of 2 x 10^6 cells was reached. Aliquots of virus inoculums were added based on the titre of the virus so that a multiplicity of infection (MOI; the ratio of viral particles to Sf9 cells) of approximately 0.1, 1, 10 and 100 was achieved. The cells were incubated at 28 ^oC for 48 hours, before being harvested by centrifugation at 3000 g for 15-20 minutes and resuspended in 0.5 ml ice cold 1x PBS lysis buffer (containing Calbiochem Protease Inhibitor cocktail set III [EDTA free] at 1x final concentration). The cell suspension was transferred to microcentrifuge tubes and sonicated twice for 10 seconds with the microprobe sonicator at 40% power.

2.5. MOLECULAR STUDIES

2.5.1. RNA extraction

RNA normally from 5-7 day old whole seedlings was extracted using RNeasy Plant Mini Kit (Qiagen) following manufacturer's instructions.

2.5.2. Reverse Transcription PCR

2 μg of total RNA was used for cDNA synthesis, RNA and oligodT primer (100 pmol) were incubated at 70 ^oC for ten minutes and then left to anneal on ice. Reverse transcription mix (5X FSB, 0.1 M DTT, 10 mM dNTP and RNase inhibitor) was added to this reaction and incubated at 42 ^oC for 2 minutes. SuperScript™ (Invitrogen) was added and left to incubate at 42 ^oC for 2 hours. The reaction was terminated by heating at 70 ^oC for 10 minutes, and the cDNA was stored at –20 ^oC.

RNA	2.5 μg
OligodT primer (50 μM)	0.5 μl
Sterile Deionised Water	< 11 μl

5X FSB	4 μl
0.1 M DTT	2 μl
dNTP (10 mM)	1 μl
RNase inhibitor	1 μl
SuperScript™	1 μl

2.5.3. DNA extraction

Plant material (normally 1-2 leaves) was ground to fine powder using liquid nitrogen. In an eppendorf 400 μl extraction buffer (200 mM Tris-HCL pH 7.5, 250 mM NaCl, 25 mM EDTA, 0.5% SDS) was added and vortexed briefly to mix. Samples were centrifuged at 16,000 x g for 2 minutes. Equal volume of isopropanol was added to the supernatant, and mixed by invertion. DNA was pelleted at 16,000 x g for 5 minutes and dried in vacuum for 10 minutes. The DNA was resuspended in 30 μl sterile water and stored at –20^{o}C.

2.5.4. Plasmid isolation

Single colonies were grown overnight in 5 ml of LB and appropriate antibiotic at 37 ^{o}C. A glycerol stock was frequently prepared for long term storage (1 ml of the culture + 0.5 ml 50 % glycerol) at -80 ^{o}C.

The rest of the culture was harvested by centrifugation at 1500 g for 3 minutes, and plasmid preparations were performed using Nucleospin® Plasmid (Macherey Nagal) following manufacturer's protocol.

2.5.5. Polymerase Chain Reaction

For routine Polymerase Chain Reaction (PCR) the general protocol and PCR program is shown below, specific details were changed based on the enzyme used,

following manufacturer's instructions. The PCR mixture was kept on an ice block (ISOfreeze, Alpha Laboratory Supply) before being placed in the PCR machine when the temperature reached 94 °C.

2.5.5.1. General protocol for Taq DNA polymerase

DNA polymerase	0.2 µl
5 X Buffer	4 µl
dNTP (10 mM)	0.4 µl
Primer Forward (10 µM)	1 µl
Primer Reverse (10 µM)	1 µl
DNA	1-2 µl
Sterile Deionised water	11.4 µl

Lid: 110 °C		
1: 94 °C	2 m	denaturation
2: 94 °C	30 s	denaturation
3: 54-60 °C	30 s	annealing
4: 72 °C	1 m	extension
5: Steps 2-4	34 x	
5: 72 °C	10 m	extension

2.5.5.2. Protocol for A-tailing

DNA polymerase	0.1 µl
5 X Buffer	2 µl
10 mM dATP	0.2 µl
Purified PCR product	1-7 µl
Sterile Deionised water	to 10 µl

Lid: 110 °C		
1: 70 °C	15 m	extension

2.5.6. PCR purification

PCR purification was done either by Gel extraction (MiniElute [Qiagen]) or by PCR clean up (GenElute^{TM} PCR Purification [Sigma]) following manufacturer's protocol.

2.5.7. DNA restriction

DNA (plasmid or PCR product) was digested with appropriate restriction enzymes (New England Biolabs), using the buffers and conditions recommended by the manufacturer. In the case of digestion of DNA with more than one restriction

enzyme, a reaction buffer compatible with both enzymes was chosen. If no compatible buffer was found then a sequential digestion was performed.

A typical reaction contained in a final volume of 20 µl; 2-12 µl DNA, 2 µl 10x buffer, and 1 µl of restriction enzyme. The digestion was performed at 37 ^{o}C for 2-3 hours.

2.5.8. Dephosphorylation

After the restriction, if required, the terminal 5' phosphate groups were removed from the linearized plasmid DNA by treatment with bacterial alkaline phosphatase (BAP, USB™), (1 µl per 20 µl reaction) for 30 minutes at 37 ^{o}C.

2.5.9. Agarose gel electrophoresis

1.0 % (w/v) agarose (Bioline) in TBE buffer (90 mM Tris-HCl, pH 8.0; 90 mM boric acid and 2 mM EDTA) with ethidium bromide added at a final concentration 0.5 µg/ml was used. DNA was electrophoresed at 100 V until bands were separated.

2.5.10. Molecular cloning

The Escherichia coli strain DH5α (Hanahan, 1983) was used for all cloning experiments and the Agrobacterium tumefaciens strain C581rif (pGV3850) (Zambryski et al, 1983) was used for all plant transformations.

DNA for cloning into plasmid vectors was PCR amplified and A-tailed if required (see section 2.5.5.2.). Both the plasmid and insert are then restricted with appropriate restriction enzymes, gel purified and ligated.

In a 10 µl ligation reaction, 100 ng of vector, an appropriate amount of insert DNA (3:1 insert to vector molar ratio), 1 µl of 10x T4 Ligase buffer, and 1 µl T4 DNA

ligase (3 U/µl) were mixed and incubated overnight at 4 ^{o}C. A ligation reaction without the insert was performed as a negative control.

2.5.11. Gateway cloning

Gateway cloning was performed as per manufacturer's instructions. Entry vectors were created by restriction and ligation based cloning with the gateway entry vector pENTR^{TM}11.

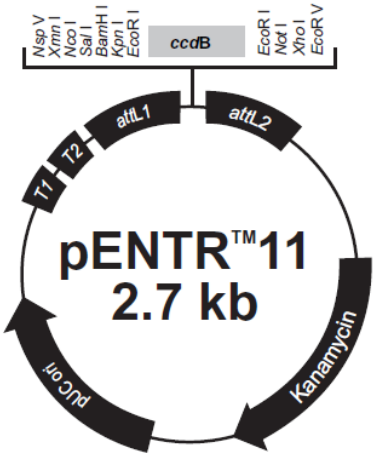

Figure 7: Plasmid map of pENTR^{TM}11 (Invitrogen)

Entry vectors were then recombined into destination vector by LR reaction as per manufacturer's instructions. A typical LR reaction contained 50-150 ng of the entry vector, 150 ng of the Destination vector, and 2 µl LR Clonase II enzyme mix in a final volume of 10 µl. The reaction was carried out at 25 ^{o}C for 2-5 hours, and terminated with 1 µl Proteinase K (Invitrogen) at 37 ^{o}C for 10 minutes.

2.5.12. Bacterial transformation

2.5.12.1. Preparation of chemical-competent E. coli cells

Prewarmed 250 ml LB was inoculated with 1 ml of overnight culture and grown at 37 ^{o}C to mid logarithmic phase (OD600 between 0.6 and 0.8). The cells were kept on ice for 15 minutes prior to centrifugation at 2500 g for 5 minutes at 4 ^{o}C. The cell pellet was gently resuspended in 100 ml of chilled TFBI solution (100 mM RbCl, 50

mM $MnCl_2$, 30 mM KOAc, 10 mM $CaCl_2$, 15% (v/v) glycerol, pH 5.8 with 0.2 N acetic acid), and kept on ice for 5 min. The cell suspension was then re-centrifuged for 5 min at 2500 rpm, at 4 ^oC, and the pellet was suspended in 10 ml of chilled TFBII solution (10 mM MOPS buffer pH 7.0, 10 mM RbCl, 75 mM $CaCl_2$, 15% (v/v) glycerol). The competent cells were divided into aliquots of 0.2 ml and stored at –80 ^oC.

2.5.12.2. E. coli transformation

DNA (1-10 µl) was mixed with 90 µl freshly thawed competent cells. The tube was then incubated on ice for 20 min, heat shocked at 42 ^oC for 90 sec, and immediately placed back on ice for 20 min. 900 µl of LB medium was added to the cells and the tubes were incubated shaking at 37 ^oC for 1 hour. Aliquots of up to 150 µl were plated onto LB agar medium containing the appropriate antibiotics and incubated overnight at 37 ^oC.

2.5.12.3. Agrobacterium tumefaciens transformation

Agrobacterium tumefaciens competent cells were thawed on ice and 1.5 µl plasmid DNA (approximately 50-100 ng) was added to 40 µl of competent cells. The cells were transferred to a pre-cooled 0.2 cm electroporation cuvette (Sarstedt) and electroporated using Gene Pulser TM (Bio-Rad). 1 ml LB was added to the cuvette and then incubated for 3 hours at 28 ^oC without shaking. Aliquots of up to 100 µl were plated on LB agar medium containing appropriate antibiotics and incubated at 28 ^oC for 2 days.

2.5.13. Plant transformation

Transformation of Arabidopsis was carried out using the floral dip method (Clough & Bent, 1998). 100 ml LB with appropriate antibiotics was inoculated with 2 ml of overnight culture, and grown at 28 ^oC until OD600 = 0.8-1.2. Sucrose (5 % w/v) and Silwet-L77 (0.5 % v/v) were added to the culture and mixed well. The aerial parts of the flowering Arabidopsis were dipped into the Agrobacterium culture for 5-20 s.

Plants were covered with folded plastic sleeves overnight to maintain humidity, the sleeves were then opened slowly and plants were left to grow.

2.6. PROTEIN STUDIES

2.6.1. Isolation of Arabidopsis thaliana microsomes

A microsomal membrane fraction was prepared by the modified methods of Kjellbom and Larsson (1984) using Arabidopsis thaliana root cultures prepared as described in section 2.3.3. Five grams of root tissue were homogenized under liquid nitrogen, using a mortar and pestle in homogenisation buffer (0.5 M sucrose, 50 mM HEPES-OH, pH 7.5, 0.5 % polyvinyl polypyrrolidone, 0.1 % [w/v] sodium ascorbate, 1.0 mM DTT and Complete Protease Inhibitor cocktail [Sigma-Aldrich]). The homogenate was filtered through 100 μm mesh nylon and the resulting filtrate centrifuged for 12 minutes at 2800 g at 4 ^{o}C to remove particulate material. A microsomal membrane fraction was pelleted further by centrifugation at 100,000 g for 1 hour at 4 ^{o}C. The supernatant was decanted and the microsomal pellet was resuspended in a solubilisation buffer (100 μL, e.g. PBS, TBS). The microsomal aliquots were frozen by liquid nitrogen and stored at – 80 ^{o}C.

2.6.2. Protein concentration measurements

Protein content was determined using a modified Lowry Assay (Bio-Rad DC Protein Assay) following the manufacturer's protocol. Bovine serum albumin (BSA; Sigma) was used to generate a standard curve (0-10 μg) and all samples were analysed in duplicates.

Modified Lowry Protein Assay	Bio-Rad
Sample/Controls	5 μl
Alkaline Copper Reagent (A)	20 μl
Folin Reagent (B)	200 μl
Leave for 15 minutes at RT	
Measure absorbance at 650-750 nm	

2.6.3. SDS-polyacrylamide gel electrophoresis

Proteins were separated on the basis of their molecular weight by the denaturing sodium dodecyl sulphate polyacrylamide gel electrophoresis (SDS-PAGE) (Laemmli, 1970) using the Bio-Rad Mini-PROTEAN apparatus (Bio-Rad Laboratories, Ltd). Protein samples were solubilised in SDS-PAGE sample buffer (31.25 mM Tris (pH 6.8), 1 % [v/w] SDS, 12.5 % [v/v] glycerol, 2.5 % [v/v] 2-mercaptoethanol, 0.005 % [w/v] bromophenol blue) and incubated at 37 ^{o}C for 30 minutes. The samples were loaded on a 5-20 % SDS-polyacrylamide pre-cast Ready Gel® (Bio-Rad) and separated electrophoretically at 200 V in Tris-Glycine running buffer (25 mM Tris, 192 mM glycine, 0.1 % [w/v] SDS).

2.6.4. Coomassie blue staining

The gels were routinely stained with a Coomassie blue protein stain (0.25 % Coomassie Blue R-250) for 1-2 hours shaking gently until the gel is a uniform blue colour. The gel was destained O/N in destaining solution (5 % [v/v] MeOH, 7.5 % [v/v] Acetic Acid) until bands are visible and destaining complete.

2.6.5. Western Blotting

After separation by electrophoresis proteins were transferred to a nitrocellulose membrane using a semi-dry transfer apparatus (Biorad) as per manufacturer's instructions. The gel was first washed in purified deionised water, and then soaked in the transfer buffer (48 mM Tris, 192 mM glycine and 20 % [v/v] methanol, and 0.0375% [w/v] SDS) for 5 minutes. The membrane and 6 pieces of Whatman™ paper were cut to the size of the gel and soaked in the transfer buffer prior to use. To prepare the paper-membrane-gel-paper sandwich, 3 Whatman™ paper sheets placed over the bottom electrode (anode), overlaid by the membrane, the gel and 3 additional Whatman™ paper sheets. The transfer was carried out by applying 15 V for 1 hour.

After the transfer, the membrane was rinsed with SDW and stained for 5 minutes with Ponceau Red (2 % ponceau S in 30 % trichloroacetic acid and 30 % sulfosalicylic acid). The membrane was washed 3-5 times with SDW to remove the stain.

2.6.6. Immuno detection

The membrane was placed in blocking solution (either 1x TBST or 1x PBST with 5 % [w/v] non-fat milk powder) with gentle shaking for 1 hour at room temperature. The membrane was then incubated with the primary antibody (1:1000 – 1:10,000, see table 2) in TBST (α-AXR4, α-BPL1, α-FLAG) or PBST (α-HA, α-HIS) with 1 % or 0.1 % (α-HIS) (w/v) non-fat milk powder, shaking overnight at 4 ^{o}C. The membrane was washed with 1x TBST (or 1 x PBST) five times for 5 minutes and then incubated with an appropriate secondary HRP (horseradish peroxidase)-labelled antibody in blocking solution at 1:1000 – 1:10,000 dilution (see table 2), for 1 hour at room temperature. The membrane was then washed five times with TBST for five minutes.

Antibody	Dilution	Source
Anti-AXR4	1:10,000	Anti-Sheep
Anti-BPL1	1:10,000	Anti-Sheep
Anti-FLAG	1:2,000	Anti-Mouse
Anti-HA	1:1,000	Anti-Mouse
Anti-HIS	1:1,000	Anti-Mouse
Anti-Mouse HRP	1:1,000	
Anti-Sheep HRP	1:10,000	

Table 2: Antibody dilution for western blots.

The membrane was developed using the enhanced chemiluminescent detection system (Pierce), following the manufacturer's instructions. The blots were exposed using RX medical X-ray film (Fuji Photo Film Co) for 1-15 minutes or until a clear signal was detected.

2.6.7. Affinity purification and immunoprecipitation of tagged protein

For the co-immunoprecipitation experiments, the Pierce® Co-Immunoprecipitation (Co-IP) Kit (Thermo Scientific) was used according to manufacturer's instructions. Anti-AXR4, Anti-FLAG and Anti-BPL1 were used at 75, 40 and 61 µg/µl respectively, with 50 µl resin. 150 µl of sample in IP Lysis/wash buffer (0.025 M Tris, 0.15 M NaCl, 0.001 M EDTA, 1 % NP-40, 5 % glycerol; pH 7.4) was added to each column for each pull down experiment, and binding occurred overnight at 4 ^{o}C. Columns were washed 3 times with IP Lysis/wash buffer, and the columns were eluted four times to completely remove any bound proteins with Elution Buffer (pH 2.8, containing primary amine). Resin was then washed, regenerated and stored for further use of the columns following manufacturer's instructions.

2.6.8. Mini-Dialysis

For use with the Co-IP Kit the antibodies were dialysed to PBS buffer using the Slide-A-Lyzer® MINI dialysis Unit (Thermo Scientific) following manufacturer's instructions. 100 µl Anti-RANI (BPL1) (1.22 µg/µl), and 50 µl Anti-AXR4 (1.22 µg/µl) were dialysed.

2.6.9. Detergent solubilisation of AXR4

A selection of common detergents (see table 3) were investigated for their suitability for the extraction of AXR4 from plant microsomal membrane preparations. Solubilisation buffer (0.025 M Tris, 0.15 M NaCl, 0.001 M EDTA, 5 % glycerol; pH 7.4) was used and the plant microsomal membrane preparations and detergents were mixed to give a final reaction volume of 100 µl with the detergent at the concentration given in table 3. These were then incubated at 4 ^{o}C for 60 minutes with end over end mixing. Insoluble material was isolated by ultracentrifugation at 100,000 g (Optima™ Max Ultracentrifuge; Beckman Coulter) for 1 hour at 4 ^{o}C and resuspended in solubilisation buffer and 10 % SDS. Solubilisation was analysed by western blotting.

Detergent	Class	Concentration (w/v) tested	Fold CMC (mM)
NP-40	Non-ionic	1 %	0.29
Dodecyl-β-maltoside (DDM)	Non-ionic	2 %	6.7
CHAPS	Zwitterionic	0.1 %	4

Table 3: Detergents used for solubilisation of AXR4 in root microsomal membrane preparations.

2.7. BIOCHEMICAL ASSAYS

2.7.1. Gus staining

Seedlings were stained for GUS activity at different stages of development (3, 5, 7, 9, 12, and 14 days) for 3 h, 6 h and 24 h; then cleared using two methods. The stained seedlings were then mounted in 50 % glycerol and staining observed using Leica microscope.

Gus Staining Protocol	
4.25 ml	50 mM phosphate buffer pH 7.2
0.25 ml	33 mg/ml K3Fe(CN)6 in PO4 buffer
0.25 ml	44 mg/ml K4Fe(CN)6 in PO4 buffer
0.25 ml	10 mg/ml X-Gluc in Dimethylformamide
5 µl	Triton X-100

Root clearing protocol 1	
Acidified methanol (Conc. HCl [4 % v/v], and MeOH [20 % v/v])	15 minutes at 50 ^{o}C
Neutralisation solution (NaOH [6 % w/v] in 60 % EtOH	15 minutes at RT
Ethanol series (40, 20 and 10 %)	Rehydrate for 5-10 minutes at each series

Root clearing protocol 2	
Chloral hydrate clearing solution (6:1:2 Chloral hydrate: glycerol: water)	24 hours at room temperature

2.7.2. Starch staining

Whole seedlings were cleared in chloral hydrate overnight (see 2.8.2) and then placed on a slide. A few drops of lugol's iodine were added and the root tip was visualised straight away under the microscope and pictures taken until the starch staining was complete.

2.8. IMAGE ANALYSIS

Seedlings were analysed for root length and phenotype. Root length was measured using ImageJ (ImageJ 1.40g) and its plugin NeuronJ (Meijering et al, 2004).

2.8.1. Gravitropic assay

Four day old seedlings grown vertically were turned 90 degrees and images of the root were taken every twenty minutes for 12 hours overnight (in dark) to observe the seedlings response to gravity. Gravitropic response was analysed using RootTrace (RootTrace V2; Naeem et al, 2011).

2.8.2. Confocal scanning microscopy

The Leica SP2 confocal laser scanning microscope (Leica Microsystems) was used to look at fluorescence within plant cells. Cell walls were stained with propidium iodide (10 μg/ml) (Sigma). Scanning settings used for one experiment were optimised to obtain the best signal-to-noise ratio, and then kept unchanged throughout the experiment. The Argon Laser was used at 488 nM and 543 nM to view fluorescence. Images were processed using the Leica SP2 Image Analysis software and figures created using Adobe Photoshop (version 6.0; Adobe Systems) and Microsoft PowerPoint 2007 (Microsoft Corporation).

2.8.3. Whole mount immunolocalization in Arabidopsis roots

3 day old seedlings were fixed and immunolocalised using various primary and secondary antibodies, and visualised using confocal microscopy. The seedlings were fixed in 4 % paraformaldehyde in MTSB (50 mM PIPES, 5 mM EGTA, 5 mM $MgSO_4$ [pH 7] adjusted with KOH). Samples were washed with MTSB/0.1 % Triton (5 x 10 min) and with deionised water (5 x 10 min). Cell walls were digested with 2 % driselase in MTSB for 30-45 min, and samples were washed with MTSB/0.1 % Triton (5 x 10 min). Seedlings were then pre-incubated in 2 % BSA/MTSB (1 hr, 37 ^{o}C). Finally, the samples were washed with MTSB/0.1 % Triton (5 x 10 min) and deionised water (5 x 10 min) and transferred into Slowfade Antifade mounting medium.

Specific primary antibodies were used at a dilution of 1:200, including anti-AXR4, anti-BPL1, anti-LAX2, anti-HA (Roche), and anti-GFP. Oregon Green or Alexa-Fluor coupled secondary anti-Rat, anti-Mouse or anti-Rabbit antibodies (Invitrogen) were used at a dilution of 1:200. Background staining was performed with Propidium Iodide (Sigma) when appropriate. Seedlings were then viewed with LEICA SP2 laser scanning confocal microscope (Leica Mircosystem, Bannockburn, IL).

2.9. GENERAL CHEMICALS AND REAGENTS

All chemicals used were of analytical grade and were supplied by the following companies; Alpha Laboratory Supply (Hampshire, U.K), Amersham Biosciences Inc (Little Chalfont, U.K), Bioline Ltd (London, U.K), Biorad Laboratories Ltd (Hemel Hempstead, U.K), Fermentas Life Science (London, U.K), Fisher Scientific (Loughborough, U.K), Fuji Photofilm UK Ltd (London, U.K), Invitrogen Ltd (Paisley, U.K), Macherey-Nagal (Hoerdt, France), New England Biolabs Ltd (Hitchin, U.K), Promega UK Ltd (Hampshire, U.K), Roche Diagnostics (West Sussex, U.K) Sarstedt (Leicester, UK), Scientific Laboratory Supply (Nottingham, U.K), Sigma-Aldrich Co. Ltd (Dorset, UK), Stratagene Ltd (Cambridge, U.K), and Thermo Fisher Scientific (Loughborough, U.K).

CHAPTER 3
IDENITYING NEW ER ACCESSORY PROTEINS

3. IDENTIFYING NEW ER ACCESSORY PROTEINS

3.1. INTRODUCTION

Approximately one third of the eukaryotic proteome travels through the endoplasmic reticulum on route to its final destination. Trafficking destinations include specific organelles such as nucleus, chloroplast, mitochondria; as well as components of the endomembrane system such as the Golgi, vacuoles, plasma membrane; and extracellular destination. Protein sorting is therefore extremely important to allow proteins to reach the correct final destination, as mentioned earlier sorting occurs at the ER, Golgi, TGN, endosomes and vacuole. Protein sorting within the ER accommodates an extraordinary variety of cargo proteins with different structures, functions and ultimate destinations. A lot of these proteins are sorted by signalling motifs within the proteins themselves; however a lot of proteins have no recognisable sorting motif. In these cases the proteins are dependent on specific accessory proteins (ER accessory proteins) for the exit from the ER. As discussed in chapter 1.4. accessory proteins can be divided into three groups; outfitters, escorts and transport receptors (Hermann et al, 1999). A large number and varied mechanisms of ER accessory proteins have been discovered in mammalian and yeast systems in the last ten years, and it is likely more will be discovered as we discover more about trafficking within the cell. Despite this ER accessory proteins are still novel in plants, with only putative ER accessory proteins AXR4, PHF1 and NAR2.1 discovered so far. This suggests that a similar mechanism exists in plants as well, and it is likely to be as numerous and varied as the other systems, with other polytopic membrane proteins requiring their own cognate ER accessory protein to facilitate folding and/or transport.

Despite having similar functions, almost all of the ER accessory proteins discovered so far share no sequence homology to each other and seem to represent novel proteins (Cooray et al, 2009). The only common feature among all these proteins is their location to the ER and their association with the ER membrane. As there is no common motif or domain, effort was focused on those proteins located within the ER with novel or unknown function.

3.2. BIOINFORMATICS

Systematic analysis of potential ER accessory proteins was done to determine ER localisation of proteins with unknown function, to do this we made use of a relatively new proteomic study of the secretory system by Dunkley et al (2006), used to determine the localisation of new proteins. This study assigned proteins to various sub-cellular compartments using a proteomics based approach LOPIT (localisation of organelle proteins by isotope tagging) (Dunkley et al, 2006). The method matches the distribution of test proteins with that of marker proteins in a density gradient to determine sub-cellular localisation (figure 8). 182 proteins were localised to the ER using this study, of these 40 were expressed proteins with unknown function (table 4)

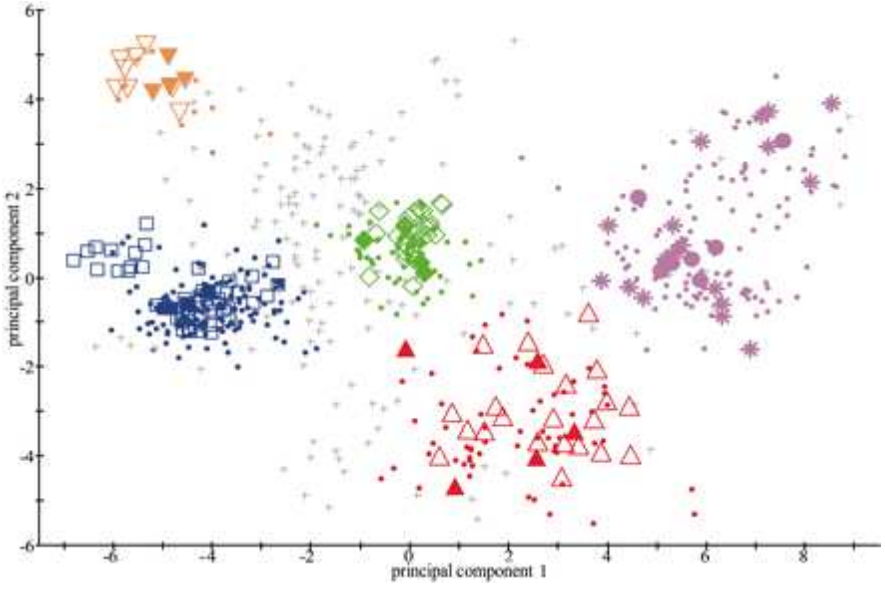

Figure 8: LOPIT clustering of proteins

PCA analysis: Clustering due to their density gradients distributions and therefore localisations. Filled shapes indicate known organelle markers allowing identification of the clusters to a certain organelle and predication of protein localisation of previously unidentified localisation (small circles). Unfilled shapes (or stars) indicate proteins with predicted localisations which were confirmed by this method. Inverted triangles = vacuolar membrane; squares = ER; diamonds = PM; circles (stars) = mitochondria/plastids; triangles = Golgi apparatus. Figure from Dunkley et al (2006).

Most known ER accessory proteins do not share any homology or motifs, and seem to represent novel proteins. Therefore, the first criteria for deciding which proteins to study were based on the fact that they have a novel or unknown function. Of the 182 proteins localised in Dr. Katherine Lilley's LOPIT database to the ER, 40 of these have unknown or novel function. The genes were prioritised based on expression in the root and whether these genes were part of a gene family. This criterion included 13 proteins encoded by a single copy gene in Arabidopsis showing high expression within the root, 5 genes that belonged to gene families where only one has significant expression in the roots, and 2 unique proteins but with low expression in the roots (table 5). A bioinformatics approach was used on the shortlisted genes to identify further information about each target, such as location of T-DNA inserts and Blast to analyse potential function of the genes (The programs Bioinformatic Harvester III (http://harvester.fzk.de/harvester) and aramemnon (http://aramemnon.botanik.uni-koeln.de/) were used).

Organelle	Number of proteins classified by the LOPIT database
Endoplasmic reticulum	182
Golgi	89
Mitochondria (Plastid)	140
Plasma membrane	92
Vacuole	24
Not Classified	162

Table 4: Summary of localisation results from Dunkley et al (2006).

Gene	T-DNA type and number	Putative annotation based on BLAST	Domain
At1g11905	Salk: N532583	BAP31-like	Protein of unknown function
At1g65270	Sail: N822782 N819022	-	Protein of unknown function
At1g70770	Salk: N665550 N66876	Transmembrane protein 214	DUF2359
At1g71780	Salk: N614289	-	Protein of unknown function
At2g16760	Salk: N663810 N513066	Six-bladed beta-propeller TolB-like, Gluconolactonase	
At2g36290	Salk: N525841		Alpha, beta hydrolase fold-1
At3g07190	Sail: N803596 Salk: N661700	BAP31-like	Protein of unknown function
At3g20450	Salk: N633340	BAP31-like	Protein of unknown function
At3g27325	Salk: N527201 N527086	GPI inositol-deacylase	PGAP1-like; Esterase lipase
At3g44330	Salk: N593742	Protein processing - putative Nicastrin-like component of gamma secretase complex	Nicalin, EF-HAND 1, Nicastrin
At3g62360	Salk N620858	NODAL modulator	Carbohydrate-binding-like fold; Collagen-binding surface protein Cna-like, B region
At4g12590	Sail: N837011	Pob	Protein of unknown function DUF850 domain
At4g16170	Sail: N829287	-	Protein of unknown function
At4g27500	Salk: N540701	PPI1 (proton pump interactor)	

Gene	T-DNA type and number	Putative annotation based on BLAST	Domain
At4g29520	Salk N665520		Saposin B
At4g32130	Salk: N663464 N637042	UPF0480 protein C15orf24 homolog precursor, TonB-dependent siderophore receptor	Carbohydrate-binding-like fold domain
At5g20520	Salk: N602859 N587030 N558588 N587022	WAV2, BEM46 family protein	Alpha/beta hydrolase fold-1
At5g42570	Sail: N822482 Salk: N642314 N597360	B-cell receptor-associated protein 31	B-cell receptor-associated 31-like
At5g48860	Salk: N600808 N600809 N660471		Protein of unknown function
At5g49945	Salk: N662942	Coiled-coil domain containing 47	Protein of unknown function DUF1682

Table 5: List of potential ER accessory protein targets

Table listing the gene, T-DNA labels, blast results and domain information. The Blast and domain results were obtained using Bioinformatic Harvester IV (beta) (http://harvester.fzk.de/harvester/), which uses the programs BLINK and NCBI Entrez Gene respectively.

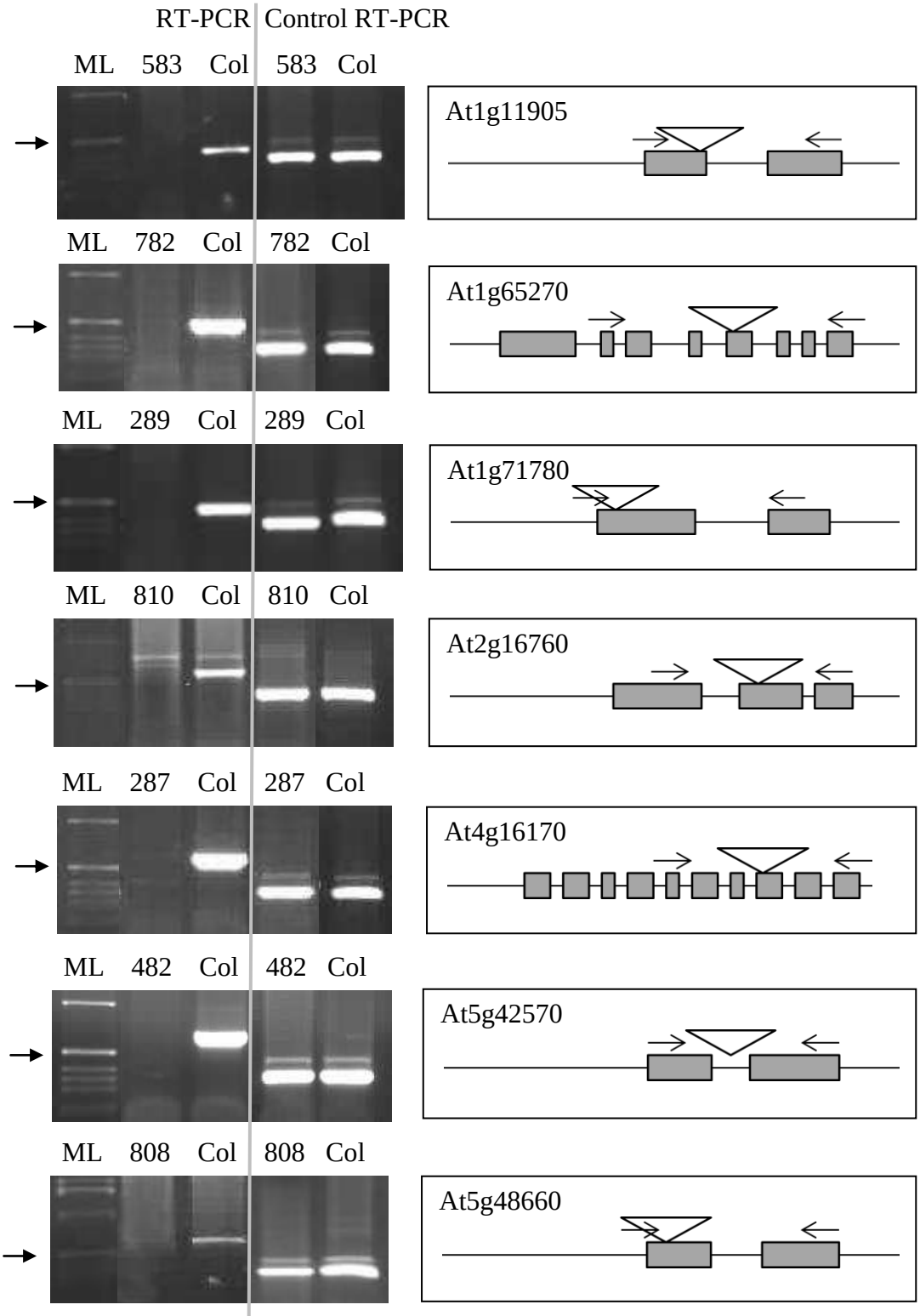

Figure 9: RT-PCR results for homozygous T-DNA Kos

Left panel shows gene specific RT-PCR (for primers see appendix 9.2). Control RT-PCR using primers 5' AUX1/3'AUX1. Right diagrams represents gene structures

with introns (line), exons (grey boxes), T-DNA (triangle) and primer positions (arrows). ML = molecular ladder. Black arrow = 500 bp.

To probe the role of these putative ER proteins, a genetic approach was used. Insertional T-DNA knock out (KO) lines were identified, and a PCR based genotyping approach was used to identify homozygous lines in the T3 generation. Using this approach of the 20 targets, 14 homozygous T-DNA insert mutants have been identified. Of these 14 homozygous knock outs (KOs) only 7 have complete loss of expression based on RT-PCR analysis (see figure 9). For those T-DNA lines where mRNA is still transcribed, in most cases it may be due to the fact that the insert is within an intron. For one line, the T-DNA insert is within the 5' UTR and it appears that the T-DNA itself is driving the expression of this gene, as a 35S promoter is less than 2 KB upstream of the right border.

3.4. PHENOTYPIC CHARACTERISATION OF TARGETS

Preliminary investigations of the knocks outs revealed no visible differences in phenotype. This may reflect non-selective conditions, therefore to reveal differences in phenotype more detailed and targeted screens were designed. Potential targets of ER accessory proteins include membrane proteins. Approximately 1000 genes (5 % of the Arabidopsis genome) encode membrane transport proteins (Mäser et al, 2001). Plants have a complex and highly regulated nutrient uptake pathway, with enormous variety in controlling nutrient uptake and distribution through membrane transporters. Due to the complexity of nutrient uptake within the plant, smart screens were designed. These screens take advantage of different levels of nutrients and minerals, at both minimal and toxic levels to produce growth inhibiting conditions (see appendix 9.4 for the solutions and treatments used). Under these conditions potential mislocalization of transporter proteins by the ER accessory proteins, may give a phenotype. These growth inhibiting conditions for nutrient deficiency or toxicity were used to analyse the KOs response to different nutrients.

3.4.1. Nutrient deficient screen

For a rapid analysis of the homozygous T-DNA KOs response to different nutrient conditions, a large screen was designed using many different nutrient deficient concentrations. By looking at comparison of root growth between different media compositions it allowed identification of lines which may show a phenotype under these screens which can then be focused on for more in depth study. Each line was compared to Wt (Col) on the control plate (Main Solution - 100 %) allowing percentage growth differences to be analysed. As the nutrient levels within the medium needed to be changed, each nutrient needed to be added separately to make up the solution. A stock solution was made up for each component and added together to give a final concentration found in the control nutrient solution (see box). Each different nutrient treatment was based on this but changed so that the nutrient of interest is in deficiency (see appendix 9 for all the different treatment concentrations).

Control nutrient solution	KH_2PO_4 24.9 mM, KOH 50.1 mM, $MgSO_4.7H_2O$ 75.0 mM, $CaCl_2.2H_2O$ 2.4 mM, FeNaEDTA 8.7 mM, $Ca(NO_3)_2.4H_2O$ 400 mM, H_3BO_3 0.31 mM, $MnSO_4.4H_2O$ 0.99 mM, $ZnSO_4.7H_2O$ 0.10 mM, $CuSO_4.5H_2O$ 0.32 mM, $Na_2MoO_4.2H_2O$ 0.41 mg/L

Screen	**Concentration**
Boron	3 μM
Nitrogen	0 μM
	50 μM
Phosphorus	0 μM (100 μM Fe)
	10 μM (100 μM Fe)
	50 μM (100 μM Fe)
Sulfate	0 μM
	100 μM

Table 6: Essential nutrient deficiency screens and concentrations used.

The different nutrient treatments, based on nutrient deficiency, should allow small differences in growth to become more apparent (for a list of the different nutrient deficient medium used for screens see table 6). For example under normal growth conditions, the phenotype may be masked due to bulk flow of the transporter or due to the expression and correct localisation of another transporter of that nutrient. However in a nutrient deficient situation this will put more pressure on the plant and small differences in nutrient availability within the plant (due to incorrect localisation of a membrane transport) may become apparent giving a deficiency phenotype. In this case the KO would show deficiency symptoms earlier or more severely than wild type (Wt), in most cases this would be observed by reduced root growth. Another phenotype which could be apparent is a weaker deficiency phenotype, which could be due to a mislocalization of a xylem or vacuole transporter; in this case more of the nutrient would be available to the plant, delaying the deficiency response.

3.4.1.1. Boron

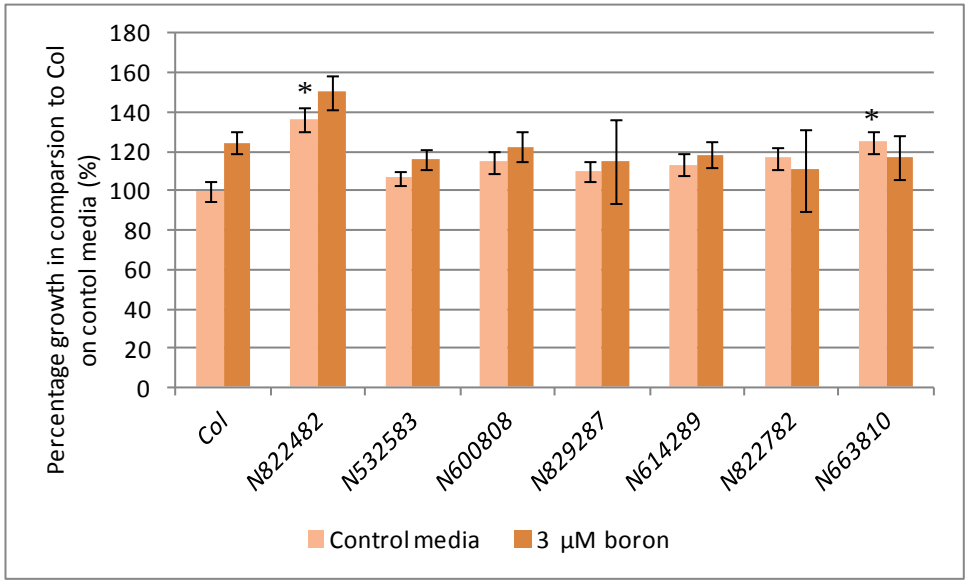

Figure 10: Boron deficiency screen

Percentage root length in sulphur screens of KO lines in comparison to Col on control media (100 %). Error bar represents standard error. Statistical difference represented by asterisks (Student's T-Test; P > 0.01), 7 day old seedlings, n = 15.

Boron (B) is an essential element in plants, and its role was first described more than 80 years ago (Takano et al, 2008). B has been shown to have an essential role in the structure and function of plant cell walls, having a role in cross-linked pectic polysaccharides (O'Neill et al, 2004), as well as a suggested structural role in membranes (Goldbach & Wimmer, 2007). B deficiency is a major problem in agriculture, and deficiency symptoms include cessation of root elongation, reduced leaf expansion, reduced fertility, all of which are due to reduced cell expansion (Dell & Huang, 1997). Due to these reasons B was chosen as a nutrient to study. Very low levels of boron are required within the plant, with wild type plants growing on as little as 3 μM. Lower (0.3 μM) concentrations result in reduction in root growth (Noguchi et al, 1997). It was reasoned that mutations that affect boron uptake may start to show these deficiency symptoms at concentrations where wild type seedlings are still growing normally. Based on these studies on B deficiency 3 μM was chosen as the limiting level as it should highlight those lines that are unable to transport boron as efficiently, while the other lines should show normal growth (Noguchi et al, 1997; Takano et al, 2006). From figure 10 it is evident that there is no obvious mutant that shows a response to B deficiency, with no statistical differences in growth.

3.4.1.2. Nitrogen

Nitrogen (N) is one of the major macronutrients for all living organisms, as it is incorporated into amino acids and nucleic acids, making it essential for growth. Nitrogen is a major limiting factor in agriculture, as N deficiency affects N and C metabolism, and the abundance of amino acids and proteins (Scheible et al, 2004). Studies have also shown the development of the root system is enhanced in NO_3^- depletion, possibly for foraging to discover new N patches within the soil (Drew & Saker, 1975). The study of nitrate transporters is therefore very interesting and while one potential ER accessory protein NAR2.1 has already been discovered, there are an extremely large number of nitrate transporters that are involved at different N status and in different organs (Dechorgnat et al, 2011; Wirth et al, 2007). Due to this large and varied number of nitrate transporters there is potential of more ER accessory proteins being involved in their regulation.

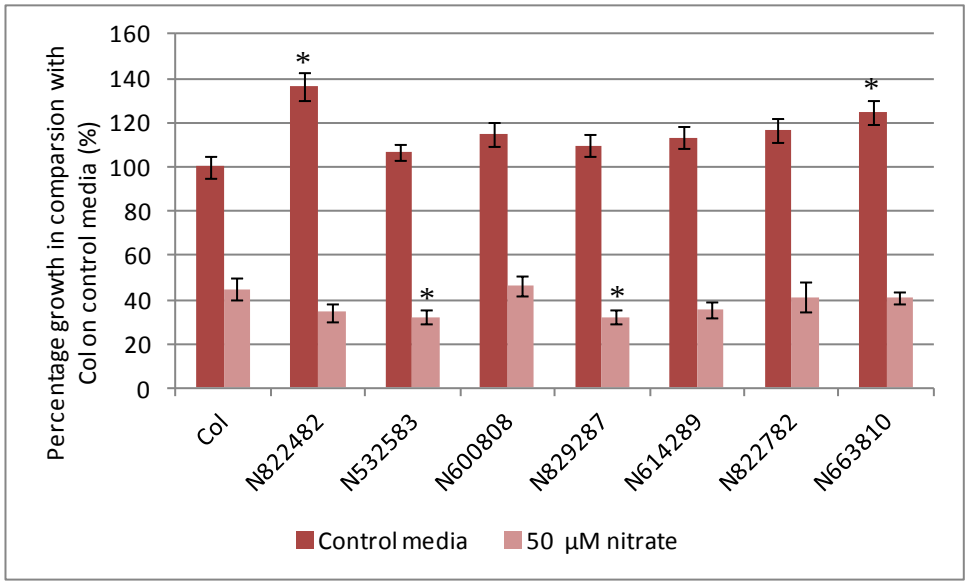

Figure 11: Nitrate deficiency screen

Percentage root length in nitrate screens in comparison to Col on control media (100 %). Error bar represents standard error. Statistical difference represented by asterisks (Student's T-Test; P > 0.05), 7 day old seedlings, n = 15.

Based on previous studies 50 µM nitrate were chosen to highlight any nitrate uptake deficiencies (Gaude et al, 2007). From figure 11 two of the KOs N532583 (At1g11905) and N829287 (At4g16170) showed significant decreased growth under the highly limiting 50 µM screens. Repeated experiment showed that N829287 differences in growth were insignificant, while N532583 was shown to be significant and is discussed in the next chapter.

3.4.1.3. Phosphorous

Phosphate (Pi) is an essential macronutrient required in plants, for metabolic processes such as energy transfer, signal transduction, photosynthesis, respiration, as well as the biosynthesis of macromolecules (Plaxton & Carswell, 1999). In Pi deficient soil a number of root modifications take place such as enhanced root growth, altered root architecture and increased production and elongation of root hairs, all aimed at enhancing Pi uptake (Bates & Lynch, 1996). Similar to nitrogen transport, an ER accessory protein has been discovered for one of the phosphate

transporters PHT1, however similarly there are a large number of phosphate transporters which may require their own ER accessory protein (González et al, 2005; Poirier & Bucher, 2002).

Based on studies in Pi deficient media, levels of 0-50 µM were chosen (Shin et al, 2004). While nutrient deficiency normally results in decreased root growth, in short term conditions, Pi deficiency causes increased growth (figure 12) which may be due to the plants foraging response to lack of Pi. Those KOs which have a defect in phosphate transport, you would expect heightened growth at 50 µM concentration, as these lines would have less Pi available. And then a sharp decrease in growth at 0 µM where they are no longer receiving enough Pi to function, and the concentration would become detrimental to growth.

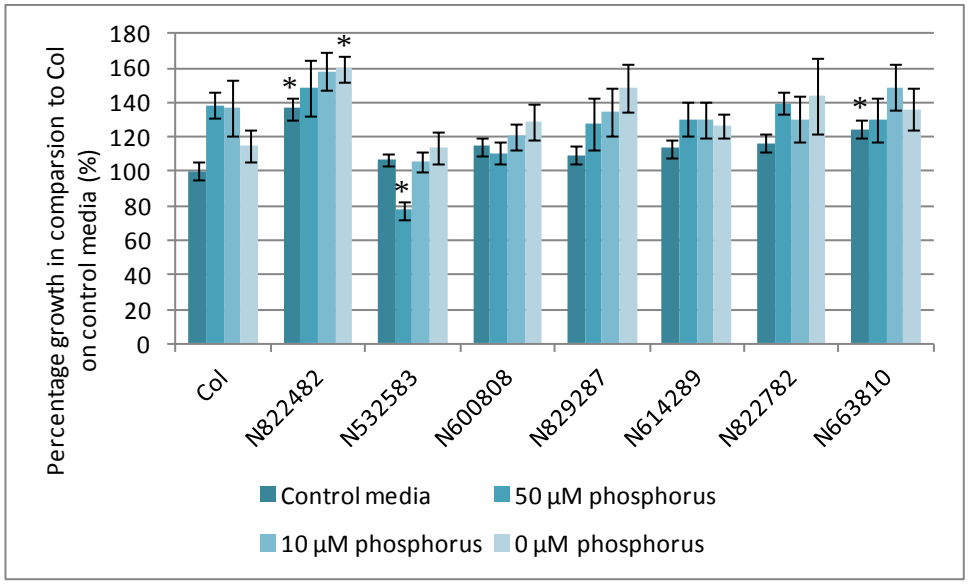

Figure 12: Phosphorous deficiency screen

Percentage root length in phosphorous screens in comparison to Col on control media (100 %). Error bar represents standard error. Statistical difference represented by asterisks (Student's T-Test; P > 0.01), 7 day old seedlings, n = 15.

While no lines are showing the same increase in growth in comparison to Wt (Col), all have increased growth under phosphorous limiting conditions. With N822482 (At5g42570) showing increased growth compared to Col in the most limiting phosphorous concentration (0 µM) which is a significant difference. This screen was

repeated, however the difference in growth in 0 µM phosphorous were no longer statistically different to Col.

3.4.1.4. Sulphate

Sulphate (S) is an essential macronutrient required for plant growth, with a wide range of compounds containing sulphur, it is utilised for the synthesis of amino acids, proteins, lipids, coenzymes, and other secondary metabolites (Saito, 2000). Deficiency symptoms are similar to those found in N deficiency, especially in field based studies (Zhao et al, 1996). From previous studies in S deficiency two sulphate concentrations were chosen, 0 µM, and 100 µM (Shibagaki et al, 2002). From figure 13 a few lines show a decreased but not significant growth in comparison to Wt (Col). N663810 (At2g16170) shows statistically increased growth in 0 µM sulphur, however this does not correspond to its growth at 100 µM which is reduced compared to control media, further screens show that there is no significant difference in growth between Col and this KO.

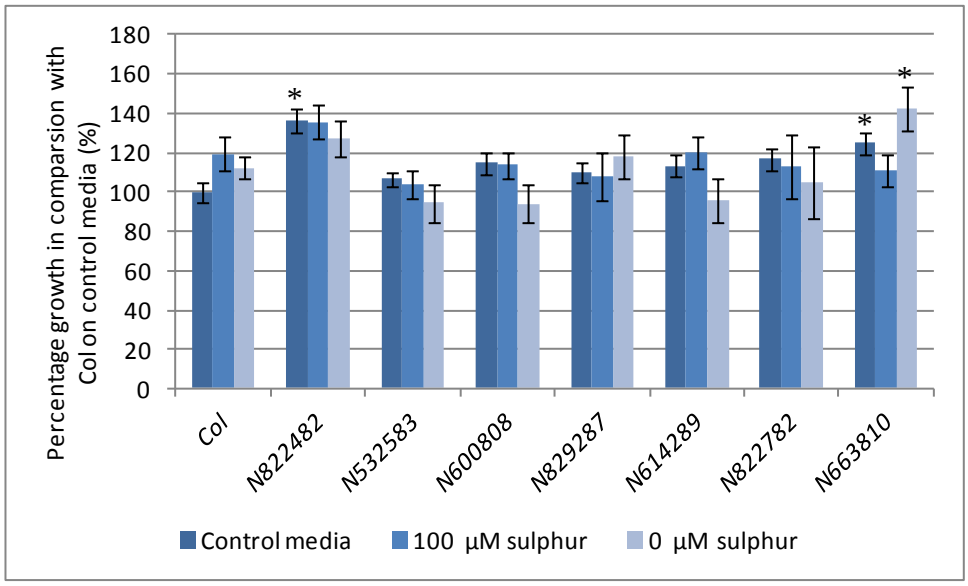

Figure 13: Sulphate deficiency screen

Percentage root length in sulphate screens in comparison to Col on control media (100 %). Error bar represents standard error. Statistical difference represented by asterisks (Student's T-Test; P > 0.05), 7 day old seedlings, n = 15.

3.4.2. Toxic screen

Besides nutrient deficiency screens, toxicity screens were also designed with the aim to identify potential defects in uptake activity (table 7). Many toxic chemicals are taken up by essential nutrient transporters, for example cadmium is transported by iron and zinc transporters, while sodium is taken up by potassium transporters. A lot of nutrients that are essential for plant growth are also toxic to the plant at higher concentrations; therefore these can also be used to look at transporter activity. Reduction in root influx transporter efficiency due to localisation defects would cause a heightened resistance compared to Wt to the specific element(s) that it can import. On the other hand localisation defects in a vacuole or xylem loading transporter would prevent the element from being sequestrated safely away where it cannot damage the plant, allowing it to build up to toxic levels quickly and causing increased sensitivity to toxic levels of the element.

Screen	Concentrations
Boron	150 μM
Copper	10 μM
	20 μM
	100 μM
Sodium	50 mM
	100 mM
Zinc	250 μM
	500 μM
	1000 μM

Table 7: Toxic mineral screen and concentration used.

3.4.2.1. Boron

As mentioned in the earlier chapter boron (B) is an essential element involved in the structure and function of cell walls (O'Neill et al, 2004). The range of B concentration between deficiency and toxicity is very narrow; however most studies

have been based on deficiency studies within Arabidopsis, with those looking at high levels of B only using 150 µM (Nable et al, 1997; Noguchi et al, 1997; Pang et al, 2010; Takano et al, 2006). This concentration was therefore taken as a starter concentration to look at B toxicity within Arabidopsis thaliana.

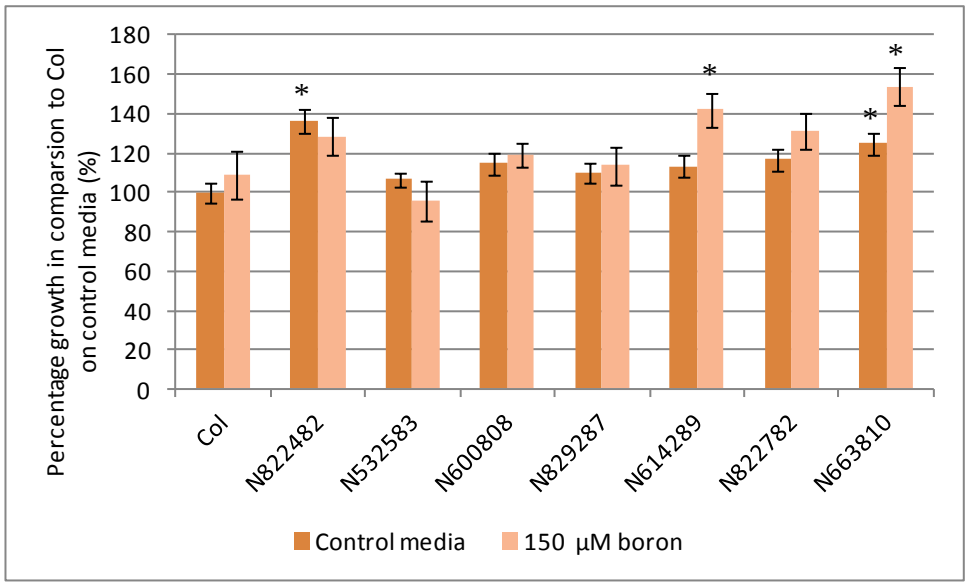

Figure 14: Boron toxicity screen

Percentage root length in boron screens in comparison to Col on control media (100 %). Error bar represents standard error. Statistical difference represented by asterisks (Student's T-Test; $P > 0.05$), 7 day old seedlings, n = 15.

From figure 14 and 15 we can see that two lines N614289 (At1g71780) and N663810 (At2g16170) have increased growth to higher levels of B in comparison to wild type (Wt). However under these conditions the high levels of B are not causing any toxicity symptoms in Wt, therefore this screen was repeated with higher levels of B to allow the phenotype to be analysed more accurately.

Higher concentrations (up to 2000 µM) were used, which gave a 30 % reduction in root growth in Wt. These higher concentrations gave opposite phenotypes, with both lines, N663810 and N614289, showing statistically heightened sensitivity to B in comparison to Wt (figure 16) at 500 µM. B toxicity is known to cause reduced root cell division leading to reduced growth of roots (Nable et al, 1990).

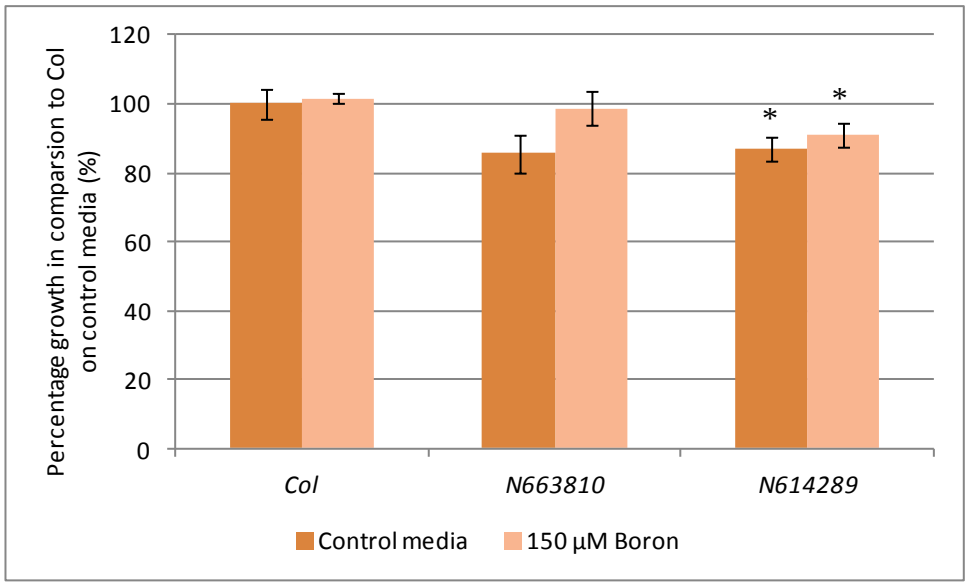

Figure 15: Boron toxicity screen

Percentage root length in boron screens in comparison to Col on control media (100 %). Error bar represents standard error. Statistical difference represented by asterisks (Student's T-Test; P > 0.05), 7 day old seedlings, n = 10.

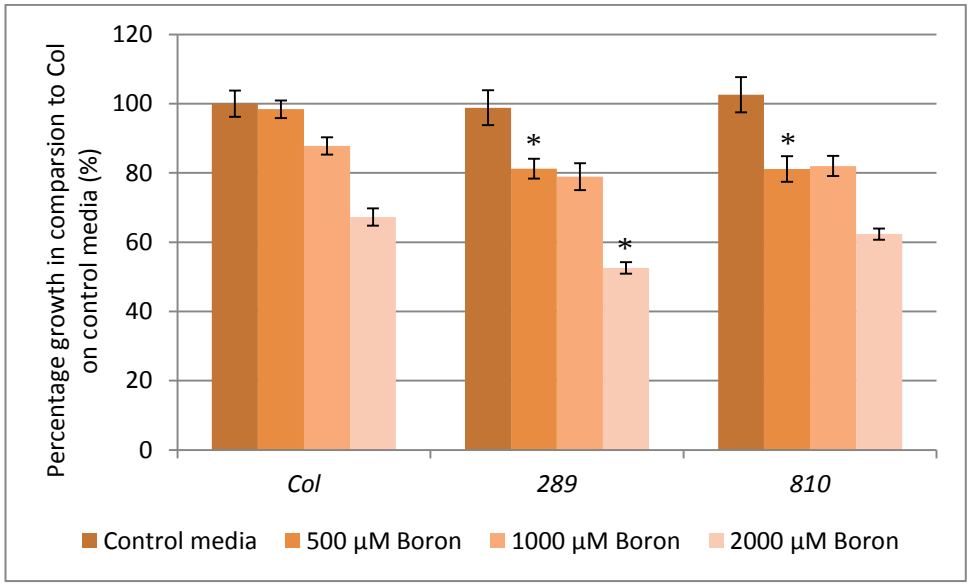

Figure 16: Boron toxicity screen

Percentage root length in boron screens in comparison to Col on control media (100 %). Error bar represents standard error. Statistical difference represented by asterisks (Student's T-Test; P > 0.01), 7 day old seedlings, n = 10.

3.4.2.2. Copper

Copper (Cu) is an essential trace element, acting as a redox-active transition metal playing critical roles in diverse reduction and oxidation reactions, such as respiration, photosynthesis hormone signalling, and oxidation stress responses (Marschner, 1995; Raven et al, 1999). Despite this importance, free Cu ions can cause toxicity, and previous studies have shown the concentrations as low as 20 μM can cause toxicity in Arabidopsis (Murphy & Taiz, 1995). Based on this and other studies, 3 concentrations were chosen (10, 20 and 50 μM) to look at copper toxicity and see if any of the lines show increased resistance to toxic levels (Kampfenkel et al, 1995). From figure 17, no lines showed increased resistance to toxic levels of Cu, however two lines (N532583 and N829287) gave increased sensitivity compared to Wt (Col) at the highest concentration (50 μM). It is likely that the increased sensitivity observed in N532583 is caused by the already reduced growth on the control media compared to Col. When N532583 is compared to itself on control media (100 %) the reduction at 50 μM Cu is no longer significant.

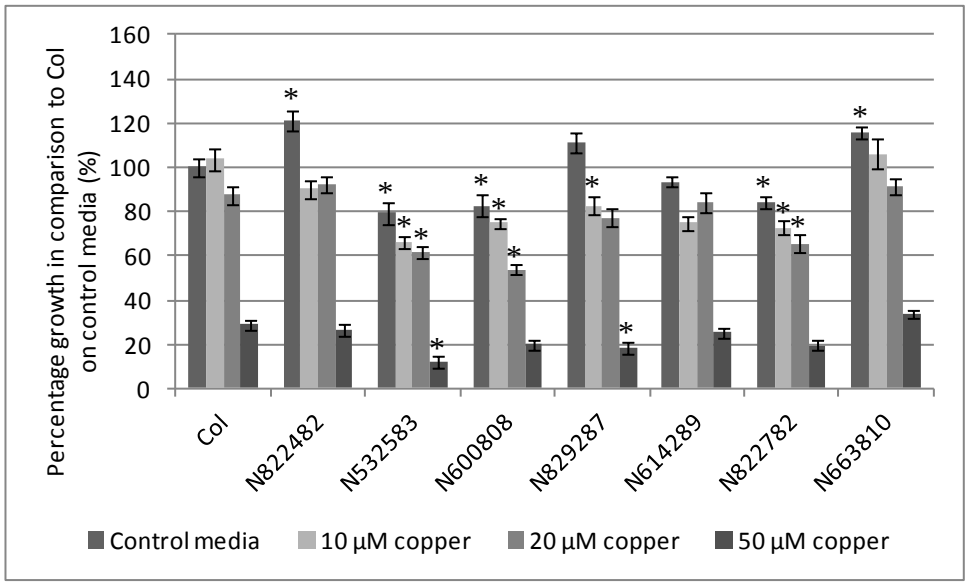

Figure 17: Copper toxicity screen

Percentage root length in copper screens in comparison to Col on control media (100 %). Error bar represents standard error. Statistical difference represented by asterisks (Student's T-Test; P > 0.01), 7 day old seedlings, n = 15.

3.4.2.3. Sodium

While sodium (Na) appears non essential for plant growth, there are a number of cation transporters which can transport Na as well as other cations such as K (Hall et al, 2006). Na is toxic to most plants at high millimolar concentration, and part of this toxicity is due to the competition of Na+ and K+ within the plant (Flowers, 1999). From previous studies a concentration of 50 mM and 100 mM were chosen to look at sodium toxicity within Arabidopsis (Lee et al, 2004; Mäser et al, 2002). Figure 18 shows that the KO N614289 (At1g71780) had a slight increase in resistance to sodium but only at the lowest sodium concentration (50 mM), further screens showed that this difference was not significant. While N532583 (At1g11905) and N600808 (At5g48860) had an increased sensitivity at all concentrations, however analysis taking into account the reduced growth on the control media showed difference was not significant.

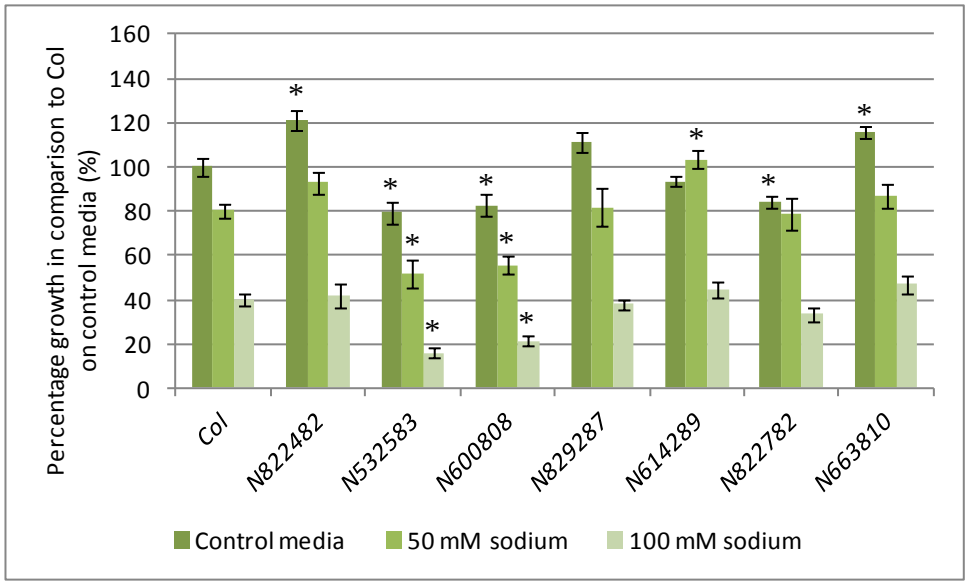

Figure 18: Sodium toxicity screen

Percentage root length in sodium screens in comparison to Col on control media (100 %). Error bar represents standard error. Statistical difference represented by asterisks (Student's T-Test; P > 0.01), 7 day old seedlings, n = 15.

3.4.2.4. Zinc

Zinc (Zn) is a micronutrient required by plants, and plays an important role in enzymes, protein-protein interactions, and transcriptional and post-transcriptional processes (Broadley et al 2007; Marschner, 1995). Zn can cause toxicity at elevated concentrations, leading to impaired growth and chlorosis (Schutzendubel and Polle, 2002). From previous Zn toxicity studies three concentrations were chosen (250, 500 and 1000 µM) to look for increased resistance to the presence of zinc (Kobae et al, 2004). Figure 19 shows that a few of the mutants have increased sensitivity to high levels of zinc with N829287 and N614289 displaying a statistically significant difference from Wt (Col) at 100 µM Zinc.

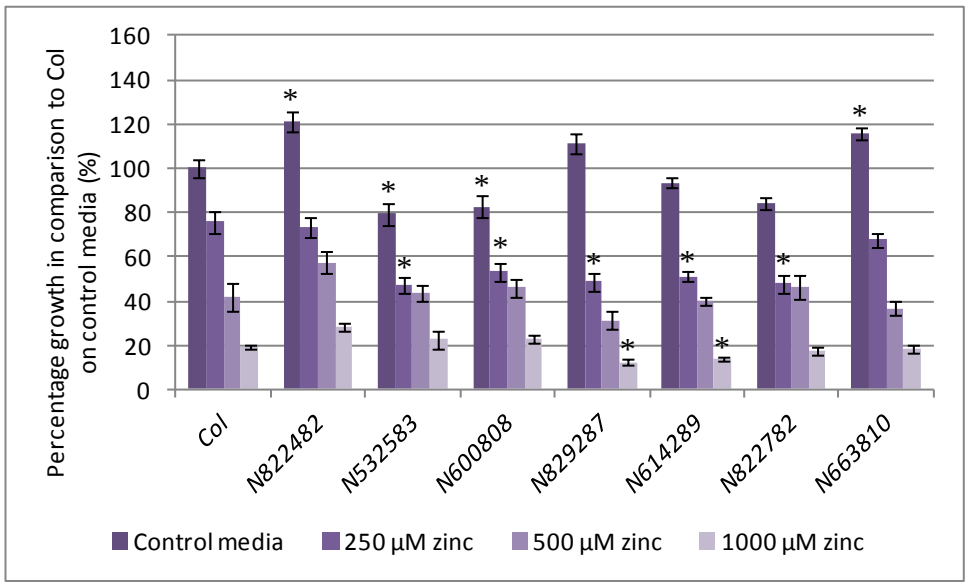

Figure 19: Zinc toxicity screen

Percentage root length in zinc screens in comparison to Col on control media (100 %). Error bar represents standard error. Statistical difference represented by asterisks (Student's T-Test; P > 0.01), 7 day old seedlings, n = 15.

3.5. ICP-MS

As well as the smart screen an inductively coupled plasma mass spectrometry (ICP-MS) analysis was done using plants grown on both nutrient rich (control media) and nutrient poor soil (minimal media). Nutrient poor soil was made up lacking the

addition of major macro nutrients (N, P, K, S) (In 55 litres: 41 litres of sphagnum moss peat, 14 litres of coarse sand, 124 g ground lime stone, 124 g magnesium limestone, 22 g fritted trace elements), this was then watered with only with water for the next two months. The nutrient rich soil was watered twice a week with a nutrient rich solution (control nutrient solution), allowing a difference in nutrients available in the two different conditions.

ICP-MS allows quantitative determination of trace metals in biological systems. It is highly sensitive and allows detection of a wide range of metals and several non-metals such as sulphur and phosphorus (Szpunar, 2005). ICP-MS may allow us to detect small differences in mineral composition which may not be very prominent in the phenotype.

Control nutrient solution	KH_2PO_4 24.9 mM, KOH 50.1 mM, $MgSO_4.7H_2O$ 75.0 mM, $CaCl_2.2H_2O$ 2.4 mM, FeNaEDTA 8.7 mM, $Ca(NO_3)_2.4H_2O$ 400 mM, H_3BO_3 0.31 mM, $MnSO_4.4H_2O$ 0.99 mM, $ZnSO_4.7H_2O$ 0.10 mM, $CuSO_4.5H_2O$ 0.32 mM, $Na_2MoO_4.2H_2O$ 0.41 mg/L

From the ICP-MS analysis there are a number of lines of interest such as N614289 (At1g71780), which has shown a phenotype in more than one screen. This line shows almost wild type nutrient levels in the nutrient rich media (B); however its nutrient levels are constantly 80 % that of Col (A), however this is not significantly different. It is possible that it has a defect in nutrient uptake or storage under nutrient limiting conditions for all nutrients. Therefore this gene may play a more extensive role than as an ER accessory protein for a single transporter. Other lines of interest are N829287 (At4g16170) which showed a significant increased Cu uptake in the minimal media compared to not only Wt (Col) on minimal media but compared to the control media. And N663810 which shows significantly decreased uptake of Mg and Ca in the minimal media compared to Col.

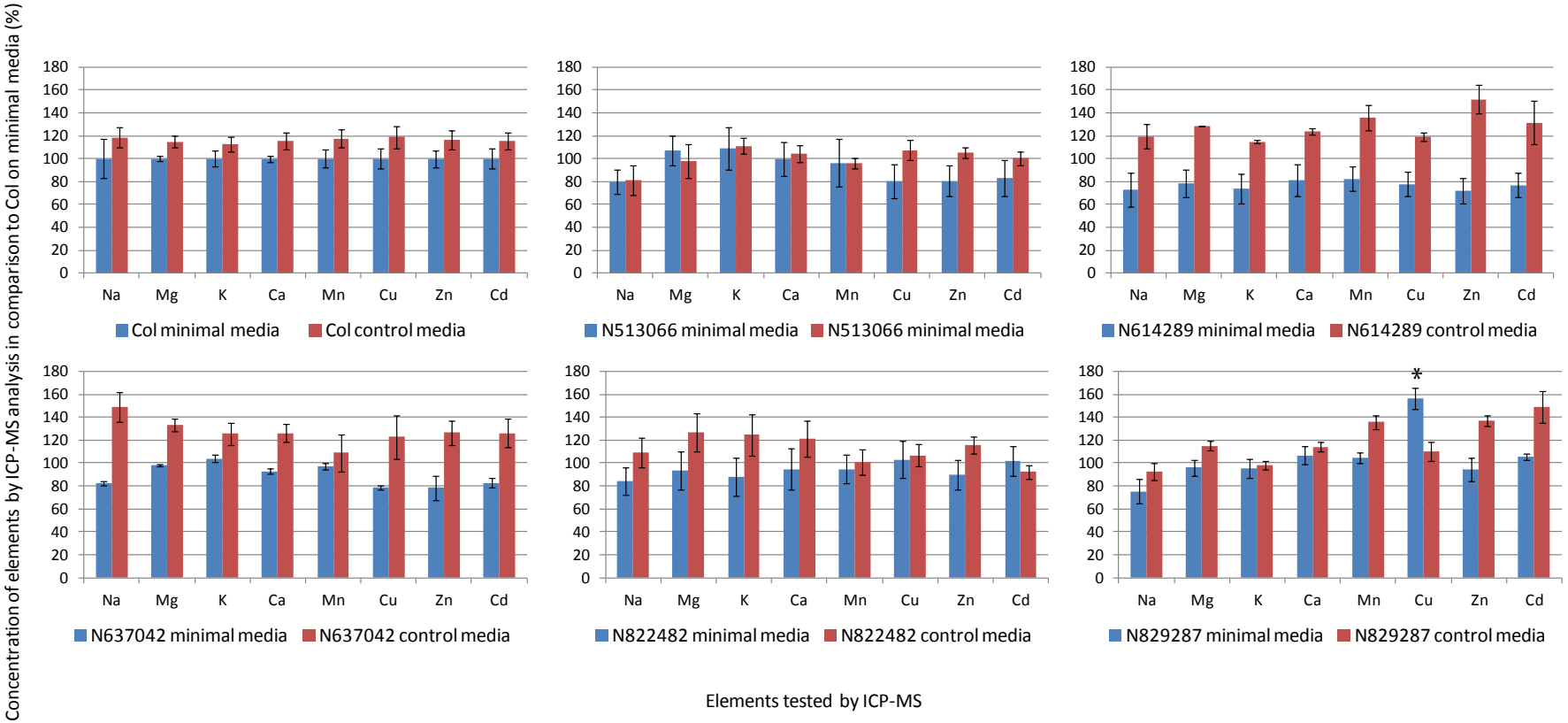
Concentration of elements by ICP-MS analysis in comparison to Col on minimal media (%)
180
160
140
120
100
80
60
40
20
0
Na
Mg
K
Ca
Mn
Cu
Zn
Cd
Col minimal media
Col control media
N513066 minimal media
N513066 minimal media
N614289 minimal media
N614289 control media
N637042 minimal media
N637042 control media
N822482 minimal media
N822482 control media
N829287 minimal media
N829287 control media
*
Elements tested by ICP-MS

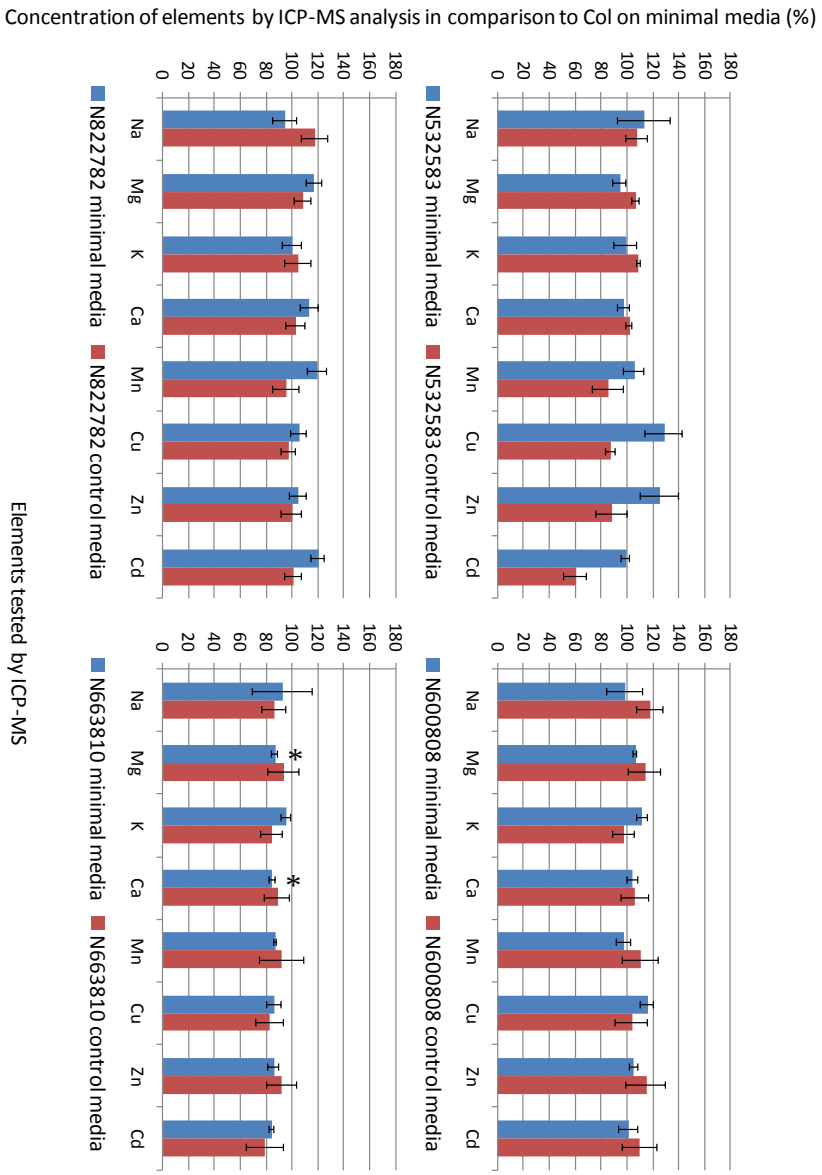

Figure 20: ICP-MS analysis of KO lines

Percentage of element concentration of KO lines in comparison to Col on minimal media (100 %). Error bar represents standard error. Statistical difference represented by asterisks (T-Test; P>0.05), n = 3.

3.6. DISCUSSION

Protein sorting within the ER accommodates an extraordinary variety of cargo proteins with different structures, functions and ultimate destination. Many of these

proteins are sorted by signalling motifs within the proteins themselves; however some proteins have no recognisable sorting motif. As well as this there are a number of multi transmembrane proteins where the order of transmembrane inserts into the membrane needs to be highly regulated, there are also proteins that need to be prevented from functioning prematurely. In these cases the proteins are dependent on specific accessory proteins (ER accessory proteins) for the correct structure and/or exit from the ER. A large number and varied mechanisms of ER accessory proteins have been discovered in mammalian and yeast systems in the last ten years, and with the discovery of potential ER accessory proteins in plants, it is likely that a similar mechanism exists in plants. So far three potential ER accessory proteins have been discovered so far; AXR4, PHF1 and NAR2.1.

AXR4 is a putative outfitter, which selectively regulates the localisation of AUX1 (an auxin influx carrier) to the plasma membrane (Dharmasiri et al, 2006). Similar to AXR4, PHF1 is an outfitter involved in the correct localisation of its target protein PHT1 (a phosphate transporter) (González et al, 2005). Mutations in AXR4 and PHF1 cause an abnormal accumulation of their target protein within the ER, however in the NAR2.1 mutant, its target protein NRT2.1 is absent from the cell. This suggests that NAR2.1 works in a different way to AXR4 and PHF1 and may be involved in preventing degradation through ERAD and allowing proper folding for vesicle transport (Wirth et al, 2007). This suggests that this mechanism is likely to be as numerous and varied as in other systems, with other polytopic membrane proteins requiring their own cognate ER accessory protein to facilitate folding and/or transport.

This area of research is therefore relatively new within Arabidopsis, and part of the project was focused on discovering new ER accessory proteins within plants. Despite having similar functions, ER accessory proteins share no sequence homology to each other, with no common motif or domain, and seem to represent novel proteins (Cooray et al, 2009). All ER accessory proteins however are localised to the ER and contain a transmembrane section, therefore to discover new ER accessory proteins a LOPIT (localisation of organelle proteins by isotope tagging) dataset was used, with the criteria for ER accessory proteins (ER localisation, transmembrane proteins,

novel or unknown function) 40 proteins were targeted by this method. The assignment of protein localisation by LOPIT appears to be reasonably accurate and have been validated experimentally by two putative ER accessory proteins (AXR4 and PHF1; Dharmasiri et al, 2006; Gonzalez et al, 2005; respectively).

Using the LOPIT dataset as a starting point, 20 proteins with unknown functions were prioritised based on high expression within the roots, single copy or multiple copy genes and whether T-DNA knock out lines were available. Of these 20 proteins, 14 homozygous lines were identified. The inability to identify homozygous lines for all the targets could be lack of T-DNA within the gene of interest or due to pollen or embryo lethality. These 14 lines were analysed for mRNA expression to see if the gene expression was completely knocked out, of these 7 showed complete loss of expression. In 6 of the 7 lines where the mRNA was still expressed, the T-DNA was located within introns and it is likely that they are still being spliced correctly, allowing normal expression level (see Appendix 9.5.). In one line the T-DNA insert was within the 5' UTR and it seems the T-DNA itself is driving the expression for this gene. Some of the T-DNA reaction used to create SALK T-DNA insertional lines are derivatives of pROK2 binary vector. pROK2 contain a 35 S promoter less than 2 Kb upstream of the left border and potentially can drive expression of flanking genes.

The homozygous KO lines were analysed for an ER accessory protein phenotype for membrane transporter proteins, based on growth on different nutrient concentrations. Membrane transport proteins are extremely important in plants, allowing regulation of a number of nutrients, chemicals, hormones and minerals within the cell. Our study is focused on the nutrient transporter proteins as these are extremely important for plant growth, and further understanding of how these are controlled may be important for crop improvement. Plants need nutrients at different concentrations for growth, with macronutrients required at comparatively large concentrations, and micronutrients required at very low concentrations. Therefore plants need to be able to control the uptake of these nutrients from the soil to ensure that they get the right quantities, one of the methods to do this is through membrane transporter proteins, and through their regulation.

Macronutrients include the elements nitrogen (N), potassium (K), sulphur (S), phosphorous (P), magnesium (Mg) and calcium (Ca). For the uptake of macronutrients and their allocation in different cellular compartments and tissues, plants employ a number of transport proteins, which differ from each other not only in their tissue and membrane location but also in their mode of energisation, substrate affinity and specificity (Blatt, 2004). The enormous variety of features displayed by transport proteins provides an invaluable pool for plants from which to select those transporters that are best suited to fulfil their nutritional demands in particular conditions. Approximately 1000 genes (5 %) of the entire genome of Arabidopsis thaliana have known or putative functions in membrane transport (Maathuis et al, 2003). A large number of membrane proteins have evolved to control the movement of ions in and out of cells and their subcellular compartments.

The expression and activity are tightly regulated in response to a number of external and internal stimuli, letting the plant make the most of its nutrient surrounding, allowing differential regulation of genes that have similar roles (e.g. ammonium transporter family). Transcript abundances of ion transporters often vary with the concentration of their substrate in the growth medium. While some transporters are induced by a decrease in substrate concentration, others are induced by an increase in substrate concentration (Amtmann & Blatt, 2009). For example, abundances of transcripts encoding high-affinity sulphate (e.g. AtSULTR1 [Buchner et al, 2004]) and phosphate (e.g. AtPT1 [Al-Ghazi et al, 2003]) transporters rise in low S and P growth medium. In contrast, up-regulation of high-affinity nitrate transporter (e.g. NRT2 [Krapp et al, 1998]) is observed when small amounts of nitrate (~50 μM) are added to N-depleted medium. The changes are not only occurring at the transcript level, but also at the protein level, such as phosphorylation, and through exocytosis/endocytosis (Amtmann & Blatt, 2009). The changes can also be dependent on time, for example the transfer of plans to N-free medium induces the expression of AtAMT1;1 and AtAMT1;3 within 3 days, whereas the induction of AtAMT1;2 and AtAMT2;1 requires more extended periods of N deficiency (Gazzarrini et al, 1999; Sohlenkamp et al, 2000). Plant membrane transporters not only regulate the uptake of nutrients from the soil, but they are also involved in the

transfer of substances throughout the plants, these include xylem loading, vacuole importers, cellular importers and exporters (Tan et al, 2002).

Therefore, plants have developed finely tuned homeostatic mechanisms aimed at coordinating systematic spatiotemporal requirements in the acquisition, distribution, and delivery of metals (Puig and Peñarrubia, 2009). Because of this it is sometimes difficult to locate proteins involved in nutrient transport, especially if it does not affect the major high affinity nutrient transporters in the system. This problem is due to overlapping functions of different genes, and tight control of expression, meaning that even if a gene is knocked out other genes may be upregulated or take over its function.

In the initial screen of homozygous KO mutants no difference to Col was observed, this is not surprising with the high level of control that the plant applies to its nutrient uptake. As mentioned earlier this could be due to overlapping functions or gene regulation masking the phenotype, but also membrane transport proteins are not active everywhere or at all times. Therefore it is possible that under the high nutrient media that was being used the potential membrane protein target may not be active. Also membrane transporters have many functions within the plant, for example uptake from the soil, distribution around the plant, xylem loading, and storage into vacuoles (Tan et al, 2002). Incorrect localisation of these transporters would have a different phenotype, with some such as vacuole importers not giving a phenotype under deficiency conditions.

Another reason for the lack of phenotypes could be due to the bulk flow mechanism of transport, which is a slow non-selective transport of proteins from the ER to the Golgi. It has been shown for some ER accessory proteins that the subcellular localisation of their target is not changed in the mutant although COPII loading has been abolished (Ladasky et al, 2006). In one case overexpression of a cargo protein has overcome the ER accessory protein mutant background, showing that it is not essential for transport (Bökel et al, 2005). In this case, however, the rescued cell lacked dorsoventral polarity, showing that bulk flow cannot control temporally and spatially precisely coordinated localisation of the cargo protein (Bökel et al, 2005).

Therefore for proteins that are highly abundant in the cell and do not need to be precisely located, the transport protein localisation could be maintained through bulk flow, reducing the phenotype observed.

Due to this difficulty we developed a number of smart screens using toxic levels of metals to probe nutrient transport function, and low nutrient levels to observe a deficiency phenotype which may be masked under normal conditions. These growth inhibiting conditions for nutrient deficiency or toxicity allow us to analyse the KOs response to different nutrients, and differences in growth which may be due the mislocalization of a nutrient membrane transporter protein. Four deficiency screens were used looking at boron, nitrogen, phosphorous and sulphate, and four toxicity screens were used looking at boron, copper, sodium and zinc. The majority of the screens and lines gave no significant difference between Wt response to the different conditions and the T-DNA KOs response to the different conditions; however a few lines gave a weak phenotype in these screens. These weak phenotypes could be due to the fact that only one out of a number of different transporter proteins is being mislocalized, or it could be that the transporter protein are still reaching the membrane at various levels through the bulk flow mechanism of transport. Due to the limitations of the nutrient and toxicity screens, an ICP-MS analysis of the nutrient content within the plants was also analysed, this allows us to see the base level of nutrient stasis within the plants. ICP-MS allows us to detect small changes in the nutrient stasis of the plants, which may be caused by a mislocalization of a nutrient transporter.

From these two methods, a few of the T-DNA KO lines showed some phenotype, and could suggest a role as an ER accessory protein. The AtBPL family (T-DNA KOs N532583) gave a weak phenotype under nitrogen limiting conditions, which is discussed in the next chapter. N663810 showed increased sensitivity to toxic levels of boron, N829287 showed increased sensitivity to toxic levels of copper and N614289 showed a weak phenotype in more than one screen.

N663810 (At2g16170) showed increased sensitivity to toxic levels of boron (> 500 μM), to date two different types of borate transporters have been discovered in

Arabidopsis; NIP5;1 and BOR1 (Takano et al, 2010). NIP5;1 is essential for efficient B import into roots under conditions of B limitation, while BOR1 homolog's are involved in toxicity tolerance in plants. As there was no decrease in growth under Boron deficiency it is unlikely that NIP5;1 localisation is effected, however it is possible that BOR1 (or BOR1 homolog's) are being affected. BOR1 is a boric acid exporter involved in xylem loading (Takano et al, 2010), and loss of boron transport into the xylem would cause boron to build up to toxic levels quicker within the root. For example BOR4 overexpression results in increased efflux of B from the roots and significant growth improvement at toxic concentrations of B (millimolar range) (Takano et al, 2010).

N614289 (At1g71780) is another line of interest having a weak phenotype in more than one screen. This line also shows increased sensitivity to toxic levels of boron, as mentioned in the previous paragraph, it could possibly be involved in the correct localisation of BOR1 or a BOR1 homolog, effecting xylem loading. Interesting N614289 also gives a reduced nutrient stasis in the minimal media for the ICP-MS analysis with an 80 % reduction in all nutrients compared to Wt. Therefore this line may play a more extensive role than an ER accessory protein for a single transporter, as it appears to affect multiple nutrient levels within the plant. It may possible be involved in general protein processing within the ER, such as a chaperone, or involved within the ERAD system.

N829287 (At4g16170) showed increased sensitivity to toxic levels of copper, as well as increased uptake of copper in minimal media in the ICP-MS analysis. Copper is an essential micronutrient that functions as a redox cofactor in multiple plant process, such as photosynthesis. So far a family of CTR-like high-affinity copper transporters have been discovered in Arabidopsis (COPT1-5), however only two of these proteins has a demonstrated role in plants. COPT1 is a high-affinity Cu transport protein involved in the uptake of Cu at the root tip, being expressed in Cu scarcity (Andrés-Colás et al, 2010; Sancenón et al, 2003, 2004), and is unlikely to be a potential target as a mislocalization would not cause heightened sensitivity to high levels of Cu. The other transport COPT5 is localised at the PVC (pre-vacuolar compartment) and is involved in the mobilisation of Cu from intracellular vesicles (Garcia-Molina et al, 2011), is also unlikely to be the target as mislocalization would cause increased

resistance to copper. In yeast excess intracellular Cu can lead to the generation of harmful reactive oxygen species that cause severe oxidative damage (Halliwell and Gutteridge, 1984). Therefore it is likely that a vacuolar influx carrier is being mistargeted; prevent the storage of Cu safely in the vacuole and away from the intracellular matrix. The lack of correct storage of Cu within the root and shoots may also cause an increased Cu concentration noticeable in the ICP-MS analysis within the shoots as more Cu is mobile for transport into the shoots. Further analysis of the other COPT2-4 transporters to see if any of these are involved in vacuolar trafficking, could allow identification of a potential target.

All phenotypes discovered were only weak phenotypes, therefore these need to be studied under more detail to discover the effect of these genes on nutrient transporters. ICP-MS has a number of limitations, and a lot of nutrients such as nitrate are unable to be measured using this method. Also the measurement of iron by ICP-MS in this study, varied enormously between the repeats and between the different lines, and thus was excluded from the results (data not shown). Because of these difficulties we were unable to validate any of the nutrient and toxicity screens phenotypes. Therefore other methods will need to be used to discover if the weak phenotype is linked to the mislocalization of a membrane transporter.

Once the phenotype has been validated a number of techniques can be used to allow further understanding of the genes function and target. For example expression analysis can be used to allow understanding of where and when the gene functions through promoter GUS constructs and by use of RT-PCR at different tissue stages and types. As ER accessory proteins such as AXR4 and PHF1 give a weak phenotype of the mutant transporter they are trafficking, mutant analysis of the KO and potential target transporter can be compared. Further validation of the phenotype can be done using metabolic profiling to show changes in the nutrient levels. To discover potential targets antibodies for the gene of interest can be used in pull downs and interaction data. Another way to do this is through a LOPIT study comparing wild type and the mutant, allowing us to detect any proteins that are mislocalized between the two databases. Yeast-two-hybrid systems can also be used to show that the two proteins do in fact interact with each other. GFP fusions will

allow protein localisation to be studied, which may give further insight into where it acts and how it functions at the cellular level. Also if we discover the target of the gene GFP fusions or specific antibodies can be used to look at localisation of the cargo protein in the mutant compared to Wt.

To conclude, a more extensive study of the potential ER accessory proteins discovered is required. The At5g42570 (BPL family), At1g71780 (N614289), and At2g16760 (N663810) need to be characterised in more detail to see whether they are responsible for the correct localisation of specific nutrient transporters. N614289 is interesting as it showed a growth defect in almost all nutrient deficient concentrations studied, and in the ICP-MS analysis showed a consistent 80 % reduction in growth in comparison to Col in the minimal media used. Therefore it is possible that this gene has a more general role as an ER protein. Due to the fact that At5g42570 contains the InterPro domain B-cell receptor-associated 31-like and has similarity to BAP31 (a known ER accessory protein) in blast searches (43% - $5e^{-10}$), it may play a similar role to mammalian BAP31 in plants. Therefore this protein was focused on in the next chapter to see whether we could discover its role in plants and to see whether it is involved as an ER accessory protein for nitrogen transport within Arabidopsis thaliana.

CHAPTER 4

AtBPL1; AN ER ACCESSORY PROTEIN?

4. **AtBPL1; AN ER ACCESSORY PROTEIN?**

4.1. BIOINFORMATIC ANALYSIS OF AtBPL1

Using the LOPIT database (Dunkley et al, 2006) as mentioned in the previous chapter, 40 novel ER proteins were identified; one of these, At5g42570 is of particular interest. Bioinformatic analysis revealed that it is related to B-cell receptor-associated protein 31 (BAP31 or BCAP31) in mammalian cells (figure 21). BAP31 is an integral ER membrane protein with three putative transmembrane domains (TMDs) and a dilysine motif at its C terminus which is an ER retrieval signal (KKXX) (Kim et al, 1994). Mammalian BAP31 has been shown to be involved in numerous processes, such as protein transport, protein processing and apoptosis. BAP31 functions as a ER accessory protein as a cargo receptor for ER export of transmembrane proteins, such as cellubrevin, class I major histocompatibility complex (MHC) molecules, CFTR, membrane-bound immunoglobulin (Ig)G, tetraspanins, cytochrome P450 2C2, tyrosine phosphatise-like B and the leukocyte integrin CD11b/CD18 (Annaert et al, 1997; Ladasky et al, 2006; Lambert et al, 2001; Paquet et al, 2004; Schamel et al, 2003; Spiliotis et al, 2002; Stojanovic et al, 2005; Szczensa-Skorupa & Kemper, 2006; Wang et al, 2004; Zen et al, 2004).

It is believed that BAP31 plays its role through quality control of these membrane proteins, allowing only correctly folded proteins to be transported out of the ER. Proteins which are not correctly folded are degraded through the ER-associated degradation pathway (ERAD); this sorts these incorrectly folded proteins to a juxtanuclear subcompartment before being retrotranslocated into the cytoplasm and degraded (Wigley et al, 1999). BAP31 has been shown to be a component of this juxtanuclear subcompartment (ER quality control compartment) (Wakana et al, 2008), and has also been shown to promote retrotranslocation of a mutated form of CFTR through interaction with components of the translocon (Wang et al, 2008).

Figure 21: Sequence alignment of HtBAP31 and At5g42570

Sequence alignment of BAP31 and At5g42570, showing 32.5% similarity. Conserved amino acids in boxed in black; dark blue box showing TM of At5g42570; light blue box showing BAP31 superfamily domain; dark red box showing TM of BAP31 (Homo sapiens); light red box showing BAP31 superfamily domain. NCBI conserved domain analysis database used for predictions (Marchler-Bauer et al, 2009). The analysis results in conserved domain Bap31 superfamily in At5g42570 (E value 2e-05) and highly conserved domain Bap31 superfamily in BCAP31 (E value 4e-33).

Transmembrane proteins which are cargo for BAP31 are especially prone to ERAD such as CFTR and class I MHC molecules (Wakana et al, 2008). It is believed that BAP31 may function by recruiting ER proteins necessary for the correct folding of these molecules (e.g. chaperones). This complex then facilitates the recruitment of these cargo proteins to the ER exit site, where correctly folded proteins then dissociate from BAP31 and are loaded into COPII vesicles (Paquet et al, 2004). This theory is supported by the fact that BAP31 has been shown to be associated with the ER chaperone calnexin, which is known to promote class I H folding and subsequent

assembly with the other chains to create MHC molecules (Vassilakoa et al, 1996). As well as this, in the absence of BAP31, the colocalization of class I MHC molecules with mSec31 (a component of mammalian coat protein complex II coats) is reduced (Paquet et al, 2004).

Despite this, BAP31 is not essential for trafficking of its cargo proteins to the plasma membrane, as loss of BAP31 does not affect levels of class I molecules to the surface of HeLA cells for example (Ladasky et al, 2006). Therefore it is likely it plays a more important job in quality control for these proteins and may prevent incorrectly folded proteins from being transported out of the ER. As well as quality control within the ER, BAP31 is also believed to be involved in retrieving class I molecules that have lost their peptides in post-ER compartments, so that they can be assembled correctly within the ER or subject to ERAD (Ladasky et al, 2006).

BAP31 has also been shown to play an important role in apoptosis in both yeast (YET3) and human cells (Delom et al, 2007; Madeo et al, 2009). In its full length form, BAP31 has anti-apoptotic activity (such as retention of cytochrome P450 2C2 in the ER), however its cytoplasmic tail is cleaved by caspase-8 during apoptosis to form p20 (proapoptotic BAP20). p20 activates pro-apoptotic signals, e.g. release of cytochrome C from the ER (Breckenridge et al, 2002; Chandra et al, 2004; Delom et al, 2007; Ng & Shore, 1998; Nguyen et al, 2000; Szczensa-Skorupa & Kemper, 2006). A mutated BAP31 which can no longer be cleaved by caspase-8 strongly inhibits Fas-induced apoptosis (Fas activates procaspase-8 at the plasma membrane to give active caspase-8), suggesting BAP31 plays a quite important role in this process (Breckenridge et al, 2003a).

Because of the similarity of At5g42570 with BAP31, this Arabidopsis homolog of BAP31 was called BAP31-like (BPL1). AtBPL1 encodes a 218 amino acid transmembrane protein, whose mRNA is expressed at a relatively high level (~400; Winter et al, 2007) in the root tissue. The gene contains 1 intron, a B-cell receptor-associated 31-like domain (Pfam), three transmembrane domains and a coiled coil stretch (Psort2) (figure 22-23) (Aceview 2006).

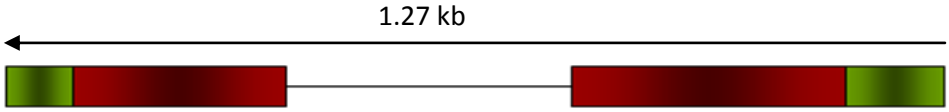

Figure 22: At5g42570 gene transcript
Non-coding region (green), coding region (red). (Swarbreck et al, 2008).

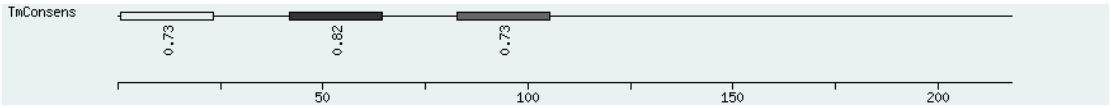

Figure 23: Consensus transmembrane spans in At5g42570 based on 16 prediction software in Aramemnon (Schwacke et al, 2003).

Bioinformatic searches reveal that a number of other plant species such as rice, maize, Medicago truncatula, grape and Ricinus communis also have a BAP31-like protein (Breckenridge et al, 2003a; Liebel et al, 2005). Predicted BAP31-like proteins in these species also terminate with the C-terminus ER retention signal (KKXX), suggesting that its role in quality control and protein transport may be conserved within plants. Recently a few studies have suggested that ER-associate protein degradation (ERAD)-like mechanism also occurs in plants (Müller et al, 2005). For example Müller et al (2005) discovered C-terminal mutants of MLO (powdery mildew resistance o) in barley (Hordeum vulgare) act as universal signals for protein quality in barley, Arabidopsis thaliana, yeast and human cells by targeting fusion proteins for degradation. Therefore the ERAD system may be conserved to some extent in all eukaryotic cells, this is supported by the fact that a number of Arabidopsis homologs have been identified for known yeast ERAD genes, such as CDC48 (Müller et al, 2005; Rancour et al, 2002; Vitale & Boston, 2008). Therefore while very little is known about the ERAD mechanism in plants, it is therefore possible that AtBPL1 could play a similar role in quality control and protein transport from the ER. BRI1-5 for example interacts with calnexin for correct folding in Arabidopsis and therefore could be a potential cargo protein for BPL1 (Hong et al, 2008).

Similar to the ERAD system in plants, little is known about whether plant cells have an apoptosis-like cell death, with caspase 8 activating pro-apoptotic proteins. In

plants controlled cell death is called programmed cell death (PCD) and several types of PCD may operate in plants, one of which is apoptotic-like PCD (AL-PCD) (Reape & McCabe, 2008). AL-PCD has characteristics of 'apoptosis' such as protoplast condensation and DNA degradation (Reape & McCabe, 2008). However caspases, which are the main activators of apoptosis in animal cells, have so far been elusive in plants. Despite this there has been evidence for caspase substrates being cleaved during plant PCD, and caspase-like proteases have been identified and been shown to have similar actions to their counterparts, such as caspase-3 like protease (Bosch et al, 2008; Bosch & Franklin-Tong, 2008; Danon et al, 2004; Woltering et al, 2002; Zhang et al, 2009). Recently caspase 8/9-like activity (LEVDase) has been discovered in Papaver during self-incompatibility, therefore it is possible that AtBPL1 may also play a similar role in apoptotic-like PCD (Bosch & Franklin-Tong, 2007). However the caspase 8 cleavage sites on BAP31 (AAVD.G) (at D^{164} and D^{238}) are not conserved in BPL1 and Breckenridge et al (2002) showed the importance of this site, as changing the asp residue to ala prevented cleavage (Breckenridge et al, 2003b). Therefore while it is possible it may play a similar role in AL-PCD it seems unlikely that it is activated by a caspase-8 like protein, therefore plants may have found a different way to control cytochrome C or they cleave BPL in an independent manner to create p20.

4.2. AtBAP31 BELONGS TO A MULTI GENE FAMILY

Database searches reveal that the Arabidopsis genome contains at least 4 other BAP31-like proteins (figure 24), however only one of these genes, At3g07190, also contains a weakly conserved BAP31 superfamily domain (7.10 e-03). At3g07190 (BPL4) is 39% identical to AtBPL1 (coverage 0.94). All 4 genes have been predicted to be located in the ER, and all except At5g48660 (BPL3) and At3g20450 (later predicted not to be part of the family) have the ER retention KKXX C-terminal motif, and have been given the preliminary function of being involved in intracellular transport and apoptosis (Schwacke et al, 2003).

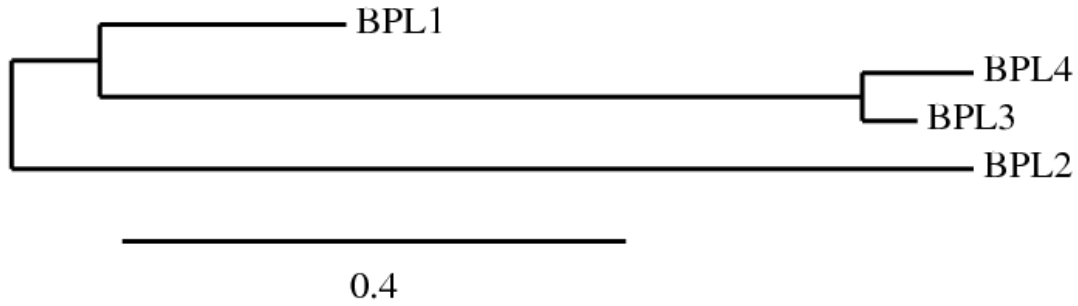

Figure 24: Phylogenetic tree of the AtBPL family members using phylogeny.fr version 2 (Dereeper et al, 2008; 2010).

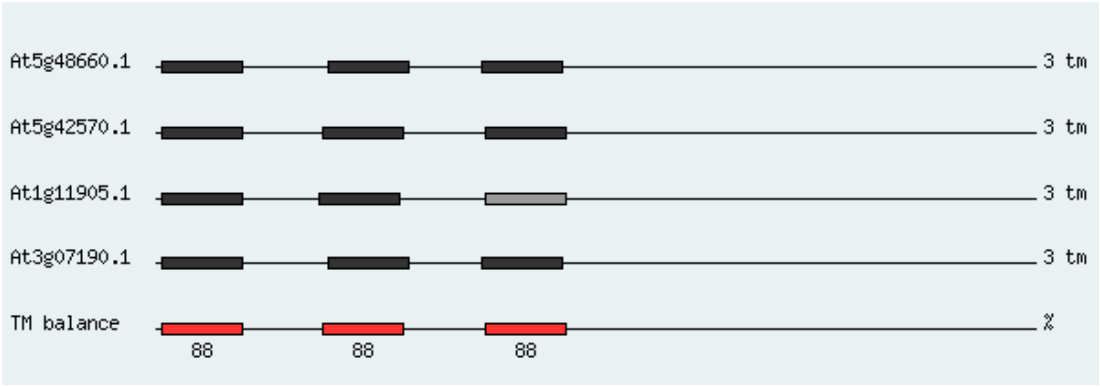

Figure 25: Predicted transmembrane regions in AtBPL family
Multiple alignment of predicted transmembrane regions in genes belonging to the AtBPL family, performed by Muscle 3.6 (Schwacke et al, 2003).

Multiple sequence alignment of the 4 genes showed that they all contain the three transmembrane domains (figure 25) and they share a slightly conserved protein sequence at the N-terminus (24% similarity) and overall they contain only 18% similarity with each other. Therefore it remains to be seen if their share a similar function. In comparison to BPL1, BPL2 shares 49 % similarity at the protein level, BPL3 shares 41 % and BPL4 shares 39%.

4.2.1. Phenotypic analysis of AtBPL family

Due to similarity of BPL1 with the mammalian BAP31 which is a known an ER accessory protein, the possibility that AtBPL1 has a similar function within plants was investigated as part of the study.

4.2.1.1. ERAD system

Very little is known about the ERAD mechanism in plants, however it is possible in common with BAP31 in animal cells, BPL plays a role in quality control and protein transport from the ER. BRASSTERIOD-INSENSITIVE 1 (BRI1) for example interacts with calnexin (a known interactor of mammalian BAP31) for correct folding in Arabidopsis and therefore could be a potential cargo protein for BPL1 (Hong et al, 2008). BRI1 encodes a cell surface receptor for brassinosteriods, and a weak bri1-5 allele (Ws-2 ecotype) carries a Cyc69Tyr mutation that causes it to be retained in the ER by the ERQC system (endoplasmic reticulum-mediated quality control) (Li et al, 2001). Hong et al (2008) have previously shown that inhibition of the ERQC/ERAD system through mutations or treatments in Arabidopsis results in a significant suppression of the bri1-5 dwarf phenotype. Therefore bri1-5 is a good model to look at the ERAD system within plants and to see whether BPL1 plays a significant role within this system. bri1-5 seeds (donated by Prof. Frans Tax, University of Arizona) were crossed with the mutant lines and the F2 generation were observed for suppression of the bri1-5 dwarf phenotype. Figure 26 shows that in the double KO lines there is no rescue of the bri1-5 dwarf phenotype, this shows that BPL1 and BPL2 are not involved the ER retention of BRI1-5 and suggest that BPL1 family does not play a very general role in the ERAD system, similar to the ER chaperones BiP and calnexin. It is possible that the members of the family have overlapping roles and redundancy between BPL1 and BPL2 could prevent the suppression of the bri1-5 mutant phenotype. Another possibly is that the BPL family may play a more specific role as an ER accessory protein focused on specific targets similar to BAP31.

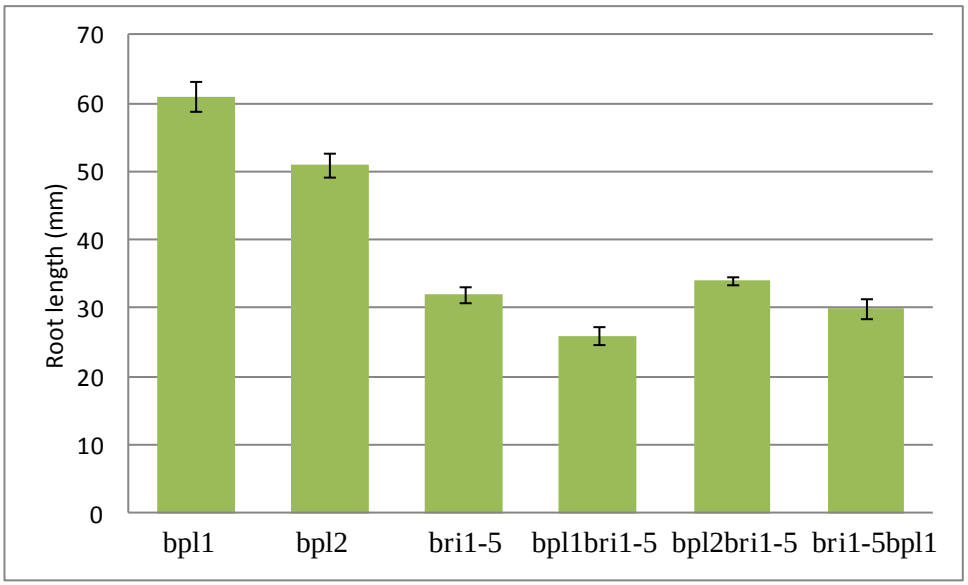

Figure 26: Root length of bri1-5 bpl1 crosses

Growth of bplbri1-5 double mutant lines, using bpl1, bpl2, bri1-5 as a control for comparison. Error bar represents standard error. No statistical difference in double mutants compared to bri1-5 (T-Test; P > 0.01), 7 day old seedlings, n = 12.

4.2.1.2. ER accessory protein

While BPL may not play a role in the general ERAD system in plants, it may have a more specific role as an ER accessory protein similar to BAP31. To investigate the role of AtBPL1 and the sequence homologs in plant development, a genetic approach was used. Homozygous T-DNA insertion knock outs (KOs) were identified in three of the five genes (At5g42570 – BPL1; At1g11905 – BPL2; At5g48660 – BPL3). The effect of these mutations on root/plant growth was analysed (Chapter 3). bpl1, bpl2, and bpl3 consistently show reduced growth on low nitrogen media, it was reasoned that this may be due to difficulties in nitrate uptake (figure 27). To investigate this further chlorate toxic screens were used. Chlorate is a toxic compound which is taken up by the nitrate transporters (Kosola & Bloom, 1996), and therefore if a nitrate transporter is being mislocalized it may prevent chlorate uptake, giving resistance to toxic levels of chlorate.

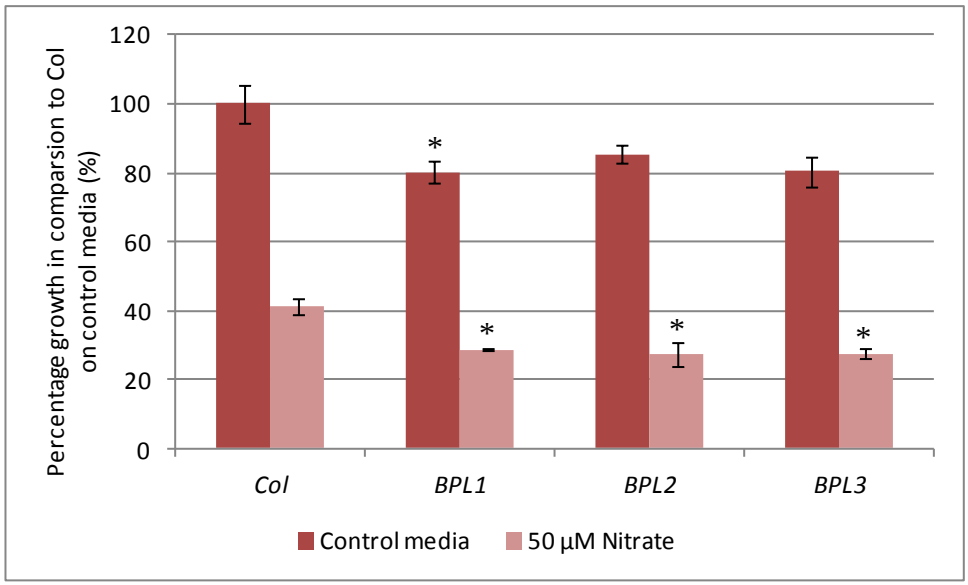

Figure 27: Nitrate deficiency screen

Percentage of growth of bpl mutant lines in comparison to Col on control media (100 %). Error bar represents standard error. Statistical difference represented by asterisks (T-Test; P > 0.01), 7 day old seedlings, n = 11.

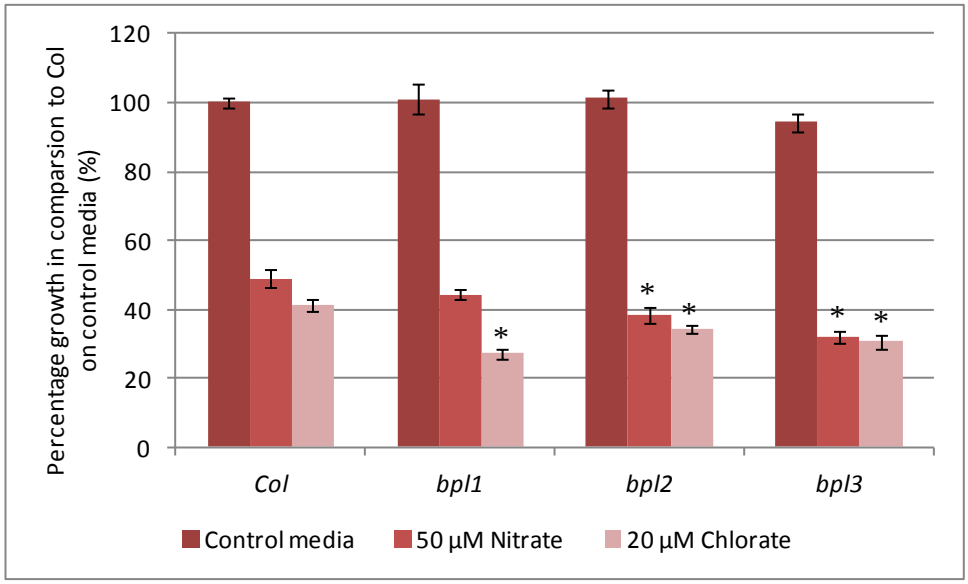

Figure 28: Chlorate toxicity screen in bpl family

Percentage of growth of bpl mutant lines in comparison to Col on control media (100 %). Error bar represents standard error. Statistical difference represented by asterisks (T-Test; P > 0.01), 7 day old seedlings, n = 11.

All three bpl mutants show increased sensitivity to chlorate (figure 28). This effect was small but consistent and was contary to what was expected if a plasma membrane transporter was mislocalised. However this can be explained if a vacuolar nitrate transporter is effected. In this case it would prevent chlorate from being sequestered safely away, therefore would cause it to build up to toxic levels quicker within the cell, causing deleterious effects. AtCLCa-1 is a vacuole anion channel involved in transport of nitrate into the vacuole (De Angeli et al, 2006). Mutation in AtCLCa shows a hypersensitivity to chlorate, with 50 % reduction in shoot fresh weight in comparison to WT (Geelen et al, 2000).

Therefore to test whether the BPL1 family is involved in the correct localisation of AtCLCa-1 protein, the phenotype of the clca mutant was checked (donated by Dr. Barbier-Brygoo, Director of Institut des Sciences du Végétal) (figure 29). Using our conditions or the conditions used by De Angeli et al (2006), no root related phenotype for clca1 or clca2 (a stronger allele) was discovered at any chlorate concentrations observed. Under the same conditions the BPL1 family mutants showed increased sensitivity to chlorate. Therefore it is possible that the BPL family are involved in nitrate transport, but as they do not phenocopy CLCa mutant it is unlikely that they are involved in only its trafficking.

The weak nitrogen deficiency phenotype and weak hypersensitivity to chlorate, is not surprising due to the complexity of the nitrate transport system within plants. Also in the mammalian BAP31 the mutant does not give a strong phenotype with almost normal expression of its target proteins at the plasma membrane in some cases. However it is still possible that lack of a clear strong phenotype may simply be due to genetic redundancy of the BPL1 family members.

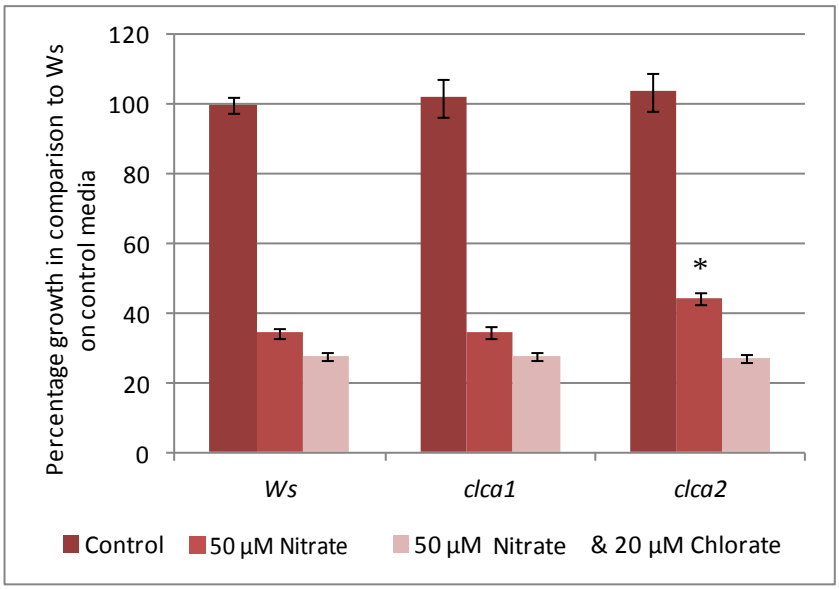

Figure 29: Chlorate toxicity screen in clc mutants

Percentage of growth of clc mutant lines in comparison to Col on control media (100 %). Error bar represents standard error. Statistical difference represented by asterisks (T-Test; P>0.05), 7 day old seedlings, n = 11.

4.3. EXPRESSION PATTERN STUDIES

To test the expression of BPL1 family members, initially microarray data was analysed using the Arabidopsis eFP browser (Winter et al, 2007). Out of five of the family members, only three have microarray data (figure 30). Therefore this approach only gave a limited view of the expression pattern for this family. To find out the expression pattern of the whole family promoter GUS constructs were made for each of the genes, and the resultant GUS expression analysed.

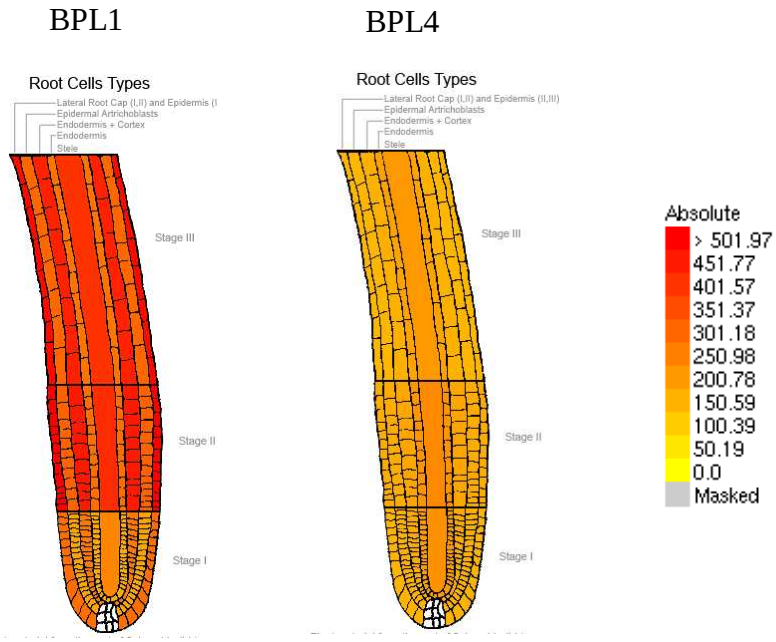

Figure 30: Expression levels of BPL family

Expression levels of the 3 genes present in the Arabidopsis eFP browser (Winter et al, 2007). At5g42570 (BPL1 - left) has a strong level of expression ~ 450 compared to At3g07190 (BPL4 – middle) which has about 50% of the expression ~200.

4.3.1. Plasmid construction

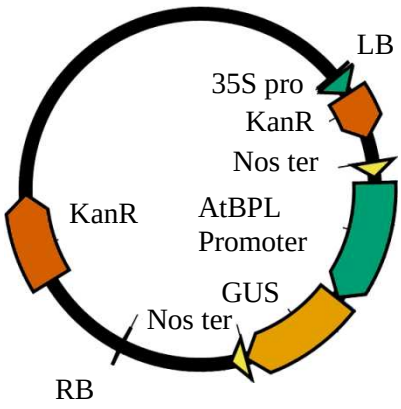

pMOG AtBPL::GUS

Figure 31: Diagram of pMOG AtBPL::GUS.

Up to 2kb of 5' upstream sequence for each gene were PCR amplified from Col-0 genomic DNA and cloned into PMOG GUS vector (figure 31). The constructs were transformed into Arabidopsis as described by Clough and Bent (1998). The transgenic lines were selected on kanamycin and the T2 generation were screened for GUS staining, and at least 3 independent lines were analysed for GUS expression in the T2 generation.

4.3.2. GUS expression patterns

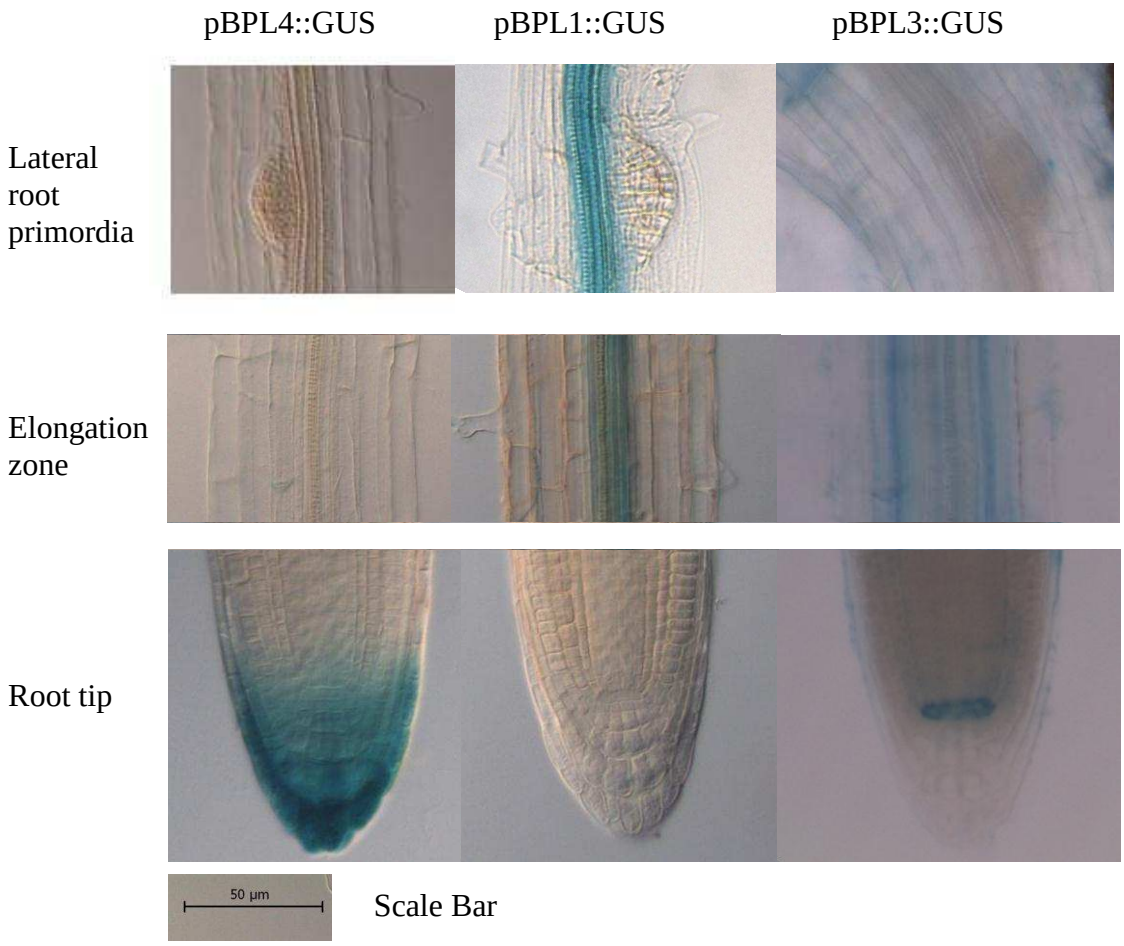

Figure 32: Promoter GUS results for BPL family

Promoter GUS expression analysis at the lateral root primordia, root elongation zone and the root tip.

The expression pattern of promoter GUS lines was observed by staining for GUS activity in 7-day old transgenic lines for 6 hours (pBPL1::GUS and pBPL4::GUS) and 24 hours (pBPL2::GUS and pBPL3::GUS) (figure 32). BPL1 has a very strong GUS expression which can be observed after 3 hours (data not shown) which is present in the vascular tissue in the elongation zone and more mature tissues. BPL4 also have a very strong GUS expression which can be observed after 3 hours (data not shown) which is present solely at the root tip in younger roots (<11 days old). Interestingly despite having two T-DNA insertion lines (1 of which is still expressed in the KO), we have been unable to isolate a homozygous KO for this gene; at this stage it is not clear if AtBPL4 is embryo or seedling lethal.

BPL3 showed a weaker GUS staining pattern than BPL1 and BPL4, therefore required longer staining. BPL3 GUS plants showed a very strong expression at the QC cells which is observed from a very young age (3 days old) (data not shown) and becomes more specific as the root matures (figure 32). Besides the QC, BPL1 GUS is also expressed in the more mature root tissue. In BPL2 there was no GUS staining after 24 hours staining suggesting that either the gene is very lowly expressed in Arabidopsis root or it is not expressed at all.

4.3.2.1. Phenotypic studies of BPL3

Because BPL3 showed a very strong QC expression, bpl3 mutants were analysed to see if they had any QC related defects. As shown in figure 33 there appears to be no defect in root patterning in the bpl3 mutant. To analyse this further, columella markers PIN3, root specific cell wall marker LM15, and starch were used as markers for fully differentiated columella cells. There appears to be no significant differences in cell differentiation or root patterning in the bpl3 mutant, as judged by starch staining, PIN3 and LM15 localisation (figure 34).

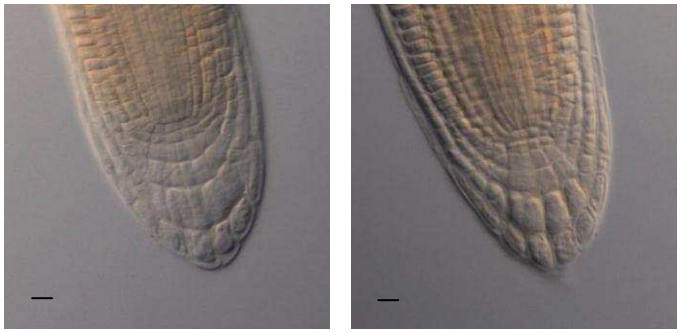

Col bpl3

Figure 33: Root patterning in bpl3

Root tip of 3 day old seedlings in Wt (Col), and bpl3 mutant. Scale bar represents 10 μM.

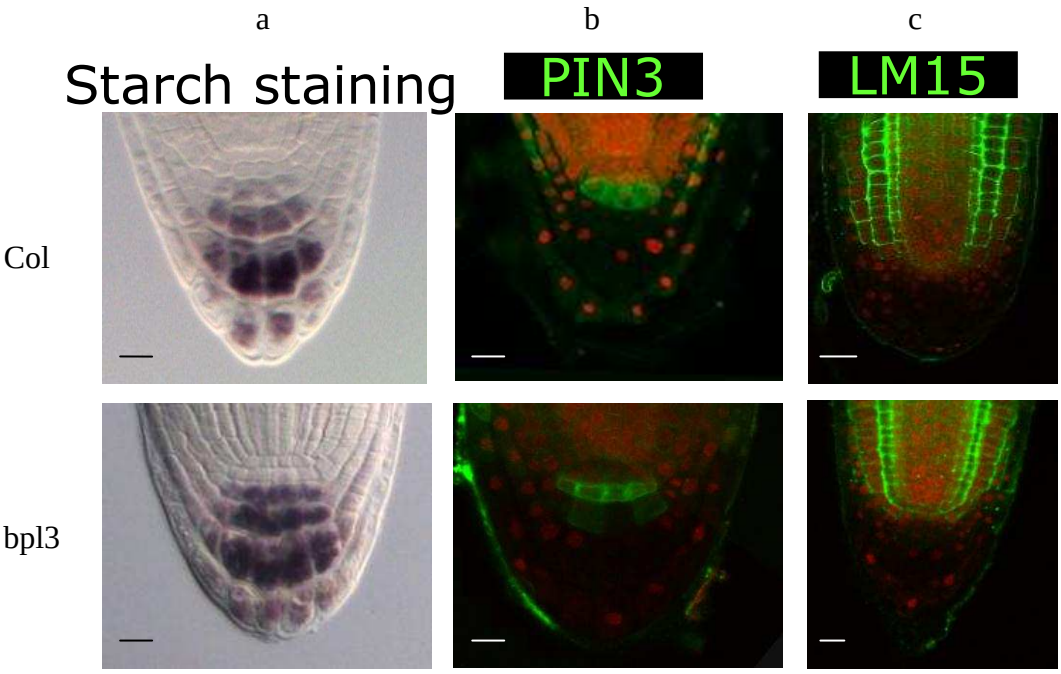

Figure 34: Phenotypic analysis of root meristem in bpl3

bpl3 mutant (bottom) compared to Col (top) for starch staining (a), PIN3 (b) and LM15 (c) localisation. Scale bar represents 10 μM.

4.4. MULTIPLE ARTIFICAL MIRNA

Due to a lack of a strong phenotype in the single mutants and unavailability of KOs in all the family members an artificial miRNA (amiRNA) approach was used. amiRNA's are a relatively new tool in gene silencing which allow highly specific silencing of genes compared to RNAi (Ossowski et al, 2008). RNAi is produced

from hairpin loops which produce a number of siRNA (small interfering RNA) sequences with varying 5' and 3' ends on both strands, making it difficult to predict off-targets for RNAi, and to optimise siRNA for silencing of specific genes (Schwab et al, 2006). miRNA on the other hand only produces 1 small RNA (the miRNA) from a single strand (see figure 35), this allows accurate analysis of potential off targets, and efficiency of targeting the gene of interest (Ossowski et al, 2008).

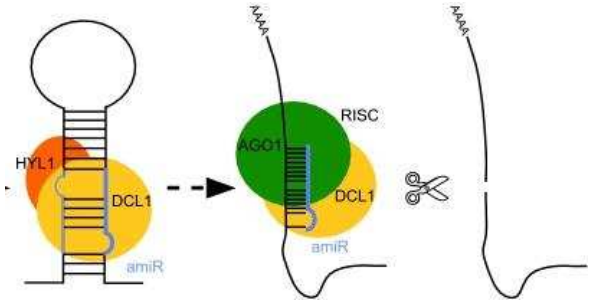

Figure 35: miRNA diagram

Figure taken from WMD3 website (Ossowski et al, 2008). 21 nucleotide miRNAs are processed from stem-loop regions of long primary transcripts by a dicer-like enzyme and are loaded into silencing complexes (RISC) where they direct the cleavage of complementary mRNAs (Jones-Rhoades et al, 2006).

AtBAP31 family amiRNA were designed using WMD (Web MircoRNA Designer platform) (Ossowski et al, 2008) which automates amiRNA design. It is designed to optimise small RNAs for maximal effectiveness, and selection of those with highest specificity for the intended target genes (Ossowski et al, 2008). Results of the 'Design' tool suggested that out of these five genes, three genes could be silenced in a single amiRNA (At3g07190, At5g42570, and At5g48660).

4.4.1. miRNA constructs

To engineer the amiRNA, three fragments containing (a) the 5' region up to the amiRNA*, (b) the loop region ranging from amiRNA* to amiRNA, and (c) the 3' region starting with the amiRNA, were amplified separately from a pBluescript template plasmid that contains the M1R319a precursor (pRS300), and the final

product was generated in a single PCR reaction (d) (figure 36) (Ossowski et al, 2008). This AtBAP31 miRNA PCR product was then cloned into pENTR1Z for cloning into PGWB402 a constitutively expressed GATEWAY™ destination vector (figure 37). The miRNA AtBAP31 constructs were then transformed into Col-0.

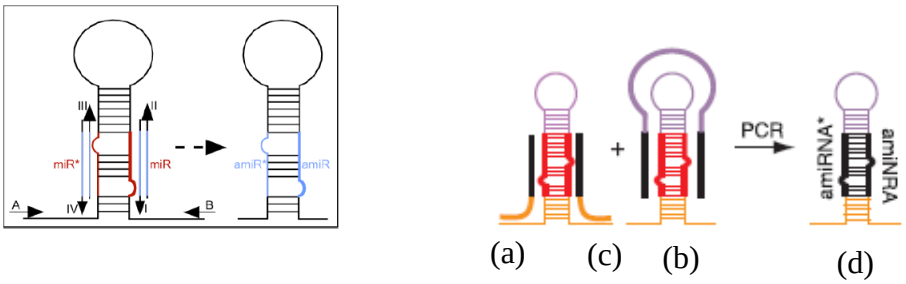

I: microRNA forward
II: microRNA reverse
III: microRNA* forward
IV: microRNA* reverse

	forward oligo	reverse oligo	template
(a)	A	IV	pRS300
(b)	III	II	pRS300
(c)	I	B	pRS300
(d)	A	B	(a)+(b)+(c)

Figure 36: Method for producing amiRNA

PCR amplification to give cloning product modified from Ossowski et al (2008). Specific primers were designed for I-IV (see appendix 9.2). The amiRNA containing precursor was generated by overlapping PCR. Three separate PCR reactions amplifies reactions (a) to (c), which are listed in the table above. These are subsequently fused in PCR (d) to give an amiRNA fragment containing the sequence for the genes of interest.

Multiple independent transgenic lines were selected based on antibiotic resistance. Eleven independent T3 lines were then screened on low nitrogen and toxic chlorate levels to see whether multiple KO effected root growth. Similar to the single KOs most lines show reduced growth on low nitrogen and increased sensitivity to chlorate, however the phenotype is no more severe than in the single KOs (figure 38), with lines PGWB402Ω miRNA 6, 7 and 9 showing the biggest reduction in growth in low nitrogen, and highest sensitivity to chlorate.

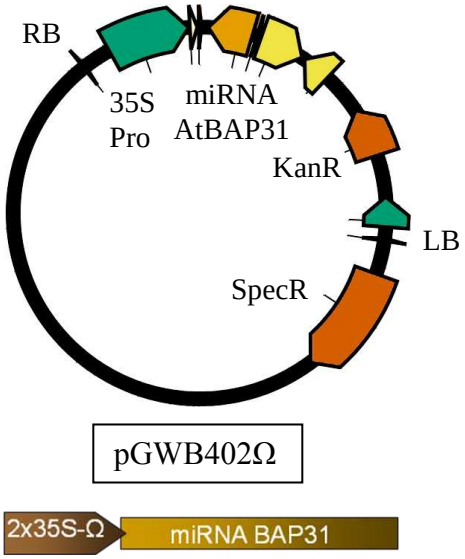

Figure 37: Diagram of constitutive expression vector pGWB402Ω.

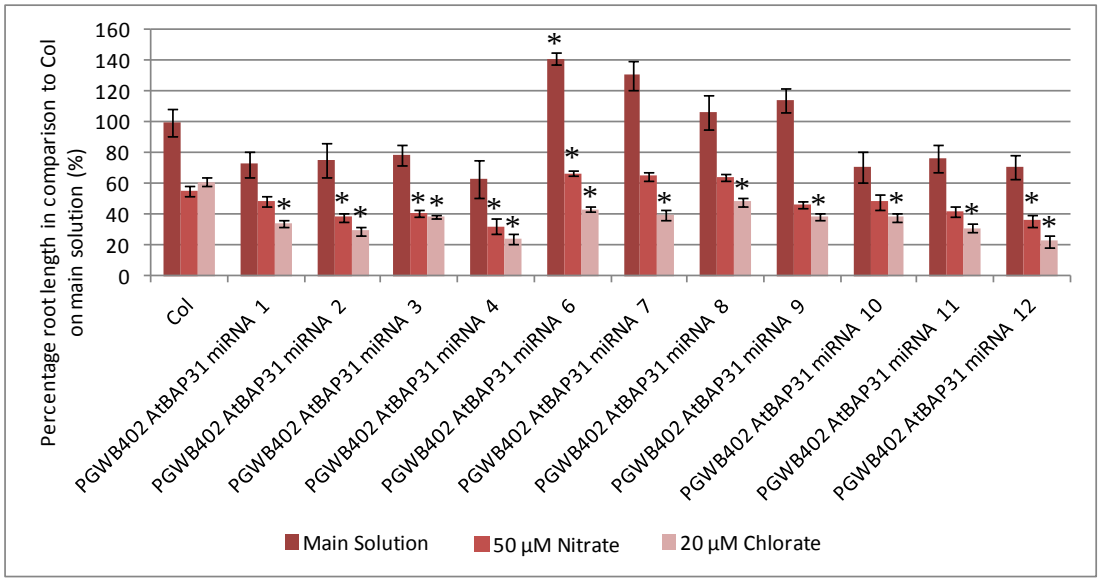

Figure 38: Chlorate toxicity screen in *PGWB402Ω AtBAP31 miRNA* lines

Percentage of growth of *PGWB402Ω AtBAP31 miRNA* lines in comparison to Col on control media (100 %). Error bar represents standard error. Statistical difference represented by asterisks (T-Test; P>0.01), 7 day old seedlings, n = 20.

4.5. AtBPL1 CHARACTERISATION

As only a weak phenotype was observed in the single KOs and amiRNA lines, further analysis was done on BPL1 to discover its role in plants. For biological characterisation of BPL1's role within plants, an antibody was raised against the C-terminal region (the last 109 amino acids). The specificity of the antibody was confirmed by Western blotting using microsomal preparation from root cultures. As shown in figure 39 a strong band at approximately 23 Kd (expected size is 24.6 Kd) was detected in the control but not the bpl1 mutant showing that it is specific to BPL1.

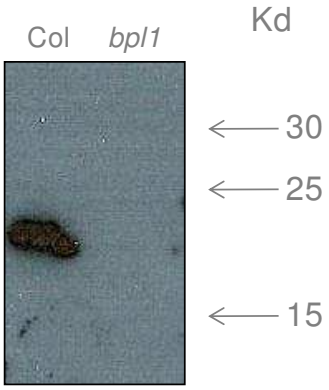

Figure 39: Western blot of BPL1 using anti-BPL1

Western blot of BPL1 using anti-BPL1 primary antibodies (1:1000) and anti-sheep HRP secondary antibodies (1:10000). The blot was exposed for 1 minute. Microsomal fraction prepared from wildtype (Col) and bpl1 root cultures.

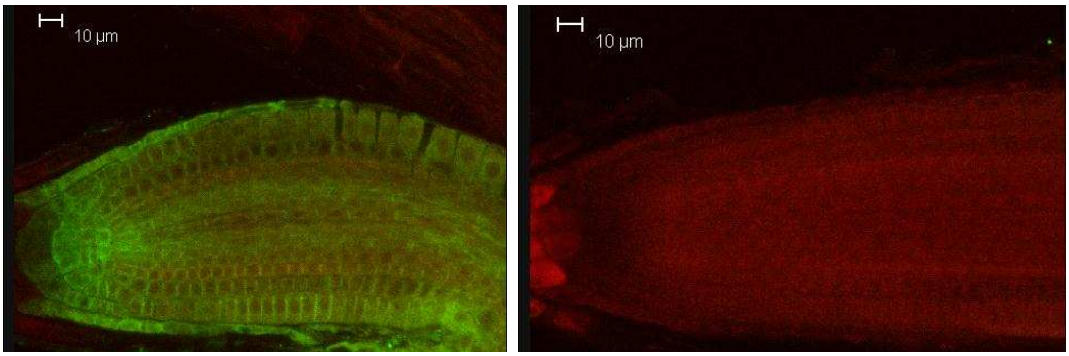

Col bpl1

Figure 40: Whole mount in situ immunolocalization of BPL1 using anti-BPL1

In situ immunolocalization of 3 day old Arabidopsis thaliana root tip using anti-BPL1 antibodies (green) in Wt (Col) and bpl1 mutant.

From the LOPIT dataset, BPL1 is suggested to be a component of the ER (Dunkley et al, 2006). To confirm this whole root in situ immunolocalizations were performed using anti-BPL1. As shown in figure 40 a strong signal was detected in the roots, and no signal was seen in the mutant, again confirming the specificity of the antibody. The ER localisation of BPL1 was further confirmed by co-localisation experiments. As presented in figure 41 BPL1 co-localises with the ER marker (Dharmasiri et al, 2006) AXR4.

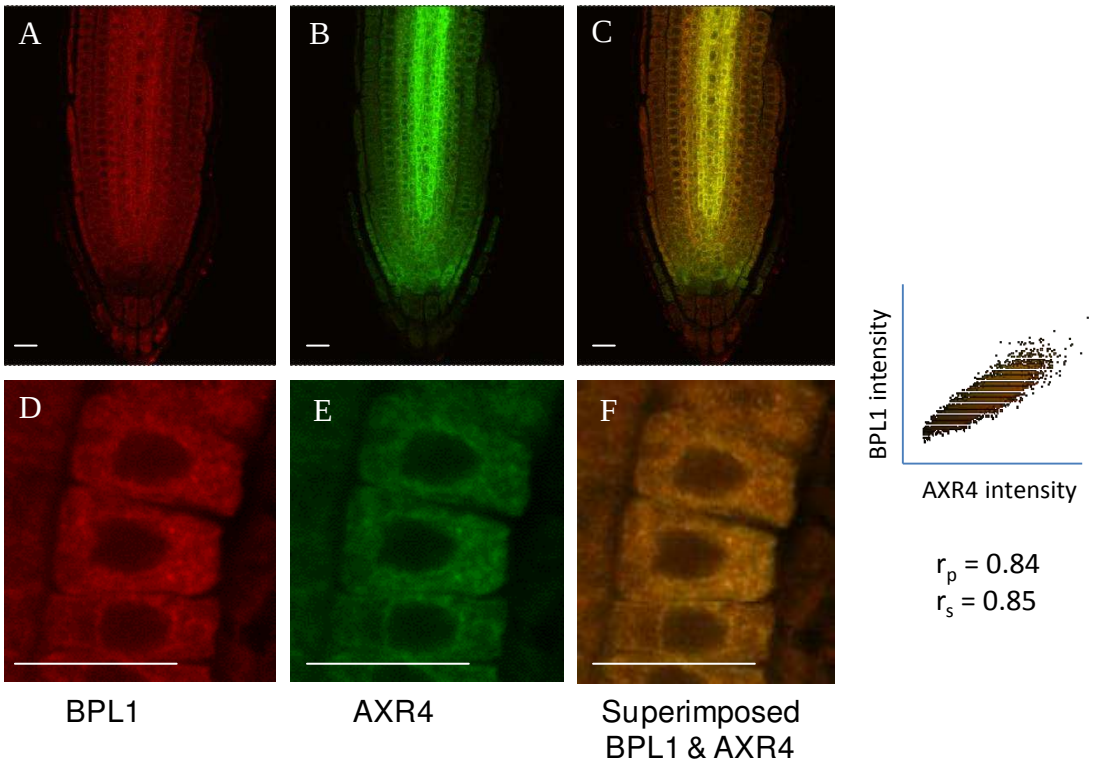

Figure 41: Whole mount in situ immunolocalization of BPL1 compared to AXR4
In situ immunolocalization of Wt (Col) Arabidopsis thaliana root type, showing BPL1 localisation (A & D) using anti-BPL1 (red) in comparison to known ER protein AXR4-GFP localisation (B & E) using anti-GFP (green), C & F represent superimposed images. A-C shows whole root tip, B-F shows zoomed in image of columella cells. Scale bar represents 10 μM. The Pearson correlation coefficient r_p and Spearman correlation coefficient r_s are indicated on the scatter plots, 1 = perfect correlation; PCS colocalisation Image J software (French et al, 2008).

4.5.1. Solubilisation of transmembrane proteins

To further investigate the role of BPL1 as a potential ER accessory protein a co-immunoprecipitation (co-IP) experiment was designed with the aim to identify its interacting partners through mass spectrometry (MS) analysis. To ensure that BPL1 is completely solubilised, a solubilisation study was carried out, using a range of detergents (table 8). Both soluble and insoluble fractions were then analysed by western blotting (figure 42). Results suggest that NP-40 was the most efficient in solubilising BPL1 and was therefore used for all subsequent studies.

Detergent	Class	Concentration (w/v) tested	Fold CMC (mM)
NP-40	Non-ionic	1 %	0.29
Dodecyl-β-maltoside (DDM)	Non-ionic	2 %	6.7
CHAPS	Zwitterionic	0.1 %	4
Triton X-100	Non-ionic	0.2 %	3.6

Table 8: Detergents trialled for BPL1 solubilisation

Table showing detergent, type, class, concentration tested and fold CMC for detergents trailed for BPL1 solubilisation.

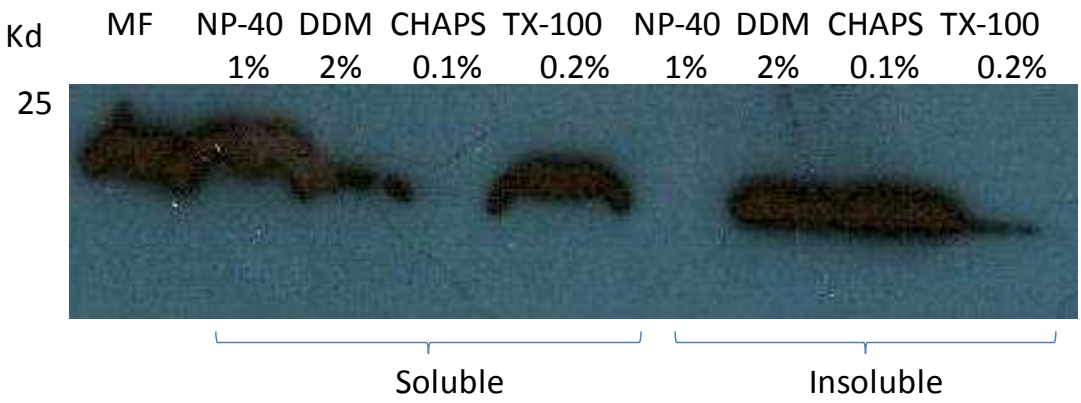

Figure 42: BPL1 protein solubilisation

Detergent solutions were added to Wt microsomal membrane fractions (MF) suspended in solubilisation buffer. These were incubated at 4 ^{o}C for 60 minutes with continuous mixing. The insoluble fraction was separated by centrifugation (100,000 g for 60 minutes) and resuspended in 10 % SDS (w/v) to allow complete solubilisation. Equivalent protein amounts of soluble and insoluble fractions were analysed by SDS-PAGE and western blotting.

4.5.2. Co-immunoprecipitation of BPL1

Co-immunoprecipitation experiments were designed to discern any interacting partners of BPL1, using proteins extracted from Col root cultures. In order to rule out non-specific interactions bpl1 mutant root cultures were used as a control. Root culture microsomal samples were solubilised in 1 % NP-40, and then immunoprecipitated using anti-BPL1 antibody. Part of the sample was analysed by western blot. BPL1 was detected in the Columbia but not in bpl1 mutant, showing that the BPL1 can be specifically immunoprecipitated under these conditions (figure 43). To show that the protein extraction was successful in the bpl1 mutant, a control antibody (AXR4) was used.

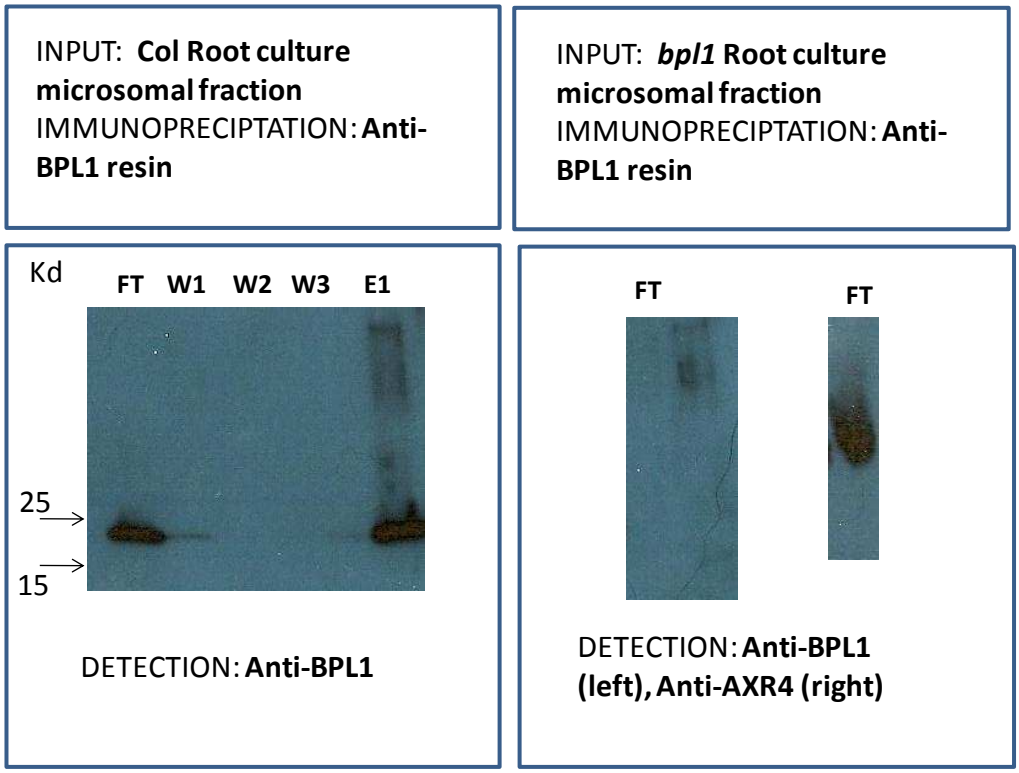

Figure 43: Western detection of BPL1after BPL1 co-immunoprecipitation
The blots were probed with anti-BPL1 at 1:10,000 dilution. A 23 kDa band of BPL1 signal was observed in the elution fraction of the anti-BPL1 pull down. Using bpl1 mutant background there was no signal showing that these antibodies are specific to BPL1. To confirm that protein was loaded on the bpl1 pull down a control protein anti-AXR4 was used. Key: FT = flow through, W1-W3 = washes 1-3, E = elution.

4.5.3. Mass Spectrometry analysis of co-immunoprecipitated BPL1 eluate

Mass spectrometry analysis of the eluate from the co-immunoprecipitation experiment using anti-BPL1 was carried out to discover the identity of any BPL1 interacting proteins. To rule out background the bpl1 mutant was also analysed as a control. Identification and characterization of the eluate by mass spectrometry analysis were conducted on a Q-TOF II mass spectrometer (BioScience Proteomics Unit) to obtain mass spectral and sequence data for the digested peptides. Identification of the fragments and peptides were obtained using MASCOT and BLAST.

Name	Gene	Expression	Localisation	Comments
ESM1 (epithiospecifier modifier 1)	At3g14210	<150	Membrane, apoplast, chloroplast (envelope), vacuole, cytosolic ribosome, nucleus, peroxisome	Carboxylesterase/hydrolase, acting on ester bonds
JR1 (jasmonate-responsive protein)	At3g16470	<300	Membrane, nucleus, chloroplast, vacuole	
Meprin and TRAF homology domain-containing protein/ MATH domain-containing protein	At3g20370	~ 1500	Membrane	
Unknown protein	At5g07170	Unknown	Unknown	
F9L1.43	At1g15480	~80	Unknown	Involved in DNA binding
Atnudt17 (Nudix hydrolase homolog 17)	At2g01670	<300	Unknown	Hydrolase
SWAP (Suppressor-of-white-Apricot)/surp domain contain protein/ D111 / G-patch domain-containing protein	At3g52120	<100	Intracellular	RNA processing
ATCSLC5 (Cellulose-synthase like C5)	At4g31590	~300	Nucleus	Cellulose synthase / transferase, transferring glycosyl groups
MLO15 (Mildew resistance locus O 15)	At2g44110	~300	Membrane	Involved in cell death. Calmodulin binding
BRXL1 (Brevis radix like 1)	At2g35600	<100	Unknown	
ATRBL5 (Arabidopsis rhomboid-like protein 5)	At1g52580	<100	Membrane	
O-methyltransferase family 2 protein	At1g77530	<50	Cytosol	Lignin biosynthesis
Band 7 family protein	At2g03510	~1000	Nucleus, endoplasmic reticulum, plasma membrane	

Table 9: MS analysis from BPL1 co-immunoprecipitation

Mass spectrum analysis of the elute from co-immunoprecipitation with anti-BPL1, showing BPL1 specific proteins.

Most proteins identified were discovered to be found in the control bpl1; however there were a few proteins (13) which were specific to BPL1 at a high probability (table 9). Surprisingly in the mass spec analysis BPL1 itself was not identified, this can be due to a number of reasons as hydrophobic membrane proteins are more difficult to analyse. Protein identification from databases is based on short segments of protein sequence obtained by mass spectrometric analysis of proteolytic peptides, however this is often ineffective with hydrophobic membrane proteins, where protease cleavage sites can be either rare or completely absent (Carroll et al, 2007). While it is not uncommon for transmembrane proteins to be absent from the analyses, it means that these results must be further confirmed. Interestingly a few membrane proteins have been 'pulled' down with BPL1 and these would be an interesting place to start to see if BPL1 is involved in the trafficking of any of these proteins. One of the membrane proteins MLO15 is also involved in cell death, which would be interesting for further study to see whether BPL1 like BAP31 is involved in ER mediated apoptosis.

4.6. DISCUSSION

The AtBPL (BAP31-like) family was discovered in the LOPIT dataset as a potential ER accessory protein target. This family gave a weak nitrogen phenotype with reduced growth in nitrogen deficient conditions, and bioinformatic analysis showed that they contained the BAP31 domain, and showed homology to BAP31. BAP31 is a polytopic integral membrane protein of the endoplasmic reticulum in mammalian cells, and is involved in various cellular functions, such as protein transport, quality control and apoptosis. Although knowledge on the functions of mammalian BAP31 is increasing, there has been little research into the BAP31 homologs in other species. There are at least 12 true or hypothetical proteins in eight different organisms: human, mouse, fruit fly, nematode, baker's yeast, fission yeast, zebra fish and Arabidopsis thaliana (Toikkanen et al, 2006). A BAP31-like protein (At5g42570 - BPL1) was discovered in our LOPIT database search, and AtBPL1 and its 3 family members were characterised to see if it plays a similar role to BAP31 in Arabidopsis thaliana. BPL1 encodes a protein of 212 amino acids, contains a BAP31 domain, and contains the C-terminal KKXX-motif which interacts with COPI vesicles in the

Golgi and returns the protein to the ER, ensuring ER localisation. The family is loosely conserved with only 39-49 % similarity; all containing the KKXX-motif except BPL3, and only BPL4 contains a loosely conserved BAP31 domain.

For further characterisation of BPL1, antibodies were raise against the C-terminal region (last 109 amino acids) of BPL1. The specificity of the antibody was confirmed by western blot and in situ immunolocalization. The calculated molecular weight of BPL1 is 24.6 kD and a band of approximately 23 kD was in the Wt and this band was missing in the bpl1 mutant. BAP31 is localised to the ER and the KKXX-motif in the C-terminal tail of BPL1 suggested that BPL1 could be an ER resident protein.

The other family members of BPL are also predicted to be localised in the ER, and may play a similar role, using promoter GUS analysis, we show that BPL1 and BPL3 have the strongest expression patterns, with localisation throughout the root in BPL3, and in the vascular tissue for BPL1. BPL2 and BPL4 however are a lot weaker, with BPL2 GUS expression undetectable, and BPL4 located just at the root tip. Due to these very specific localisation patterns, it is unlikely that these genes have overlapping functions, and may possibly be involved in the same function but in different locations to allow tightly controlled regulation by the plant. Therefore these KO lines were analysed to see whether they have a BAP31-like function within Arabidopsis thaliana.

Previous studies have demonstrated that there are specific molecular mechanisms, which are required for the export of proteins from the ER to their final destination. Mammalian BAP31 participates in the regulation of protein transport at the ER, causing a delay in the ER to Golgi transport of MHC class I molecules, and preventing the transport of tetraspanins CD9 and CD81 to the plasma membrane (Wakana et al, 2008). BAP31 also has a role in the ER quality control process of a subset of specific proteins, were it is required to mediate ER retention of mutant cystic fibrosis transmembrane conductance regulator (CFTR) (Wang et al, 2008).

A new way of looking at the ERAD system in plants and understanding how it works is to use the bri1-5 mutant which is kept within the ER due to the ERAD system. Hong et al (2008) have shown that by mutating components of the ERAD system such as calnexin, it allows a suppression of the bri1-5 mutant dwarf phenotype, as the mutant protein can escape the ER and function normally. Genetic analysis of double mutants of bri1-5 and bpl family (bri1-5bpl1, bpl1bri1-5, and bpl2bri1-5) showed no suppression of the bri1-5 dwarf phenotype. This suggests that BPL1 and BPL2 do not function as general members of the ERAD system.

BAP31 also has a more specific role as an ER accessory protein, where its absence prevents the transport of transport of tetraspanins CD9 and CD81 to the plasma membrane (Stojanovic et al, 2005). To study this, smart screens using low nutrient and toxic nutrients/heavy metals were designed (see chapter 3), this showed that the BPL family members have a weak nitrogen defect, with reduced growth in low levels of nitrate and an increased sensitivity to chlorate. Chlorate is a toxic mineral which is taken up by the nitrate transporters. This weak phenotype could be due to a mislocalization of a vacuole transporter, preventing sequestration of chlorate away from the metabolically active areas of the cell, and therefore a build up to toxic levels, for example CLCa. However when looking at clca mutant phenotype in comparison to the BPL mutants, there is no increased sensitivity to chlorate under the conditions used. This suggests that BPL family may be affecting more than one vacuole transporter, as CLC a-c, and g are also localised to the vacuole membrane (Lv et al, 2009), or it could possibly be affecting another nitrogen transporter gene.

To further analyse the family's function within the plant, miRNA lines were produced to knock out more than a single gene at a time, and give a stronger phenotype. These lines were screened on low levels of nitrogen and a weak chlorate screen, all showed a weak phenotype with reduced growth on both of the treatments; however none of these showed a more significant phenotype in comparison to the single KOs. Therefore it is likely that the reduced expression levels of all the genes are enough to keep its function.

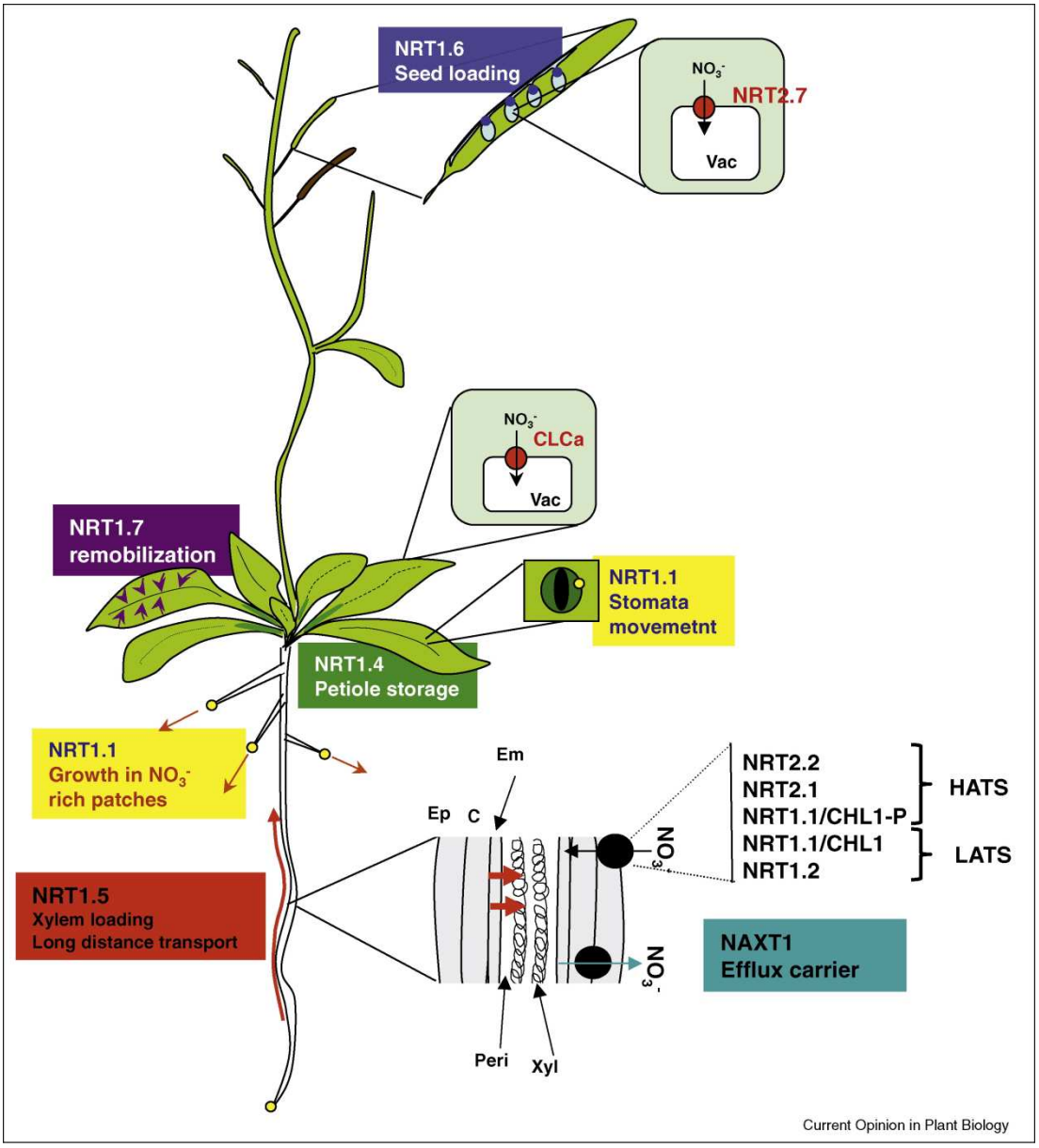

Figure 44: Nitrogen transport within Arabidopsis thaliana

Nitrate transporters within the whole plant (figure taken from Krouk et al, 2010).

Regulation of nitrogen uptake within plants is extremely complex with numerous transporter genes which are up regulated in low or high nitrogen (figure 44). While it does not appear to be involved in the correct localisation of CLCa, or CLCa singularly, it is possible that the BPL family are affecting alternative genes such as the xylem loader NRT1.5. Further investigations looking at the mutants of these nitrogen transporters should allow BPL function to be determined. Analysis of the transporters for immunolocalization in the mutant would also allow us to discover if

any proteins are becoming mislocalized in the mutants. An alternative to this is to do a LOPIT study, comparing wild type to the bpl1 mutant to see if any proteins have their location changed between the two studies, for example becoming localised in the ER rather than the plasma membrane or vacuole.

BPL1 function was also analysed using mass spectrometry on the eluate from the in planta co-immunoprecipitation experiment. This identified 13 proteins that were specific to BPL1 at a high probability, and were not found in the control bpl1. BPL1 itself, however, was not identified in the MS; this can be due to a number of reasons as hydrophobic membrane proteins are more difficult to analysis than soluble proteins. To identify proteins by mass spectrometry, proteolytic peptides are analysed, however in hydrophobic membrane proteins this can be ineffective as protease cleavage sites can be either rare or completely absent (Carroll et al, 2007). While it is not uncommon for transmembrane proteins to be absent from the analyses, it means that these results must be further confirmed. A few membrane proteins have been identified as possible BPL1 targets or interacting partners, and it would be an interesting place to start to see if BPL1 is involved in the trafficking of any of these proteins. One of the membrane proteins MLO15 is also involved in cell death, which would be interesting for further study to see whether BPL1 like BAP31 is involved in ER related apoptosis.

To conclude, 3 out of the 4 members of the BPL family have had single KOs identified, and these all give a subtle nitrogen phenotype, with reduced growth in nitrate limiting conditions and in chlorate toxicity studies. As this family has homology to BAP31 a known ER accessory protein it is possible that they have a similar function within Arabidopsis, involved in the correct localisation of a nitrate transporter. These 4 genes have different expression patterns, and therefore it is possible that they have similar functions but in different cells types to allow tight control. This level of control is often seen in controlling nutrient membrane transporters, with over 53 NRT1 genes involved in nitrogen transport within the plant.

CHAPTER 5

AXR4 REGULATES TRAFFICKING OF THE AUX1/LAX FAMILY

5. AXR4 REGULATES TRAFFICKING OF THE AUX1/LAX FAMILY

5.1. INTRODUCTION

Auxin is regarded to be the most important hormones in plants, involved in every aspect of growth and development, and therefore have been extensively studied. The majority of auxin is synthesised in the tissue of young leaves and requires movement or transport to its sites of action. Auxin is extremely important in a number of auxin-related developmental processes, such as gravitropism, vascular differentiation, and organ development (Benkova et al, 2003; Blilou et al, 2005; Luschnig et al, 1998; Swarup et al, 2005). To achieve this transport, specific auxin influx and efflux carriers are required; such as AUX1/LAX, PIN-FORMED (PIN), and ABCB families (figure 45). Asymmetric distribution of these transport proteins allows formation of gradients or maxima which are important for auxin influence on a number of developmental processes, such as gravitropism (Sorefan et al, 2009; Swarup et al, 2005; Tanaka et al, 2006).

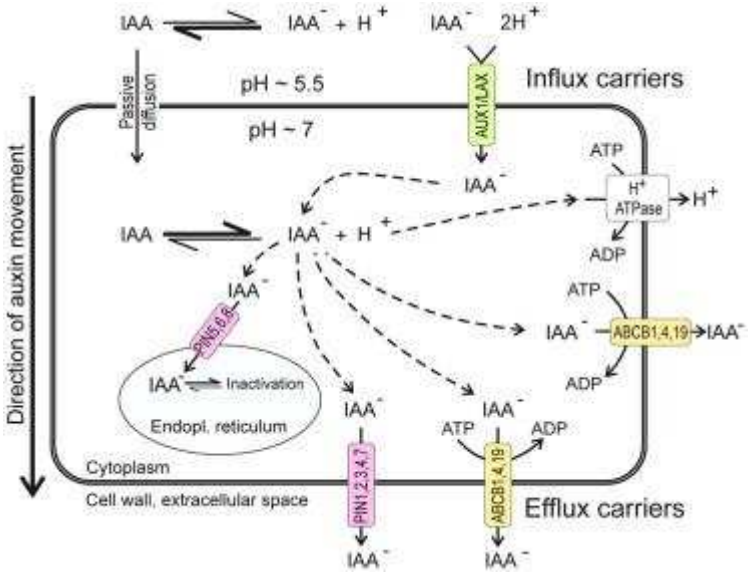

Figure 45: Model of intracellular auxin transport

Figure taken from Friml (2010), undissociated IAA molecules enter cells by passive diffusion, whereas the less lipophilic (less permeable) dissociated auxin anions require transporter proteins. Asymmetric, subcellular localisation of efflux carriers determines direction of auxin flow.

The PIN and ABCB families are involved in auxin efflux within the plant. The PIN comprises of a large number of genes involved in auxin transport, which were originally discovered based on their mutant phenotypes. There are eight family members within Arabidopsis and homologous genes are found throughout the plant kingdom (Paponov et al, 2005). They have roles in the auxin regulated developmental processes, such as root meristem patterning, lateral root organ development, vascular development and embryo development (Benková et al, 2003; Blilou et al, 2005; Friml et al, 2002, 2003; Reinhardt et al, 2003; Sauer et al, 2006; Scarpella et al, 2006; Weijers et al, 2005; Xu et al, 2006) Three members of the MULTIDRUG RESISTANCE/P-GLYCOPROTEIN (ABCB) family have been attributed to auxin transport in plants (ABCB1, ABCB4, and ABCB19), with their mutants showing reduced growth, defects in lateral root formation and gravitropic response (Noh et al, 2001).

The AUX/LAX family of proteins comprise of AUXIN RESISTANT 1 (AUX1) and the LIKE-AUXIN RESISTANT 1 (LAX) group of influx carriers. The aux1 mutant showed reduced sensitivity in root elongation to auxin (Maher and Martindale, 1980), and an agravitropic phenotype that could be rescued by the membrane permeable auxin 1-NAA but not the membrane-impermeable 2,4-D (Marchant et al, 1999; Yamamoto and Yamamoto, 1998). Cloning of the AUX1 gene (485 amino acids) revealed that it shared similarity with a family of amino acid permeases, which have a predicted topology of 11 membrane spanning helices and function by proton symport (Bennett et al, 1996; Young et al, 1999).

Genetic analysis of axr4 and aux1 single and double mutants show that these two proteins function in the same pathway, regulating auxin related root development (Dharmasiri et al, 2006; Hobbie & Estelle, 1995). axr4 mutant have a weak aux1 like phenotype, identified originally in screens for auxin resistance (Hobbie & Estelle, 1995). Both aux1 and axr4 mutant roots are agravitropic, and have a decreased amount of laterals. axr4 mutants similar to aux1 mutants are resistant to applications of auxins that require transporter proteins (2,4-D and IAA), but not membrane permeable auxins (1-NAA), and both mutant phenotypes are rescued by the

application of 1-NAA (Marchant et al, 1999; Yamamoto & Yamamoto, 1998, 1999). Cloning of axr4 revealed a novel transmembrane protein of 473 amino acids which is localised to the ER. Because of these similarities with aux1 it was possible that AXR4 was an auxin influx carrier in its own right, or that it regulated the trafficking or function of AUX1. Dharmisiri et al (2006) showed that AUX1 trafficking was affected in the axr4 mutant background, with accumulation of AUX1 within the ER rather than correct localisation to the plasma membrane. Due to this mislocalization of AUX1 to the ER in the axr4 mutant it was suggested that AXR4 is involved in trafficking of AUX1 to the plasma membrane. Dharmisiri et al (2006) proposed that AXR4 may act as an ER accessory protein for AUX1. ER accessory proteins are ER localised proteins, which are important for the correct localisation of their target proteins. In the absence of the ER accessory proteins their cognate target proteins have been shown to accumulate within the ER (Kota et al, 2007).

The mammalian ER accessory protein RAP is involved in the correct localisation of low-density lipoprotein (LDL) receptor family, its absence causes the LDL receptors to aggregate within the ER (Bu et al, 1995; Bu & Schwartz, 1998). Similarly loss of PHF1 in Arabidopsis leads to abnormal accumulation of its target protein PHT1 (a phosphate transporter) within the ER, and loss of correct localisation to the plasma membrane (González et al, 2005). In yeast, Shr3p is required for the trafficking of amino acid permeases (e.g. Gap1p) to the plasma membrane (Ljungdahl et al, 1992). In the Shr3p mutant Gap1p is no longer folded correctly and the proteins aggregate together, preventing Gap1p from being loaded into COPII vesicles and causing accumulation within the ER.

These ER accessory proteins are highly specific to their cognate target proteins, for example the mammalian TANGO1 ER accessory protein is involved in the correct targeting of collagen VII solely and has been shown not to influence the transport of the related protein collagen I (Saito et al, 2009). Pho86p in yeast has been shown to be highly specific for the regulation of Pho84p, and does not influence the trafficking of other members of the hexose transporter family which Pho84 belongs to (Lau et al, 2000). Dharmasiri et al (2006) provided evidence that AXR4 was specific to

AUX1 as the axr4 mutation had no effect on the localisation of other plasma membrane proteins such as PIN1, PIN2 and H^+-ATPase (figure 46).

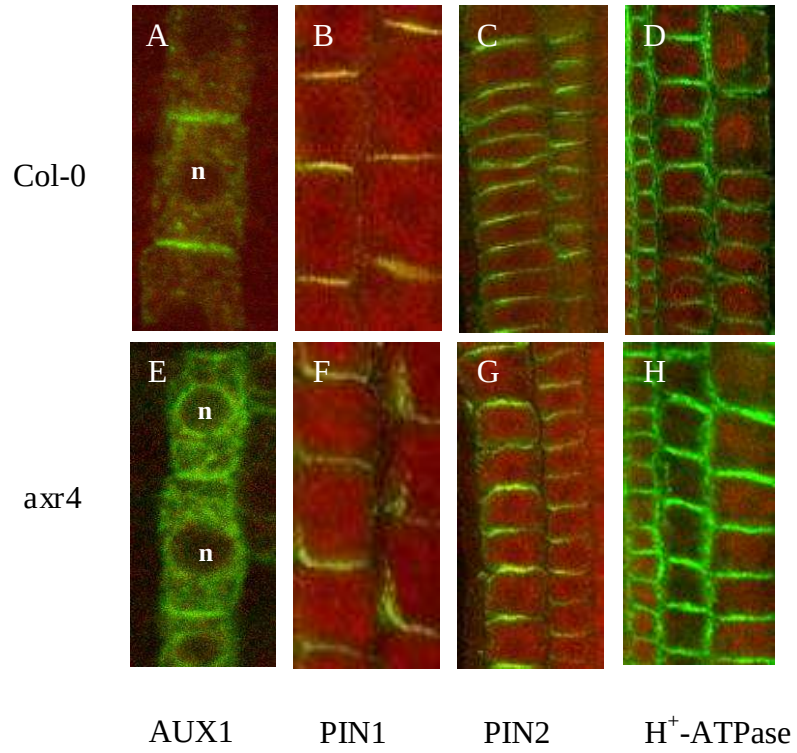

Figure 46: AUX1 trafficking is affected in the axr4 mutant
Hemagglutinin (HA)-AUX1 localisation in the protophloem of Col-0 (A) and axr4-2 (E); PIN1 localisation in Col-0 (B) and axr4-2 (F); PIN2 localisation in Col-0 (C) and axr4-2 (G); and localisation of plasma membrane H^+-ATPase in Col-0 (D) and axr4-2 (H). n = nucleus (from Dharmasiri et al, 2006).

5.2. THE AUX1/LAX FAMILY

AUX1 belongs to a family of auxin influx transporters, the AUX/LAX family, which is made up of four highly conserved genes (figure 47) (Bennett et al, 1996; Carrier et al, 2008; Yang et al, 2006). AUX1 and its homologues LAX1, LAX2 and LAX3 (LIKE AUXIN RESISTANT) are multi membrane spanning proteins (11 transmembrane domains) and share a high level of homology with each other (76-82 %), with well conserved exon/intron boundaries (Péret et al, unpublished). All four genes have a role in auxin transport, with mutants affecting auxin regulated

gravitropism, phyllotaxis and lateral root formation (Bainbridge et al, 2008; Dubrovsky et al, 2006; Marchant et al, 1999; Parry et al, 2001; Reinhardt et al, 2003; Swarup et al, 2003, 2008). aux1 has developmental defects in auxin related root growth, such as root gravitropism and lateral root production (Marchant et al, 2002). lax3 also shows a root phenotype in the mutant, resulting in delayed lateral root emergence. It acts together with AUX1 to regulate lateral root formation, with LAX3 effecting emergence (Swarup et al, 2008) and AUX1 regulating the initiation steps (Marchant et al, 2002).

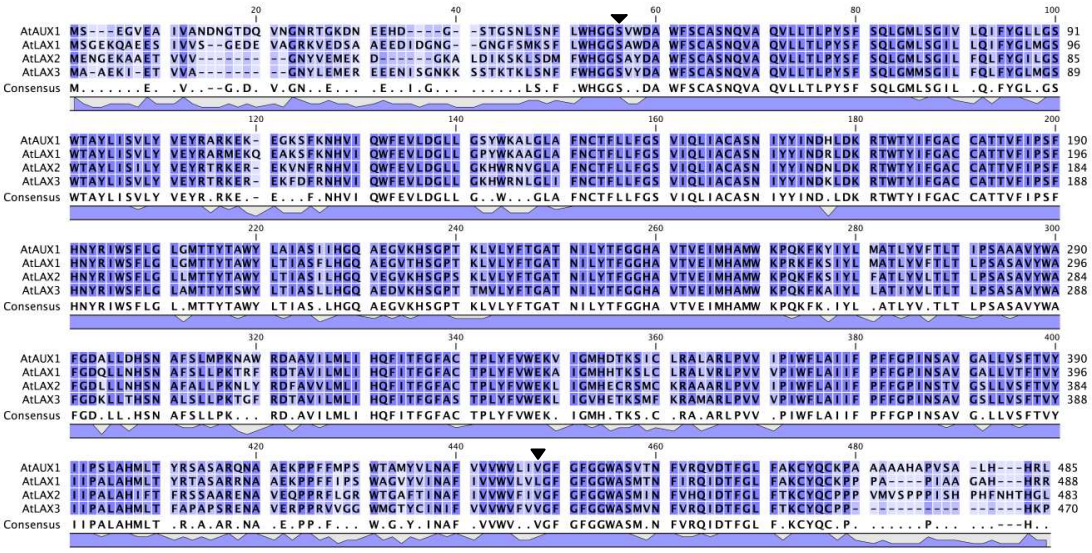

Figure 47: Multiple sequence alignment of AUX1/LAX family
Multiple sequence of AUX1, LAX1, LAX2 and LAX3, dark blue showing conserved residues between the four proteins.

lax1 mutants however have phyllotaxis related defects (Bainbridge et al, 2008) and lax2 mutants have vascular developmental defects in the cotyledons, with a higher propensity of discontinuity in the vascular strands (Péret et al, unpublished). Auxin is known to regulate phyllotaxis and vascular development and many auxin transport mutants have defects in their development (Petrášek & Friml, 2009; Reinhardt, 2003). Therefore all four genes are involved in auxin related developmental processes. In addition to this, recent work has shown that the whole family are capable of transporting IAA in heterologous systems (Péret et al, unpublished; Swarup et al, 2008; Yang et al, 2006), which is consistent with their roles as auxin influx proteins.

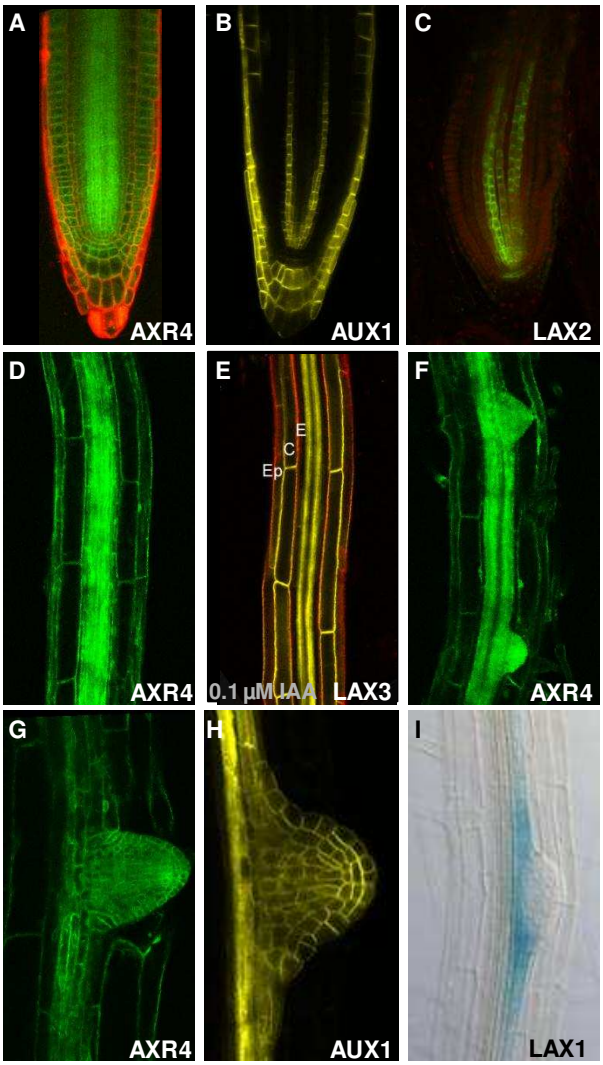

Figure 48: AXR4 and AUX1/LAX family expression domains

AXR4 (A, D, F, G) is expressed in the expression domains of the whole AUX1/LAX family; AUX1 is found in the epidermis, stele, columella, root cap cells (B), and during lateral root development (H); LAX1 is located in mature regions of the primary root vascular tissue (I); LAX2 is found in quiescent centre and columella cells (C), LAX3 is located in the central stele and cortical/epidermal cells when induced by 0.1 µM IAA (E) (Péret et al, unpublished).

Expression studies have shown that the expression patterns of the AUX/LAX genes are mostly non-redundant and complementary within the root (figure 48). Expression studies have revealed that AUX1 is expressed in a variety of tissues, such as the

vascular elements, abaxial epidermis of leaf primordia and meristem L1 layer (Bainbridge et al, 2008; Marchant et al, 2002; Reinhardt et al, 2003), and in the root it has been observed in the epidermis, stele, columella and lateral root cap cells (Swarup et al, 2001, 2005). LAX3 is expressed in the L1 layer of the shoot meristem, and in the root it has been observed in central stele (Bainbridge et al, 2008), and in small groups of cortical and epidermal cells of the root flanking meristem development (Swarup et al, 2008). Recently Péret et al (unpublished) has shown that LAX1 is expressed in the mature regions of the primary root vascular tissues, while LAX2 is located in young vascular tissues, quiescent centre and columella cells. AXR4 is found throughout the root, and its expression patterns overlap with all of the AUX1/LAX family members (figure 48). This posses an interesting question; is AXR4 involved in the trafficking of other members of the AUX1/LAX family.

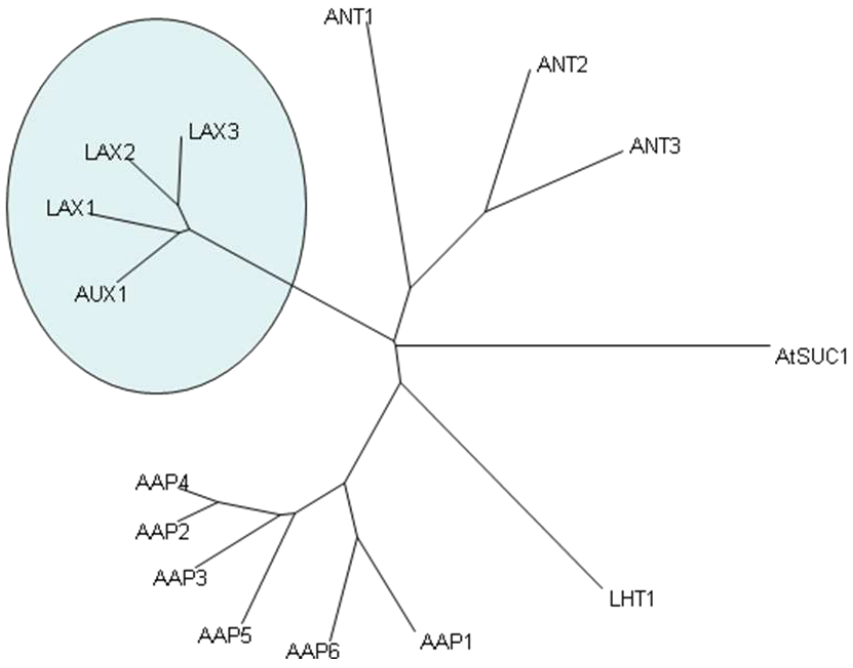

Figure 49: Diagram of amino acid/auxin permease superfamily
AUX1 belongs to a small family of auxin influx carriers within the amino acid/auxin permease superfamily.

The ER accessory protein Shr3p is required for the correct targeting of a whole family (18 members) of the amino acid permease (AAP) within yeast, this is highly

specific as other proteins localisation are unaffected in the Shr3p mutant (Gilstring et al, 1999; Kota & Ljungdahl, 2005). AUX1 belong to a small gene family within the amino acid/auxin permease super family in Arabidopsis (figure 49); therefore it shares similarity with AAP at the protein level (Young et al, 1999). If AXR4 is acting like Shr3p as an ER accessory protein, it may be involved the correct targeting of the whole family.

5.3. AXR4 IS INVOLVED IN THE TRAFFICKING OF THE AUX1/LAX FAMILY.

In order to test if AXR4 regulates the trafficking of other AUX1/LAX genes, LAX2 and LAX3 were localised in the axr4 mutant background. Subcellular fractionation and confocal microscopy studies showed that AUX1 localises at the plasma membrane (Carrier et al, 2009; Swarup et al, 2004), and is mislocalized to the ER in axr4 mutant lines (Dharmasiri et al, 2006). Using a functional LAX3 YFP protein, Swarup et al (2008) have shown that LAX3 is localised to the plasma membrane in cells in front of the lateral root primordia. They also showed that LAX3 expression is auxin inducible, and can be induced by the application of IAA in mature cortical and epidermal cells. To test if AXR4 regulates the trafficking of LAX3, LAX3-YFP was introgressed into the axr4 background, and auxin inducibility of LAX3 was exploited. LAX3 YFP was induced with 0.5 µM 1-NAA for 24 hours in the Wt and axr4 background and then its localisation was studied using confocal laser microscopy.

As shown in figure 50, LAX3 YFP appears to be mislocalized in axr4 mutant. Dharmasiri et al (2006) have shown that AUX1 accumulates within the ER in the axr4 mutant. The cortical and epidermal cells are highly vacuolated making it difficult to determine plasma membrane and ER localisation, however in the axr4 mutant you can see the tell tale localisation around the nucleus which is specific to ER localisation, and you would not see this in a plasma membrane localisation. To test if LAX3 also accumulates in the ER in the axr4 background, in situ co-immunolocalization were done on 4 day old NAA 0.5 µM treated LAX3 YFP (in axr4 background) using ER marker BiP and anti-GFP antibodies. These results show

that LAX3 YFP co-localises with the ER marker BiP in the axr4 mutant background suggesting that like AUX1, LAX3 is also under AXR4 regulation.

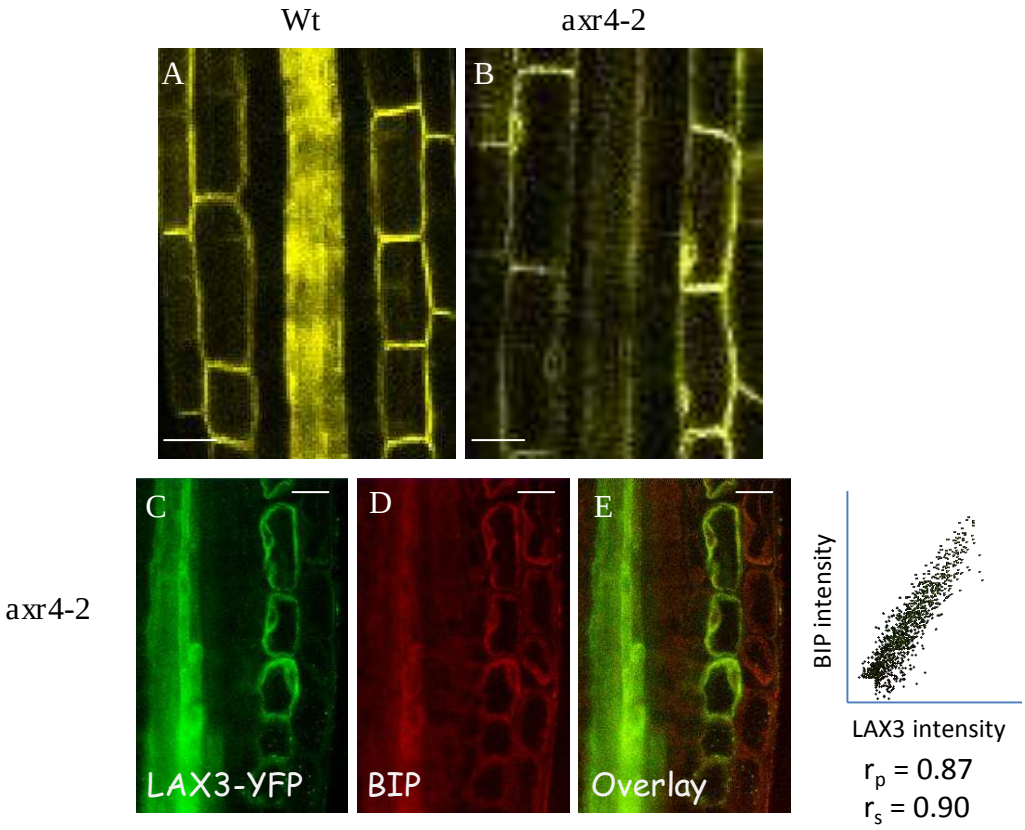

Figure 50: Localisation of LAX3 in Wt and axr4 background

Localisation of LAX3 in 4 day old seedlings using LAX3-YFP tagged line and YFP antibodies, after LAX3 induction with 0.5 µM NAA for 24 hours. Localisation of LAX3 within Wt (A) and axr4 (B) in the vascular and cortical cells. Localisation of LAX3-YFP in axr4 mutant using anti-YFP (C), in comparison to ER localised BIP (anti-BIP) (D), overlay showing LAX3-YFP and BIP (E). Scale bare represents 10 µM. The Pearson correlation coefficient r_p and Spearman correlation coefficient r_s are indicated on the scatter plot, 1 = perfect correlation. PCS colocalisation Image J software (French et al, 2008).

To test if AXR4 also regulates LAX2 targeting, LAX2 was localised in axr4 background by in situ immunolocalization using anti-LAX2 antibodies. LAX2 antibody was provided by Dr. Eric Nielson and has since been raised under the CPIB antibody program (J Oh, MJ Bennett and R Swarup – personal communication). The

results show that LAX2 antibody is very specific and broadly matches the expression of LAX2 GUS. LAX2 has been shown to be expressed in the quiescent centre and columella cells (Péret et al, unpublished).

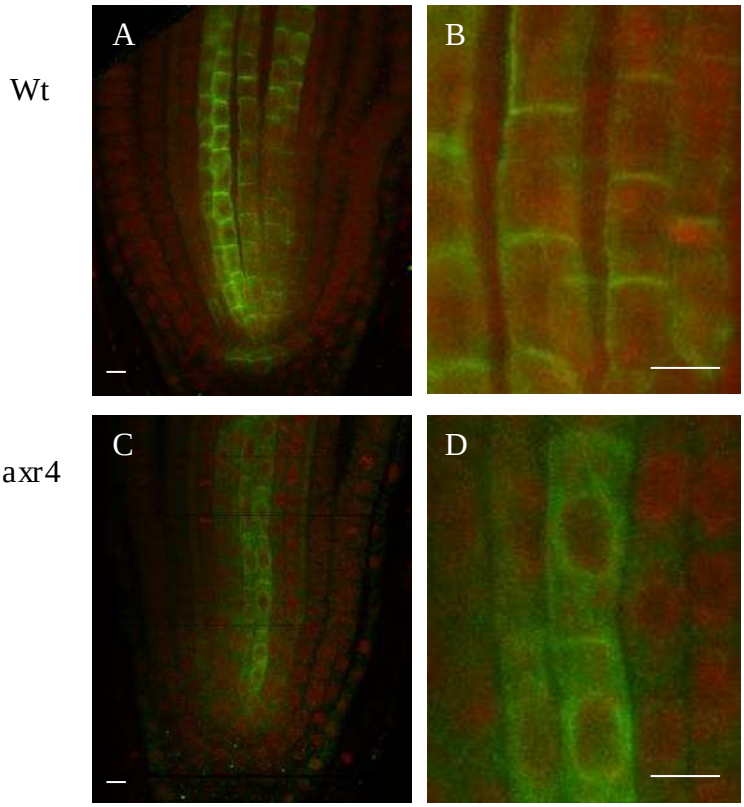

Figure 51: Localisation of LAX2 in Wt and axr4 background
Localisation of LAX2 using LAX2 specific antibodies. Localisation of LAX2 in 4 day old seedlings at the root tip within Wt (A) and axr4 (C). Close up of the columella cells in Wt (B) and axr4 (D). Scale bar represents 10 μM.

As shown in figure 51, LAX2 also appears to be mislocalized in axr4 mutant, giving a similar localisation pattern to AUX1 in the axr4 background (Dharmasiri et al, 2006). To confirm that LAX2 also accumulates in the ER in the axr4 background, in situ co-immunolocalization were done on 4 day old axr4 seedlings using the ER marker BPL1 (Dunkley et al, 2006) and anti-LAX2 (data not shown). These results show that similar to LAX3 and AUX1, LAX2 co-localises with the BPL1 ER marker, suggesting that LAX2 is also under AXR4 regulation. These results suggest that AXR4 is involved in the targeting of LAX2, LAX3 and AUX1, suggesting a

conserved mechanism for trafficking from the ER to the plasma membrane for the AUX1/LAX family.

5.3.1.1.Genetic analysis

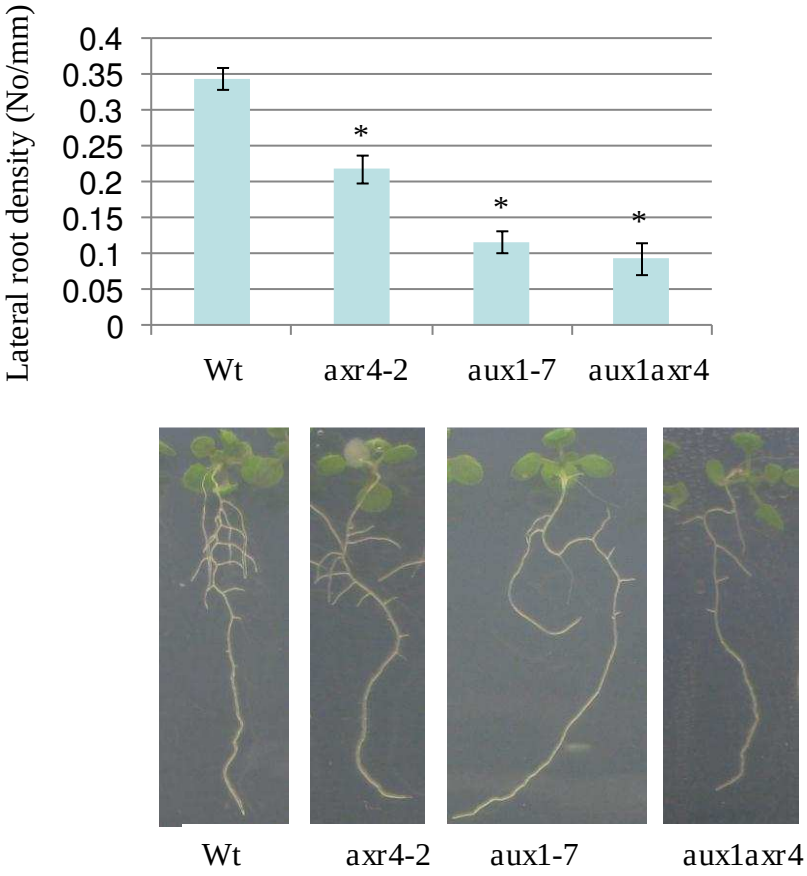

Figure 52: aux1 and axr4 mutant analysis

Showing lateral root density (number of laterals per mm in primary root) in Wt, axr4-2, aux1-7 and aux1axr4 double mutant and comparative images of 12 day old seedlings (bottom). Error bar represents standard error. Statistical difference represented by asterisks (Students T-Test, $P<0.01$), 12 day old seedlings, n =20.

We have shown that AXR4 regulates LAX3 and LAX2 targeting to the plasma membrane; it was therefore investigated to see if like in aux1, axr4 phenocopies lax3 and lax2. lax3 mutants have been shown to have a defect in lateral root emergence (Swarup et al, 2008). Previous studies have shown that axr4 mutants also have a reduction in lateral root numbers, and that the double aux1axr4 mutant have more

severe defect than found in the single mutants (Hobbie & Estelle, 1995) (figure 52). At the time it was not very clear why the double mutant showed an additive phenotype, our localisation results indicate that the additive phenotype may be due to a defect in LAX3 localisation in axr4 background. To test this double lax3axr4 were created and their lateral root phenotype studied. Results show that the lax3axr4 double mutant have a more severe phenotype than single mutants (figure 53), therefore showing that AXR4 is regulating both LAX3 and AUX1 localisation to the plasma membrane.

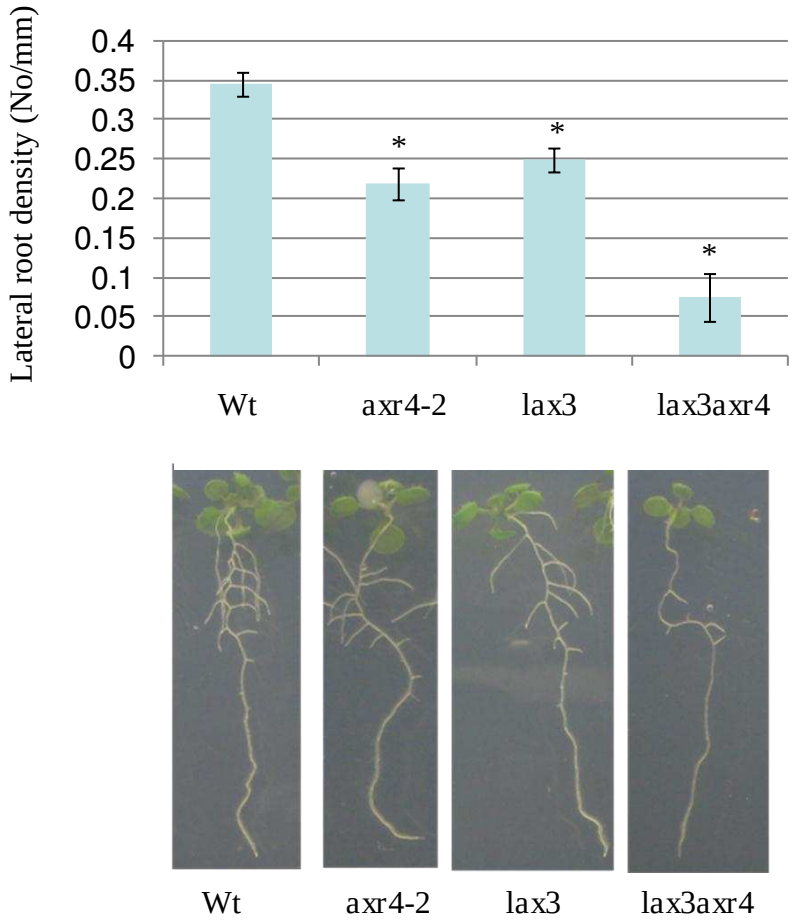

Figure 53: lax3 and axr4 mutant analysis

Showing lateral root density (number of laterals per mm in primary root) in Wt, axr4-2, aux1-7 and aux1axr4 double mutant and comparative images of 12 day old seedlings (bottom). Error bar represents standard error. Statistical difference represented by asterisks (Students T-Test, $P<0.01$), 12 day old seedlings, n =20.

To further probe the role of AXR4 in the regulation of LAX2 targeting, genetic studies were done to test if the axr4 mutant is exhibiting any lax2 related defects, as we have shown that axr4 phenocopies aux1 and lax3 defect. LAX2 promter:GUS studies have shown that LAX2 expression is associated with procambial and vascular tissues during embryogenesis, and lax2 mutants have been shown to have a defect in vascular development in cotyledons (Péret et al, unpublished). As shown in figure 54 compared to control both lax2 and axr4 mutants have a higher propensity of discontinuity in vascular strands. This shows that AXR4 is involved in vascular development in cotyledons, most likely due to the trafficking of LAX2.

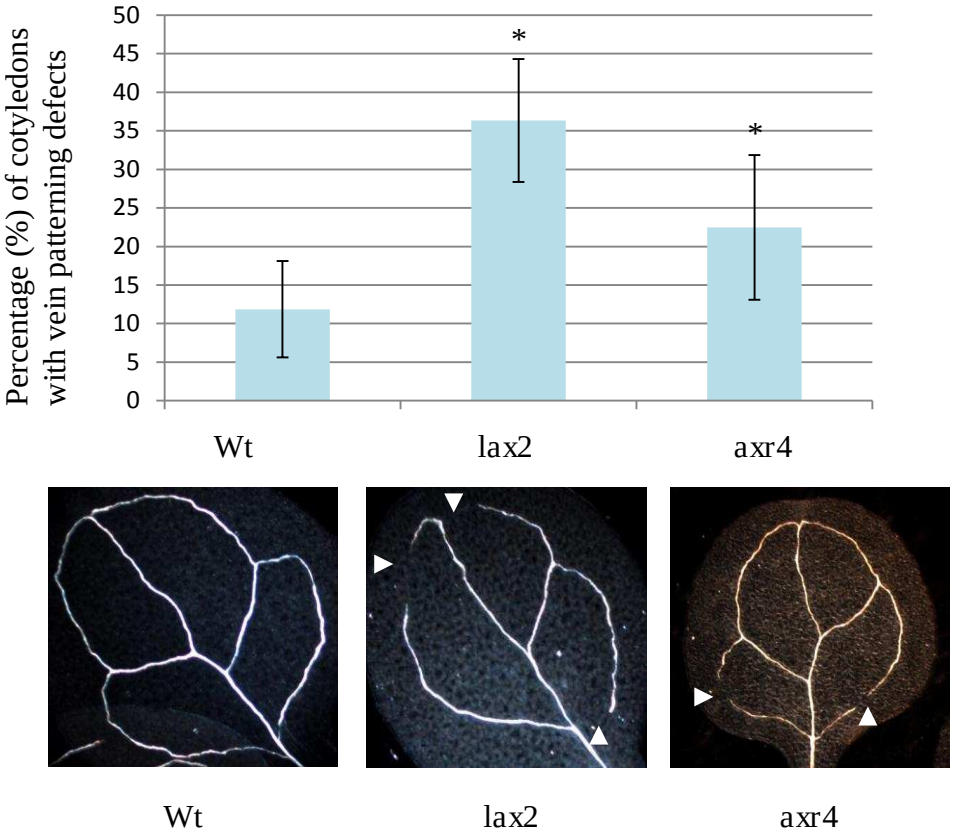

Figure 54: lax2 and axr4 mutant analysis

Percentage of vein breaks in patterning in lax2 and axr4 in comparsion to Wt, with comparative images of 5 day old cotyledons (bottom). Error bar represents standard error, triangle represent vein breakage. Stastical difference represented by asterisks (Students T-Test, $P<0.05$), 5 day old seedlings, n = 100.

5.4. DISCUSSION

Both genetic and physiological data have indicated that AUX1 and AXR4 function together in the same biological process to regulate auxin transport (Dharmasiri et al, 2006; Hobbie & Estellle, 1994). axr4 mutants have a weak aux1 like phenotype, identified originally in screens for auxin resistance (Hobbie & Estelle, 1995). Cloning of axr4 revealed a novel transmembrane protein of 473 amino acids which is localised to the ER. AXR4 has been previously shown by Dharmasiri et al (2006) to be required for the correct targeting of AUX1 to the plasma membrane, and in the absence of AXR4, AUX1 is retained in the ER.

ER accessory proteins are required for the correct targeting of their cognate transporter protein to the correct destination, and achieve this through a number of different mechanisms, such as providing correct tertiary folding or structure, interacting directly with COPII vesicles, or by preventing premature activity/binding (Herrmann et al, 1999). Loss of function of ER accessory proteins often causes an accumulation of their cognate target within the ER, for example RAP, PHFI and Shr3p (Bu et al, 1995; González et al, 2005; Ljungdahl et al, 1992; respectively). The absence of the mammalian RAP ER accessory proteins leads to an aggregation of its target low-density lipoprotein (LDL) receptor family within the ER (Bu et al, 1995; Bu & Schwartz, 1998). Similarly loss of PHF1 in Arabidopsis and Shr3p in yeast causes an abnormal accumulation of their target proteins PHT1 and amino acid permeases, respectively (González et al, 2005; Ljungdahl et al, 1992; respectively). All ER accessory proteins are transmembrane proteins and are located to the ER, however they do not appear to share any more similarity than that, even two proteins from different species involved in the correct trafficking of a phosphate transporter (PHT1 and Pho86; González et al, 2005 and Lau et al, 2000, respectively). As AXR4 is also localised to the ER, contains a transmembrane domain, and is required for the correct localisation of AUX1, it is possible that AXR4 acts as an ER accessory protein for AUX1.

Numerous studies have shown that ER accessory proteins are highly specific to their cognate target proteins. For example Pho86p in yeast has been shown to be highly

specific for the regulation of Pho84p, and does not affect the trafficking of other members of the hexose transporter family (Lau et al, 2000). Mammalian TANGO1 ER accessory protein is involved in the correct targeting of collagen VII and has been shown not to influence the correct transport of a related protein collagen I (Saito et al, 2009). AXR4 has previously been shown to be specific for AUX1, with the mutant not effecting the localisation of other plasma membrane proteins such as PINs and H^+-ATPase (Dharmasiri et al, 2006). This is another line of evidence that AXR4 may be acting as an ER accessory protein for AUX1.

While ER accessory proteins are highly specific to their cognate target, some are involved specifically in the correct trafficking of a whole family of proteins, rather than just a single target. Shr3p for example is involved in the trafficking of the amino acid permeases family (AAP) to the plasma membrane (Ljungdahl et al, 1992). Again this is highly specific only to the 18 members of the AAP gene family within yeast, as other membrane proteins are unaffected in the shr3p mutant (Gilstring et al, 1999; Kota & Ljungdahl, 2005). AUX1 belongs to a small gene family within the amino acid/auxin permease super family in Arabidopsis, and therefore shares similarity with AAP targets of Shr3p (Young et al, 1999), therefore if AXR4 is acting like Shr3p as an ER accessory protein, it may be involved in the trafficking of the whole family.

AUX1 belongs to a family of four highly conserved genes (AUX1, LAX1, LAX2 and LAX3), all of which encode multi-membrane transmembrane proteins that share similarities to amino acid transporters. The family has been shown to be involved in phyllotactic patterning, which is known to be regulated by auxin (Bainbridge et al, 2008). Recently all members of the family have been shown to have auxin uptake activity (Péret et al, unpublished), AUX1 and LAX3 have previously been demonstrated to be high influx auxin carriers (Carrier et al, 2008; Swarup et al, 2008; Yang et al, 2006). All members share a high identity with each other (76-86 %), therefore due to this similarity it is possible that AXR4 is involved in the trafficking of the whole family of proteins. It has also been shown that AXR4 expression patterns is not limited to AUX1 expression, AXR4 is present in LAX1, LAX2 and LAX3 expression domains are well. If AXR4 was only involved in the

trafficking of AUX1 it would likely be limited to AUX1 expression zone, therefore AXR4 could potentially traffic the whole family.

Mutant analysis was done of the AUX1/LAX family and AXR4 to see whether there was any correlation in the phenotype. Out of the four members of the family, only aux1 and lax3 have a mutant root phenotype, with reduced lateral root density, both affecting lateral root development, with AUX1 affecting initiation of lateral roots, and LAX3 is involved in emergence of lateral roots (Marchant et al, 2002; Swarup et al, 2008; respectively). Previous studies by Hobbie & Estelle (1995) have shown that the aux1axr4 double mutant has an additive effect of producing fewer lateral roots than in either single mutant. One possible explanation for this phenotype is that AXR4 is required for the localisation of the other auxin influx carriers within this family (Hobbie, 2006; Parry et al, 2001). The mutant phenotype of lax3 was compared to axr4, and both have a similar weak lateral root phenotype; however the double mutant of lax3axr4 had a severe phenotype similar to that of aux1axr4 suggesting that AXR4 is involved in the correct localisation of LAX3 as well as AUX1.

As mentioned earlier, mutant axr4 cause an accumulation of AUX1 within the ER, preventing it from reaching its final destination. We have shown that the localisation of LAX3 within the axr4 mutant is also mislocalized to the ER. This, with the mutant studies shows that AXR4 is involved in the trafficking of LAX3 as well as AUX1; therefore it may be involved in the trafficking of the whole AUX1/LAX family. No mutant phenotype has been discovered for lax1, and there is no antibody or transgenic line available to study the localisation of LAX1 within the axr4 mutant. However LAX2 does have a mutant phenotype in the cotyledons and antibodies have been raised for this line, allowing localisation within axr4 mutant.

lax2 mutants have a vascular developmental defect in cotyledons, resulting in a higher propensity of discontinuity in the vascular strands. We have shown that similar to aux1, axr4 has a weak lax2 phenotype, with a higher percentage of discontinuity of veins than in Wt. This phenocopy of the lax2 phenotype, suggests that AXR4 may also play a role in the correct trafficking of LAX2. To confirm this,

we looked at the localisation of LAX2 within the axr4 mutant; this showed that similar to AUX1 and LAX3, LAX2 is also mislocalized within the mutant, causing an accumulation of the protein within the ER.

In this study we have shown that AXR4 is also required for two other members of the AUX1/LAX family, LAX2 and LAX3, as well as AUX1 where the axr4 mutant results in these proteins accumulating within the ER. While we currently have no data for LAX1, it is likely that AXR4 functions as a chaperone or accessory protein for the whole family, and is required for their correct localisation.

CHAPTER 6

MODEL FOR AXR4 FUNCTION

6. MODEL FOR AXR4 FUNCTION

6.1. INTRODUCTION

AUXIN RESISTANT4 (axr4) was identified in screens for auxin resistant root elongation, where it showed a similar phenotype to aux1 showing 2,4-D resistance (Hobbie & Estelle, 1995). The axr4 mutant also shares other characteristics with aux1 such as reduced lateral root number, defects in root gravitropism and similar responses to applications of different types of auxin, for example phenotype rescued by application of NAA (Marchant et al. 1999; Yamamoto & Yamamoto, 1998, 1999). As discussed in the previous chapter the aux1 mutant was first identified by Maher & Martindale (1980) as it showed resistance to the herbicide 2,4-D, a synthetic auxin analogue. This was later identified as the AUXIN RESISTANT 1 (AUX1) gene by Bennett et al (1996) and recent work has shown that it encodes a high affinity auxin influx (IAA-H^+ symporter) (Carrier et al, 2008; Yang et al, 2006). Subcellular fractionation and confocal microscopy studies showed that AUX1 localises at the plasma membrane (Carrier et al, 2009; Swarup et al, 2004). However subcellular localisation studies have shown that AXR4 is localised in the endoplasmic reticulum (ER) based on two independent studies (Dharmasiri et al, 2006; Dunkley et al, 2006).

Genetic and mutant studies have suggested that AXR4 and AUX1 are involved in the same pathway (Marchant et al, 1999; Yamamoto & Yamamoto, 1999), and due to the similarities with aux1 it was possible that AXR4 was an auxin influx carrier in its own right, or that it regulated the trafficking or function of AUX1. Dharmisiri et al (2006) showed that AUX1 trafficking was affected in the axr4 mutant background, with accumulation of AUX1 within the ER rather than correct localisation to the plasma membrane. Due to this mislocalization of AUX1 to the ER in the axr4 mutant it was suggested that AXR4 is involved in trafficking of AUX1 to the plasma membrane.

Plant Species	Gene Sequence Name
Arabidopsis	At1g54990
Barley	BQ470218 BQ764572
Cotton	TC101021
Grape	TC91603
Lettuce	TC20522 TC26389
Maize	TC340552
Medicago	TC123134
Popular	TC105021
Potato	TC164950 TC168469
Rice	Os11g34140
Rye	BE704484
Soybean	TC253523
Sugarcane	TC54289
Wheat	BQ246926 CA620981 CA625375 CA726799

Table 10: AXR4-like gene sequences in different plant species
Table showing sequence plant species which contain an AXR4-like gene sequence, obtained using The Gene Index Project – Eukaryotic Gene Orthologs.

AXR4 is a single copy gene within Arabidopsis thaliana, and database searches of genomic databases revealed that it encodes a plant specific protein. Each plant species encodes a single AXR4-like gene (table 10). The AXR4 gene encodes a protein of 473 amino acids and is predicted as a type II membrane protein with one single transmembrane domain located near the N-terminus (spanning between 56-70 amino acids) (figure 55). Two conserved domains have been identified in the AXR4 protein using the NCBI, conserved domains database designed for domain family

analysis (Marchler-Bauer et al, 2009). The analysis revealed two weakly-conserved esterase lipase superfamily domains (figure 56). Esterases and lipases are enzymes which act on carboxylic esters by nucleophilic attack on the carbonyl carbon atom of the ester bond, and are found in several classes of enzymes such as lipid hydrolase/transferases (Holmquist, 2000). The active site of this molecule involves three residues (catalytic triad); a serine, a glutamate or aspartate, and a histidine (Marchler-Bauer et al, 2009).

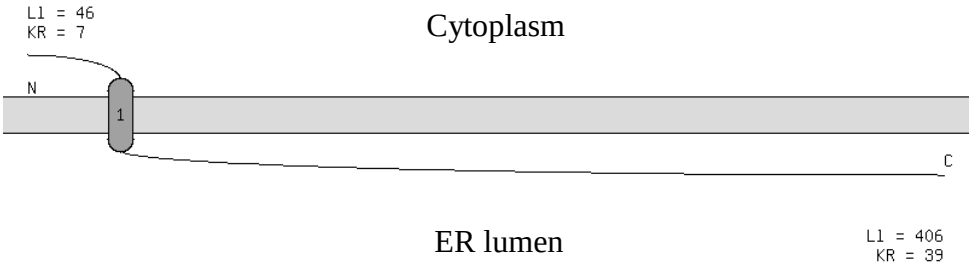

Figure 55: TOPPRED membrane topology analysis of AXR4

TOPPRED predicts that AXR4 is an integral membrane protein with one putative transmembrane domain (Claros and Von Heine, 1994).

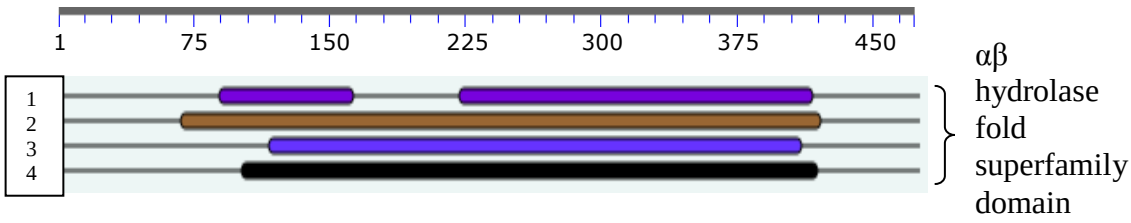

Figure 56: Domain analysis of the AXR4

Domain analysis of AXR4 using Gene3D (1; Yeats et al, 2008); Panther (2; Mi et al, 2005); Pfam (3; Finn et al, 2010); superfamily 1.75 (4; Gough et al, 2001). All analysis revealed a weakly conserved alpha beta hydrolase fold superfamily domain located between ~75 and 420 amino acids of the AXR4 C-terminal cytoplasmic domain.

A few models have been proposed for AXR4 and how it may regulate the trafficking of AUX1. Such as by regulating lipid composition of the endoplasmic reticulum exit site (ERES), having a role as an ER accessory protein or as a post-translational modifying enzyme. AXR4 could affect AUX1 trafficking by regulating the lipid

composition of the ERES. It is believed that the ERES has a different lipid composition to other areas of the ER, allowing exclusion of ER-resident membrane proteins from this area (Ronchi et al, 2008). Affecting the lipid composition would likely have a large effect on all traffic from the ER involving COPII vesicles and it would be unlikely that it would only affect the trafficking of AUX1 from the ER.

Dharmasiri et al (2006) proposed that AXR4 may function as an ER accessory protein and facilitate correct folding of AUX1 in the ER. In yeast it has been shown that Shr3p and Gsf2p are involved in the correct folding of their cargo proteins (AAP and Hxt1p respectively) to allow trafficking from the ER and prevent aggregation of their cargo proteins (Kota & Ljungdahl, 2005). In shr3p mutants its target protein such as Aap1 are no longer folded correctly and the proteins aggregate together within the ER. In addition to the mislocalization of AUX1 in the axr4 mutant, Tendot Abu Baker (2007) has shown that the co-expression of AXR4 and AUX1 in insect cells prevented AUX1 aggregation in vitro in a dose dependent fashion. AAP1 and AUX1 are both transmembrane spanning protein and share reasonable similarity at the protein level. Therefore it is possible that similarly AXR4 may be required to fold AUX1 into the correct tertiary structure required for ER exit and to prevent aggregation of AUX1 within the ER. Despite these similarities between Shr3p and AXR4, there is no similarity either at the protein level or structural level between AXR4 and Shr3p. AXR4 only has one transmembrane spanning region compared to Shr3p and Gsf2p which have multiple transmembrane spanning regions (Ljungdahl et al, 1992; Kota & Ljungdahl, 2005).

Alternatively AXR4 may act as a post-translational modifying enzyme, as AXR4 contains two α/β hydrolase domains within the C-terminus. This domain is found in several classes of proteins including lipid hydrolases and lipid transfereases. Genetic studies suggest that the C-terminal of AXR4 is required for its function, and it is known that C-terminal of AXR4 residues within the ER lumen (Tendot Abu Baker, 2007). Post translation modifications often influence a protein's activity, localisation, turnover and interaction with other proteins. Post translational modifications are events in which primary structure of proteins are covalently modified through proteolytic cleavage, or by the addition or removal of groups such as

phosphorylation, acylation, glycosylation, nitration and ubiquitination (Mann & Jenson, 2003). The addition of mannose 6-phosphate (M6P) residues to soluble acid hydrolases for example is required for the correct sorting of these proteins, by recognition by M6P receptors which allow trafficking from the Golgi to the lysosomes (Braulke & Bonifacino, 2009). While there has been no evidence of post-translational modifications involved in the sorting of multiple membrane-spanning proteins such as AUX1 (Hobbie, 2006), evidence exists that AUX1 may be subjected to post translational modifications. Kargul (1998) showed that plant AUX1 appears to show a reduction in mobility on the SDS-PAGE when compared to recombinant AUX1 expressed in insect cells. It is possible that this shift may be caused by post-translational modification of AUX1 in planta.

In order to investigate the role of the α/β hydrolase fold domain in AXR4 function. Multiple sequence alignment covering over 100 sequences containing α/β hydrolase fold domains was used to identify the most conserved amino acids in AXR4. We then mutagenesised highly conserved amino acids within the α/β hydrolase fold domain

6.2. AXR4 - A POST-TRANSLATIONAL MODIFYING ENZYME?

A multiple sequence alignment of plant AXR4-like genes (20 sequences) suggest that the large C terminal domain of AXR4 is highly conserved (figure 57; appendix 9.6). Within the C-terminus are two α/β hydrolase fold domains which may be important for AXR4 function as a post translational modifying enzyme. To discover highly conserved amino acids within the α/β hydrolase domain, a multiple sequence alignment with proteins containing these esterase lipase domains was performed (approximately 100 proteins). 18 amino acid residues were highly conserved, 9 of these were selected for site directed mutagenesis to probe their role in AXR4 function (figure 58). One of these residues occurs in the catalytic triad HDS, which has been shown to be important for α/β hydrolase domain function.

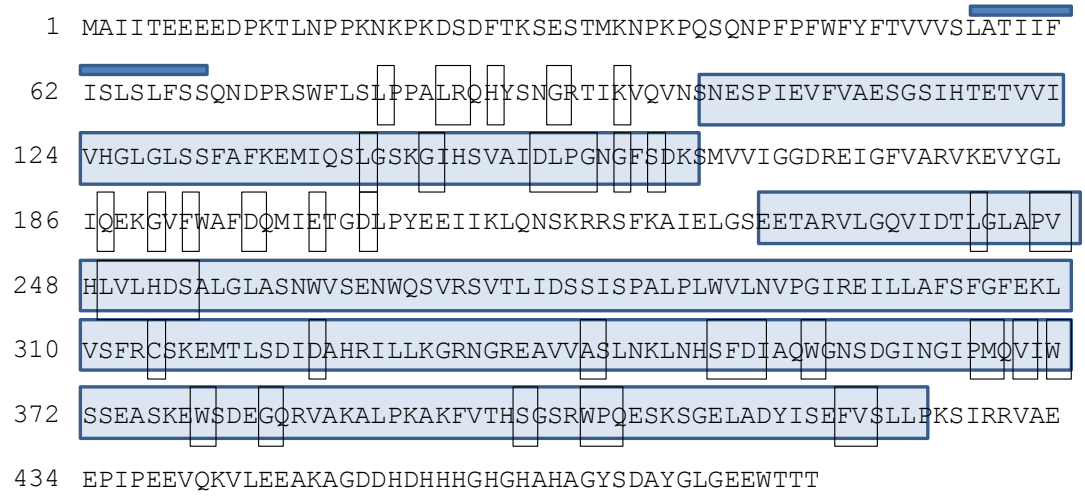

Figure 57: Highly conserved amino acids from multiple sequence alignment of plant AXR4-like sequences

Graphic representation of AtAXR4 showing TM (dark blue box), alpha beta hydrolase domain (light blue box) and highly conserved residues (black outline box) from the multisequence alignment of AXR4-like sequences (for alignment see appendix 9.6).

To probe the role of these amino acids within AXR4 function, a site directed mutagenesis approach was used. Site directed mutagenesis is a highly targeted approach to investigate the function of particular amino acids; however it only results in a single amino acid change. To allow more flexibility within our approach, primers were designed so that random mutations were created at chosen target sites, allowing a single amino acid to be replaced with up to 16 different amino acid combinations (appendix 9.2 for list of primers).

A three step PCR approach was used to generate mutations. PCR product was then cloned into pENTR11 AXR4 GFP replacing Wt gene. Clones were probed for mutated gene (randomly selected), and then over 100 colonies were combined and recombined into PGWB7 GATEWAY^{TM} destination vector (see figure 59). DNA from a pool of colonies was then electroporated into Agrobacterium C58. Transformed plants were screened on kanamycin, and GFP expression was observed to prevent choosing non-sense mutations and frame shifts (or recombinations). Kanamycin and GFP positive seedlings were sequenced to discover the amino acid

change. Creation of the AXR4 random site directed mutagenesis library is illustrated in figure 60.

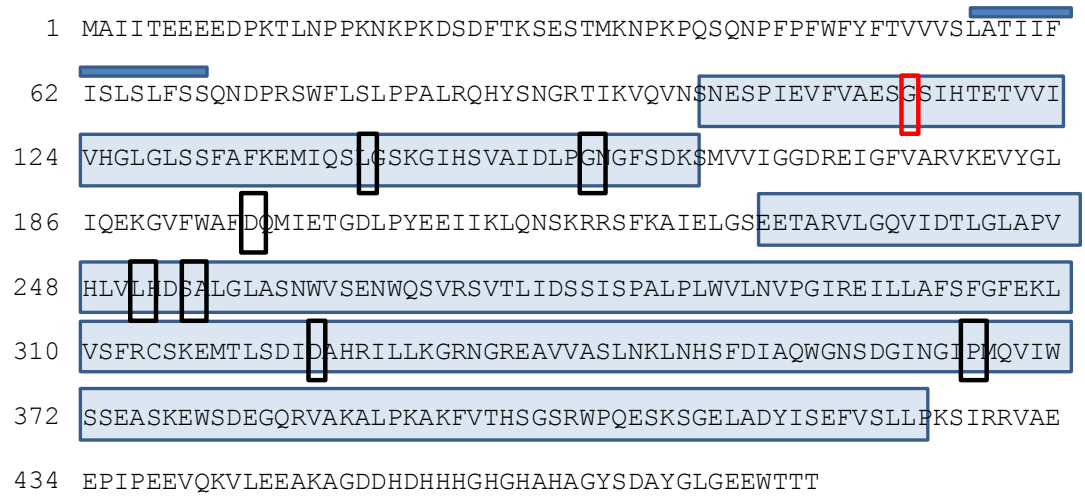

Figure 58: Sites chosen for site directed mutagenesis

Graphic representation of AtAXR4 showing TM (dark blue box), alpha beta hydrolase domain (light blue box) and highly conserved amino acids chosen for site directed mutagenesis (black outline box), and control amino acid (red outline box) from the multisequence alignment of alpha beta hydrolase domain in inter-kingdom species.

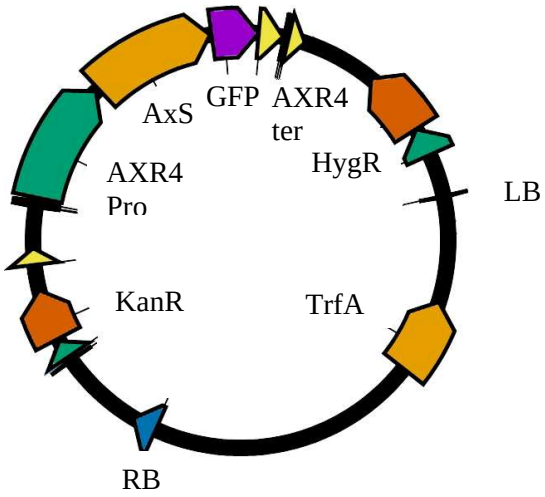

Figure 59: Diagram of PGWB7 pAXR4::AxS-GFP.

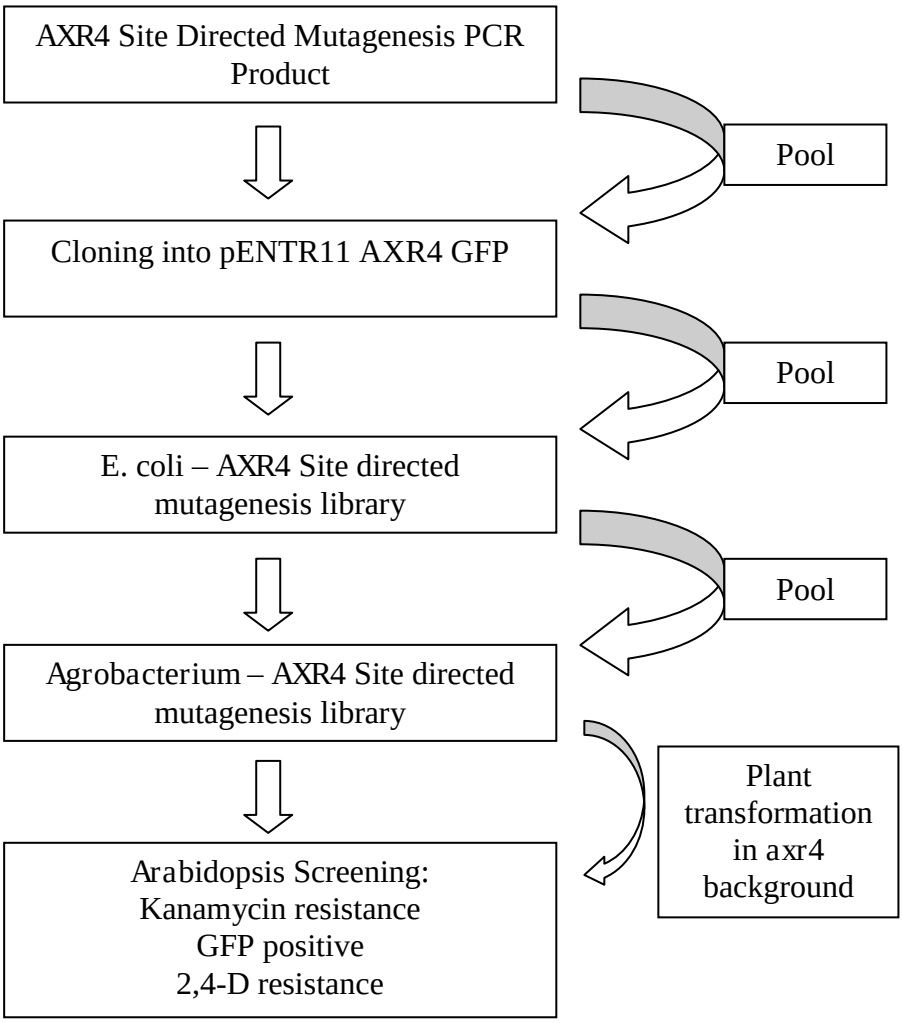

Figure 60: Scheme of random site directed mutagenesis

For the construction of library of AXR4 site directed mutant genes – AxS.

6.2.1. AXR4 site directed mutagenesis

Generation of mutagenesised AXR4 product was achieved through a three step PCR approach whereby specific mutations are introduced in a DNA sequence (site-directed mutagenesis). This is accomplished by PCR amplification using mutagenesis oligonucleotides primers that already incorporate the desired mutation. As the mutagenic primers are incorporated into each new copy of the template DNA during PCR, the result is the amplification of a new, mutated DNA sequence. The primers for this site directed mutagenesis were designed by Primer X and then the first two bases of the amino acid of interest were substituted by 'N', allowing up to 16 different amino acid changes at a single amino acid position.

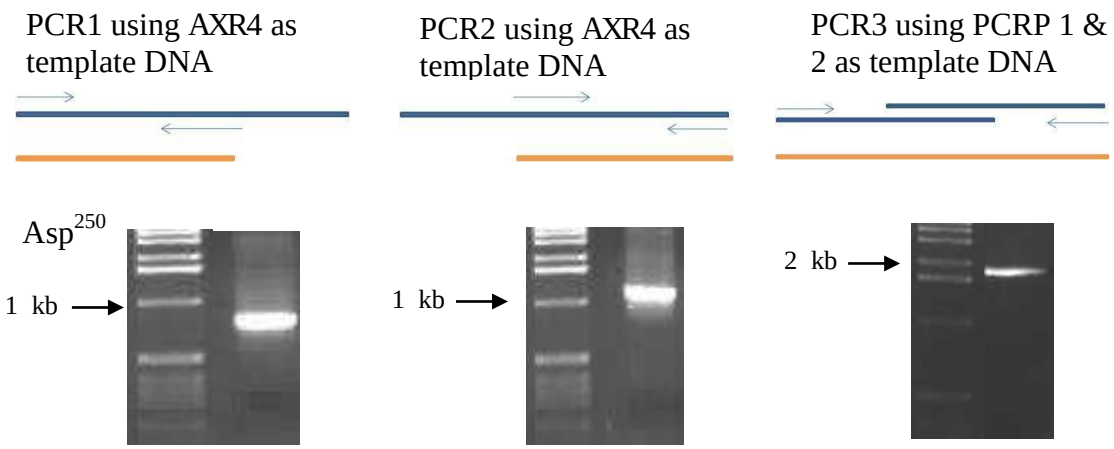

Figure 61: Random Site Directed Mutagenesis protocol
Showing the 3 PCR steps, and an example PCR product from each step. (For all PCR products see appendix 9.7).

A three step PCR approach was used to generate mutations (figure 61). PCR product was then cloned into pENTR11 AXR4 GFP replacing Wt gene. To examine the success of the mutagenesis, the final PCR product was sequenced. Poor quality in the sequencing (Quality 0-9) will indicate the presence of different nucleotides at this specific site showing that the approach has worked (see figure 62 for example).

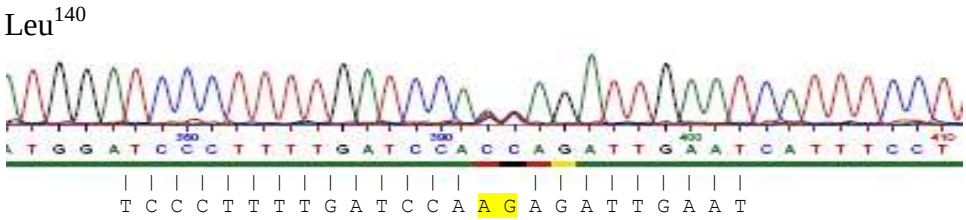

Figure 62: Sequencing result for AxS PCRP
Shows chromograph and blast results for Leu^{140} showing poor sequencing results at the target nucleotides AG, in the sequencing they are shown as CC showing that the approach is working.

6.2.2. Plasmid and expression library construction

PENTR11 Random Site Directed Mutagenesis construct	Normal Codon	New Codon	Wt Amino Acid	Mutated Amino Acid
AxS 113	GGT	GGT	Gly	Gly
		AAT		Asn
		No blast results		
AxS 151	GAT	AAT	Asp	Asn
		GGT		Gly
		GAT		Asp
AxS 246	TTG	ACG	Leu	Thr
		TCG		Ser
		TCG		Ser
AxS 250	GAT	GGT	Asp	Gly
		TCT		Ser
		AGT		Arg
AxS 320	GAT	TCT	Asp	Ser
		CCT		Pro
		AGT		Arg
AxS 361	CCG	ATG	Pro	Met
		CGG		Arg
		TGG		Trp

Table 11: Sequencing results for pENTR11 AxS lines
Sequence from individual colonies of the pENTR11 AXR4::AxS-GFP constructs.

The AXR4 random site directed mutagenesis (AxS) PCR products generated were cloned into pENR11-AXR4::AXR4-GFP construct (Gateway entry vector) between BglII and Asp718 sites replacing the Wt gene (figure 63). Ligated DNA was

transformed into competent DH5α cells, subsequently generating a randomized library consisting of AXR4 mutants. To ensure that the cloning was working efficiently 3 colonies for each site specific mutagenesis were randomly sequenced (table 11). From the results almost all amino acids were replaced with a site specific change, showing that this method is working well. 80-100 colonies were then collected by scraping all the clones together and then inoculated in LB-kanamycin broth, and plasmid extracted

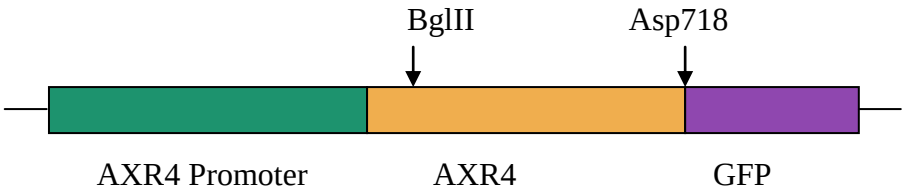

Figure 63: AXR4 gene showing restriction enzyme sites used for cloning.

6.2.3. Cloning into Binary vectors

The resulting pENTR11-AXR4::AXS-GFP plasmids were recombined into PGWB7 destination vector (Nakagawa et al, 2007) using LR reaction and then transformed into competent DH5*α* cells. 80-100 colonies were collected pooled together and plasmid extracted. These constructs were then transformed into C58 Agrobacterium competent cells, and transformed into Arabidopsis (in axr4 and NHA AUX1 axr4 backgrounds). NHA AUX1 axr4 background was used for transformation, so that AUX1 can be localised within the mutant lines to see if it is localised correctly to the plasma membrane or is mislocalized to the ER.

6.2.4. Screening of Site Directed Mutagenesis lines

Primary selection of transformed lines was screened using kanamycin in axr4-2 background and hygromycin in the NHA AUX1 axr4-2 background. Antibiotic resistant T1 seedlings were then checked for GFP expression and then transferred to soil. The T2 seedlings were screened on 2,4-D plates to see whether they could rescue the axr4 mutant phenotype. axr4 mutants are resistant to the inhibitory effect of 2,4-D which prevents root growth. A growth repression curve was initially

performed to identify a concentration for the 2,4-D screen. As shown in figure 64, axr4 roots can be distinguished from Wt roots at 25 nM 2,4-D concentration. At this concentration Wt root growth was inhibited by over 50 % while only having a small inhibitory effect on axr4 and NHA AUX1 axr4. Therefore to enable us to identify lines that may give a partial rescue of AXR4 phenotype in the initial screen, the lower 25 nM 2,4-D concentration was chosen for initial studies, and then rescue confirmed using higher 2,4-D concentrations.

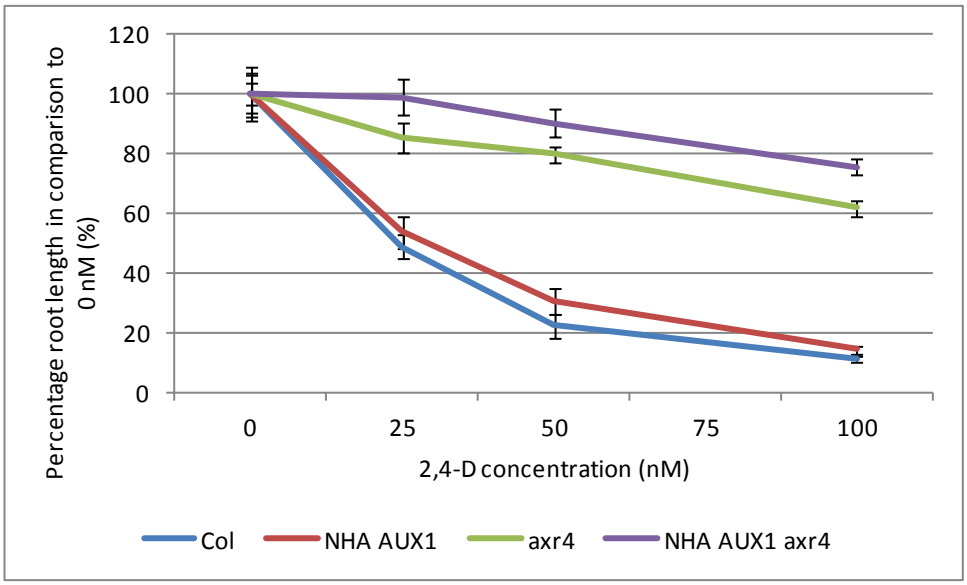

Figure 64: 2,4-D growth response curve

Growth response curve for 2,4-D for axr4, NHA AUX1 axr4, NHA AUX1 and Col, showing percentage growth in comparison to control (0 nM 2,4-D). Error bars represent standard error. 5 day old seedlings used, n = 15.

Amino acid substitution were confirmed by sequencing and several seedlings were transferred to soil for the selection of homozygous lines (see table 12 for a summary of site directed mutagenesis lines). Several homozygous lines were identified and were subsequently used for further studies. A 2,4-D dose response study revealed that the majority of these lines rescue axr4 mutant phenotype (figure 65). Results suggest that some amino acid substitutions results in only a partial rescue at lower 2,4-D concentrations (140 L-V; 154 G-L; 201 D-C; 246 L-A; 246 L-E; 246 L-T). However at 100 nM 2,4-D concentration, all these lines show full rescue of axr4 phenotype. This study suggests that those amino acids do not have an obligate

requirement in AXR4 function. Furthermore, for some of the targets where no homozygous lines have yet been identified, similar observations have also been made on the basis of studies performed in the T2 generation (figure 66). The results presented in figure 66 are based on GFP positive seedlings (therefore allowing identification of mutagenesised AXR4) and suggests that most lines appear to rescue axr4 mutant to some degree.

Amino acid position	Amino acid change
113	Gly → Asn; Gly → Ser
140	Leu → Gly; Leu → Val
154	Gly → Arg; Gly → Gln; Gly → Glu; Gly → Leu; Gly → Lys
201	Asp → Asn; Asp → Cys; Asp → Pro; Asp → Ser
246	Leu → Ala; Leu → Glu; Leu → Thr
250	Asp → Ala; Asp → Asn; Asp → His; Asp → Gly; Asp → Leu; Asp → Phe; Asp → Ser; Asp → Tyr; Asp → Val
320	Asp → Arg; Asp → Asn; Asp → Cys; Asp → Ile; Asp → Ser
361	Pro → Arg; Pro → Glu; Pro → Leu; Pro → Trp

Table 12: Summary of transformed AxS lines.

Interesting, all substitutions at amino acid position 246 result in a weak phenotype at 25 nM 2,4-D suggesting that this amino acid substitution may play an important role in AXR4 function. Another amino acid position of interest is 140, and although a subtle L-V substitution results in only partial rescue of axr4 phenotype, other substitutions on this position appear to rescue the function (figure 66). This is further supported by the in situ immunolocalization studies that show that both LAX2 (figure 68) and NHA-AUX1 (figure 69) localisation are restored at 140 L-V line.

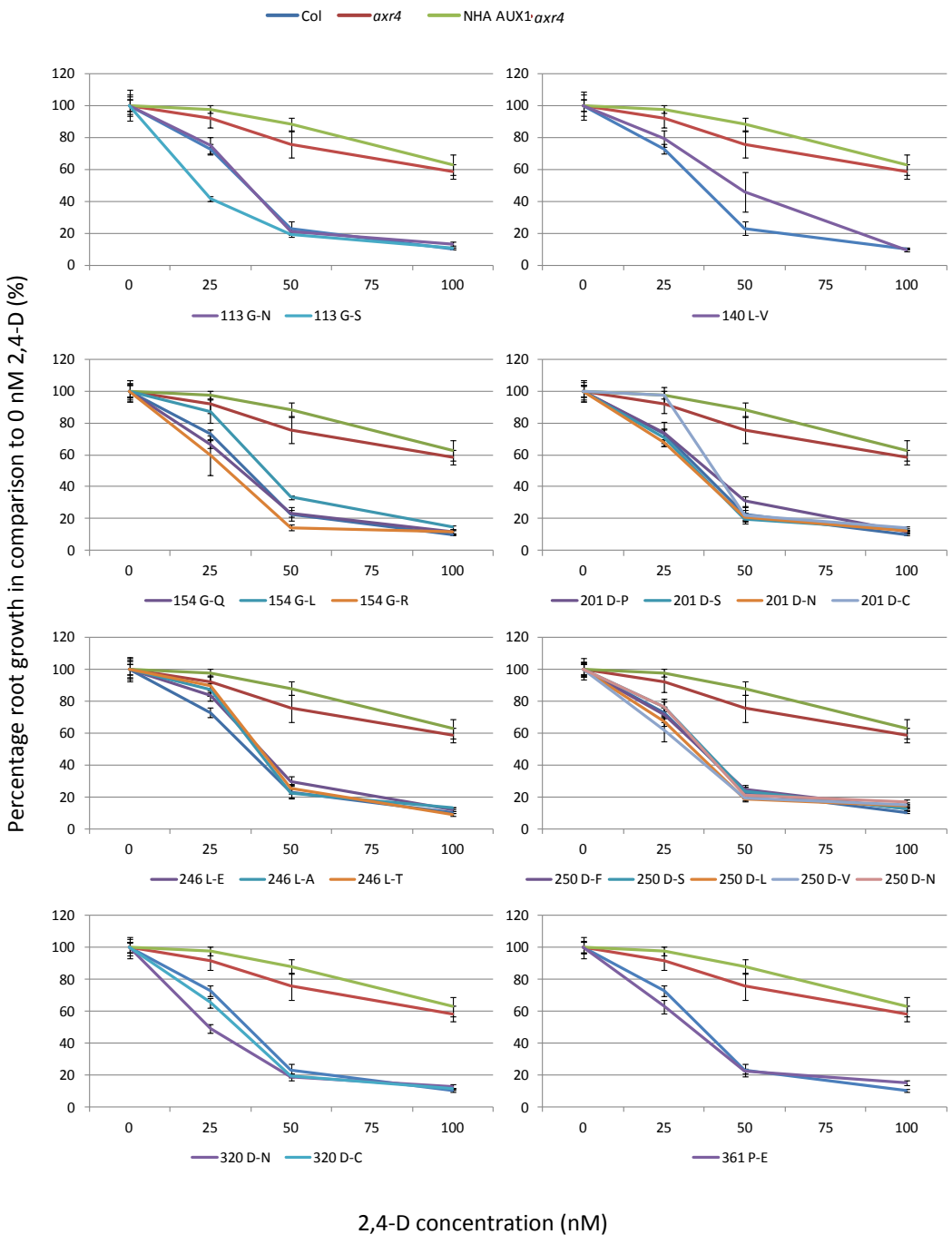

Figure 65: Dose response curve of homozygous AxS transformed lines.

2,4-D dose response screen showing percentage growth compared to control (0 nM 2,4-D on ½ MS) for the AxS (AXR4 site directed mutagenesis) transgenic lines with Col, axr4-2 and NHA AUX1 axr4 as a control. Error bars represent standard error. 5 day old seedlings n = 15.

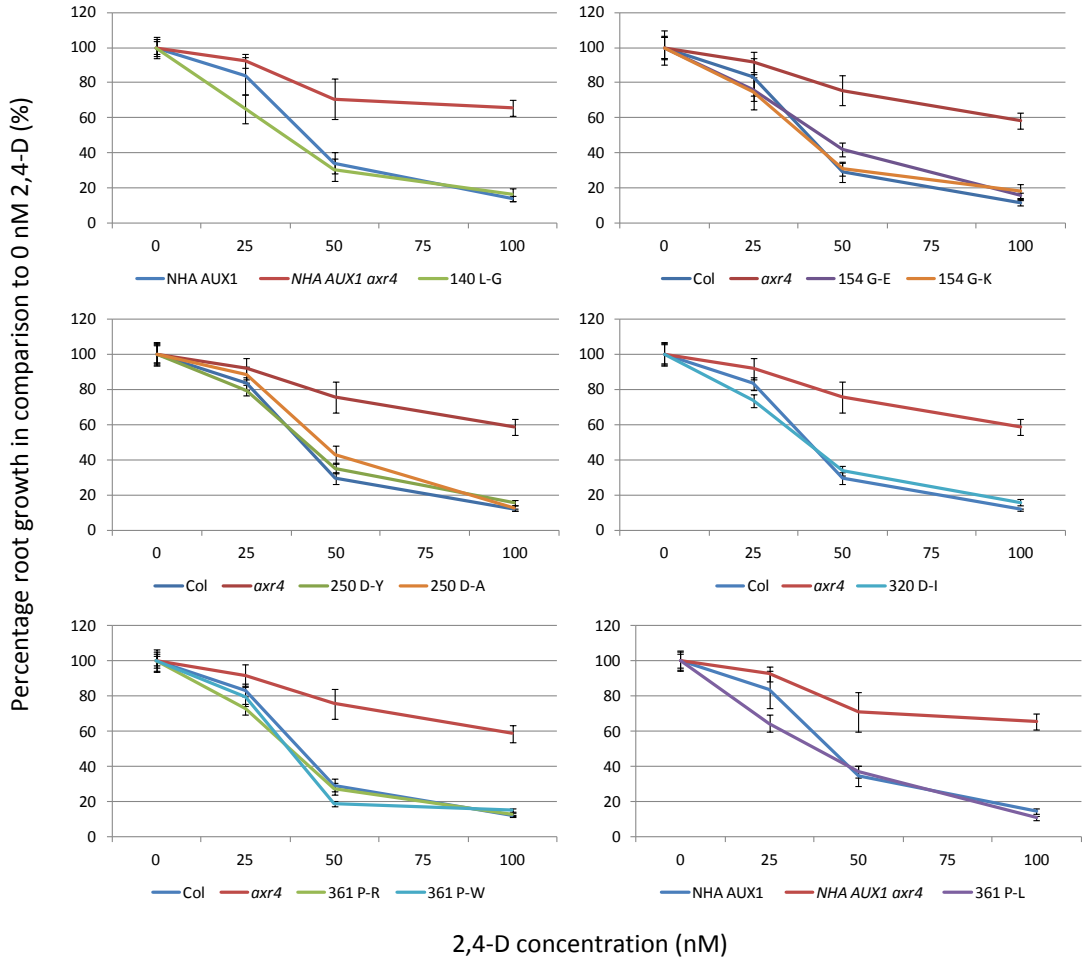

Figure 66: Dose response curve of heterozygous AxS transformed lines
2,4-D dose response screen showing percentage growth compared to control (0 nM 2,4-D on ½ MS) for the AxS (AXR4 site directed mutagenesis) transgenic lines with Col, axr4-2 and NHA AUX1 axr4 as a control. Error bars represent standard error. 5 day old seedlings, n = 15.

As well as looking at the transgenic lines in a dose response 2,4-D screen, their response to gravity was also observed to see if they can rescue axr4 mutant phenotype. axr4 respond slowly to gravity in comparison to wild type (Col), and under the time frame used axr4-2 does not have a gravitropic response. As you can see all the mutants respond to gravity (50 % seedlings) in the ten hour time frame (figure 67), showing that all lines rescue axr4 phenotype. However some lines respond slower than Col, noticeably 201 D-N, 201 D-C and 250 D-S, suggesting that while these lines rescue axr4 they may not be as efficient in AXR4 function, possibly due to small structural changes.

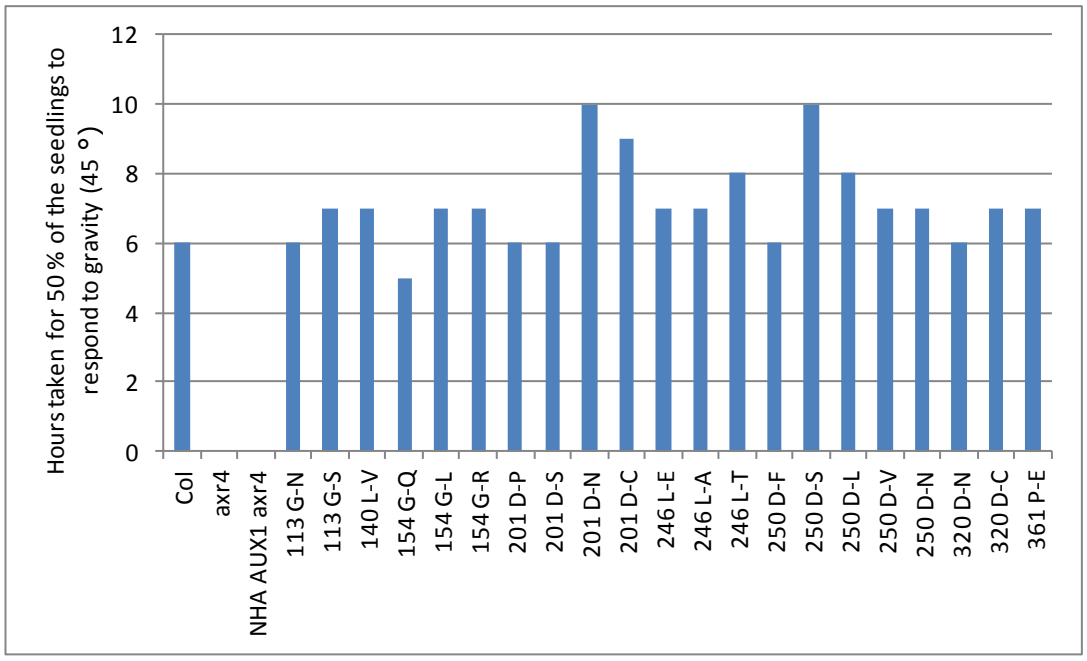

Figure 67: Response to gravity in homozygous AxS transformed lines
Gravity response screen showing hours taken for 50 % of the seedlings to respond to gravity (45 °) for the AxS (AXR4 site directed mutagenesis) transgenic lines with Col, axr4, and NHA AUX1 axr4 as a control. 5 day old seedlings, n = 12.

6.2.5. AUX/LAX localisation in site directed mutants

As discussed in the previous chapter LAX2 and NHA-AUX1 are mislocalized to the ER in the axr4 mutant background. Their localisation was then examined in the lines that gave complete or partial rescue to see if there is any difference in the localisation of these target proteins of AXR4.

From figure 68 it can be seen that LAX2 localisation is completely restored in all lines analysed, giving strong plasma membrane signal. Similarly NHA-AUX1 localisation was also restored in the lines analysed which were transformed into the NHA AUX1 axr4 background (figure 69). These results further support the genetic analysis that AXR4 is functional in the different site directed mutants. It is therefore unlikely that the alpha beta hydrolase fold plays an important role in AXR4 function, and it may be more likely that the actual structure of AXR4 is more important for its

role. To confirm this prediction software was used to look at the 3D structure of AXR4 and the amino acid changes.

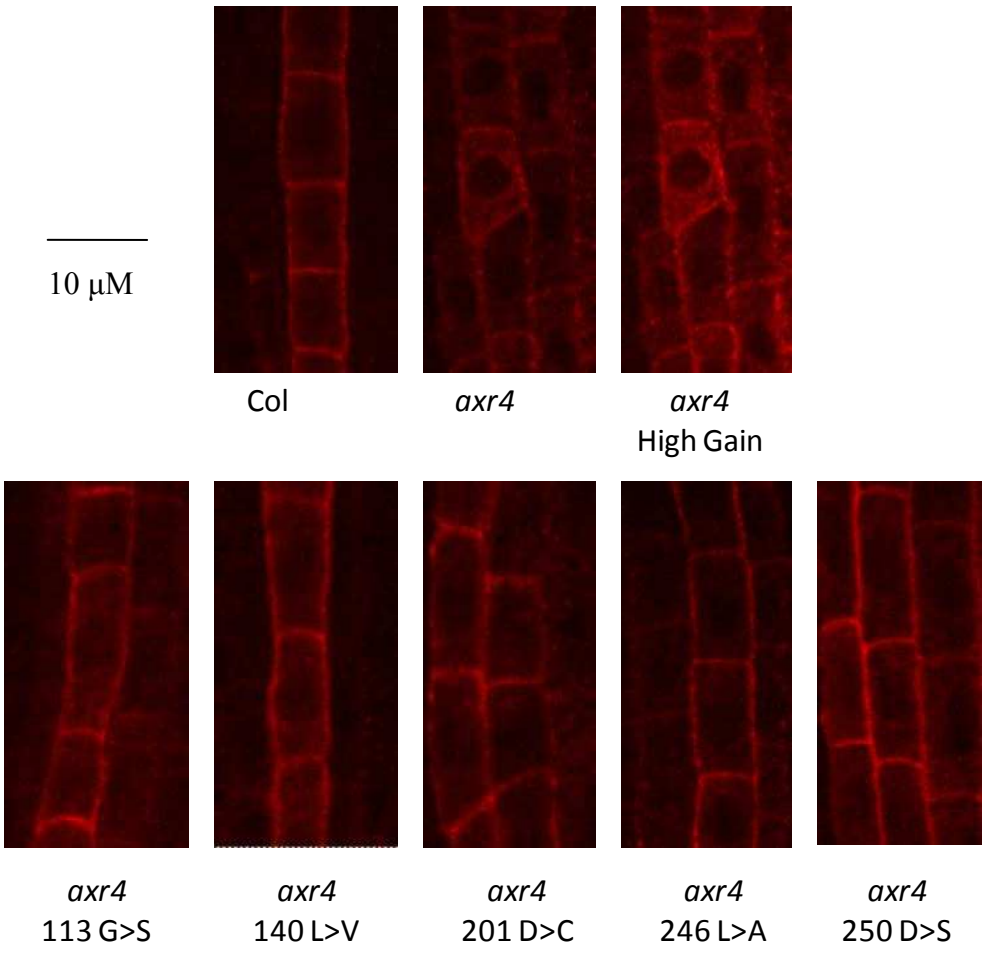

Figure 68: LAX2 localisation in AxS transgenic lines

Localisation of AxS lines (AXR4 site directed mutagenesis), compared to Col and axr4 using anti-LAX2 antibodies in 4 day old seedlings in the columella cells.

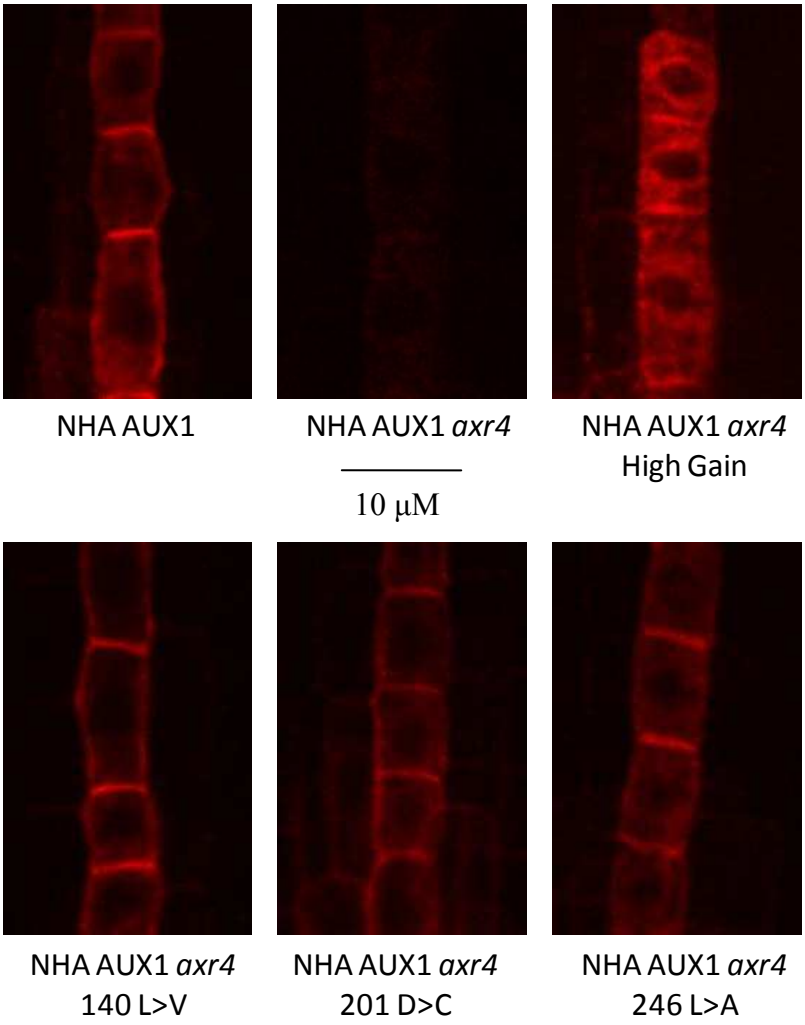

Figure 69: AUX1 NHA localisation in AxS transgenic lines
Localisation of AxS (AXR4 site directed mutagenesis) compared to NHA AUX1 and NHA AUX1 axr4 using anti-HA antibodies in 4 day old seedlings in the protophloem cells.

6.2.6. Protein structure analysis of Site Directed Mutagenesis lines

CPH model 3.0 (Nielsen et al, 2010) was used to predict the 3D structure of AXR4 and the site directed amino acid mutants, so an idea of the effect of the changes on the 3D structure could be analysed. The different amino acid changes were highlighted on the 3D model of AXR4, so positions of the changes could be observed (figure 70). From this, those that are located on the outside of the 3D structure all completely restored axr4 function; therefore it is likely that these positions can take

great variety in amino acid change. However the residues buried deep in the AXR4 structure are those that give varied restoration of axr4 function. Despite giving varied restoration, they all give up to a least 80 % restoration, and therefore even major changes in amino acid used, such as L-E, which appear to change the 3D structure, still allow AXR4 to function (figure 71). Each specific amino acid change was observed and a predicted 3D model was created. From figure 71, although a lot of the amino acid changes cause a loop to become free of the structure, all of them keep the tight bundled structure of AXR4. Therefore it may be this structure itself that allows AXR4 to function, and those that disrupt it in small ways, such as causing a loop to become free, may reduce the efficiency that AXR4 can function, give a slight partial phenotype.

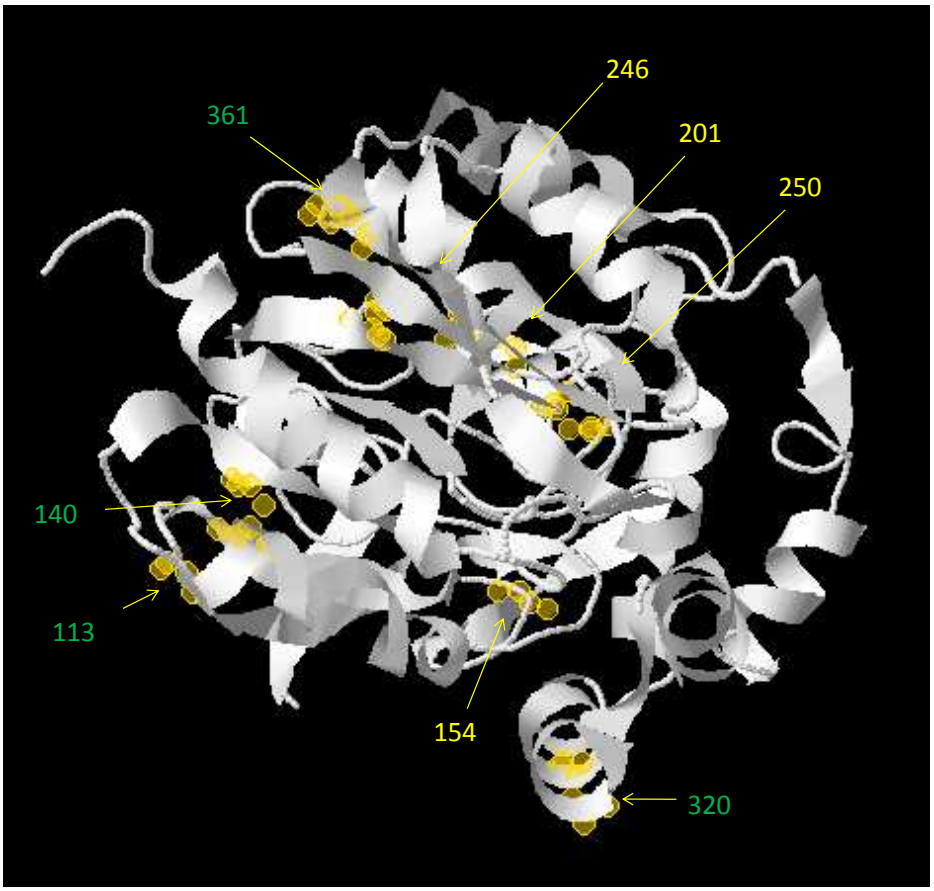

Figure 70: 3D model of AXR4 and a summary of amino acid sites targeted
Amino acid positions marked to whether they all rescue axr4 phenotype (green) or partially rescue axr4 phenotype (yellow).

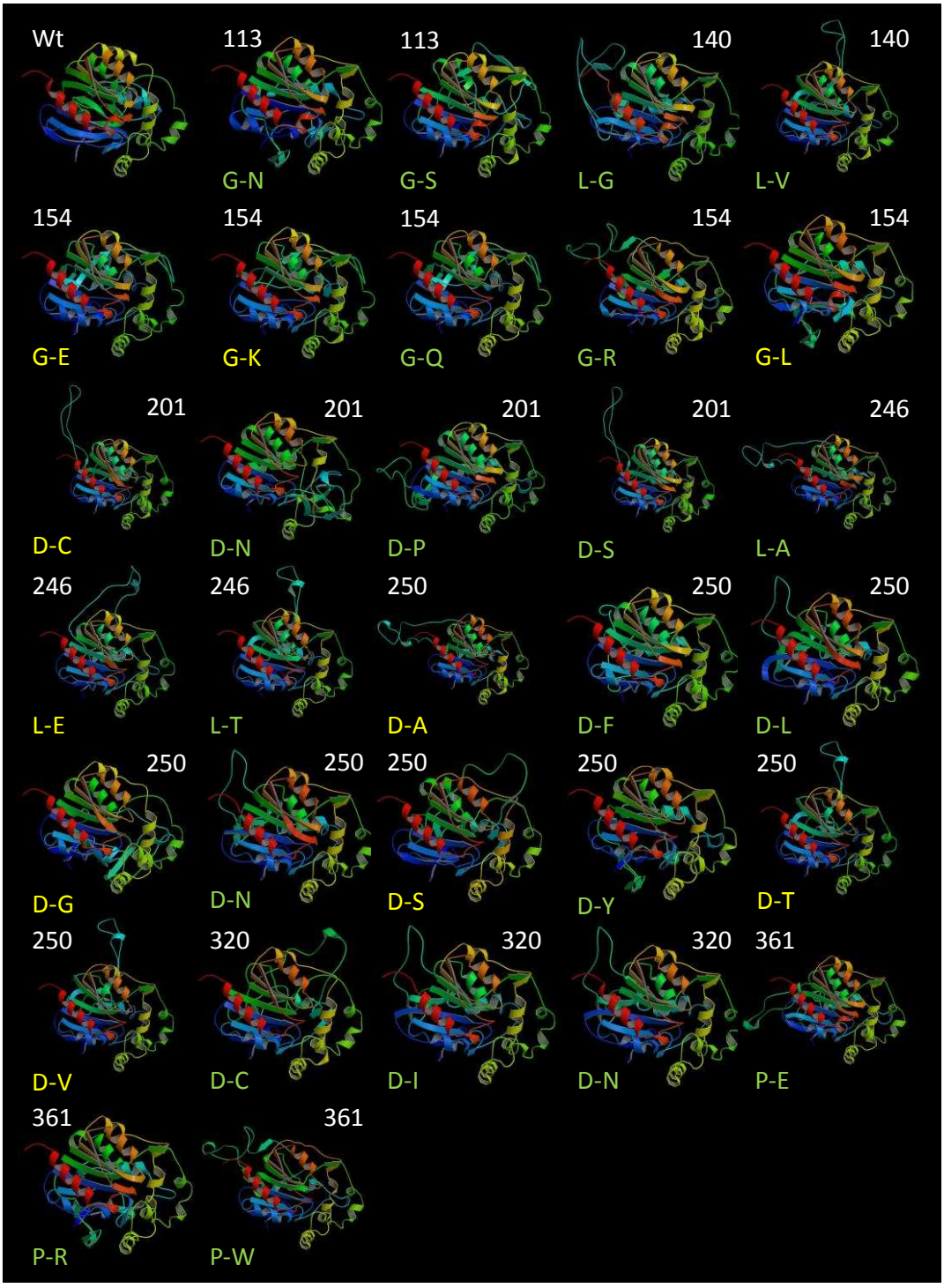

Figure 71: 3D structure of each amino acid change

3D model predicted by CPH models, showing complete rescue (green), or partial rescue (yellow).

Due to the fact that AXR4 can accommodate numerous mutations within the alpha beta hydrolase domain, with all amino acid changes resulting in a functional AXR4

protein, it appears that the domain does not play a role in AXR4 function. It is therefore unlikely that AXR4 is acting as a post translational modifying enzyme, as if it had an enzymatic function, this would be more sensitive to amino acid changes. The alternative hypothesis is that AXR4 is functioning as an ER accessory protein, probably as an ER chaperone, providing correct folding, or preventing AUX1 aggregation.

6.3. AXR4 – AN ER ACCESSORY PROTEIN?

As mentioned previously ER accessory proteins have been shown to be involved in providing correct folding and preventing aggregation. For example the loss of PHF1 in Arabidopsis leads to an abnormal accumulation of its target protein PHT1 (a phosphate transporter) within the ER, and loss of correct localisation to the plasma membrane (González et al, 2005). And other ER accessory proteins have shown that this abnormal accumulation is the result of aggregation, the mammalian low-density lipoprotein (LDL) receptor family aggregates in the ER in the absence of its ER accessory protein RAP (Bu et al, 1995; Bu & Schwartz, 1998). Similarly Shr3p is required for the correct trafficking of amino acid permease (e.g. Gap1p) family (18 members) to the plasma membrane, and its absence cause aggregation of its targets, preventing loading into COPII vesicles and accumulation within the ER (Ljungdahl et al, 1992). AUX1 belongs to the amino acid/auxin permease family within Arabidopsis and shares similarities to Shr3p AAP targets at the protein level; therefore it is possibly that AXR4 is playing a similar role to Shr3p in providing an ER accessory protein function. AXR4 has many similarities with ER accessory proteins, as it is localised to the ER and it is involved in the correct localisation of its target proteins; the AUX1/LAX family, with accumulation of these target proteins within the ER in axr4. Evidence also suggests that AXR4 prevents aggregation of AUX1 in vivo (Tendot Abu Baker, 2007). Kota et al (2007) have shown that Shr3p interacts directly with its targets, therefore to see if AXR4 plays a similar role as an ER accessory protein for AUX1, we looked at co-immunolocalization in vivo and in planta, to look for interaction between the two proteins.

6.3.1. AUX1 and AXR4 interaction in vivo

6.3.1.1. Recombinant AUX1 and AXR4 co-expression in Baculovirus System

The baculovirus expression system has been widely used to produce recombinant functional heterologous proteins, giving high expression levels (Hunte et al, 2003; reviewed by Hu, 2005). The baculovirus system is advantageous as insect cells are higher eukaryotes and possess post translational modification activities, allowing correct folding, oligomerisation and modifications, producing recombinant proteins that are antigenically, immunologically and functionally similar to the homologous proteins. Once baculovirus have infected insect cells, the viral DNA un-coats, highjack's the cell protein production machinery and replicates.

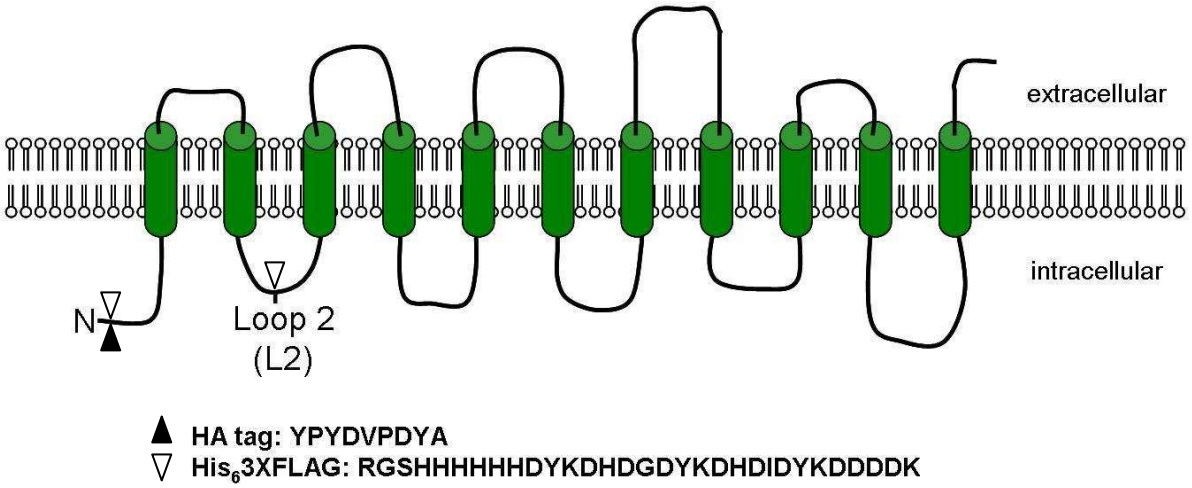

Figure 72: Diagram of AUX1 showing sequence tag positions
Diagrammatic representation of AUX1 showing position of epitope tags (HA or $His_6$3XFLAG) either at amino acid position 3 (N) or 116 (L2). The predicted membrane topology of AUX1 is shown with TM helices represented as cylinders (Swarup et al, 2004).

In order to gain more insight into the interactions between AUX1 and AXR4, co-expression studies were carried out using the baculovirus expression system. Co-

expression is accomplished by infecting the same insect cell with AUX1 and AXR4 viruses. The following three AUX1 constructs were used; N-HA-AUX1; N-$His_6$3xFLAG-AUX1; L2-$His_6$3xFLAG-AUX1 (figure 72); and one AXR4 construct; His_6HA-AXR4 (Carrier, 2009; Tendot Abu Baker, 2007).

For the co-expression study Sf9 insect cell cultures were infected with AUX1 and/or AXR4 at 0.1, 1 or 10 MOI (multiplicity of infection – the ratio of viral particles to Sf9 cells) based on titre of viruses (table 13). The viruses were optimised based on expression levels so that equal concentrations of proteins were used for co-expression.

Virus	P3 Titre (pfu/ml)
AXR4-HA-His	2×10^9
AUX1-N-His-FLAG	2×10^9
AUX1-L2-His-FLAG	1×10^9
NHA-AUX1	2×10^9

Table 13: Titre of virus stocks
Titre of the AXR4-HA-His, AUX1-N-His-FLAG, AUX1-L2-His-FLAG, NHA AUX1 viruses. Data courtesy of Dr Ian Kerr (Nottingham University).

Western blots were performed to confirm the expression of tagged AUX1 and AXR4 protein. Cells were harvested by centrifugation after 48 hours; lysed and 20 μg of the cell lysate was loaded and separated on 15 % SDS-PAGE gel followed by blotting onto a nitrocellulose membrane. Western detection of proteins was performed using anti-FLAG (1:2000 dilution), anti-His (1:1000 dilution), anti-HA (1:1000 dilution), and anti-AXR4 (1:10000 dilution) antibodies.

Figure 73 shows the immunodetection of AXR4-HA-His, AUX1-N-His-FLAG, AUX1-L2-His-FLAG and AUX1-HA, using anti-HA, anti-FLAG, anti-HIS and anti-AXR4 antibodies after infection. A ~ 55 kDa band corresponding to the recombinant AXR4 protein was detected in the blot with anti-HA, anti-His and anti-AXR4 (shown by the arrow). As shown in figure 73 anti-AXR4 is a highly specific for AXR4 and

works well at low titre. A ~ 48 kDa band corresponding to the recombinant AUX1 protein was detected in the blot with anti-HA, anti-His and anti-FLAG (shown by the star). MOI for each construct was chosen based on equal expression on western blot.

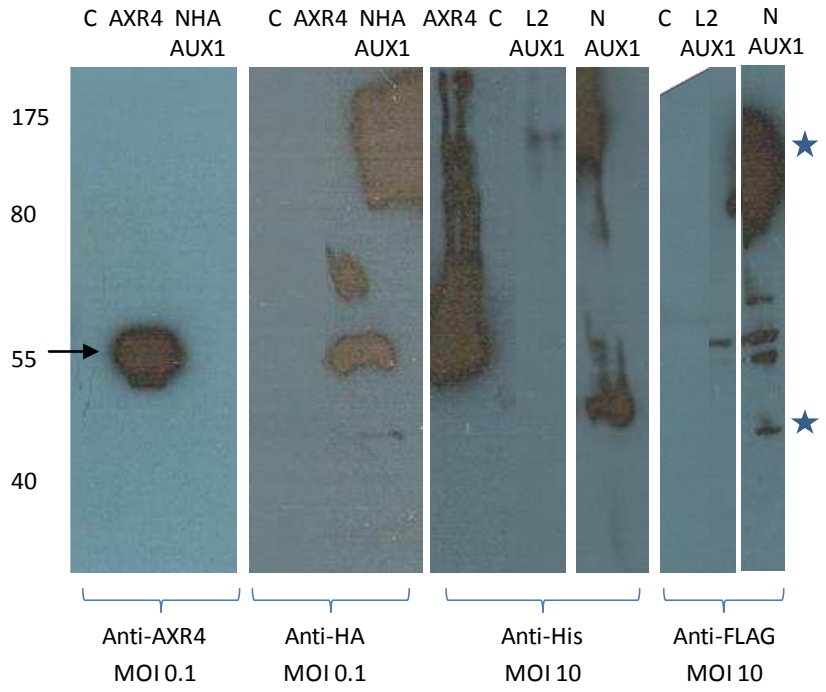

Figure 73: Western blot of recombinant proteins in insect cells

Western immunodetection of recombinant AXR4-HA-His, AUX1-N-His-FLAG, AUX1-L2-His-FLAG, and NHA AUX1 protein. P3 baculovirus stocks were used to infect Sf9 cells at MOI of 0.1 and 10. After culture for 48 hours at 28 ^{o}C cells were harvested, lysed and the lysate (10 μg) resolved by SDS-PAGE and expression verified by immunoblotting, with anti-AXR4 (first panel), anti-HA (second panel), anti-His (third panel), and anti-FLAG (fourth panel) antibodies. ★ represents AUX1. C = non infected control.

6.3.1.2. Co-immunoprecipitation of AUX1 and AXR4

The co-expression studies were carried out based on the optimised conditions achieved in MOI for the AXR4 and AUX1 protein to give similar levels of recombinant protein. As previously mentioned ER accessory proteins such as Shr3p have been shown to interact with their target proteins (Kota et al, 2007). Therefore to

see if AXR4 interacts directly with AUX1 co-immunoprecipitation experiments were done to test for a physical interaction. Co-immunoprecipitation (Co-IP) enables isolation of native protein complexes from a lysate by directly immobilising purified antibodies through covalently coupling them onto an amine-reactive resin. Co-IP is a common approach to study protein:protein interactions that use an antibody to immunoprecipitate the antigen (bait protein) and co-immunoprecipitate any interacting proteins (prey proteins).

The Co-IP experiments were performed on baculovirus cell lysates using anti-FLAG or anti-AXR4 resin, and as a control, uncoupled resin. Co-expressed recombinant AUX1 and AXR4 were used to test AUX1 and AXR4 interaction, and was immunoprecipitated using anti-FLAG, anti-AXR4 and control resin. Singly expressed recombinant AUX1 or AXR4 was used as a control to show that the proteins themselves do not interact directly with the antibodies (anti-AXR4 and anti-FLAG respectively). In the Co-IP experiments, anti-FLAG was used to immunoprecipitate AUX1-N-His-FLAG in co-expressed cell lysate, and then western analysis using anti-AXR4 was performed to see if there is any AUX1/AXR4 interaction. This was also performed the other way round, so that anti-AXR4 was used to immunoprecipitate AXR4 His-HA in co-expressed cell lysate, and then western analysis using anti-FLAG was used performed to detect AUX1 and see if there was any AXR4/AUX1 interaction. Appropriate controls using single expressed cell lysate and uncoupled resin were performed. The protocol used for the co-immunoprecipitation of AXR4 and AUX1 is described in chapter 2.6.7. Co-immunoprecipitation was carried out overnight at 4 ^{o}C, and then samples were separated on a gradient 10-20 % SDS PAGE before being transferred to nitrocellulose membrane.

Affinity purification of AUX1 N-His-FLAG using the antibody against FLAG was successful in immunoprecipitating AUX1 N-His-FLAG when detected by the anti-FLAG antibody by western blot analysis. Interaction between the recombinant AUX1 and AXR4 in vitro was confirmed in figure 74, showing co-immunoprecipitation of AXR4 HA-His. No signal was detected for AXR4 in any of

the controls suggesting that this is a specific interaction between AUX1 and AXR4 recombinant protein with the insect cells.

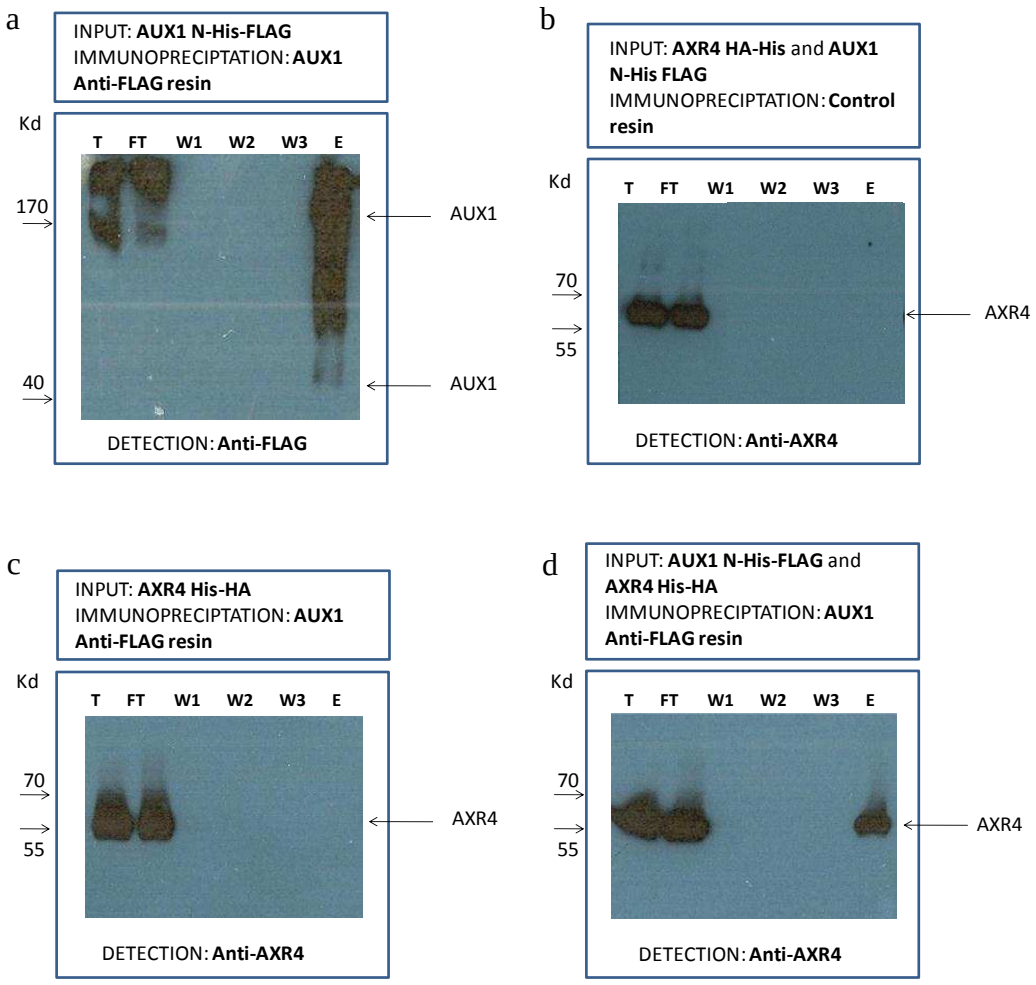

Figure 74: Co-immunoprecipitation of AUX1 and AXR4 using Anti-FLAG

a) AUX1 N-His-FLAG immunoprecipitated using anti-FLAG resin. b) AXR4 His-HA immunoprecipitated using anti-FLAG resin. c) AXR4 His-HA immunoprecipitated with the control resin. d) AXR4 His-HA and AUX1 N-His-FLAG co-expressed immunoprecipitated with anti-FLAG resin. Key: T = Total Input, FT = Flow through sample after affinity purification, W1-W3 = Washes, E = Elute after affinity purification

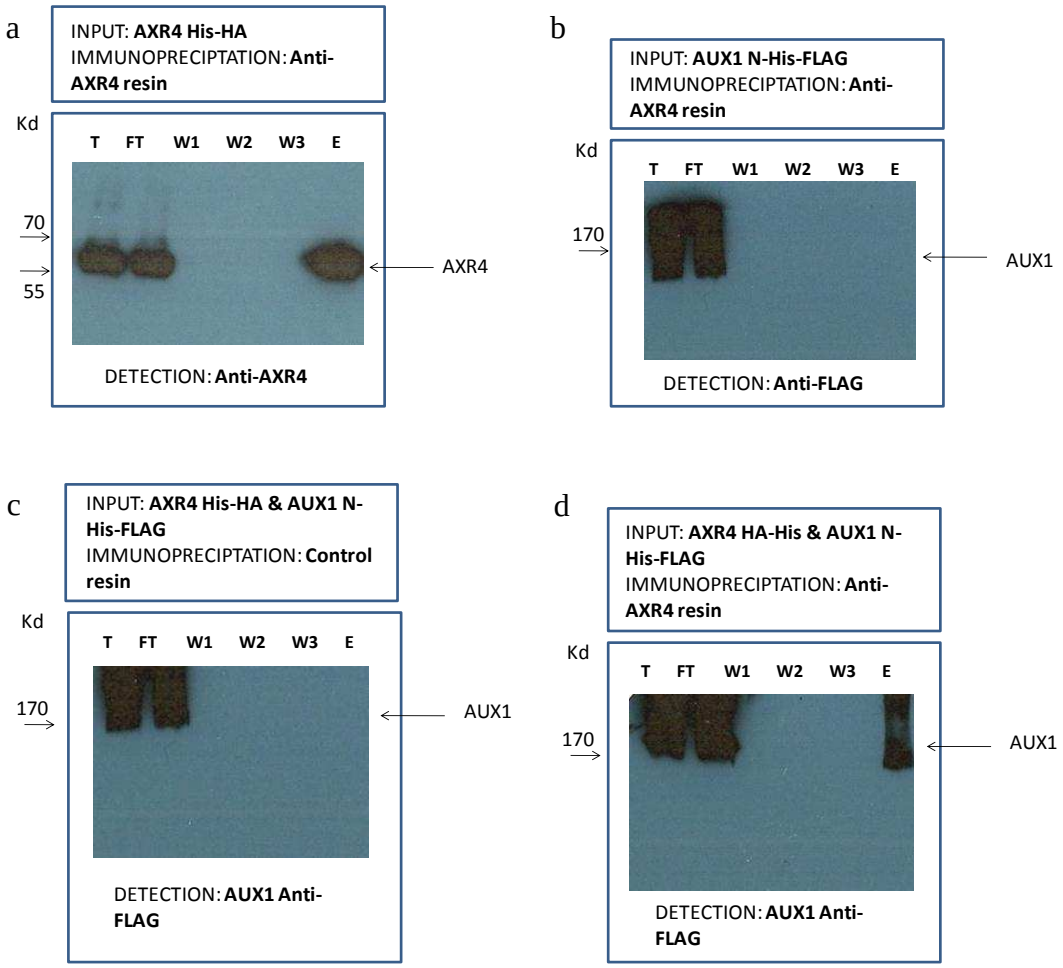

Figure 75: Co-immunoprecipitation of AXR4 and AUX1 using anti-AXR4.

a) AXR4 His-HA immunoprecipitated using anti-AXR4 resin. b) AUX1 N-His FLAG immunoprecipitated using anti-AXR4 resin. c) AUX1 N-His FLAG immunoprecipitated with the control resin. d) AUX1 N-His FLAG and AXR4 His-HA co-expressed immunoprecipitated with anti-AXR4 resin. Key: T = Total Input, FT = Flow through sample after affinity purification, W1-W3 = Washes, E = Elute after affinity purification

Affinity purification of AXR4-HA-His using the antibody against AXR4 was successful in immunoprecipitating AXR4 when detected by the anti-AXR4 and anti-His (data not shown) antibody by western blot analysis. Also interaction between AUX1 and AXR4 was further reinforced by the fact that when immunoprecipitating AXR4, AUX1 N-His-FLAG is also co-immunoprecipitated (figure 75), while AUX1

was not detected in any of the controls. The lack of AXR4 or AUX1 within any of the controls suggests that co-immunoprecipitation was not due to cross reaction with a non-specific protein.

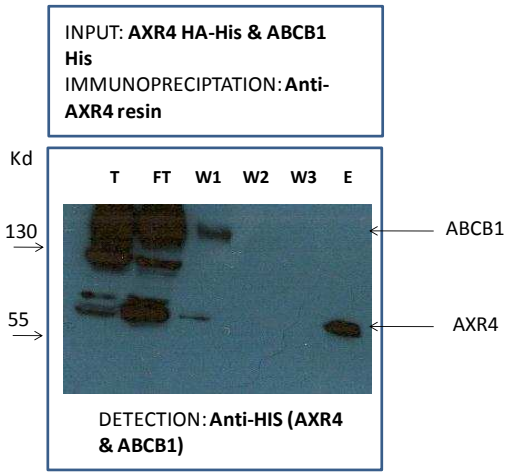

Figure 76: Co-immunoprecipitation of AXR4 and ABCB1
Co-expressed AXR4-HA-His and ABCB1-His immunoprecipitated using anti-AXR4 resin and detected with anti-His. Key: T = Total Input, FT = Flow through sample after affinity purification, W1-W3 = Washes, E = Elute after affinity purification

In order to rule out the possibility that the interaction seen above is not simply due to overexpression of two highly expressed membrane proteins. A control co-immunoprecipitation experiment was designed where AXR4 was co-expressed with a control protein ABCB1-His_6. The rationale for using the same epitope tag (His) for both AXR4 and ABCB1 was that the two proteins could be distinguished based on their size differences; AXR4 (55 Kb) and ABCB1 anti-HIS (130 Kb). Figure 76 shows that while AXR4 is still immunoprecipitated using anti-AXR4 resin, while ABCB1 is not detected. This shows that despite both of them being highly expressed in insect cells, ABCB1 cannot be pulled down. Therefore ruling out that the interaction detected between AUX1 and AXR4 within insect cells, is not just an artefact due to high expression levels. In summary, co-immunoprecipitation experiments have detected a specific interaction between AXR4 and AUX1 consistent with AXR4 functioning as an ER accessory protein.

6.3.2. AUX1 and AXR4 interaction in planta

While we have shown that AUX1 and AXR4 interact in vitro we wanted to look at their interaction in natural conditions, therefore we did a similar experiment looking at co-immunoprecipitation using anti-AXR4 in Arabidopsis thaliana root cultures.

6.3.2.1. Solubilisation of AXR4 in planta

To test for AXR4 solubilisation a range of detergents were used; Non-ionic detergents NP-40 (1 %), Dodecyl- β-maltoside (DDM) 2%, and zwitterionic detergent (0.1 %). All solubilisations were at 4 ^{o}C for 1 hour to prevent proteolysis and help with retention of protein function. After incubation to allow solubilisation, centrifugation was used to pellet the un-solubilised proteins. Both soluble and insoluble fractions were analysed by western blotting (figure 77). The results suggest that out of the detergents tested NP-40 is the most efficient at completely solubilising AXR4, NP-40 was therefore used for the Co-IP experiments.

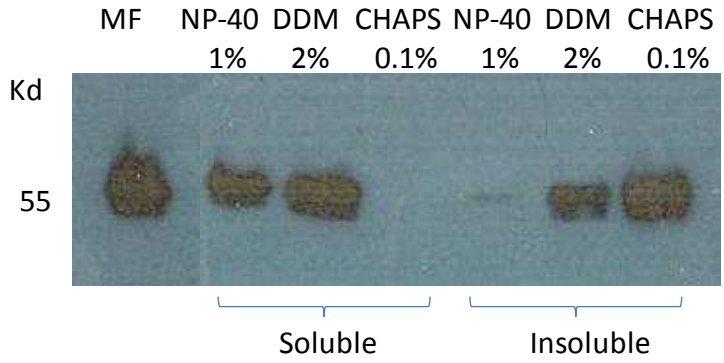

Figure 77: Detergent trials for AXR4 solubilisation.
Detergent solutions were added to Wt microsomal membrane fractions suspended in solubilisation buffer, to achieve the desired detergent concentration and to give a final protein concentration of 1 mg/ml. The insoluble fraction was separated from the soluble fraction by centrifugation (100,000 g for 60 minutes) and resuspended in 10% SDS (w/v) to allow complete solubilisation.

6.3.2.2. Immunoprecipitation of AXR4 in planta

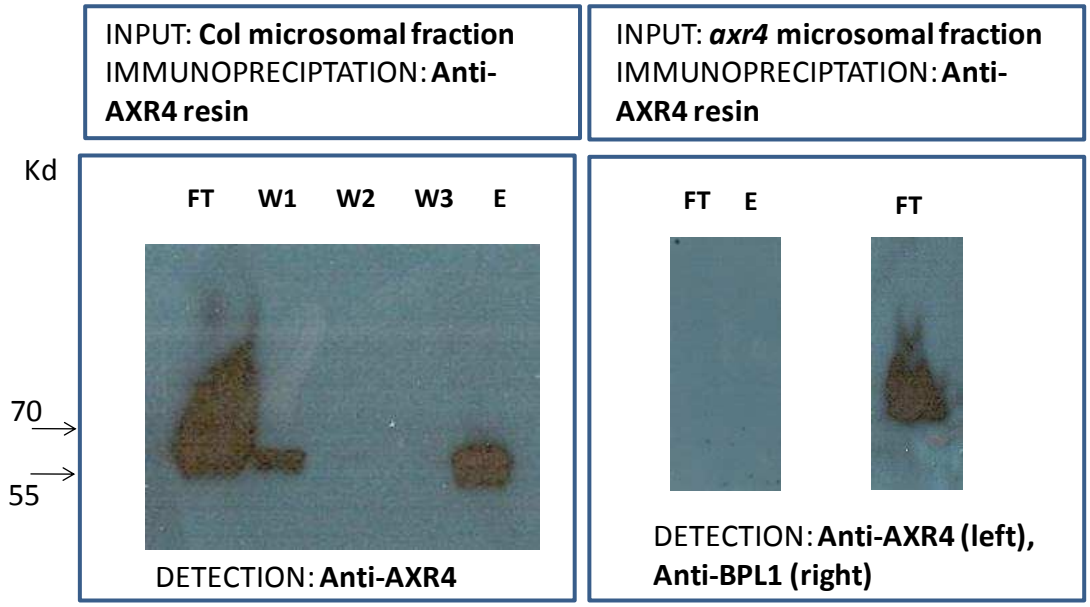

Figure 78: Western detection of AXR4 after anti-AXR4 immunoprecipitation
Affinity purification of AXR4 in the Columbia (Wild type) background was carried out as in chapter 2.6.7. Aliquots of the samples were loaded onto 10-20 % SDS PAGE and were blotted onto nitrocellulose membrane. The blots were probed with anti-AXR4 at 1:10,000 dilution. A 55 kDa band of AXR4 signal was observed in the elution fraction of the anti-AXR4 pull down. To confirm that protein was loaded on the axr4-2 pull down a control protein anti-BPL1 was used. Key: FT = Flow through, W1-W3 = washes 1-3, E = elution.

For the co-immunoprecipitation experiment in planta, NHA-AUX1 (Swarup et al, 2001) root cultures were used to allow analysis of AUX1 and AXR4 interaction within Arabidopsis. Western blot analysis was performed on 10 % of the elution fraction. Detection of AXR4 was detected in the wildtype (Columbia) background but not the axr4-2 mutant background or the uncoupled resin, showing that the AXR4 can be immunoprecipitated under these conditions (figure 78). To confirm that the protein solubilisation was successful in the axr4 mutant, a control antibody (anti-BPL1) was used.

While the AXR4 immunoprecipitation experiment was successful, AUX1 was not detected within the flow through or the elution after co-immunoprecipitation (data not shown). This may be due to the fact that AUX1 is expressed only in a few cell files within the root, and therefore may be below detection levels.

6.4. DISCUSSION

Genetic analysis of axr4 and aux1 show that these two proteins function in the same pathway, regulating auxin related root development (Dharmasiri et al, 2006). axr4 mutant have a weak aux1 like phenotype, identified originally in screens for auxin resistance (Hobbie & Estelle, 1995). Both aux1 and axr4 mutant roots are agravitropic, and have a decreased amount of lateral roots. axr4 mutants similar to aux1 mutants, are resistant to applications of auxins that require transporter proteins (2,4-D and IAA), but not membrane permeable auxins (NAA), and both mutant phenotypes are rescued by the application of NAA (Marchant et al, 1999; Yamamoto & Yamamoto, 1998, 1999). Cloning of AXR4 revealed a novel transmembrane protein of 473 amino acids which is localised to the ER. Because of these similarities with aux1 it was possible that AXR4 was an auxin influx carrier in its own right, or that it regulated the trafficking or function of AUX1. Dharmisiri et al (2006) showed that AUX1 trafficking was affected in the axr4 mutant background, with accumulation of AUX1 within the ER rather than correct localisation to the plasma membrane. In the previous chapter we have shown that AXR4 is also required for the correct localisation of LAX2 and LAX3, and is likely to be involved in trafficking for the whole AUX1/LAX family. In the axr4 mutant, AUX1, LAX2 and LAX3 become mislocalized and accumulate within the ER, however how AXR4 provides this targeting is unknown.

There are a number of different hypotheses about its function, such as acting as an ER accessory protein providing correct folding and attainment of tertiary structure. This would allow AUX1 to be folded correctly and inserted into the ER membrane, possibly by acting as a helix storage site before AUX1 is ready for incorporation into the ER membrane and preventing self aggregation (Dharmasiri et al, 2006). Hobbie (2006), suggested that AXR4 may regulate the lipid composition at the ERES

allowing AUX1 exit, as axr4 knockouts had a different membrane lipid composition during phosphate starvation (Kobayashi et al, 2006). Alternatively AXR4 could act as a post translational enzyme, modifying AUX1 to allow exit from the ER and targeting information. Glycosylation and acylation have been shown to affect protein localisation and therefore post translational modification can provide targeting information. For example, glycosylation of the glycine transporter GLYT2 affects its polar localisation (Zafra and Gimenez, 2001).

Post translational modifications are covalent processes that involve the alteration of the primary structure of the protein after protein translation and folding. More than 300 different protein modifications have been documented, such as addition or removal of functional groups (acetate, phosphate, lipids and carbohydrates), addition of proteins or peptides, changing the chemical nature of the amino acids (citrullination) and structural changes of the protein (disulfide bridges) (Mann and Jensen, 2003).

Bioinformatic analysis identifies two weakly conserved alpha beta hydrolase fold motifs in the C-terminal domain of AXR4, which is a common feature of a wide range of enzymes including the acyltransferase family. Alpha beta hydrolase fold domain superfamily of proteins are known to subserve three general functions: 1) catalysing the hydrolysis of ester and amide substrates as with acetylcholinesterase (AChE); 2) serving as chaperones for section of hormone precursors such as with thyroglobulin (Tg); 3) mediating heterophilic synaptic adhesion interactions as found for neuroligin (NLGN) (De Jaco et al, 2010). The α/β hydrolase fold family is one of the most versatile and widespread protein folds known, and over 50 structures have been solved, including proteases, lipases, esterases, dehalogenases, peroxidises and epoxide hydrolases (Nardini & Dijkstra, 1999). The common structure of the α/β-hydrolase fold domain shared by the members of this family, suggests that despite the different functions, these proteins share common mechanisms of protein folding and processing (De Jaco et al, 2010). As AXR4 contains two putative alpha beta hydrolase fold these were analysed using site directed mutagenesis to determine if these domains are active in AXR4 function.

When Arabidopsis thaliana AXR4 was aligned with AXR4 homologous proteins from other plant species, the amino acid similarity was very high especially in the large C terminal domain of AXR4 (appendix 9.6). Possible functional amino acids were then further narrowed down by comparing this alignment with proteins in other kingdoms containing the alpha beta hydrolase domain, highlighting conserved amino acids within this domain. Site directed mutagenesis was then used to target nine different amino acids and generate random mutations at these specific sites. 34 different amino acid changes were identified and these were screened on 50 nM 2,4-D. The majority of the lines rescue the axr4 phenotype, with a few lines showing a partial rescue such as 140 L-V, 154 G-L, 201 D-C, 246 L-A, 246 L-E and 246 L-T. 154 G-L is interesting where the small hydrophobic glycine changes to a hydrophobic aliphatic leucine. It is likely that the amino acid change is affecting the structure in some way, and therefore reducing AXR4 efficiency. In the other case (201 D-C) amino acid change from the small negatively charged polar aspartate to a small polar cysteine, a highly disfavoured change in membrane proteins (Betts & Russel, 2003). Interestingly, all substitutions at amino acid 246 result in a weak phenotype at 25 nM 2,4-D suggesting that this amino acid substitution may play an important role in AXR4 function.

On the whole, however we have shown that AXR4 is tolerant to amino acid changes even in highly conserved amino acids without losing function. This suggests that none of these conserved amino acids in the alpha beta hydrolase fold are essential for AXR4 function, and therefore it is likely that the α/β hydrolase fold does not play a role in AXR4 function. The inability to identify a single amino acid substitution that results in loss of function makes AXR4 a very interesting protein for structural studies. This may also explain why missense alleles of axr4 have not been identified in numerous 2,4-D screens. The only mutations discovered for AXR4 are insertions (T-DNA and γ-radiated) and those EMS mutants that result in stop codons (figure 79). The lack missense mutations in AXR4 that cause loss of function, could be because AXR4 has flexibility within its structure and can cope with single amino acid changes without losing function.

To confirm that AXR4 function was restored in the mutant lines, in situ localisation of LAX2 and NHA-AUX1 were used to see whether they are correctly targeted to the plasma membrane. As shown previously AXR4 is required for the correct plasma membrane localisation, the axr4 mutant resulting in accumulation of these proteins in the ER. The results confirm that LAX2 and AUX1 are correctly targeted within the mutants, suggesting that all the amino acid changes lead to a functional AXR4 protein. It may be that the lines that partially rescue axr4 are those that slightly affect the structure of AXR4 causing it to be less efficient functionally.

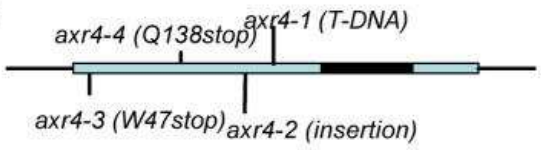

Figure 79: Diagram of AXR4 KO lines
Showing two EMS mutants, γ-irradiated and T-DNA mutant.

It appears therefore that the alpha beta hydrolase domain does not play a role in AXR4 function; therefore it is possible that AXR4 is acting as an ER accessory protein, providing correct AUX1 structure or preventing aggregation of AUX1 within the ER. Therefore it may be possible that AXR4 structure itself is important to allow function, therefore 3D models were created of AXR4 and the mutations to see if there are any differences in the prediction. Membrane proteins are notoriously difficult to work with, and so far only 187 membrane proteins have had their 3D structures resolved (White, 2009). This represents only a small fraction of membrane proteins, as they comprise of 20-30 % of all proteins in both prokaryotic and eukaryotic organisms (Kunji et al, 2005). In comparison the number of 3D structures of soluble proteins identified is well over 10,000 (Grissammer and Buchanan, 2006). Due to this lack of known structures of membrane proteins, it is difficult to model predictions. Therefore the 3D models produced by CPH models 3.0 should be used as a rough model of AXR4 3D structure. From this model a lot of the amino acid changes cause a loop to become free of the structure, however they all keep the tightly bundled structure of AXR4 which may be necessary for its function. Those changes that disrupt it in small ways, such as causing a loop to become free, may

reduce the efficiency with which AXR4 can function, give a partial phenotype rather than complete rescue. This agrees with the model of AXR4 as an ER accessory protein.

ER accessory proteins are important for the correct localisation of their targets, and loss of function mutants result in accumulation of their target within the ER. The mammalian ER accessory protein RAP, for example, is involved in the correct localisation of low-density lipoprotein (LDL) receptor family; its absence causes the LDL receptors to aggregate within the ER (Bu et al, 1995; Bu & Schwartz, 1998). Similarly loss of PHF1 in Arabidopsis leads to abnormal accumulation of its target protein PHT1 (a phosphate transporter) within the ER, and loss of correct localisation to the plasma membrane (González et al, 2005). In yeast, Shr3p is required for the trafficking of amino acid permeases (e.g. Gap1p) to the plasma membrane (Ljungdahl et al, 1992). In the Shr3p mutant Aap1 is no longer folded correctly and the proteins aggregate together, preventing Aap1 from being loaded into COPII vesicles and causing accumulation within the ER. AXR4 has been previously shown by Dharmasiri et al (2006) to be required for the correct targeting of AUX1 to the plasma membrane with the axr4 mutant resulting in AUX1 retention in the ER

These ER accessory proteins are highly specific to their cognate target proteins, for example the mammalian TANGO1 ER accessory protein is involved in the correct targeting of collagen VII solely and has been shown not to influence the transport of the related protein collagen I (Saito et al, 2009). Pho86p in yeast has been shown to be highly specific for the regulation of Pho84p, and does not influence the trafficking of other members of the hexose transporter family to which Pho84 belongs to (Lau et al, 2000). Dharmasiri et al (2006) provided evidence that AXR4 was specific to AUX1 as the axr4 mutation had no effect on the localisation of other plasma membrane proteins such as PIN1, PIN2 and H^+-ATPase. A number of ER accessory proteins have been shown to be specific for the trafficking of a whole family of proteins, such as RAP and Shr3p, which is involved in the trafficking of LDL receptor, and AAP families respectively. We have also shown in the previous chapter that AXR4 is required for the correct localisation of LAX2 and LAX3 as well, and is likely involved in the trafficking of the whole family. AUX1/LAX family belongs to

the amino/acid permease super family within Arabidopsis, therefore it is possible that AXR4 has a similar function to Shr3p. Recently Kota et al (2007) has shown that Shr3p interacts directly with its target proteins. To see if AXR4 is playing a similar role to Shr3p as an ER accessory protein for AUX1, we looked for direct interaction between the two proteins in vitro and in planta.

Data from the co-immunoprecipitation studies of AXR4 and AUX1 provides strong evidence that these two proteins interact. In the control studies using the opposite antibody (e.g. anti-AXR4 for AUX1) or control columns, we show that there is no immunoprecipitation. This shows that neither AXR4 nor AUX1 interact with the column itself, or cross react with each other's antibodies. Only when both proteins are present co-immunoprecipitation occurs, indicating that the interaction between the two proteins is specific. To rule out the possibility that the interaction is artificial and only occurring because of the very high protein levels of the co-expressed protein another control was used. AXR4 was co-expressed with ABCB1 which is a multiple transmembrane protein. We have shown that ABCB1 cannot be detected after co-immunoprecipitation with anti-AXR4, indicating that the AXR4 and AUX1 interaction is specific.

The interaction of AXR4 with AUX1 is consistent with the proposed role as an ER accessory protein, functioning as a molecular chaperone providing correct structure or reducing aggregation (Dharmasiri et al, 2006). A known ER accessory protein Shr3p in yeast is involved in preventing aggregation of a family of amino acid permeases, by providing correct folding and attainment of tertiary structure (Kota and Ljungdahl, 2005). The AUX1/LAX family belong in the amino acid permease group, and while there is little similarity in structure between Shr3p and AXR4, it is possible that AXR4 is playing a similar role in plants. This is further supported by work by Tendot Abu Baker (2007) and Carrier (2009), showing that AXR4 prevented aggregation of AUX1 in a dose dependent manner.

As the co-immunoprecipitation showed interaction between AUX1 and AXR4 in vivo, the experiment was repeated in plant cells. Due to the low expression levels of AUX1 within Arabidopsis, AXR4 was chosen as the target for immunoprecipitation,

and the eluate was analysed for AUX1 (anti-HA) expression by western blotting. While we have shown that AXR4 is easily detectable under the conditions used, and that the pull down experiments were successful, unfortunately in the western analysis we were unable to detect the NHA-AUX1 using anti-HA antibody. But these in planta experiments are technically challenging for several reasons: 1) AUX1 is expressed only in a subset of root cells. 2) AUX1 is a polytopic membrane protein that is hard to solubilise and only weak detergents were used to allow interactions between AXR4 and other proteins to be observed. 3) AUX1 is a plasma membrane protein whereas AXR4 is an ER protein; therefore any interaction is only transient, further limiting the likelihood of observing AUX1.

Despite these difficulties co-expression studies using heterologous expression system have shown that AXR4 and AUX1 interact in vivo, supporting the theory that AXR4 is an ER accessory protein for AUX1 providing correct targeting, possibly through preventing AUX1 aggregation within the ER.

CHAPTER 7

CONCLUSION

7. CONCLUSION

7.1. INTRODUCTION

Protein sorting within the ER accommodates an extraordinary variety of cargo proteins with different structures, functions and ultimate destinations. A lot of these proteins are sorted by signalling motifs found within the proteins themselves; however some proteins have no recognisable sorting motif. There are also a number of polytopic transmembrane proteins where the order of transmembrane insertions into the membrane needs to be highly regulated. Some proteins are also prevented from becoming functionally active prematurely before they reach their final destination. In these cases the proteins are dependent on specific accessory proteins (ER accessory proteins) for the correct structure and/or exit from the ER. A large number of different proteins and varied mechanisms for ER accessory proteins have been discovered in mammalian and yeast systems in the last ten years. In recent years three potential ER accessory proteins have been discovered in plants suggesting that similar mechanisms exist in plants too. It is likely that this mechanism is as numerous and varied in plants as in other systems; with polytopic membrane proteins requiring their own cognate ER accessory protein to facilitate folding and/or transport.

7.2. DISCOVERING NEW ER ACCESSORY PROTEINS

ER accessory proteins in plants are a relatively new area of research within Arabidopsis thaliana, and part of the project was focused on discovering new ER accessory proteins within plants. While ER accessory proteins have similar functions, almost all ER accessory proteins share no homology with each other, with no common motif or domain (Cooray et al, 2009). Despite this they are all localised to the ER with a transmembrane domain. A protein localisation data set (LOPIT – Dunkley et al, 2006) was used to identify targets which could possibly be ER accessory proteins, based on ER localisation and an unknown or novel function. Two of the known ER accessory proteins in Arabidopsis thaliana AXR4 and PHF1 were

identified using this method, suggesting this is a suitable method for ER accessory protein discovery.

These candidate proteins (40) were then prioritised based on expression within the roots, whether they were single or multi copy genes and if T-DNA KOs were available. This narrowed the list of candidates from 40 to 20 targets. Of these 20 targets, 14 homozygous T-DNA KOs were isolated, 7 of which showed complete loss of mRNA expression. Those lines where homozygous T-DNA KOs were obtained, but still there was not a complete loss of mRNA expression, insertions were mostly located within the introns, suggesting that the transcript was spliced correctly despite the T-DNA insert. For one of the lines the T-DNA insert was located within the 5' UTR and in this case the 35 S promoter within the T-DNA likely drove the expression of the gene. The lines where no homozygous lines have been identified were mainly due to lack of T-DNA insertion within the gene of interest. For these targets other mutation/insertion lines could be analysed if available. Alternatively an RNAi approach can be used to obtain knock down lines in these genes of interest.

The homozygous KO lines were subjected to phenotypic analysis including deficiency screens, toxicity screens and ICP-MS analysis of nutrient content within the aerial tissue. The rationale of these phenotypic analysis was that if the Wt (wild type) protein functions as an ER accessory protein for a membrane transporter; then in the KO lines the membrane transporter will not be correctly localised and is expected to affect uptake or transport of nutrient/mineral and give a phenotype under these conditions. For example an observed increased resistance to toxicity screens, could be due to the reduced ability to uptake the toxic chemical caused by a mislocalisation of a plasma membrane transporter protein.

A few lines gave a weak phenotype in these screens, suggesting that they may play a role as an ER accessory proteins. Mutations in At2g16170 (N663810) gave an increased sensitivity to toxic levels of boron (>500 μM Boron). If it plays a role as an ER accessory protein, this phenotype could be caused by mislocalization of a xylem loader protein such as BOR1, or a vacuole importer. The bor1 phenotype has reduced

growth in boron limiting conditions and increased resistance to toxic levels of boron (Noguchi et al, 1997; Takano et al, 2010). Future work in discovering whether At2g16170 is involved in the trafficking of a boron transporter would be to locate boron transporters in the At2g16170 mutant background.

Mutation in AtBPL and related family members gave a weak phenotype under nitrate limiting conditions, with reduced growth compared to Wt. This would suggest that one of the transporters involved in uptake is deficient, leading to a reduction in nitrate uptake and therefore increased deficiency within the plant. There are a large number of nitrogen transporters within the plants (53 NRT1 genes in Arabidopsis) and it is likely that AtBPL family only regulate trafficking of some of these membrane transporters, therefore only have a weak phenotype. A possible target could be CHL1 (AtNRT1.1) which is constantly expressed and responsible for high affinity uptake under low nitrate conditions, if this was mistargeted it would give reduced growth, as less nitrogen is available to the plant.

Mutation in At1g71789 (N614289) gave a weak phenotype in a number of screens, with an increased sensitivity to boron. Also, in the ICP-MS analysis it gave an 80 % reduction in nutrient concentration. This suggests that this line may play a more extensive role than an ER accessory protein for a single transporter protein, as it appears to affect multiple nutrient levels within the plant. It may possibly be involved in general protein processing within the ER, such as a chaperone, or being involved in the ERAD system. Hong et al (2008) have previously shown that inhibition or mutants with the ERQC/ERAD system result in significant suppression of the bri1-5 dwarf phenotype. BRI1 encodes a cell surface receptor for brassinosteriods, and a weak bri1-5 allele carries a mutation that causes it to be retained in the ER by the ERQC (Li et al, 2001). Genetic analysis of the double mutant (At1g71789 and bri1-5) would clarify whether At1g71789 plays a general role in the ERAD system in Arabidopsis.

Genetic analysis of these potential ER accessory protein candidates only resulted in a weak phenotype. It is not surprising considering the complexity of the nutrient transport system within the plant. There are large numbers of transporter proteins in

plants, differing not only in their tissue and membrane location but also in their mode of energisation, substrate affinity and specificity (Blatt, 2004).

Further characterisation of these lines will clarify their role as an ER accessory protein. Besides identification of their targets which would be another challenge. A number of techniques can be used including expression analysis, genetic analysis, metabolic profiling, pull down studies and yeast two-hybrid analysis. Once the target protein is known localisation studies in planta will reveal if they are mislocalised in their cognate mutant backgrounds.

7.3. AtBPL – AN ER ACCESSORY PROTEIN?

Bioinformatic analysis suggested that one of the candidate genes was similar to mammalian BAP31. In animal systems, BAP31 has been shown to act as an ER accessory protein for MHC class I molecules and tetraspanins CD9 and CD81 (Stojanovic et al, 2005); hence AtBPL1 was a promising candidate as a potential ER accessory protein. In situ immunolocalisation using highly specific BPL1 antibodies revealed that BPL1 colocalises with ER markers confirming its location in the ER.

Genetic analysis of the AtBPL1 knock out showed reduced root growth in nitrogen deficient conditions. In Arabidopsis, there are three other AtBPL1 like genes (designated AtBPL2-4). Of the four members of the BPL1 family homozygous knock out lines were obtained for BPL1, BPL2 and BPL3, however no homologous line was identified for BPL4 (using two idependant T-DNA insertion lines). For one of the BPL4 T-DNA insertion lines, the T-DNA insert was located in the intron and the mRNA level was normal in this knock out, suggesting that in this line the gene is still transcribed correctly due to mRNA splicing. In the other case (N803596) though the T-DNA is located in the exon, seed germination was very poor in this line and so it could not be determined if our inability to identify a homozygous line for AtBPL4 suggests an embryo lethal phenotype. Further analysis of the heterozygous lines would confirm if there is an embryo or seedling lethal phenotype.

AtBPL family was further investigated using a miRNA approach targeting all members of the family. Using single KOs and miRNA lines, we show that the mutant bri1-5 phenotype cannot be suppressed, suggesting that the BPL family is not involved in a general role in ER quality control. We also showed that all lines had a weak phenotype on nitrate deficiency screens and chlorate toxicity screens, with reduced growth. It is possible that BPL family is involved in targeting a nitrate transporter, possibly a vacuole or xylem loading transporter, such as CLCa. We have shown that the mutant phenotypes do not phenocopy clca under the conditions used in our lab and it is possible that the BPL family is involved in the trafficking of other nitrate transporters. Further studies will involve discovering potential targets of BPL, which can then be clarified looking at the localisation within the bpl mutants.

To try and discover BPL1 role in plants and identify interacting partners, a mass spectrum analysis was performed on BPL1 pull downs in planta, in comparsion to the bpl1 mutant. While this highlighted some proteins that are only found in the BPL1 pull down, the BPL1 protein itself was not pulled down. It is possible that BPL1 peptides do not fly well in our conditions but care must be taken in interpreting this data. There are a few interesting candiates such as MILDEW RESISTANCE LOCUS O 15 (MLO15); a polytopic membrane protein, known to be involved in cell death in plants (source NCBI BLink). BAP31 is involved in apoptosis in mammalian systems and therefore identification of MLO15 in our pull down is exciting. Future work of these targets would be to look at mutant phenotypes and see if they are similar to BPL family phenotype. Yeast two hybrid screens can be used to confirm interaction of the two proteins.

7.4. AXR4 – AN ER ACCESSORY PROTEIN OR POST TRANSLATIONAL MODIFYING ENZYME?

AXR4 has been previously shown by Dharmasiri et al (2006) to be required for the correct targeting of AUX1 to the plasma membrane with the axr4 mutant exhibiting AUX1 retention in the ER. This ER retention of the target protein is typical of a mutated ER accessory protein such as Shr3p, RAP, LMAN1-MCFDC (Ljungdahl et al, 1992; Bu et al, 1995; Appenzeller et al, 1999; respectively). However

bioinformatic analysis suggest that AXR4 contains two weakly conserved alpha beta hydrolase fold motifs in its C-terminal domain. Alpha beta hydrolase fold domain is a common feature of a wide range of enzyme including the acyltransferase family. Though evidence suggests that AXR4 acts as an ER accessory protein the possibility that it functions as a post-translational modifying enzyme could not be ruled out. To test the role of the alpha beta hydrolase domain on AXR4 function, site directed mutagenesis was performed on highly conserved amino acids within these domains.

10 sites were chosen for mutagenesis, and 34 different amino acid subsitutions were made. Phenotypic analysis suggested that the majority of the lines completely rescued axr4 phenotype. This was further confirmed by in situ immunolocalisation through the localisation of LAX2 and AUX1 (NHA-AUX1) in the in vitro mutagenesis AXR4 background. All lines analysed not only rescued the axr4 phenotype, they also showed a wildtype (Wt) membrane localisation of LAX2 and AUX1.

Our work clearly shows that AXR4 can still function despite amino acid changes even in highly conserved amino acids in the alpha beta hydrolase fold domain suggesting that none of these conserved amino acids are essential for AXR4 function. Therefore it is likely that the α/β hydrolase fold does not play a role in AXR4 function and AXR4 functions as an ER accessory protein. This is further supported by work of Tendot Abu Baker (2007) and Carrier (2009) who showed that AXR4 reduces AUX1 aggregation in insect cells as has been shown for several ER accessory proteins in yeast (Kota and Ljungdahl 2005).

7.4.1. AXR4 is required for the correct localisation of the AUX1/LAX family

It has been hypothesised that AXR4 acts as an ER accessory protein for AUX1. One ER accessory protein Shr3p in yeast is required for the trafficking of amino acid permeases family (18 members) to the plasma membrane (Gilstring et al, 1999; Kota & Ljungdahl, 2005). AUX1 belong to a small gene family of four highly conserved genes (AUX1, LAX1, LAX2, and LAX3) within the amino acid/auxin permease super

family in Arabidopsis (Young et al, 1999), and all have been shown to have auxin uptake activity (Carrier et al, 2008; Péret et al, manuscript under preparation; Swarup et al, 2008; Yang et al, 2006).

To discover if AXR4 is involved in the correct targeting of the whole family, localisation studies of LAX2 and LAX3 within the axr4 background were carried out and compared to Wt. Our work using cell biological approaches show that AXR4 also regulates the trafficking of LAX2 and LAX3. This is futher supported by genetic studies that suggest that axr4 mutants show weak aux1, lax2, and lax3 phenotypes. For example, lax2 mutants show a vascular developmental defect in cotyledons, a similar but weaker phenotype is also seen in axr4. The double mutant (lax2 and axr4) is currently being produced to see whether they have an additive phenotype.

Similarly, both lax3 and axr4 mutants show defect in lateral root emergence and a double mutant between lax3 and axr4 show a more severe lateral root emergence defect. Hobbie & Estelle (1995) have shown that the aux1axr4 double mutant had an additive effect of producing fewer lateral roots than in either single mutant. Our work provides an explanation for this phenotype as this is likely due to mis-targeting of both AUX1 (Dharmasiri et al, 2006) and LAX3 in axr4 background.

At present it is not clear if AXR4 regulates targeting of LAX1 as well. Currently efforts are underway to investigate this. A LAX1-YPET line (Swarup & Bennett, personal communication) has been crossed with axr4 and homozygous lines are being screened.

7.4.2. AXR4 interacts directly with AUX1

In this study we provide evidence that AXR4 acts as an ER accessory protein and is required for the trafficking of two other members of the AUX1/LAX family, LAX2 and LAX3. Recent work into ER accessory proteins has shown that in some cases they interact directly with their targets (Kota et al, 2007). To test if AXR4 interacts directly with AUX1, pull down experiments were designed.

Results provide strong evidence that AUX1 and AXR4 proteins interact in vivo. A control experiment using ABCB1 and AXR4 do not show any interaction ruling out the possibility of an artefact due to high protein levels, and confirming that the AXR4 and AUX1 interaction is specific.

The pull down experiment were also performed in planta, however AUX1 was not observed within the protein extract or elute. This may be due to the fact that AUX1 is only expressed in a few cell files within the root, and therefore may be too low for detection. As well as this the interaction between AUX1 and AXR4 is likely to be transient within the ER, with the majority of AUX1 on the plasma membrane and therefore not interacting with AXR4. Other approaches such as FRET or pull down studies using plant protoplasts should be used to prove AUX1 and AXR4 interaction in planta.

To conclude we have shown that AXR4 functions as an ER accessory protein to regulate the targeting of AUX1, LAX2 and LAX3.

8. REFERENCES

AceView: a comprehensive cDNA-support gene and transcripts annotation. 2006. Genome Biology **7** (Suppl 1): S12

Adams MD, Celniker SE, Holt RA, Evans CA, Gocayne JD, Arnanatides PG, Scherer SE, Li PW, Hoskins RA, Galle RF, George RA, Lewis SE, Richards S, Ashburner M, Henderson SN, Sutton GG, Wortman JR, Yandell MD, Zhang Q, Chen LX, Brandon RC, Rogers Y-HC, Blazej RG, Champe M, Pfeiffer BD, Wan KH, Doyle C, Baxter EG, Helt G, Nelson CR, Gabor Miklos GL, Abril JF, Agbayani A, An H-J, Andrews-Pfannkoch C, Baldwin D, Ballew RM, Basu A, Baxendale J, Bayrataroglu L, Beasley EM, Beeson KY, Benos PV, Berman BP, Bhandari D, Bolshakov S, Borkova D, Botchan MR, Bouck J, Brokstein P, Brottier P, Burtis KC, Busam DA, Butler H, Cadieu E, Center A, Chandra I, Cherry M, Cawley S, Dahlke C, Davenport LB, Davies P, de Pablos B, Delcher A, Deng Z, Deslattes Mays A, Dew I, Dietz SM, Dodson K, Doup LE, Downes M, Dugan-Rocha S, Dunkov BC, Dunn P, Durbin KJ, Evangelista CC, Ferraz C, Ferriera S, Fleischmann W, Fosler C, Gabrielian AE, Garg NS, Gelbart WM, Glasser K, Glodek A, Gong F, Gorrell JH, Gu NS, Gelbart WM, Glasser K, Glodek A, Gong F, Gorrell JH, Gu Z, Guan P, Harris M, Harris NL, Harvey D, Heiman TJ, Hernandez JR, Houck J, Hostin D, Houston KA, Howland TJ, Wei M-H, Ibegwam C, Jalai M, Kalush F, Karpen GH, Ke Z, Kennison JA, Ketchum KA, Kimmel BE, Kodira CD, Kraft C, Kravitz S, Kulp D, Lai Z, Lasko P, Lei Y, Levitsky AA, Li J, Li Z, Laing Y, Lin X, Liu X, Mattei B, McIntosh TC, McLeod MP, McPherson D, Merkulov G, Milshina NV, Mobarry C, Morris J, Moshrefi A, Mount SM, Moy M, Murphy B, Murphy B, Murphy L, Muzny DM, Nelson DL, Nelson DR, Nelson KA, Nixon K, Nusskern DR, Pacleb JM, Palazzolo M, Pittman GS, Pan S, Pollard J, Puri V, Reese MG, Reinert K, Remington K, Saunders RDC, Scheeler F, Shen H, Shue BC, Sidén-Kiamos I, Simpson M, Skupski MP, Smith T, Spier E, Spradling AC, Stapleton M, Strong R, Sun E, Svirskas R, Tector C, Turner R, Venter E, Wang AH, Wang X, Wang Z-Y, Wassarman DA, Weinstock GM, Weissenbach J, Williams SM, Woodage T, Worley KC, Wu D, Yang S, Yao

QA, Ye J, Yeh R-F, Zaveri JS, Zhan M, Zhang G, Zhao Q, Zheng L, Zheng XH, Zhong FN, Zhong W, Zhong W, Zhou X, Zhu S, Zhu X, Smith HO, Gibbs RA, Myers EW, Rubin GM, and Venter JC. 2000. The genome sequence of Drosophila melanogaster. Science **287**: 2185-2195

Al-Ghazi Y, Muller B, Pinloche S, Tranbarger TJ, Nacry P, Rossignol M, Tardieu F, and Doumas P. 2003. Temporal responses of Arabidopsis root architecture to phosphate starvation: evidence for the involvement of auxin signalling. Plant, Cell & Environment **26**: 1053-1066

Alaimo A, Gómez-Posada JC, Aivar P, Etxeberria A, Rodriguez-Alfaro JA, Areso P, and Villarroel A. 2009. Calmodulin activation limits the rate of KCNQ2 K^+ channel exit from the endoplasmic reticulum. Journal of Biological Chemistry **284**: 20668-20675

Amtmann A, and Blatt MR. 2009. Regulation of macronutrient transport. New Phytologist **181**: 35-52

Anchour L, Scott MGH, Shirvani H, Thuret A, Bismuth G, Labbé-Jullié C, and Marullo S. 2009. CD4-CCR5 interaction in intracellular compartments contributes to receptor expression at the cell surface. Blood **113**: 1938-1947

Andreeva AV, Xheng H, Saint-Jore CM, Kutuzov MA, Evans DE, Hawes CR. 2000. Organization of transport from endoplasmic reticulum to Golgi in higher plants. Biochemical Society Transactions **28**: 505-512

Andrés-Colás N, Perea-García A, Puig S, and Peñarrubia L. 2010. Deregulated copper transport affects Arabidopsis development especially in the absence of environmental cycles. Plant Physiology **153**: 170-184

Anelli T, and Sitia R. 2008. Protein quality control in the early secretory pathway. The EMBO Journal **27**: 315-327

Anisimova M, and Gascuel O. 2006. Approximate likelihood ratio tests for branches: A fast, accurate and powerful alternative. System Biology **55**: 539-552

Annaert WG, Becker B, Kistner U, Reth M, and Jahn R. 1997. Export of cellubrevin from the endoplasmic reticulum is controlled by BAP31. The Journal of Cell Biology **139**: 1397-1410

Antonny B, and Schekman R. 2001. ER export: public transportation by the COPII coach. Current Opinion in Cell Biology **13**: 438-443

Appenzeller C, Andersson H, Kappeler F, and Hauri H-P. 1999. The lectin ERGIC-53 is a cargo transport receptor for glycoproteins. Nature Cell Biology **1**: 330-334

Aridor M, Fish KN, Bannykh S, Weissman J, Roberts TH, Lippincott-Schwartz J, and Balch WE. 2001. The Sar1 GTPase coordinates biosynthetic cargo selection with endoplasmic reticulum export site assembly. The Journal of Cell Biology **152**: 213-230

Bainbridge K, Guyomarc'h S, Bayer E, Swarup R, Bennett M, Mandel T, and Kuhlemeier C. 2008. Auxin influx carriers stabilize phyllotactic patterning. Genes and Development **22**: 810-823

Baines AC, and Zhang B. 2007. Receptor-mediated protein transport in the early secretory pathway. TRENDS in Biochemical Sciences **32**: 381-388

Baker EK, Colley NJ, and Zuker CS. 1994. The cyclophilin homolog NinaA functions as a chaperone, forming a stable complex in vivo with its protein target rhodopsin. The EMBO Journal **13**: 4886-4895

Bar-Peled M, and Raikhel NV. 1997. Characterization of AtSEC12 and AtSAR1. Proteins likely involved in endoplasmic reticulum and Golgi transport. Plant Physiology **114**: 315-324

Barlowe C, and Schekman R. 1993. SEC12 encodes a guanine-nucleotide-exchange factor essential for transport vesicle budding from the ER. Nature **365**: 347-349

Barlowe C, d'Enfert C, and Schekman R. 1993. Purification and characterization of SAR1p, a small GTP-binding protein required for transport vesicle formation from the endoplasmic reticulum. Journal of Biological Chemistry **268**: 873-879

Barlowe C, Orci L, Yeung T, Hosobuchi M, Hamamoto S, Salama N, Rexach MF, Ravazzola M, Amherdt M, and Schekman R. 1994. COPII: A membrane coat formed by Sec proteins that drive vesicle budding from the endoplasmic reticulum. Cell **77**: 895-907

Bates TR, and Lynch JP. 1996. Stimulation of root hair elongation in Arabidopsis thaliana by low phosphorous availability. Plant Cell Environment **19**: 529-538

Beck R, Ravet M, Wieland FT, and Cassel D. 2009. The COPI system: Molecular mechanisms and function. FEBS Letters **583**: 2701-2709

Belden WJ, and Barlowe C. 2001. Role of Erv29p in collecting soluble secretory proteins into ER-derived transport vesicles. Science **294**: 1528-1531

Benková E, Michniewicz M, Sauer M, Teichmann T, Seifertová D, Jürgens G, and Friml J. 2003. Local, efflux-dependent auxin gradients as a common module for plant organ formation. Cell **115**: 591-602

Bennett MJ, Marchant A, Green HG, May ST, Ward SP, Millner PA, Walker AR, Schultz B, and Feldmann KA. 1996. Arabidopsis AUX1 gene: A permease-like regulator of root gravitropism. Science **273**: 948-950

Bermak JC, Li M, Bullock C, and Zhoi QY. 2001. Regulation of transport of the dopamine D1 receptor by a new membrane-associated ER protein. Nature Cell Biology **3**: 492-498

Betts MJ, and Russel RB. 2003. Amino acid properties and consequences of substitutions. In Bioinformatics for Geneticists, Barnes MR and Gray IC, editors. Wiley, 2003

Bhairi SM. 2001. A guide to the properties and uses of detergents in biological systems. Calbiochem

Bickford LC, Mossessova E, and Goldberg J. 2004. A structural view of the COPII vesicle coat. Current Opinion of Structural Biology **14**: 147-153

Blatt MR. 2004. Membrane transport in plants. Oxford, UK; Blackwell Publishing.

Blilou I, Xu J, Wildwater M, Willemsen V, Paponov I, Friml J, Heidstra R, Aida M, Palme K, and Scheres B. 2005. The PIN auxin efflux facilitator network controls growth and patterning in Arabidopsis roots. Nature **433**: 39-44

Boevink P, Oparka K, Santa Cruz S, Martin B, Betteridge A, and Hawes C. 1998. Stacks on tracks: The plant Golgi apparatus traffics on an actin/ER network. The Plant Journal **15**: 441-447

Bökel C, Dass S, Wilsch-Bräuninger M, and Roth S. 2005. Drosophila Cornichon acts as cargo receptor for ER export of the TGFα-like growth factor Gurken. Development **133**: 459-470

Bonifacino JS, and Rojas R. 2009. Retrograde transport from endosomes to the trans-Golgi network. Nature Reviews Molecular Cell Biology **7**: 568-579

Bosch M, Poulter NS, Vatovec S, and Franklin-Tong VE. 2008. Initiation of programmed cell death in self-incompatibility and several caspase-like activities. Molecular Plant **1**: 879-887

Bosch M, and Franklin Tong VE. 2007. Temporal and spatial activation of caspase-like enzymes induced by self-incompatibility in Papaver pollen. Proceedings of the National Academy of Science of the United States of America **104**: 18327-18332

Bosch M, and Franklin Tong VE. 2008. Self-incompatibility in Papaver: Signalling to trigger PCD in incompatible pollen. Journal of Experimental Botany **59**: 481-490

Braulke T, and Bonifacino JS. 2009. Sorting of lysosomal proteins. Biochimica et Biophysica Acta **1793**: 605-614

Breckenridge DG, Germain M, Mathai JP, Nguyen M, and Shore GC. 2003. Regulation of apoptosis by endoplasmic reticulum pathways. Oncogene **22**: 8608-8618

Breckenridge DG, Nguyan M, Kuppig S, Reth M, and Shore GC. 2002. The procaspase-8 isoform, procaspase-8L, recruited to the BAP31 complex at the endoplasmic reticulum. Proceedings of the National Academy of Sciences of the United States of America **99**: 4331-4336

Breckenridge DG, Stojanovic M, Marcellus RC, and Shore GC. 2003. Caspase cleavage product of BAP31 induces mitochondrial fission through endoplasmic reticulum calcium signals enhancing cytochrome c release to the cytosol. Journal of Cell Biology **31**: 1115-1127

Broadley MR, White PJ, Hammond JP, Zelko I, and Lux A. 2007. Zinc in plants. New Phytologist **173**: 677-702

Bu G, and Schwartz AL. 1998. RAP, a novel type of ER chaperone. Trends in Cell Biology **8**: 272-276

Bu G, Geuze HJ, Strous GJ, and Schwartz AL. 1995. 39 kDa receptor-associated protein is an ER resident protein and molecular chaperone for LDL receptor-related protein. The EMBO Journal **14**: 2269-2280

Buchner P, Takahashi H, and Hawkeford MJ. 2004. Plant sulphate transporters; co-ordination of uptake, intracellular and long-distance transport. Journal of Experimental Botany **55**: 1765-1773

Buck TM, Wright CM, and Brodsky JL. 2007. The activities and function of molecular chaperones in the endoplasmic reticulum. Seminars in Cell & Developmental Biology **18**: 751-761

Bue CA, and Barlowe C. 2009. Molecular dissection of Erv26p indentifies separable cargo binding and coat protein sorting activities. The Journal of Biological Chemistry **284**: 24049-24060

Bue CA, Bentivoglio CM, and Barlowe C. 2006. Erv26p directs pro-alkaline phosphatase into endoplasmic reticulum-derived coat protein complex II transport vesicles. Molecular Biology of the Cell **17**: 4780-4789

Carrel D, Masson J, Al Awabdh S, Capra CB, Lenkei X, Hamon M, Emerit MB, and Darmon M. 2008. Targeting of the 5-HT1A serotonin receptor to neuronal dendrites is mediated by Yif1B. Journal of Neuroscience **28**: 8063-8073

Carrier DJ. 2009. The Arabidopsis auxin transporter AUX1: Heterologous expression, characterisation and purification. University of Nottingham Thesis

Carrier DJ, Bakar NT, Swarup R, Callaghan R, Napier RM, Bennett MJ, and Kerr ID. 2008. The binding of auxin to the Arabidopsis auxin influx transporter AUX1. Plant Physiology **148**: 529-535

Carroll J, Altman MC, Fearnley IM, and Walker JE. 2007. Identification of membrane proteins by tandem mass spectrometry of protein ions. PNAS **104**: 14330-14335

Castresana J. 2000. Selection of conserved blocks from multiple alignments for their use in phylogenetic analysis. Molecular Biology Evolution **17**: 540-552

Chandra D, Choy G, Deng X, Bhatia B, Daniel P, and Tang DG. 2004. Association of active caspase 8 with the mitochondrial membrane during apoptosis: potential roles in cleaving BAP31 and caspase 3 and mediating mitochondrion-endoplasmic reticulum cross talk in etoposide-induced cell death. Molecular Cell Biology **24**: 6592-6607

Chen Y-F, Wang Y, and Wu W-H. 2008. Membrane transporters for nitrogen, phosphate and potassium uptake in plants. Journal of Integrative Plant Biology **50**: 835-848

Chevenet F, Brun C, Banuls AL, Jacq B, and Chisten R. 2006. TreeDyn: towards dynamic graphics and annotations for analyses of trees. BMC Bioinformatics **10**: 439

Claros MG, and von Heijne G. 1994. TopPredII: an improved software for membrane protein structure predictions. Bioinformatics **10**: 685-686

Clough SJ, and Bent AF. 1998. Floral dip: A simplified method for Agrobacterium-mediated transformation of Arabidopsis thaliana. The Plant Journal **16**: 735-743

Cohen CK, Fox TC, Garvin DF, and Kochian LV. 1998. The role of iron-deficiency stress responses in stimulating heavy-metal transport in plants. Plant Physiology **116**: 1063-1072

Colley NJ, Baker EK, Stamnes MA, and Zuker CS. 1991. The cyclophilin homolog ninaA is required in the secretory pathway. Cell **67**: 255-263

Contreras I, Yang Y, Robinson DG, and Aniento F. 2004. Sorting signals in the cytosolic tail of plant p24 proteins involved in the interaction with the COPII coat. Plant and Cell Physiology **45**: 1779-1786

Cooray SN, Chan L, Webb TR, Metherell L, and Clark AJ. 2009. Accessory proteins are vital for the function expression of certain G protein-coupled receptors. Molecular and cellular endocrinology **300**: 17-24

Cunningham MA, Pipe SW, Zhang B, Hauri H-P, Ginsburg D, and Kaufman RJ. 2003. LMAN1 is a molecular chaperone for the secretion of coagulation factor VIII. Journal of Thrombosis and Haemostasis **1**: 2360-2367

Danon A, Rotari VI, Gordon A, Mailhac N, and Gallois P. 2004. Ultraviolet-C overexposure induces programmed cell death in Arabidopsis, which is mediated by caspase-like activities and which can be suppressed by caspase inhibitors, p35 and defender against apoptotic death. Journal of Biological Chemistry **279**: 779-787

daSilva LL, Snapp EL, Denecke J, Lippincott-Schwartz K, Hawes C, and Brandizzi F. 2004. Endoplasmic reticulum export sites and Golgi bodies behave as single mobile secretory units in plant cells. The Plant Cell **16**: 1753-1771

d'Enfert C, Gensse M, and Gaillardin C. 1992. Fission yeast and a plant have functional homologues of the Sar1 and Sec12 proteins involved in ER to Golgi traffic in budding yeast. The EMBO Journal **11**: 4205-4211

De Angeli A, Monchello D, Ephritikhine G, Frachisse JM, Thomine S, Gambale F, and Barbier-Brygoo H. 2006. The nitrate/proton antiporter AtCLCa mediates nitrate accumulation in plant vacuoles. Nature Letters **442**: 939-942

De Jaco A, Lin MZ, Dubi N, Comoletti D, Miller MT, Camp S, Ellisman M, Butko MT, Tsien RY, and Taylor P. 2010. Neuroligin trafficking deficiencies

arising from mutations in the α/β hydrolase fold protein family. The Journal of Biological Chemistry **285**: 28674-28682

Dechorgnat J, Nguyen CT, Armengaud P, Jossier M, Diatloff E, Filleur S, Daniel-Vedel F. 2011. From the soil to the seeds: the long journey of nitrate in plants. Journal of Experimental Botany **62**: 1349-1359

Dell B, and Huang L. 1997. Physiological response of plants to low boron. Plant and Soil **193**: 103-120

Delom F, Fessart D, and Chevet E. 2007. Regulation of calnexin sub-cellular localization modulates endoplasmic reticulum stress-induced apoptosis in MCF-7 cells. Apoptosis **12**: 293-305

Denecke J, Botterman J, and Deblaere R. 1990. Protein secretion in plant cells can occur via a default pathway. The Plant Cell **2**: 51-59

Dereeper A, Audic S, Claverie JM, and Blanc G. 2010. BLAST-EXPLORER helps you building datasets for phylogenetic analysis. BMC Evolutionary Biology **12**: 8

Dereeper A, Guignon V, Blanc G, Audic S, Buffet S, Chevenet F, Dufayard JF, Guindon S, Lefort V, Lescot M, Claverie JM, and Gascuel O. 2008. Phylogeny fr: robust phylogenetic analysis for the non-specialist. Nucleic Acids Research **1**: W465-W469

Deutscher P. 1990. Guide to protein purification. Vol 182. Academic press, London

Dharmasiri S, Swarup R, Mockaitis K, Dharmasiri N, Singh SK, Kowalchyk M, Marchant A, Mills S, Sandberg G, Bennett MJ, and Estelle M. 2006. AXR4 is required for localization of the auxin influx facilitator AUX1. Science **312**: 1218-1220

Drew MC, and Saker LR. 1975. Nutrient supply and the growth of the seminal root system in barley: II. Localized, compensatory increases in lateral root growth and rates of nitrate uptake when nitrate supply is restricted to only part of the root system. Journal of Experimental Botany **26**: 79-90

Dubrovsky JG, Gambetta GA, Hernández-Barrera A, Shishkova S, and González I. 2006. Lateral root initiation in Arabidopsis: Developmental window, spatial patterning, density and predictability. Annuals of Botany **97**: 903-915

Dunkley TPJ, Hester S, Shadforth IP, Runions J, Weimar T, Hanton SL, Griffin JL, Bessant C, Brandizzi F, Hawes C, Watson RB, Dupree P, and

Lilley KS. 2006. Mapping the Arabidopsis organelle proteome. Proceedings of the National Academy of Sciences of the United States of America **103**: 6518-6523

Dwyer ND, Troemel ER, Sengupta P, and Bargmann CI. 1996. Odorant receptor localization to olfactory cilia is mediated by ODR-4, a novel membrane-associated protein. Cell **93**: 455-466

Edgar RC. 2004. MUSCLE: multiple sequence alignment with high accuracy and high throughput. Nucleic Acid Research **19**: 1792-1797

Fath S, Mancias JD, Bi X, and Goldberg J. 2007. Structure and organization of coat proteins in the COPII cage. Cell **129**: 1325-1336

Fernández-Sánchez E, Díez-Guerra FJ, Cubelos B, Giménez C, and Zafra F. 2008. Mechanisms of endoplasmic-reticulum export of glycine transporter-1 (GLYT1). The Biochemical Journal **409**: 669-681

Ferreira PA, Nakayama TA, Pak WL, and Travis GH. 1996. Cyclophilin-related protein RanBP2 acts as chaperone for red/green opsin. Nature **383**: 637-640

Filleur S, and Daniel-Vedele F. 1999. Expression analysis of a high-affinity nitrate transporter isolated from Arabidopsis thaliana by differential display. Planta **207**: 461-469

Finn RD, Mistry J, Tate J, Coggill P, Heger A, Pollington JE, Gavin OL, Gunesekaran P, Ceric G, Forslund K, Holm L, Sonnhammer EL, Eddy SR, and Bateman A. 2010. The Pfam protein families database. Nucleic Acid Research: D211-D222

Flowers TJ. 1999. Salinisation and horticultural production: Preface. Scientia Horticulturae **78**: 1-4

Forsthoefel NR, Wu Y, Schultz B, Bennett MJ, and Feldman KA. 1992. T-DNA insertion mutagenesis in Arabidopsis: prospects and perspectives. Australian Journal of Plant Physiology **19**: 353-366

French AP, Mills S, Swarup R, Bennett MJ and Pridmore TP. 2008. Colocalization of fluorescent markers in confocal microscope images of plant cells. Nature Protocols **3**: 619-628

Friml J. 2010. Subcellular trafficking of PIN auxin efflux carriers in auxin transport. European Journal of Cell Biology **89**: 231-235

Friml J, Benková E, Blilou I, Wisniewska J, Hamann T, Ljung K, Woody S, Sandberg G, Scheres B, Jürgens G, and Palme K. 2002. AtPIN4 mediates sink driven auxin gradients and patterning in Arabidopsis roots. Cell **108**: 661-673

Friml J, Vieten A, Sauer M, Weijers D, Schwarz H, Hamann T, Offringa R, and Jürgens G. 2003. Efflux-dependent auxin gradients establish the apical-basal axis of Arabidopsis. Nature **426**: 147-153

Garcia-Molina A, Andrés-Colás N, Perea-García A, del Valle-Tascón S, Peñarrubia L, and Puig S. 2011. The intracellular Arabidopsis COPT5 transport protein is required for photosynthetic electron transport under severe copper deficiency. The Plant Journal **65**: 848-860

Gazzarrini S, Lejay T, Gojon A, Ninnemann O, Frommer WB, von Wiren N. 1999. Three functional transporters for constitutive, diurnally regulated, and starvation-induced uptake of ammonium into Arabidopsis roots. Plant Cell **11**: 937-947

Geelen D, Lurin C, Bouchez D, Frachisse J-M, Leliévre F, Courtial B, Barbeir-Brygoo H, and Maurel C. 2000. Disruption of putative anion channel gene AtCLC-a in Arabidopsis suggests a role in the regulation of nitrate content. The Plant Journal **21**: 259-267

Geldner N. 2004. The plant endosomal system – it's structure and role in signal transduction and plant development. Planta **219**: 547-560

Geldner N, Anders N, Wolters H, Keicher J, Kornberger W, Muller P, Delbarre A, Ueda T, Nakano A, and Jürgens G. 2003. The Arabidopsis GNOM ARF-GEF mediates endosomal recycling, auxin transport, and auxin-dependent plant growth. Cell **112**: 219-230

Gilstring CF, Melin-Larsson M, and Ljungdahl. 1999. Shr3p mediates specific COPII coatomer-cargo interactions required for the packaging of amino acid permeases into ER-derived transport vesicles. Molecular Biology of the Cell **10**: 3549-3565

Goldbach HE, and Wimmer MA. 2007. Boron in plants and animals: Is there a role beyond cell-wall structure. Journal of Plant Nutritional Soil Science **170**: 39-48

González G, Solano R, Rubio V, Leyva A, and Paz-Ares J. 2005. PHOSPHATE TRANSPORTER TRAFFIC FACILITATOR1 is a plant-specific SEC12-related

protein that enables the endoplasmic reticulum exit of a high-affinity phosphate transporter in Arabidopsis. The Plant Cell **17**: 3500-3512

Gough J, Karplus K, Hughey R, and Chothia C. 2001. Assignment of homology to genome sequences using a library of hidden Markov models that represent all proteins of known structure. Journal of Molecular Biology **313**: 903-919

Greenberg JT. 1996. Programmed cell death: A way of life for plants. Proceedings of the National Academy of Sciences of the United States of America **93**: 12094-12097

Grissammer R, and Buchanan SK. 2006. Structural biology of membrane proteins. RSC Publishing, Cambridge

Guade N, Bréhélin C, Tischendorf G, Kessler F, and Dörmann P. 2007. Nitrogen deficiency in Arabidopsis affects galactolipid composition and gene expression and results in accumulation of fatty acid phytl esters. The Plant Journal **49**: 729-739

Guidon S, and Gascuel O. 2003. A simple, fast, and accurate algorithm to estimate large phylogenies by maximum likelihood. System Biology **52**: 696-704

Hadlington JL, and Denecke J. 2000. Sorting of soluble proteins in the secretory pathway of plants. Current Opinion in Plant Biology **3**: 461-468

Hall D, Evans AR, Newbury HJ, and Pritchard J. 2006. Functional analysis of CHX21: a putative sodium transporter in Arabidopsis. Journal of Experimental Botany **57**: 1201-1210

Halliwell B, and Gutteridge JM. 1984. Oxygen toxicity, oxygen radicals, transition metals and disease. Biochemistry Journal **219**: 1-14

Hanahan D. 1983. Studies on transformation of Escherichia coli with plasmids. Journal of Molecular Biology **166**: 557-580

Hanton SL, Bortolotti LE, Renna L, Stefano G, and Brandizzi F. 2005b. Crossing the divide – transport between the Endoplasmic Reticulum and Golgi apparatus in plants. Traffic **6**: 267-277

Hanton SL, Chatre L, Renna L, Matheson LA, and Brandizzi F. 2007. De novo formation of plant endoplasmic reticulum export sites is membrane cargo induced and signal mediated. Plant Physiology **143**: 1640-1650

Hanton SL, Matheson LA, and Brandizzi F. 2006. Seeking a way out: Export of proteins from the plant endoplasmic reticulum. Trends in Plant Science **11**: 335-343

Hanton SL, Renna L, Bortolotti LE, Chatre L, Stefano G, and Brandizzi F. 2005a. Diacidic motifs influence the export of transmembrane proteins from the endoplasmic reticulum in plant cells. The Plant Cell **17**: 3081-3093

Hauri H-P, and Schweizer A. 1992. The endoplasmic reticulum-Golgi intermediate compartment. Current Opinion in Cell Biology **4**: 600-608

Hawes C, and Satiat-Jeunemaitre B. 2005. The plant Golgi apparatus – going with the flow. Biochimica et Biophysica Acta **1744**: 93-107

Heinzer S, Wörz S, Kalla C, Rohr K, and Weiss M. 2008. A model for the self-organization of exit sites in the endoplasmic reticulum. Journal of Cell Science **121**: 55-64

Helliwell CA, Wesley SV, Wielopolska AJ, and Waterhouse PM. 2002. High-throughput vectors for efficient gene silencing in plant. Functional Plant Biology **29**: 1217-1255

Herrmann JM, Malkus P, and Schekman R. 1999. Out of the ER – outfitters, escorts and guides. Trends In Cell Biology **9**: 5-7

Higashio H, Kimata Y, Kiriyama T, Hirata A, and Kohno K. 2000. Sfb2p, a yeast protein related to Sec24p, can function as a constituent of COPII coats required for vesicle budding from the endoplasmic reticulum. Journal of Biological Chemistry **275**: 17900-17908

Hobbie LJ. 2006. Auxin and cell polarity: The emergence of AXR4. Trends in Plant Science **11**: 517-518

Hobbie L, and Estelle M. 1995. The axr4 auxin-resistant mutants of Arabidopsis thaliana define a gene important for root gravitropism and lateral root initiation. The Plant Journal **7**: 221-220

Hofte H, and Chrispeels MJ. 1992. Protein sorting to the vacuolar membrane. The Plant Cell **4**: 995-1004

Holmquist M. 2000. Alpha/beta hydrolases fold enzymes: structures, functions and mechanisms. Current Protein Peptide Science **1**: 209-235

Hong Z, Jin H, Tzfira T, and Li J. 2008. Multiple mechanism-mediated retention of a defective brassionsteroid receptor in the endoplasmic reticulum of Arabidopsis. The Plant Cell **20**: 3418-3429

Hu YC. 2005. Baculovirus as a highly efficient expression vector in insect and mammalian cells. Acta Pharmacologica Sinica **26**: 405-416

Huang M, Weissman JT, and Balch WE. 2001. Crystal structure of Sar1-GDP at 1.7A resolution and the role of the NH2 terminus in ER export. Journal of Cell Biology **155**: 937-948

Hunte C, Von Jagow G, and Schägger H. 2003. Membrane protein purification and crystallization: A practical guide. Ed second edition. Academic Press, New York

Inaba T, and Schnell DJ. 2008. Protein trafficking to plastids: one theme, many variations. Biochemical Journal **413**: 15-28

Jaquinod M, Villiers F, Kieffer-Jaquinod S, Hugouvieux V, Bruley C, Garin J, and Bourguignon. 2006. A proteomics dissection of Arabidopsis thaliana vacuole isolated from cell culture. Molecular Cellular Proteomics **6**: 394-412

Johnannes L, and Popoff V. 2008. Tracing the retrograde route in protein trafficking. Cell **135**: 1175-1187

Jones-Rhoades MW, Bartel DP, and Bartel B. 2006. MicroRNAs and their regulatory role in plants. Annual Review of Plant Biology **57**: 19-53

Jürgens G, and Geldner N. 2002. Protein secretion in plants: from the trans-Golgi network to the outer space. Traffic **3**: 605-613

Kampfenkel K, Kushnir S, Babiychuk E, Inzé D, and Van Montagu M. 1995. Molecular characterization of a putative Arabidopsis thaliana copper transporter and its yeast homologue. The Journal of Biological Chemistry **270**: 28479-28486

Kang B-H, and Staehelin LA. 2008. ER-to-Golgi transport by COPII vesicles in Arabidopsis involves a ribosome-excluding scaffold that is transferred with the vesicles to the Golgi matrix. Protoplasma **234**: 51-64

Kappeler F, Klopfenstein DR, Forguet M, Paccaud JP, and Hauri HP. 1997. The recycling of ERGIC53 in the early secretory pathway. ERGIC53 carries a cytosolic endoplasmic reticulum-exit determinant interacting with COPII. Journal of Biological Chemistry **272**: 31801-31808

Kargul JM. 1998. Biochemical characterization of AUX1 protein from Arabidopsis thaliana. PhD thesis. University of Warwick. United Kingdom

Karimi M, Inze D, and Depicker A. 2002. Gateway vectors for Agrobacterium-mediated plant transformation. Trends in Plant Science **7**: 193-195

Kasajima I, and Fujiwara T. 2007. Identification of novel Arabidopsis thaliana genes which are induced by high levels of boron. Plant Biotechnology **24**: 355-360

Kim K-M, Adachi T, Nielsen PJ, Terashima M, Lamera MC, Köhler G, and Reth M. 1994. Two new proteins preferentially associated with membrane immunoglobulin D. The EMBO Journal **13**: 3793-3800

King LA, and Posse RD. 1992. The Baculovirus Expression System. 106-119. Chapman and Hall. London

Kjellnom P, and Larsson C. 1984. Preparation and polypeptide composition of chlorophyll-free plasma membranes from leaves of light grown spinach and barley. Plant Physiology **62**: 501-509

Kobae Y, Uemura T, Sato MH, Ohnishi M, Mimura T, Nakagawa T, and Maeshima M. 2004. Zinc transporter of Arabidopsis thaliana AtMTP1 is localized to vacuolar membranes and implicated in zinc homeostasis. Plant Cell Physiology **45**: 1749-1758

Kobayashi K, Masuda T, Takamiya K, and Ohta H. 2006. Membrane lipid alteration during phosphate starvation is regulated by phosphate signalling and auxin/cytokinin cross-talk. The Plant Journal **47**: 238-248

Kosola KR, and Bloom AJ. 1996. Chlorate as a transport analog for nitrate absorption by roots of tomato. Plant Physiology **110**: 1293-1299

Kota J, and Ljungdahl PO. 2005. Specialized membrane-localized chaperones prevent aggregation of polytopic proteins in the ER. The Journal of Cell Biology **168**: 79-88

Kota J, Gilstring CF, and Ljungdahl. 2007. Membrane chaperone Shr3 assists in folding amino acid permeases preventing precocious ERAD. The Journal of Cell Biology **176**: 617-628

Kramer EM. 2004. PIN and AUX/LAX proteins: Their role in auxin accumulation. Trends In Plant Science **9**: 578-582

Krapp A, Fraiser V, Scheible WR, Quesada A, Gojon A, Stitt M, Caboche M, and Daniel-Vedele F. 1998. Expression studies of NRT2: 1Np, a putative high-affinity nitrate transporter: evidence for its role in nitrate uptake. The Plant Journal **14**: 723-731

Krouk G, Crawford NM, Coruzzi GM, and Tsay Y-F. 2010. Nitrate signalling: adaption to fluctuating environments. Current Opinion in Plant Biology **13**: 266-273

Kuehn MJ, Herrmann JM, and Schekman R. 1998. COPII-cargo interactions direct protein sorting into ER-derived transport vesicles. Nature **391**: 187-190

Kuehn MJ, Schekman R, and Ljungdahl PO. 1996. Amino acid permeases require COPII components and the ER resident membrane protein Shr3p for packaging into transport vesicles in vitro. The Journal of Cell Biology **135**: 585-595

Kunji ER, Chen KW, Slotbloom DJ, Floyd S, O'Conner R, and Monne M. 2005. Eukaryotic membrane protein overproduction in Lactococcus lactis. Current Opinion in Biotechnology **16**: 546-551

Ladasky JJ, Boyle S, Seth M, Li H, Pentcheva T, Abe F, Steinberg SJ, and Edidin M. 2006. Bap31 enhances the endoplasmic reticulum export and quality control of human class I MHC molecules. The Journal of Immunology **177**: 6172-6181

Laemmli, UK. 1970. Cleavage of structural proteins during the assembly of the head of bacteriophage T4. Nature **227**: 680-685

Lambert G, Becker B, Schreiber R, Boucherot A, Reth M, and Kunzelmann K. 2001. Control of cystic fibrosis transmembrane conductance regulator expression by BAP31. Journal of Biological Chemistry **276**: 20340-20345

Lau W-TW, Howson RW, Malkus P, Schekman R, and O'Shea EK. 2000. Pho86p, and endoplasmic reticulum (ER) resident protein in Saccharomyces cerevisiae, is required for ER exit of the high-affinity phosphate transporter Pho84p. Proceedings of the National Academy of Sciences of the United States of America **97**: 1107-1112

Lee EK, Kwon M, Ko J-H, Yi H, Hwang MG, Chang S, and Cho MH. 2004. Binding of sulfonylurea by AtMRP5, an Arabidopsis multidrug resistance-related protein that functions in salt tolerance. Plant Physiology **134**: 528-538

Lee MCS, and Miller EA. 2007. Molecular mechanisms of COPII vesicle formation. Seminars in Cell & Developmental Biology **18**: 424-434

Levanony H, Rubin R, Altschuler Y, and Galili G. 1992. Evidence for a novel route of wheat storage proteins to vacuoles. Journal of Cell Biology **119**: 1117-1128

Li J, Lease KA, Tax FE, and Walker JC. 2001. BRS1, a serine carboxypeptidase regulates BRI1 signalling in Arabidopsis thaliana. PNAS **98**: 5916-5921

Liebel U, Kindler B, and Pepperkok R. 2005. Bioinformatic "Harvester": a search engine for genome-wide human, mouse, and rat protein resources. Methods in Enzymology **404**: 19-26

Ljungdahl PO, Gimeno CJ, Styles CA, and Fink GR. 1992. SHR3: A novel component of the secretory pathway specifically required for localization of amino acid permeases in yeast. Cell **71**: 463-478

Luschnig C, Gaxiola RA, Grisafi P, and Fink GR. 1998. EIR1, a root-specific protein involved in auxin transport, is required for gravitropism in Arabidopsis thaliana. Genes Development **12**: 2175-2187

Lv Q-D, Tang R-J, Liu H, Gao X-S, Zheng H-Q, and Zhang H-X. 2009. Cloning and molecular analyses of the Arabidopsis thaliana chloride channel gene family. Plant Science **176**: 650-661

Maathuis FJ, Filatov V, Herzyk P, Krijger GC, Axelsen KB, Chen S, Green BJ, Li Y, Madagan KL, Sanchez-Fernandez R, Forde BG, Palmgren MG, Rea PA, Williams LE, Sanders D, and Amtmann A. 2003. Transcriptome analysis of root transporters reveals participation of multiple gene families in response to cation stress. The Plant Journal **35**: 675-692

Madeo F, Durchschlag M, Kepp O, Panaretakis T, Zitvogel L, Fröhlich K-U, and Kroemer G. 2009. Phylogenetic conservation of the preapoptotic calreticulin exposure pathway from yeast to mammals. Cell Cycle **8**: 639-642

Maher EP, and Martindale SJ. 1980. Mutants of Arabidopsis thaliana with altered responses to auxins and gravity. Biochemical Genetics **18**: 1041-1053

Malamy JE, and Benfy PN. 1997. Organization and cell differentiation in lateral roots of Arabidopsis thaliana. Development **124**: 33-44

Malkus P, Graham LA, Stevens TH, and Schekman R. 2004. Role of Vma21p in assembly and transport of the yeast vacuolar ATPase. Molecular Biology of the Cell **15**: 5075-5091

Malkus P, Jiang F, and Schekman R. 2002. Concentrative sorting of secretory cargo proteins into COPII-coated vesicles. Journal of Cell Biology **159**: 915-921

Mann M, and Jenson ON. 2003. Proteomic analysis of post-translational modifications. Nature Biotechnology **21**: 255-261

Marchant A, Bhalerao R, Casimiro I, Eklof J, Casero PJ, Bennett MJ, and Sandberg G. 2002. AUX1 promotes lateral root formation by facilitating indole-3-acetic acid distribution between sink and source tissue in the Arabidopsis seedling. The Plant Cell **14**: 589-597

Marchant A, Kargul J, May ST, Muller P, Delbarre A, Perrot-Rechenmann C, and Bennett MJ. 1999. AUX1 regulates root gravitropism in Arabidopsis by facilitating auxin uptake within root apical tissues. EMBO Journal **18**: 2066-2073

Marchler-Bauer A, Anderson JB, Derbyshire MK, DeWeese-Scott C, Gonzales NR, Gwadz M, Hao L, He S, Hurwitz DI, Jackson JD, Ke Z, Krylov D, Lanczycki CJ, Liebert CA, Liu C, Lu F, Lu S, Marchler GH, Mullokandov M, Song JS, Thanki N, Yamashita RA, Yin JJ, Zhang D, and Bryant SH. 2007. CCD: A conserved domain database for interactive domain analysis. Nucleic Acid Research **35**: 237-240

Marschner H. 1995. Mineral nutrition of higher plants. Marschner H, Editor. Academic Press, London

Mäser P, Thomine S, Schroeder JI, Ward JM, Hirschi K, and Sze H. 2001. Phylogenetic relationship within cation transporter families of Arabidopsis. Plant Physiology **126**: 1646-1667

Mäser P, Eckelman B, Vaidyanathan R, Horie T, Fairbairn DJ, Kubo M, Yamagami M, Yamagami K, Nishimura M, Uozumi N, Robertson W, Sussman MR, and Schroeder JI. 2002. Altered shoot/root Na^+ distribution and bifurcating salt sensitivity in Arabidopsis by genetic disruption of the Na^+ transporter AtHKT1. FEBS Letters **531**: 157-161

Mayer MP. 2010. Gymnastics of molecular chaperones. Molecular Cell **39**: 321-331

McLatchie LM, Fraser NJ, Main MJ, Wise A, Brown J, Thompson N, Solari R, Lee MG, and Foord SM. 1998. RAMPs regulate the transport and ligand specificity of the calcitonin-receptor-like receptor. Nature **393**: 333-339

Meijering E, Jacob M, Sarria J-CF, Steiner P, Hirling H, and Unser M. 2004. Design and validation of a tool for neurite tracing and analysis in fluorescence microscopy images. Cytometry Part A **58**: 167-176

Mellman I, and Warren G. 2000. The road taken past and future foundations of membrane traffic. Cell **100**: 99-112

Memon AR. 2004. The role of ADP-ribosylation factor and SAR1 in vesicular trafficking in plants. Biochimica et Biophysica Acta **1664**: 9-30

Mi H, Lazareva-Ulitsky B, Loo R, Kejariwal A, Vandergriff J, Rabkin S, Guo N, Muruganujan A, Doremieux O, Campbell MJ, Kitano H, and Thomas PD. 2005. The PANTHER database of protein families, subfamilies, functions and pathways. Nucleic Acids Research **33**: D284-D288

Mikosch M, Hurst AC, Hertel B, and Homann U. 2006. Diacidic motif is required for efficient transport of the K^+ channel KAT1 to the plasma membrane. Plant Physiology **142**: 923-930

Miller EA, Beilharz T, Malkus P, Lee M, Hamamoto S, Orci L, and Schekman R. 2003. Multiple cargo binding sites on the COPII subunit Sec24p ensure capture of diverse membrane proteins into transport vesicles. Cell **114**: 497-509

Mitsuhashi N, Hayashi Y, Koumoto Y, Shimada T, Fukasawa-Akada T, Nishimura M, and Hara-Nishimura I. 2001. A novel membrane protein that is transported to protein storage vacuoles via precursor-accumulating vesicles. The Plant Cell **13**: 2361-2372

Mochizuki S, Harada A, Inada S, Sugimoto-Shirasu K, Stacey N, Wada T, Ishiguro S, Okada K, and Sakai T. 2005. The Arabidopsis WAVY GROWTH 2 protein modulates root bending in response to environmental stimuli. The Plant Cell **17**: 537-547

Monacello D, Allot M, Oliva S, Krapp A, Daniel-Vedele F, Barbier-Brygoo H, and Ephritikhine G. 2009. Two anion transporters AtCLCa and AtCLCe fulfil interconnecting but not redundant roles in nitrate assimilation pathways. New Phytologist **183**: 88-94

Moore CA, Bowen HC, Scrase-Field S, Knight MR, and White PJ. 2002. The deposition of Suberin lamellae determines the magnitude of cytosolic Ca2+ elevations in root endodermal cells subjected to cooling. The Plant Journal **30**: 457-465

Mossessova E, Bickford LC, and Goldberg J. 2003. SNARE selectivity of the COPII coat. Cell **114**: 483-495

Müller J, Piffanelli P, Devoto A, Miklis M, Elliott C, Ortman B, Schulze-Lefert P, and Panstruga R. 2005. Conserved ERAD-like quality control of a plant polytopic membrane protein. The Plant Cell **17**: 149-163

Muñiz M, Nuoffer C, Hauri H-P, and Riezman H. 2000. The Emp24 complex recruits a specific cargo molecule into endoplasmic reticulum-derived vesicles. The Journal of Cell Biology **148**: 925-930

Munro S, and Pelham HR. 1986. An Hsp70-like protein in the ER: Identity with the 78 Kd glucose-regulated protein and immunoglobulin heavy chain binding protein. Cell **46**: 291-300

Murashige T, and Skoog F. 1962. A revised medium for rapid growth and bioassays with tobacco tissue cultures. Plant Physiology **15**: 473-497

Murphy A, and Taiz L. 1995. A new vertical mesh transfer technique for metal tolerance studies in Arabidopsis. Plant Physiology **108**: 29-38

Nable RO, Bañuelos GS, and Paull JG. 1997. Boron toxicity. Plant and Soil **193**: 181-198

Nable RO, Cartwright B, and Lance RC. 1990. Genotypic differences in boron accumulation in barley: Relative susceptibilities to boron deficiency and toxicity. In: El Bassam N, Dambroth M, Loughman B, eds. Genetic Aspects of Plant Mineral Nutrition. Kluwer Academic Publishers, Dordrecht, The Netherlands: 243-251

Naeem A, French AP, Wells DM, and Pridmore TP. 2011. High-throughput feature counting and measurement of roots. Bioinformatics **27**: 1337-1338

Nakagawa T, Kurose T, Hino T, Tanaka K, Kawamukai M, Niwa Y, Toyooka K, Matsuoka K, Jinbo T, and Kimura T. 2007. Development of series of Gateway Binary Vectors pGWBs for realizing efficient construction of fusion genes for plant transformation. Journal of Bioscience and Bioengineering **104**: 34-41

Nakamura T, Hayashi T, Nasu-Nishimura Y, Sakaue F, Morishita Y, Okabe T, Ohwada S, Matsuura K, and Akiyama T. 2008. PX-RICS mediate ER-to-Golgi transport of the N-cadherin/β-catenin complex. Genes & Development **22**: 1244-1256

Nakanishi H, 2007. Erv14 family cargo receptors are necessary for ER exit during sporulation in Saccharomyces cerevisiae. Journal of Cell Science **120**: 908-916

Nanjo Y, Oka H, Ikarashi N, Kaneko K, Kitajima A, Mitsui T, Munoz FJ, Rodriguez-Lopez M, Baroja-Fernandez E, and Pozueta-Romero J. 2006. Rice plastidial N-glycosylated nucleotide pyrophosphatase/phosphodiesterase is transported from the ER-Golgi to the chloroplast through the secretory pathway. The Plant Cell **18**: 2582-2592

Nardini M, and Dijkstra BW. 1999. α/β hydrolase fold enzymes: the family that keeps growing. Current Opinion in Structural Biology **9**: 732-737

Nebenführ A. 2002. Vesicle traffic in the endomembrane system: a tale of COPs, Rabs and SNARES. Current Opinion in Plant Biology **5**: 507-512

Nebenführ A, Gallagher LA, Dunahay TG, Frohlick JA, Mazurkiewicz AM, Meehl JB, and Staehelin LA. 1999. Stop-and-GO movements of plant Golgi stacks are mediated by the acto-myosin system. Plant Physiology **121**: 1127-1141

Neumann U, Brandizzi F, and Hawes C. 2003. Protein transport in plant cells: in and out of the Golgi. Annals of Botany **92**: 167-180

Ng FWH, and Shore GC. 1998. Bcl-X_L cooperatively associates with the Bap31 complex in the endoplasmic reticulum dependent on procaspase-8 and Ced-4 adaptor. The Journal of Biological Chemistry **273**: 3140-3143

Nguyen M, Breckenridge DG, Ducret A, and Shore GC. 2000. Caspase-resistant BAP31 inhibits Fas-mediated apoptotic membrane fragmentation and release of cytochrome c from mitochondria. Molecular and Cellular Biology **20**: 6731-6740

Nielsen M, Lundegaard C, Lund O, and Petersen TN. 2010. CPHmodels-3.0 – Remote homology modelling using structure guided sequence profiles. Nucleic Acids Research **38**: W576-581

Nishimura N, and Balch WE. 1997. A di-acidic signal required for selective export from the endoplasmic reticulum. Science **227**: 556-558

Noguchi K, Yasumori M, Imai T, Naito S, Matsunaga T, Oda H, Hayashi H, Chino M, and Fujiwara T. 1997. Bor1-1, an Arabidopsis thaliana mutant that requires a high level of boron. Plant Physiology **115**: 901-906

Noh B, Murphy AS, and Spalding EP. 2001. Multidrug resistance-like genes of Arabidopsis required for auxin transport and auxin-mediated development. Plant Cell **13**: 2441-2454

Nyfeler B, Zhang B, Ginsburg D, Kaufman RJ, and Hauri H-P. 2006. Cargo selectivity of the ERGIC-53/MCFD2 transport receptor complex. Traffic **7**: 1473-1481

O'Neill MA, Ishii T, Albersheim P, and Darvill AG. 2004. Rhamnogalacturonan II: structure and function of a borate cross-linked cell wall pectic polysaccharide. Annual Review of Plant Biology **55**: 109-139

Obayashi T, Hayashi S, Saeki M, Ohta H, and Kinoshita K. 2009. ATTED-II provides coexpressed gene networks for Arabidopsis. Nucleic Acid Research **37**: D987-D991

Obayashi T, Hayashi S, Shibaoka M, Saeki M, Ohta H, and Kinoshita K. 2008. COXPRESdb: A database of coexpressed gene networks in mammals. Nucleic Acid Research **36**: D77-D82

Obayshi T, Nishida K, Kasahara K, and Kinoshita K. 2011. ATTED-II uptakes: condition-specific gene coexpression analyses and applications to a broad range of flowering plants. Plant Cell Physiology **52**: 213-219

Orsel M, Chopin F, Leleu O, Smith SJ, Krapp A, Daniel-Vedele F, and Miller AJ. 2006. Characterization of a two-component high-affinity nitrate uptake system in Arabidopsis: physiology and protein-protein interaction. Plant Physiology **142**: 1304-1317

Ossowski S, Schwab R, and Weigel D. 2008. Gene silencing in plants using artificial microRNAs and other small RNAs. The Plant Journal **53**: 674-690

Otegui MS, and Spitzer C. 2008. Endosomal functions in plants. Traffic **9**: 1589-1598

Otte S, and Barlowe C. 2002. The Erv41p-Erv46p complex. Multiple export signals are required in trans for COPII-dependent transport from the ER. EMBO Journal **21**: 6095-6104

Pagano A, Letourneur F, Garcia-Estefania D, Carpentier J-L, Orci L, and Paccaud J-P. 1999. Sec24 proteins and sorting at the endoplasmic reticulum. Journal of Biological Chemistry **274**: 7833-7840

Palade G. 1975. Intracellular aspects of the process of protein synthesis. Science **189**: 347-358

Pang Y, Li L, Ren F, Lu P, Wei P, Cai J, Xin L, Zhang J, Chen J, and Wang X. 2010. Overexpression of the tonoplast aquaporin AtTIP5;1 conferred tolerance to boron toxicity in Arabidopsis. Journal of Genetics and Genomics **37**: 389-397

Paponov IA, Teale WD, Trebar M, Blilou I, and Palme K. 2005. The PIN auxin efflux facilitators: evolutionary and functional perspectives. Trends in Plant Science **10**: 170-177

Paquet ME, Cohen-Doyle M, Shore GC, and Williams DB. 2004. Bap29/31 influences the intracellular traffic of MHC class I molecules. Journal of Immunology **172**: 7548-7555

Parry G, Marchant A, May S, Swarup R, Swarup K, James N, Graham N, Allen T, Martucci T, Yemm A, Napier R, Manning K, King G, and Bennett M. 2001. Quick on the uptake: Characterization of a family of plant auxin influx carriers. Journal of Plant Growth Regulation **20**: 217-225

Pertea G, Huang X, Liang F, Antonescu V, Sultana R, Karamycheva S, Lee Y, White J, Cheung F, Parvizi B, Tsai J, and Quackenbush J. 2003. TIGR Gene Indices clustering tools (TGICL): A software system for fast clustering of large EST datasets. Bioinformatics **19**: 651-652

Petrášek J, and Friml J. 2009. Auxin transport routes in plant development. Development **136**: 2675-2688

Phillipson BA, Pimpl P, daSilva LL, Crofts AJ, Taylor JP, Movafeghi A, Robinson DG, Denecke J. 2001. Secretory bulk flow of soluble proteins is efficient and COPII dependent. The Plant Cell **13**: 2005-2020

Plaxton WC, and Carswell MC. 1999. Metabolic aspects of the phosphate starvation response in plants. Lemer HR, Editor. Plant Responses to Environmental Stresses: From Phytohormones to Genome Reorganization, Dekker, New York 349:372

Poirier Y, and Bucher M. 2002. Phosphate transport and homeostasis in Arabidopsis. The Arabidopsis Book **1**: e0024

Powers J, and Barlowe C. 1998. Transport of Axl2p depends on Erv14p, an ER-vesicle protein related to the Drosophila cornichon gene product. The Journal of Cell Biology **142**: 1209-1222

Powers J, and Barlowe C. 2002. Erv14p directs a transmembrane secretory protein into COPII-coated transport vesicles. Molecular Biology of the Cell **13**: 880-891

Prasad MNV. 2004. Heavy metal stress in plants – from biomolecules to ecosystems. Verlag, India: Springer. ISBN: 3-540-40131-8

Prydz K, Dick G, and Tveit H. 2008. How many ways through the Golgi maze? Traffic **9**: 299-304

Puig S, and Peñarrubia L. 2009. Placing metal micronutrients in context: transport and distribution in plants. Current Opinion in Plant Biology **12**: 299-304

Rancour DM, Dickey CE, Park S, and Bednarek SY. 2002. Characterization of AtCDC48. Evidence for multiple membrane fusion mechanisms at the cell division in plants. Plant Physiology **130**: 1241-1253

Rausch C, and Bucher, M. 2002. Molecular mechanisms of phosphate transport in plants. Planta **216**: 23-37

Raven JA, Evans MCW, and Korb RE. 1999. The role of trace metals in photosynthetic electron transport in O_2-evolving organisms. Photosynthesis Research **60**: 111-149

Reape TJ, and McCabe PF. 2008. Apoptotic-like programmed cell death in plants. New Phytologist **180**: 13-26

Reinhardt D. 2003. Vascular patterning: more than just auxin? Current Opinion in Biology **13**: R485-R487

Reinhardt D, Pesce ER, Stieger P, Mandel T, Baltensperger K, Bennett M, Traas J, Friml J, and Kuhlemeier C. 2003. Regulation of phyllotaxis by polar auxin transport. Nature **426**: 255-260

Reiterer V, Maier S, Sitte HH, Kriz A, Rüegg MA, Hauri H-P, Freissmuth M, and Farhan H. 2008. Sec 24- and ARFGAP1-dependent trafficking of GABA Transport-1 is a prerequisite for correct axonal targeting. The Journal of Neuroscience **28**: 12453-12464

Richter S, Voβ U, and Jürgens G. 2009. Post-Golgi traffic in plants. Traffic **10**: 819-828

Roberg KJ, Crotwell M, Espenshade P, Gimeno R, and Kaiser CA. 1999. LST1 is a SEC24 homologue used for selective export of plasma membrane ATPase from the endoplasmic reticulum. Journal of Cell Biology **145**: 659-672

Ronchi P, Colombo S, Francolini M, and Borgese N. 2008. Transmembrane domain-dependent partitioning of membrane proteins within the endoplasmic reticulum. Journal of Cell Biology **181**: 105-118

Rouse DT, Marotta R, and Parish RW. 1996. Promoter and expression studies on an Arabidopsis thaliana dehydrin gene. FEBS Letters **381**: 252-256

Rouillé Y, Rohn W, and Hoflack B. 2000. Targeting of lysosomal proteins. Seminars in Cell and Developmental Biology **11**: 165-171

Saheki Y, and Bargmann CI. 2009. Presynaptic CaV2 calcium channel traffic requires CALF-1 and the $\alpha_2\delta$ subunit UNC-36. Nature Neuroscience **12**: 1257-1265

Saito K. 2000. Regulation of sulfate transport and synthesis of sulfur-containing amino acids. Current Opinion in Plant Biology **3**: 188-195

Saito K, Chen M, Bard F, Chen S, Zhou H, Woodley D, Polischuk R, Schekman R, and Malhotra V. 2009. TANGO1 facilitates cargo loading at endoplasmic reticulum exit sites. Cell **136**: 891-902

Sambrook J, Fritsch E, and Maniatis T. 1989. Molecular cloning: A laboratory manual. Cold Spring Harbor Laboratory Press, Cold Spring Harbour, NY, USA. **ISBN**: 0-87969-309-6

Sancenón V, Puig S, Mateu-Andrés I, Dorcey E, Thiele DJ and Peñarrubia L. 2004. The Arabidopsis copper transporter COPT1 functions in root elongation and pollen development. Journal of Biological Chemistry **279**: 15348-15355

Sancenón V, Puig S, Mira H, Thiele DJ, and Peñarrubia L. 2003. Identification of a copper transporter family in Arabidopsis thaliana. Plant Molecular Biology **51**: 577-587

Sato K, and Nakano A. 2003. Oligomerisation of a cargo receptor directs protein sorting into COPII-coated transport vesicles. Molecular Biology of the Cell **14**: 3055-3063

Sato K, and Nakano A. 2007. Mechanisms of COPII vesicle formation and protein sorting. FEBS Letters **581**: 2076-2082

Sauer M, Balla J, Luschnig C, Wiśniewska J, Reinöhl V, Friml J, and Benková E. 2006. Canalization of auxin flow by Aux/IAA-ARF dependent feed-back regulation of PIN polarity. Genes Development **20**: 2902-2911

Scarpella E, Marcos D, Friml J, and Berleth T. 2006. Control of leaf vascular patterning by polar auxin transport. Genes Development **20**: 1015-1027

Schamel WW, Kuppig S, Becker B, Gimborn K, Hauri HP, and Reth M. 2003. A high-molecular-weight complex of membrane proteins BAP29/BAP31 is involved in the retention of membrane-bound IgD in the endoplasmic reticulum. Proceedings of the National Academy of Sciences of the United States of America **19**: 9861-9866

Scheible W-R, Morcuende R, Czechowski T, Fritz C, Osuna D, Palacios-Rojas N, Schindelasch D, Thimm O, Udvardi MK, and Stitt M. 2004. Genome-wide reprogramming of primary and secondary metabolism, protein synthesis, cellular growth processes, and the regulatory infrastructure of Arabidopsis in response to nitrogen. Plant Physiology **136**: 2483-2499

Schekman R, and Orci L. 1996. Coat proteins and vesicle budding. Science **271**: 1526-1533

Schutzendubel A, and Polle A. 2002. Plant responses to abiotic stresses: heavy metal-induced oxidative stress and protection by mycorrhization. Journal of Experimental Botany **53**: 1351-1365

Schwab R, Ossowski S, Riester M, Warthmann N, and Weigel D. 2006. Highly specific gene silencing by artificial microRNAs in Arabidopsis. Plant Cell **18**: 1121-1133

Schwacke R, Schneider A, Van Der Graaf E, Fischer K, Catoni E, Desimone M, Frommer WB, Flugge UI, and Kunze R. 2003. ARAMEMNON, a novel database for Arabidopsis integral membrane proteins. Plant Physiology **131**: 16-26

Sharpe LJ, Luu W, and Brown AJ. 2011. Akt phosphorylates Sec24: New clues into the regulation of ER-to-Golgi trafficking. Traffic **12**: 19-27

Sherwood PW, and Carlson M. 1999. Efficient export of the glucose transporter Hxt1p from the endoplasmic reticulum requires Gsf2p. Proceedings of the National Academy of Sciences of the United States of America. **96**: 7415-7420

Shibagaki N, Rose A, McDermott JP, Fujiwara T, Hayashi H, Yoneyama T, and Davies JP. **2002.** Selenate-resistant mutants of Arabidopsis thaliana identified Sultr1;2, a sulfate transporter required for efficient transport of sulfate into roots. The Plant Journal **29**: 475-486

Shin H, Shin H-S, Dewbre GR, and Harrison MJ. 2004. Phosphate transport in Arabidopsis: Pht1;1 and Pht1;4 play a major role in phosphate acquisition from both low- and high-phosphate environments. The Plant Journal **39**: 629-642

Sieben C, Mikosch M, Brandizzi F, and Homann U. 2008. Interaction of the K+-channel KAT1 with the coat protein complex II coat component Sec24 depends on a di-acidic endoplasmic reticulum export motif. The Plant Journal **56**: 997-1006

Simmons C, Migliaccio F, Masson P, Caspar T, and Söll D. 1995. A novel root gravitropism mutant of Arabidopsis thaliana exhibiting altered auxin physiology. Physiologia Plantarum **93**: 790-798

Sohlenkamp C, Shelden M, Howitt S, Udvardi M. 2000. Characterization of Arabidopsis AtAMT2, a novel ammonium transporter in plants. FEBS Letters **467**: 273-278

Sorefan K, Grin T, Lijegren SJ, Ljung K, Robles P, Galván-Ampudia CS, Offringa R, Friml J, Yanofsky MF, and Østergaard L. 2009. A regulated auxin maxima is required for seed dispersal in Arabidopsis. Nature **459**: 583-586

Soulie S, Moller JV, Falson P, le Marie M. 1996. Urea reduces the aggregation of membrane proteins on sodium dodecyl sulfate-polyacrylamide gel electrophoresis. Analytical Biochemistry **236**: 363-364

Spiliotis ET, Pentcheva T, and Edidin M. 2002. Probing for membrane domains in the endoplasmic reticulum: Retention and degradation of unassembled MHC class I molecules. Molecular Biology of the Cell **13**: 1566-1581

Staehelin A, and Kang B-H. 2008. Nanoscale architecture of Endoplasmic Reticulum export sites and of Golgi membrane as determined by electron tomography. Plant Physiology **147**: 1454-1468

Stefano G, Renna L, Chatre L, Hanton SL, Moreau P, Hawes C, Brandizzi F. 2006. In tobacco leaf epidermal cells, the integrity of protein export from the endoplasmic reticulum and of ER export sites depends on active COPI machinery. The Plant Journal **46**: 95-110

Stojanovic M, Germain M, Nguyen M, and Store GC. 2005. BAP31 and its caspase cleavage product regulate cell surface expression of tetraspanins and integrin-mediated cell survival. The Journal of Biological Chemistry **280**: 30018-30024

Suaud L, Miller K, Alvey L, Yan W, Robay A, Kebler C, Kreindler JL, Guttentag S, Hubbard MJ, and Rubenstein RC. 2011. ERp29 regulates ΔF508 and wild type CFTR trafficking to the plasma membrane in CF and non-CF epithelial cells. The Journal of Biological Chemistry **doi:** 10.1074/jbc.M111.240267

Sucic S, El-Kasaby A, Kudlacek O, Sarker S, Sitte HH, Marin P, and Freissmuth M. 2011. The serotonin transporter is an exclusive client of the coat protein complex II (COPII) component SEC24C. The Journal of Biological Chemistry **286**: 15482-16490

Surpin M, and Raikhel N. 2004. Traffic jams affect plant development and signal transduction. Nature Reviews Molecular Cell Biology **5**: 100-109

Swanton E, High S, and Woodman P. 2003. Role of calnexin in the glycan-independent quality control of proteolipid protein. EMBO Journal **22**: 2948-2958

Swarbreck D, Wilks C, Lamesch P, Berardini TZ, Garcia-Hernandez M, Foerster H, Li D, Meyer T, Muller R, Ploetz L, Radenbaugh A, Singh S, Swing V, Tissier C, Zhang P, and Huala E. 2008. The Arabidopsis Information Resource (TAIR): Gene structure and function annotation. Nucleic Acids Research **36**: D1009-D1014

Swarup R, Friml J, Marchant A, Ljung K, Sandberg G, Palme K, and Bennett M. 2001. Localization of the auxin permease AUX1 suggests two functionally distinct hormone transport pathways operate in the Arabidopsis root apex. Genes & Development **15**: 2648-2653

Swarup R, Kargul J, Marchant A, Zadik D, Rahman A, Mills R, Yemm A, May S, Williams L, Millner P, Tsurumi S, Moore I, Napier R, Kerr ID, and Bennett MJ. 2004. Structure-function analysis of the presumptive Arabidopsis auxin permease AUX1. Plant Cell **16**: 3069-3083

Swarup R, Kramer EM, Perry P, Knox K, Ottoline Leyser HM, Haseloff J, Beemster GTS, Bhalerao R, and Bennett MJ. 2005. Root gravitropism

requires lateral root cap and epidermal cells for transport and response to a mobile auxin signal. Nature Cell Biology **7**: 1057-1065

Szczensa-Skorupa E, and Kemper B. 2006. BAP31 is involved in the retention of cytochrome P450 2C2 in the endoplasmic reticulum. Journal of Biological Chemistry **281**: 4142-4148

Szpunar J. 2005. Advances in analytical methodology for bioinorganic speciation analysis: metallomics, metalloproteomics and heteroatom-tagged proteomics and metabolomics. Analyst **130**: 442-465

Tanaka H, Dhonukshe P, and Friml J. 2006. Spatio-temporal asymmetric auxin distribution: means to coordinate plant development. Cellular Molecular Life Science **63**: 2738-2754

Takano J, Miwa K, and Fujiwara T. 2008. Boron transport mechanisms: collaboration of channels and transporters. Trends in Plant Science **13**: 451-457

Takano J, Noquchi K, Yasumori M, Kobayashi M, Gajdos Z, Miwa K, Hayashi H, Yoneyama T, and Fujiwara T. 2002. Arabidopsis boron transporter for xylem loading. Nature **420**: 337-340

Takano J, Tanaka M, Toyoda A, Miwa K, Kasai K, Fuji K, Onouchi H, Naito S, and Fujiwara T. 2010. Polar localization and degradation of Arabidopsis boron transporters through distinct trafficking pathways. PNAS **doi**: 10.1073/pnas.0910744107

Takano J, Wada M, Ludewig U, Schaaf G, von Wirén N, and Fujiwara T. 2006. The Arabidopsis major intrinsic protein NIP5;1 is essential for efficient boron uptake and plant development under boron limitation. The Plant Cell Online **18**: 1498-1509

Tan X, Qin Z, and Zheng R. 2002. Uptake and distribution of trace metal elements in wheat seedlings. Biological Trace Element Research **85**: 77-85

Tendot Abu Baker N. 2007. Characterization of AXR4 protein function from Arabidopsis thaliana. University of Nottingham Thesis. United Kingdom.

The Gene Index Database, Dana Farber Cancer Institute, Boston, MA 02115 (URL: http://www.danafarber.org/) [11/2008 accessed].

Thomine S, Wang R, Ward JM, and Crawford NM. 2002. Cadmium and iron transport by members of a plant metal transporter family in Arabidopsis with homology to Nramp genes. PNAS **97**: 4991-4996

Thomine S, Wang R, Ward JM, Crawford NM, and Schroeder JI. 2000. Cadmium and iron transport by members of a plant metal transporter family in Arabidopsis with homology to Nramp genes. PNAS **97**: 4991-4996

Timpte C, Lincoln C, Picket FB, Turner J, and Estelle M. 1995. The AXR4 and AUX1 genes of Arabidopsis function in separate auxin-response pathways. The Plant Journal **8**: 561-568

Toikkanen JH, Fatal N, Hildén P, Makarow M, and Kuismanen E. 2006. YET1, YET2 and YET3 of Saccharomyces cerevisiae encode BAP31 homologs with partially overlapping functions. Journal of Biological Sciences **6**: 446-456

Trilla JA, Durám A, and Roncero C. 1999. Chs7p, a new protein involved in the control of protein export from the endoplasmic reticulum that is specifically engaged in the regulation of chitin synthesis in Saccharomyces cerevisiae. The Journal of Cell Biology **145**: 1153-1163

Tsay YF, Chiu CC, Tsal CB, Ho CH, Hsu PK. 2007. Nitrate transporters and peptide transporters. FEBS Letters **581**: 2290-2300

Ueda T, and Nakano A. 2002. Vesicular traffic: An integral part of plant life. Current Opinion in Plant Biology **5**: 513-517

Ugartechea-Chirino Y, Swarup R, Swarup K, Péret B, Whitworth M, Bennett M, and Bougourd S. 2010. The AUX1 LAX family of auxin influx carriers is required for the establishment of embryonic root cell organization in Arabidopsis thaliana. Annuals of Botany **105**: 227-289

van Vilet C, Thomas EC, Merino-Trigo A, Teasdale RD, and Gleeson PA. 2003. Intracellular sorting and transport of proteins. Progress in Biophysics and Molecular Biology **83**: 1-45

Vandenberghe W, Nicoll RA, and Bredt DS. 2005. Interaction with the unfolded protein response reveals a role for stargazin in biosynthetic AMPA receptor transport. The Journal of Neuroscience **25**: 1095-1102

Vandenbussche F, Petrásek J, Zádníková P, Hoyerová K, Pesek B, Raz V, Swarup R, Bennett M, Zazímalová E, Benková E, and Van Der Straeten D. 2010. The auxin influx carriers AUX1 and LAX3 are involved in auxin-ethylene interactions during apical hook development in Arabidopsis thaliana seedlings. Development **137**: 597-606

Vassilakos A, Cohen-Doyle MF, Peterson PA, Jackson MR, and Williams DB. 1996. The molecular chaperone calnexin facilitates folding and assembly of class I histocompatibility molecules. The EMBO Journal **15**: 1495-1506

Vaughn JL, Goodwin RH, Tompkins GJ, and McCawley P. 1977. The establishment of two cell lines from the insect Spodoptera frugiperda (Lepidoptera; Noctuidae). In Vitro **13**: 213-217

Verbruggen N, Hermans C, and Schat H. 2009. Mechanisms to cope with arsenic or cadmium excess in plants. Current Opinion in Plant Biology **12**: 1-9

Vert G, and Chory J. 2009. A toggle switch in plant nitrate uptake. Cell **138**: 1064-1066

Vitale A, and Boston RS. 2008. Endoplasmic reticulum quality control and the unfolded protein response: insights from plants. Traffic **9**: 1581-1588

Vitale A, and Hinz G. 2005. Sorting of proteins to storage vacuoles: how many mechanisms? Trends in Plant Science **10**: 316-323

Vitale A, and Raikhel N. 1999. What do proteins need to reach different vacuoles? Trends in Plant Science **4**: 149-155

Von Heijne G. 2006. Membrane-protein topology. Nature Review of Molecular Cell Biology **7**: 909-918

Wakana Y, Takai S, Nakajima KI, Tani K, Yamamoto A, Watson P, Stephens DJ, Hauri HP, and Tagaya M. 2008. Bap31 is an itinerant protein that moves between the peripheral endoplasmic reticulum (ER) and a juxtanuclear compartment related to ER-associated degradation. Molecular Biology of the Cell **19**: 1825-1836

Wang B, Heath-Engel H, Zhang D, Nguyen N, Thomas DY, Hanrahan JW, and Shore GC. 2008. BAP31 interacts with Sec61 translocons and promotes retrotranslocation of CFTRDeltaF508 via the derlin-1 complex. Cell **13**: 1080-1092

Wang B, Pelletier J, Massaad MJ, Herscovics A, and Shore GC. 2004. The yeast split-ubiquitin membrane protein two-hybrid screen identifies BAP31 as a regulator of the turnover of endoplasmic reticulum-associated protein tyrosine phosphatase-like B. Molecular and Cellular Biology **24**: 2767-2778

Ward JM. 2001. Identification of novel families of membrane proteins from the model plant Arabidopsis thaliana. Bioinformatics **17**: 560-563

Webb TR, Chan L, Cooray SN, Cheetham ME, Chapple JP, and Clark AJ. 2009. Distinct melanocortin 2 receptor accessory protein domains are required for melanocortin 2 receptor interaction and promotion of receptor trafficking. Endocrinology **150**: 720-726

Weijers D, Sauer M, Meurette O, Friml J, Ljung K, Sandberg G, Hooykass P, and Offringa R. 2005. Maintenance of embryonic auxin distribution for apical-basal patterning by PIN-FORMED-dependent auxin transport in Arabidopsis. Plant Cell **17**: 2517-2516

Wendeler MW, Paccaud J-P, and Hauri H-P. 2007. Role of Sec24 isoforms in selective export of membrane proteins from the endoplasmic reticulum. EMBO Reports **8**: 258-264

Welsh LM, Tong AHY, Boone C, Jensen ON, and Otte S. 2006. Genetic and molecular interactions of the Erv41p-Erv46p complex involved in transport between the endoplasmic reticulum and Golgi complex. Journal of Cell Science **119**: 4730-4740

White SH. 2009. Biophysical dissection of membrane proteins. Nature **459**: 344-346

White SH and von Heijne G. 2005. Transmembrane helices before, during and after insertion. Current Opinion in Structural Biology **15**: 378-386

Wielopolska A, Townley H, Moore I, Waterhouse P, and Helliwell C. 2005. A high-throughput inducible RNAi vector for plants. Plant Biotechnology Journal **3**: 583-590

Wigley WC, Fabunmi RP, Lee MC, Marino CR, Muallem S, DeMartino GN, and Thomas PJ. 1999. Dynamic association of proteasomal machinery with the centrosome. Journal of Cell Biology **145**: 481-490

Willemsen V, Wolkenfelt H, Vrieze G, Weisbeek P, and Sheres B. 1998. The HOBBIT gene is required for formation of the root meristem in the Arabidopsis embryo. Development **125**: 521-531

Winter D, Vinegar B, Nahal H, Ammar R, Wilson GV, and Provart NJ. 2007. An "Electronic Fluorescent Pictograph" browser for exploring and analyzing large-scale biological data sets. PLoS ONE **2**: e718

Wirth J, Chopin F, Santoni V, Viennois G, Tillard P, Krapp A, Lejay L, Daniel-Vedele F, and Gojon A. 2007. Regulation of root nitrate uptake at the NRT2.1

protein level in Arabidopsis thaliana. Journal of Biological Chemistry **282**: 23541-23552

Wiseman RL, Powers ET, Buxbaum JN, Kelly JW, and Balch WE. 2007. An adaptable standard for protein export from the endoplasmic reticulum. Cell **131**: 809-821

Woltering EJ, van der Bent A, and Horberichts FA. 2002. Do plant caspases exist? Plant Physiology **130**: 1764-1769

Xu C, Fan J, Cornish AJ, and Benning C. 2008. Lipid trafficking between the endoplasmic reticulum and the plastid in Arabidopsis require the extraplastidic TGD4 protein. The Plant Cell **20**: 2190-2204

Xu J, Hofhuis H, Heidstra R, Sauer M, Friml J, and Scheres B. 2006. A molecular framework for root regeneration. Science **311**: 385-388

Yamamoto M, and Yamamoto KT. 1998. Differential effect of 1-napthaleneacetic acid, indole-3-acetic acid and 2,4-dichlorophenoxyacetic acid on the gravitropic response of roots in an auxin-resistant mutant of Arabidopsis, aux1. Plant Cell Physiology **39**: 660-664

Yamamoto M, and Yamamoto KT. 1999. Effects of natural and synthetic auxins on the gravitropic growth habit of roots in two auxin-resistant mutants of Arabidopsis, axr1 and axr4: evidence for defects in the auxin influx mechanism of axr4. Journal of Plant Research **112**: 391-396

Yamamoto K. 2009. Intracellular lectins involved in folding and transport in the endoplasmic reticulum. Biological & Pharmaceutical Bulletin **32**: 767-773

Yang Y, Hammes UZ, Taylor CG, Schachtman DP, and Nielsen E. 2006. High-affinity auxin transport by the AUX1 influx carrier protein. Current Biology **16**: 1123-1127

Yang Y-D, Elamawi R, Bubeck J, Pepperkok R, Ritzenhaler C, and Robinson DG. 2005. Dynamics of COPII vesicles and the Golgi Apparatus in cultured Nicotiana tabacum BY-2 cells provides evidence for transient association of Golgi stacks with Endoplasmic Reticulum exit sites. The Plant Cell **17**: 1513-1531

Yeats C, Lees J, Reid A, Kellam P, Martin N, Liu X, and Orengo C. 2008. Gene3D: comprehensive structural and functional annotation of genomes. Nucleic Acid Research **36**: D414-D418

Yoshihisa T, Barlowe C, and Schekman R. 1993. Requirement for a GTPase-activating protein in vesicle budding from the endoplasmic reticulum. Science **259**: 1466-1468

Young GB, Jack DL, Smith DW, and Saier MH. 1999. The amino acid/auxin: protein symport permease family. Biochimie Biophysica Acta **1415**: 306-322

Yuasa K, Toyooka K, Fukuda H, and Matsuoka K. 2004. Membrane-anchored prolyl hydroxylase with an export signal from the endoplasmic reticulum. The Plant Journal **41**: 81-94

Zaarour N, Demaretz S, Defontaine N, Mordasini D, and Laghmani K. 2009. A highly conserved motif at the COOH terminus dictates endoplasmic reticulum exit and cell surface expression of NKCC2. Journal of Biological Chemistry **284**: 21752-21764

Zafra F, and Gimenez C. 2001. Molecular determinants involved in the asymmetrical distribution of glycine transporters in polarized cells. Biochemical Society Transactions **29**: 746-750

Zambryski P, Joos H, Genetello C, Leemans J, Montagu MV, and Schell J. 1983. Ti plasmid vector for the introduction of DNA into plant cells without alteration of their normal regeneration capacity. The EMBO Journal **2**: 2143-2150

Zelazny E, Miecielica U, Borst JW, Hemminga MA, and Chaumont F. 2008. An N-terminal diacidic motif is required for the trafficking of maize aquaporins ZmPIP2:4 and ZmPIP2:5 to the plasma membrane. The Plant Journal **57**: 346-355

Zen K, Utech M, Liu Y, Soto I, Nusrat A, and Parkos CA. 2004. Association of BAP31 with CD11b/CD18. Potential role in intracellular trafficking of CD11b/CD18 in neutrophils. Journal of Biological Chemistry **279**: 44924-44930

Zhang B, Kaufman RJ, and Ginsburg D. 2005. LMAN1 and MCFD2 form a cargo receptor complex and interact with coagulation factor VII in the early secretory pathway. Journal of Biological Chemistry **280**: 25881-25886

Zhang L, Xu Q, Xing D, Gao C, and Xiong H. 2009. Activation in vivo using fluorescence resonance energy transfer during plant programmed cell death induced by ultraviolet C overexposure. Plant Physiology **150**: 1773-1783

Zhao FJ, Hawkesford MJ, Warrilow AGS, McGrath SP, and Clarkson DT. 1996. Responses of two wheat varieties to sulphur addition and diagnosis of sulphur deficiency. Plant and Soil **181**: 317-327

9. APPENDIX

9.1. SEED LINES

Line	At Code	Description
N532583	At1g11905	T-DNA insert
N598336	At1g65020	T-DNA insert
N510039	At1g65020	T-DNA insert
N822782	At1g65270	T-DNA insert
N523673	At1g70770	T-DNA insert
N614289	At1g71780	T-DNA insert
N663810	At2g16760	T-DNA insert
N513066	At2g16760	T-DNA insert
N525841	At2g36290	T-DNA insert
N519285	At3g07190	T-DNA insert
N803596	At3g07190	T-DNA insert
N633340	At3g20450	T-DNA insert
N527201	At3g27325	T-DNA insert
N593742	At3g44330	T-DNA insert
N620858	At3g62360	T-DNA insert
N837011	At4g12590	T-DNA insert
N829287	At4g16170	T-DNA insert
N522300	At4g29520	T-DNA insert
N663464	At4g32130	T-DNA insert
N637042	At4g32130	T-DNA insert
N602859	At5g20520	T-DNA insert
N587030	At5g20520	T-DNA insert
N822482	At5g42570	T-DNA insert
N600808	At5g48660	T-DNA insert
N662942	At5g49945	T-DNA insert
axr4-2	At1g54990	γ-radiated insertion line
aux1-21	At2g38120	KO line

lax1	At5g01240	KO line
lax2	At2g21050	KO line
lax3	At1g77690	KO line
AXR4 GFP	At1g54990	GFP protein fusion line
NHA AUX1	At2g38120	NHA protein fusion line
NHA AUX1 axr4-2	At2g38120	NHA protein fusion line in axr4 background
LAX3 YFP	At1g77690	YFP protein fusion line
SR123		p35S GFP protein line

Table 14: Seed lines used

9.2. PRIMERS

Strategy	**Gene**	**Primer Name**	**Primer Sequence (5' – 3')**
For genotyping T-DNA insert	At1g11905	583 F1	CTCACGACTTCAACTTTCCTCCTT
		583 R1	TAGAAAACCACCTGGAAGAAACAC
	At1g65020	336 F1	CGGCGGAGATTAGATTACGA
		336 R1	CCTTCACAAACCCAGCTACC
		039 F1	CTGGCGGAGGTCAAGAAAC
		039 R1	AAATGGAGACAAGCGACGAT
	At1g65270	K 782-1	GAACATGCCTTCGGTGAC
		K 782-2	CATCCAAGCCATCCCGTGGTA
	At1g70770	K 673-1	AGCCAAGGAAGCTACAGC
		K 673-2	GCATACACTTATGTTCAAGAG
	At1g71780	K 289-1	GAAGTACTGTATCATCCC
		K 289-2	CACAGACCGACCATTCC
	At2g16760	810 F1	GACCACGTCAGAAACCGTCT
		810 R1	TGTAGCCGACGAGACTACCC
		066 F1	TTTGACCAGCTCAAGACACG
		066 R1	CGACAAGGAGACGGTTTCTG
	At2g36290	841 F1	TAACGCTTGTTGCTCCAGTG
		841 R1	CCATGCAAACACAAACACAAG
	At3g07190	285 F1	GGTGCGATTGCGTTCTTACT
		285 R1	GCTGTTTCGAGCTTCGTTTC
		596 F1	TACTCTATGAACTCGCTGCTGACC
		596 R1	TTCAAGCCAAATCAGCAGACAAGA
	At3g20450	340 F3	TTGCATATTTTGTTCCGATTGT
		340 R1	TCCCGAACCGATTGATAAGAACTA

	At3g27325	201 F1	TTGAGCGCACATTTTACCAG
		201 R1	ATGTTCCATTGACAGCCACA
	At3g44330	K 742-1	CATATCTATGGTCACCAAGG
		K 742-2	GAGAGGCATACAACCAAAC
	At3g62360	K 858-1	GCTGTAGTGTCAAAAGATGG
		K 858-2	GTTCTATAGCCAGTGTTGAAGG
		842 F1	GGGCTTTGTTATTTGATTGTTGTC
		842 R1	GATTTGGCTTTGGAGATGTTGG
	At4g12590	011 F1	CGAGAGGCTCAGTATCAGCA
		011 R1	AAGCTTTCAATGGAATCCACA
	At4g16170	K 287-1	AGACCTCACACGCGCATG
		K 287-2	CCAGCCACAAGTATTCCT
	At4g29520	K 300-1	TGCTGAAATGGACAAG
		K 300-2	GTTCTCTCATAAGAAGCAG
	At4g32130	464 F1	GCACTGGGCTACTTCTTCTCC
		464 R1	AGAGCAAAACATTCACCATCAA
		042 F1	ATTCCCATGTGCACGTCTTT
		042 R1	CCATGAACGGAGGTTTCAGA
	At5g20520	K 859-1	TGGTGGACTCGCAAATGAAC
		K 859-2	CATCTCCAGACGATGAGCG
		030 F1	GCCTCCTTTTATCACCCCCACTG
		859 R1	GGCAGCCGCTTTCGCATACAG
	At5g42570	K 482-1	CTTTACACAGTGATCTTCG
		K 482-2	CCCTTCTTTCCCTCAG
		RS3	CAGCACCTTCTTCTATACGAGCAG
		RS9	TTGGAAATCGAATAAGGGAACA
	At5g48660	809 F1	TGCTTGCTTTCTCTTCATTCTCC
		809 R1	TCAATTATAAAGCCGAGAAAAAGT
	At5g49945	942 F1	CATCAATCGCAGCTGTTCAA
		942 R1	TCTCATCTTTACAAGGAACAACCA
MRNA Expression Studies	AUX1	AUXGEN sphI	GATTATGCATGCTATGTGG
		3’ AUX3	TAATAGCTAAGAACCAAATAGG
	At1g11905	583 F2	TCGCTGTTGTTCTCTTCGAG
		583 R2	CTGGCCTTAACACCTTCCAA
	At1g65020	039 F1	CTGGCGGAGGTCAAGAAAC
		039 R1	AAATGGAGACAAGCGACGAT
	At1g65270	782 F1	ACCTGGAGTCATGGCGGAAAG
		782 R1	GCTTGTGTCACGGCATTCATCA
	At1g70770	673 F1	CTGTTAGGAAGGGAGAGCGTTTGA
		673 R1	CCCTCAGTGATGACCTCCTCG
	At1g71780	289 F1	ATGACGGAGAAGGAGAAGGAGAG
		289 R1	TGATTCTGGTGATGGGTTTGAGCA
	At2g16760	810 F1	GACCACGTCAGAAACCGTCT
		810 R1	TGTAGCCGACGAGACTACCC
	At2g36290	841 F1	TAACGCTTGTTGCTCCAGTG
		841 R2	CTCCCAAGTTCCAAATCCAA
	At3g07190	285 F1	GGTGCGATTGCGTTCTTACT

		285 R1	GCTGTTTCGAGCTTCGTTTC
	At3g20450	340 F2	TTCACAATCGTGACAATCGAA
		340 R2	CGGTTTTGCCCTTCTTTACA
	At3g27325	201 F1	TTGAGCGCACATTTTACCAG
		201 R1	ATGTTCCATTGACAGCCACA
	At3g44330	742 F1	TGGAAAATGCTGGAAGTCTGTCTG
		742 R1	AGGAGGCCGGCGAAATAAGC
	At3g62360	K 858-1	GCTGTAGTGTCAAAAGATGG
		K 858-2	GTTCTATAGCCAGTGTTGAAGG
	At4g12590	011 F2	ACATGTTCCCAAGGGAGAAG
		011 R2	TCCTTCTCTGCACCCAGACT
	At4g16170	K 287-1	AGACCTCACACGCGCATG
		K 287-2	CCAGCCACAAGTATTCCT
	At4g29520	300 F2	CGTCGGCGTTATTACCTGTT
		300 R2	TTGCAACAAATGGTTCTCCA
		300 R3	GACGATCCAAGTCCTTTCCA
	At4g32130	464 F2	TGCTTCCACTCTTCCGATCT
		464 R2	GGCTCCAAAACCAGCTCA
	At5g20520	859 F1	ACATCGCTCATCGTCTGGAG
		859 R1	GGCAGCCGCTTTCGCATACAG
	At5g42570	K 482-1	CTTTACACAGTGATCTTCG
		K 482-2	CCCTTCTTTCCCTCAG
	At5g48660	842 F2	GTAAAGGTCCTGCCACTGTGA
		842 R1	GATTTGGCTTTGGAGATGTTGG
	At5g49945	942 F2	AATTCTACGCGAGTGGTCGT
		942 R2	ATATGGAATTAGCGCCACCA
For cloning	Promoter GUS – At1g11905	P1G11 F1	ggCTCGAGTTTCGTAATTTAGCGGACTTCTC
		P1G11 R1	ggTCTAGACGTCTTTGATCTCAGAAGCGATA
	Promoter GUS – At3g07190	P3G07 F1	ggCTCGAGAACAATCATTGGGAAATGAACAG
		P3G07 R1	ggTCTAGAGTCCGATTCCCCCTCTTCCCAGTT
	Promoter GUS – At3g20450	P3G20 F1	ggCTCGAGCGACTTAAAATGGCAAAAGTTCA
		P3G20 R1	ggTCTAGATTTTTATTAGTACATGGAGAAGTTTAG
	Promoter GUS – At5g42570	RS1	AAATTTTTCTTGGAGGCACTGACA
		RS10	ggTCTAGATGTTCGTCGCCGGTGAGAGTAA
	Promoter GUS – At5g428660	P5G48 F1	ggCTCGAGGTATTTTGGAGTTGATGCCAGAG
		P5G48 R1	ggTCTAGAGTCTGAATGAGTTCTCCCCCTAA
	AtBAP31 RNAi cloning	RS11	ggGGATCCAAATGGCACTGATCCTTCTCCTC

	into Psilent1, PK7GW1WG2 & POPOF2H	RS12	ggCTCGAGTTACATACCCTTCTTTCCCTCAG
	AtBAP31 GFP RNAi cloning into Psilent1, PK7GW1WG2 & POPOF2H	RS13	ggGTCGACAAATGGCACTGATCCTTCTCCTC
		RS14	ggGGTACCTTACATACCCTTCTTTCCCTCAG
	AtBAP31 Family RNAi cloning into PK7GW1WG2 & POPOF2H	R1G11 F1	ggCCATGGGTTGATTATGAGCTTGGATCGTT
		R1G11 R1	ggGCATGCGGATTCACTACACCATCTTCGAT
		R3G07 F1	ggACTAGTGGGAGCTTGTAATGAAGAGCTTA
		R3G07 R1	ggGTCGACTGATATTCATGAGATTCGACAGG
		R3G20 F1	CTGCTAGACCTATCAAAGCAAGG
		R3G20 R1	TTGTGTGGATTTGAATAGTGCTG
		RS11	ggGGATCCAAATGGCACTGATCCTTCTCCTC
		RS14	ggGGTACCTTACATACCCTTCTTTCCCTCAG
		R5G48 F1	ggTCTAGAAGATTGGTCCTTTGAGAGAGCTT
		R5G48 R1	ACAGACATAGTTCCAGCGATTGT
	AtBAP31 Family miRNA cloning into PDEX00 & PGWB402Ω	miR I	gaTAATCTATCATACTCTAGCAGTCTCTCTTTTGTATTCC
		miR II	gaCTGCTAGAGTATGATAGATTATCAAAGAGAATCAATGA
		miR III	gaCTACTAGAGTATGTTAGATTTTCACAGGTCGTGATATG
		miR IV	gaAAATCTAACATACTCTAGTAGTCTACATATATATTCCT
		miR A	CTGCAAGGCGATTAAGTTGGGTAAC
		miR B	GCGGATAACAATTTCACACAGGAAACAG
	Random site directed mutagenesis of AXR4 for cloning into PGWB7	AXS 113 F1	GTAGCTGAATCANNTTCGATTCATACAGAGACTG
		AXS 113 R1	CTGTATGAATCGAANNTGATTCAGCTACAAAGAC
		AXS 140 F1	GAAATGATTCAATCTNNTGGATCAAAAGGGATCCATAG
		AXS 140 R1	CCTTTTGATCCANNAGATTGAATCATTTCC
		AXS 151 F1	GTGTTGCTATTNNTTTACCTGGAAATGGGTTCTC

		AXS 151 R1	CATTTCCAGGTAAANNAATAGCAACACTATGGATC
		AXS 154 F1	GCTATTGATTTACCTGGAAATGGGTTCTCTGATAAGTC
		AXS 154 R1	GAGAACCCATTTNNAGGTAAATCAATAGCAACAC
		AXS 201 F1	GATTGAAACTGGANNTTTGCCTTATGAGGAGATC
		AXS 201 R1	CTCATAAGGCAAANNTCCAGTTTCAATCATCTG
		AXS 246 F1	GCTCCTGTGCATNNGGTTCTTCATGATTCAGC
		AXS 246 R1	CATGAAGAACCNNATGCACAGGAGCTAAACC
		AXS 250 F1	GGTTCTTCATNNTTCAGCTTTAGGGTTAGCTTC
		AXS 250 R1	CCTAAAGCTGAANNATGAAGAACCAAATGCACAG
		AXS 320 F1	CTTTATCGGATATTNNTGCTCATAGGATACTTTTGAAG
		AXS 320 R1	GTATCCTATGAGCANNAATATCCGATAAAGTCATC
		AXS 361 F1	GGATTAATGGTATTNNGATGCAAGTGATTTGGTCTAG
		AXS 361 R1	CACTTGCATCNNAATACCATTAATCCCATCTG
		AXS 414 F1	CATATCAGAANNTGTCTCTCTCCTCCCTAAATC
		AXS 414 R1	GAGGAGAGAGACANNTTCTGATATGATTACTGCAAG
For screening and sequencing of constructs		PK7 R1	AGGTGGCACTTGTTGGTATG
		35S 1	ACTATCCTTCGCAAGAC
		Cat Intron Rev	GAGAAAAGGGTCCTAACCAAGA
		35S F	GGAAGTTCATTTCATTTGGA
		RB inward	CCGCCAATATATCCTGTCAA
		5'GUSR1	GAATGCCCACAGGCCGTCG
		R1G11 R2	GTACACGCTCGTCACCAGAA
		P1G11 F2	TGAAAGCCCCGAAACTAAAA
		P3G07 F2	CGCTCTTGGTTACACGCATA
		P3G20 F2	TTTGAGTCTTTGTATGTTTAATTTGA
		P5G48 F2	TTGCTTTTACAAAGGCATGAG
		RS1	AAATTTTTCTTGGAGGCACTGACA
		RS2	TTTTGGAGGTGGAAGGAGGAC
		RS3	CAGCACCTTCTTCTATACGAGCAG
		RS4	TAAGTCGATGCTCAAGGCGTCTCT
		RS5	CATTTTATTTCCATTGACCGACAC

		RS6	TGCTGTTCTTAATCCCACTGA
		RS7	TGAGGAAGACAATGGAGACTGC
		RS8	ACGGTGGTTCCTATGGTTTTGACG
		RS9	TTGGAAATCGAATAAGGGAACA
		RS10	ggTCTAGATGTTCGTCGCCGGTGAGAGTAA
		RS11	ggGGATCCAAATGGCACTGATCCTTCTCCTC
		RS12	ggCTCGAGTTACATACCCTTCTTTCCCTCAG
		RS13	ggGTCGACAAATGGCACTGATCCTTCTCCTC
		RS14	ggGGTACCTTACATACCCTTCTTTCCCTCAG
		RS15	CGTGGTCCCGTCGTCGTCA
		RS16	CTTCCCCGAGCGCTTTCACTT
		GFP5	GACGGGAACTACAAGACACG
		GFP6	CCAACTTGTGGCCGAGGATG

Table 15: PCR primers used.

9.3. SMART SCREEN STOCK SOLUTIONS

Ingredient		Concentration in stock solution	
Stock Solution	Molecular weight	Molarity (M)	g l-1
$Ca(H_2PO_4)_2$	252.07	0.0667	16.81
$Ca(NO_3)2.4H_2O$	236.15	0.5	118.075
$CaCl_2.2H_2O$	147.02	0.0125	1.84
$CaSO_4.4H_2O$	172.17	0.01	1.145
$CdSO_4$	256.5	0.01	2.565
$CuCl_2.2H_2O$	170.48	0.003	0.51
$CuSO_4.5H_2O$	249.68	0.003	0.75
$CuSO_4.5H_2O$	249.68	0.1	24.97
FeNaEDTA	367.05	0.05	18.35
$FeSO_4.7H_2O$	278.02	0.01	2.78
H_3BO_3	61.83	0.03	1.85
K_2SO_4	174.25	0.1333	23.23
KH_2PO_4	136.09	0.2667	36.3
KOH	56.1	0.5333	29.92
$MgCl_2.6H_2O$	203.31	0.75	152.48
$MgSO_4.7H_2O$	246.47	0.375	92.43
$MnCl_2.4H_2O$	197.9	0.01	1.98
$MnSO_4.4H_2O$	223.06	0.01	2.23
$Na_2EDTA.2H_2O$	372.24	0.05	18.61
$Na_2MoO_4.2H_2O$	241.95	0.0005	0.12
NaCl	58.44	1	58.44
$ZnCl_2$	136.3	0.1	13.6
$ZnSO_4.7H_2O$	287.55	0.001	0.29
$ZnSO_4.7H_2O$	287.55	0.1	28.76

Table 16: Smart screen stock solutions.

9.4. SMART SCREEN TREATMENTS

9.4.1. Main Solution

Main solution - control	Concentration in stock (M)	Volume required for 1L (ml)	Concentration of final solution (mM)
KH_2PO_4	0.2667	0.938	0.25
KOH	0.5333	0.938	0.50
$MgSO_4.7H_2O$	0.3750	2	0.75
$CaCl_2.2H_2O$	0.0125	2	0.025
FeNaEDTA	0.0500	2	0.10
$Ca(NO_3)_2.4H_2O$	0.5	8	4.00
Micronutrients	mM		µM
H_3BO_3	30.0	1	30.0
$MnSO_4.4H_2O$	10.0	1	10.0
$ZnSO_4.7H_2O$	1.0	1	1.0
$CuSO_4.5H_2O$	3.0	1	3.0
$Na_2MoO_4.2H_2O$	0.5	1	0.5

Table 17: Main solution

9.4.2. Boron

3 µM Boron	Concentration in stock (M)	Volume required for 1L (ml)	Concentration of final solution (mM)
KH_2PO_4	0.2667	0.938	0.25
KOH	0.5333	0.938	0.50
$MgSO_4.7H_2O$	0.3750	2	0.75
$CaCl_2.2H_2O$	0.0125	2	0.025
FeNaEDTA	0.0500	2	0.10
$Ca(NO_3)_2.4H_2O$	0.5	8	4.00
Micronutrients	mM		µM
H_3BO_3	30.0	0.1	3.0
$MnSO_4.4H_2O$	10.0	1	10.0
$ZnSO_4.7H_2O$	1.0	1	1.0
$CuSO_4.5H_2O$	3.0	1	3.0
$Na_2MoO_4.2H_2O$	0.5	1	0.5

Table 18: 3 µM boron solution.

150 µM Boron	Concentration in stock (M)	Volume required for 1L (ml)	Concentration of final solution (mM)
KH_2PO_4	0.2667	0.938	0.25
KOH	0.5333	0.938	0.50
$MgSO_4.7H_2O$	0.3750	2	0.75
$CaCl_2.2H_2O$	0.0125	2	0.025
FeNaEDTA	0.0500	2	0.10
$Ca(NO_3)_2.4H_2O$	0.5	8	4.00
Micronutrients	mM		µM
H_3BO_3	30.0	5	150.0
$MnSO_4.4H_2O$	10.0	1	10.0
$ZnSO_4.7H_2O$	1.0	1	1.0
$CuSO_4.5H_2O$	3.0	1	3.0
$Na_2MoO_4.2H_2O$	0.5	1	0.5

Table 19: 150 µM boron solution.

150 µM Boron	Concentration in stock (M)	Volume required for 1L (ml)	Concentration of final solution (mM)
½ MS		2.15	30
H_3BO_3	30.0	4	120.0

Table 20: 150 µM boron solution in ½ MS.

300 µM Boron	Concentration in stock (M)	Volume required for 1L (ml)	Concentration of final solution (mM)
½ MS		2.15	30
H_3BO_3	30.0	9	270

Table 21: 300 µM boron solution in ½ MS.

9.4.3. Copper

10 µM Copper	Concentration in stock (M)	Volume required for 1L (ml)	Concentration of final solution (µM)
½ MS (Sigma)		2.15 g	0.1
$CuSO_4$	0.1	0.099	9.9

Table 22: 10 µM copper solution.

20 µM Copper	Concentration in stock (M)	Volume required for 1L (ml)	Concentration of final solution (µM)
½ MS (Sigma)		2.15 g	0.1
$CuSO_4$	0.1	0.199	19.9

Table 23: 20 µM copper solution.

50 µM Copper	Concentration in stock (M)	Volume required for 1L (ml)	Concentration of final solution (µM)
½ MS (Sigma)		2.15 g	0.1
$CuSO_4$	0.1	0.499	49.9

Table 24: 50 µM copper solution.

9.4.4. Nitrogen

Zero Nitrogen	Concentration in stock (M)	Volume required for 1L (ml)	Concentration of final solution (mM)
KH_2PO_4	0.2667	0.938	0.25
KOH	0.5333	0.938	0.50
$MgSO_4.7H_2O$	0.3750	2	0.75
$CaCl_2.2H_2O$	0.0125	2	0.025
FeNaEDTA	0.0500	2	0.10
$CaSO_4.4H_2O$	0.01	400	4.00
Micronutrients	mM		µM
H_3BO_3	30.0	1	30.0
$MnSO_4.4H_2O$	10.0	1	10.0
$ZnSO_4.7H_2O$	1.0	1	1.0
$CuSO_4.5H_2O$	3.0	1	3.0
$Na_2MoO_4.2H_2O$	0.5	1	0.5

Table 25: 0 µM nitrogen solution.

50 μM Nitrogen	Concentration in stock (M)	Volume required for 1L (ml)	Concentration of final solution (mM)
KH_2PO_4	0.2667	0.938	0.25
KOH	0.5333	0.938	0.50
$MgSO_4.7H_2O$	0.3750	2	0.75
$CaCl_2.2H_2O$	0.0125	2	0.025
FeNaEDTA	0.0500	2	0.10
$CaSO_4.4H_2O$	0.01	400	4.00
$Ca(NO_3)_2.4H_2O$	0.5	0.01	0.05
Micronutrients	mM		μM
H_3BO_3	30.0	1	30.0
$MnSO_4.4H_2O$	10.0	1	10.0
$ZnSO_4.7H_2O$	1.0	1	1.0
$CuSO_4.5H_2O$	3.0	1	3.0
$Na_2MoO_4.2H_2O$	0.5	1	0.5

Table 26: 50 μM nitrogen solution.

9.4.5. Phosphorus

Zero Phosphorus 100 μM Fe	Concentration in stock (M)	Volume required for 1L (ml)	Concentration of final solution (mM)
K_2SO_4	0.1333	0.938	0.125
KOH	0.5333	0.938	0.50
$MgSO_4.7H_2O$	0.3750	2	0.75
$CaCl_2.2H_2O$	0.0125	2	0.03
FeNaEDTA	0.0500	2	0.10
$Ca(NO_3)_2.4H_2O$	0.5	8	4.00
Micronutrients	mM		μM
H_3BO_3	30.0	1	30.0
$MnSO_4.4H_2O$	10.0	1	10.0
$ZnSO_4.7H_2O$	1.0	1	1.0
$CuSO_4.5H_2O$	3.0	1	3.0
$Na_2MoO_4.2H_2O$	0.5	1	0.5

Table 27: 0 μM phosphorus and 100 μM iron solution.

10 μM Phosphorus 100 μM Fe	Concentration in stock (M)	Volume required for 1L (ml)	Concentration of final solution (mM)
KH_2PO_4	0.2667	0.038	0.01
K_2SO_4	0.1333	0.863	0.115
KOH	0.5333	0.938	0.50
$MgSO_4.7H_2O$	0.3750	2	0.75
$CaCl_2.2H_2O$	0.0125	2	0.03
FeNaEDTA	0.0500	2	0.10
$Ca(NO_3)_2.4H_2O$	0.5	8	4.00
Micronutrients	mM		μM
H_3BO_3	30.0	1	30.0
$MnSO_4.4H_2O$	10.0	1	10.0
$ZnSO_4.7H_2O$	1.0	1	1.0
$CuSO_4.5H_2O$	3.0	1	3.0
$Na_2MoO_4.2H_2O$	0.5	1	0.5

Table 28: 10 μM phosphorus and 100 μM iron solution.

50 μM Phosphorus 100 μM Fe	Concentration in stock (M)	Volume required for 1L (ml)	Concentration of final solution (mM)
KH_2PO_4	0.2667	0.19	0.05
K_2SO_4	0.1333	0.563	0.075
KOH	0.5333	0.938	0.50
$MgSO_4.7H_2O$	0.3750	2	0.75
$CaCl_2.2H_2O$	0.0125	2	0.03
FeNaEDTA	0.0500	2	0.10
$Ca(NO_3)_2.4H_2O$	0.5	8	4.00
Micronutrients	mM		μM
H_3BO_3	30.0	1	30.0
$MnSO_4.4H_2O$	10.0	1	10.0
$ZnSO_4.7H_2O$	1.0	1	1.0
$CuSO_4.5H_2O$	3.0	1	3.0
$Na_2MoO_4.2H_2O$	0.5	1	0.5

Table 29: 50 μM phosphorus and 100 μM iron solution.

9.4.6. Sodium

50 mM Sodium	Concentration in stock (M)	Volume required for 1L (ml)	Concentration of final solution (mM)
½ MS (Sigma)		2.15 g	0.1
NaCl	1	49.9	49.9

Table 30: 50 mM sodium solution.

100 mM Sodium	Concentration in stock (M)	Volume required for 1L (ml)	Concentration of final solution (mM)
½ MS (Sigma)		2.15 g	0.1
NaCl	1	99.9	99.9

Table 31: 100 mM sodium solution.

200 mM Sodium	Concentration in stock (M)	Volume required for 1L (ml)	Concentration of final solution (mM)
½ MS (Sigma)		2.15 g	0.1
NaCl	1	199.9	199.9

Table 32: 200 mM sodium solution.

9.4.7. Sulphate

Zero Sulphate	Concentration in stock (M)	Volume required for 1L (ml)	Concentration of final solution (mM)
KH_2PO_4	0.2667	0.938	0.25
KOH	0.5333	0.938	0.50
$MgCl_2$	0.75	1	0.75
$CaCl_2.2H_2O$	0.0125	2	0.025
FeNaEDTA	0.0500	2	0.10
$Ca(NO_3)_2.4H_2O$	0.5	8	4.00
Micronutrients	mM		µM
H_3BO_3	30.0	1	30.0
$MnCl_2.4H_2O$	10.0	1	10.0
$ZnCl_2$	100	0.01	1.0
$CuCl_2.2H_2O$	3.0	1	3.0
$Na_2MoO_4.2H_2O$	0.5	1	0.5

Table 33: 0 µM sulphate solution.

0.1 mM Sulphate	Concentration in stock (M)	Volume required for 1L (ml)	Concentration of final solution (mM)
KH_2PO_4	0.2667	0.938	0.25
KOH	0.5333	0.938	0.50
$MgCl_2$	0.75	0.86	0.65
$MgSO_4.7H_2O$	0.3750	0.26	0.1
$CaCl_2.2H_2O$	0.0125	2	0.025
FeNaEDTA	0.0500	2	0.10
$Ca(NO_3)_2.4H_2O$	0.5	8	4.00
Micronutrients	mM		µM
H_3BO_3	30.0	1	30.0
$MnCl_2.4H_2O$	10.0	1	10.0
$ZnCl_2$	100	0.01	1.0
$CuCl_2.2H_2O$	3.0	1	3.0
$Na_2MoO_4.2H_2O$	0.5	1	0.5

Table 34: 0.1 mM sulphate solution.

9.4.8. Zinc

250 µM Zinc	Concentration in stock (M)	Volume required for 1L (ml)	Concentration of final solution (µM)
½ MS (Sigma)		2.15 g	1
$ZnSO_4.7H_2O$	0.1	2.49	249

Table 35: 250 µM zinc solution.

500 µM Zinc	Concentration in stock (M)	Volume required for 1L (ml)	Concentration of final solution (µM)
MS - Sigma		4.3 g	1
$ZnSO_4.7H_2O$	0.1	4.99	499

Table 36: 500 µM zinc solution.

1000 µM Zinc	Concentration in stock (M)	Volume required for 1L (ml)	Concentration of final solution (µM)
MS - Sigma		4.3 g	1
$ZnSO_4.7H_2O$	0.1	9.99	999

Table 37: 1000 µM zinc solution.

9.5. DNA AND RNA RESULTS FROM T-DNA KO LINES

9.5.1. At1g11905 – TDNA insert N532583

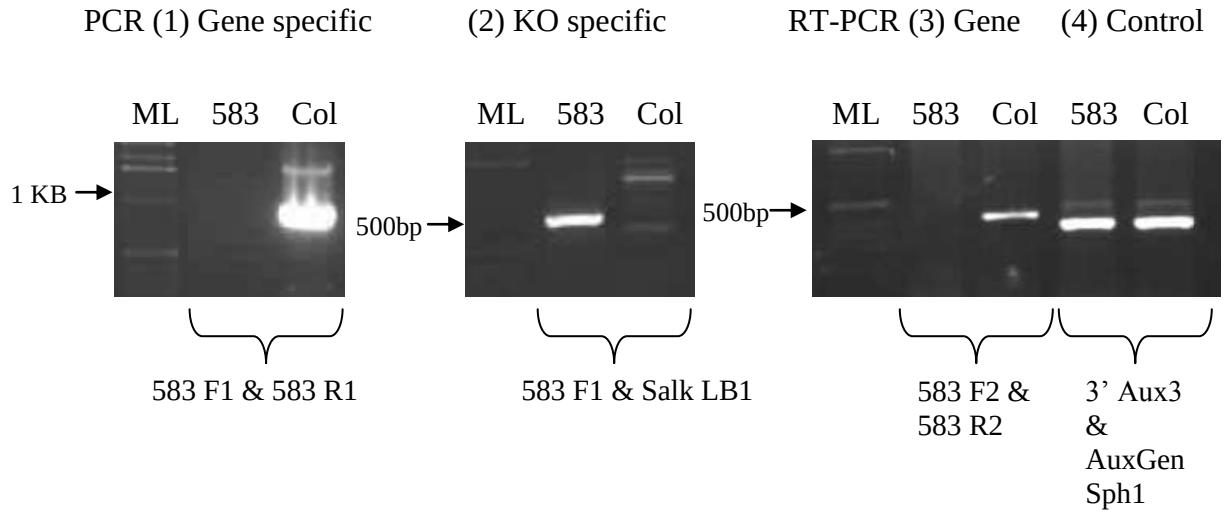

Figure 80: Genotyping and RT-PCR for N535583

N535583 (583) T-DNA insert is a homozygous KO line with complete loss of mRNA expression.

9.5.2. At1g65270 – TDNA insert N822782

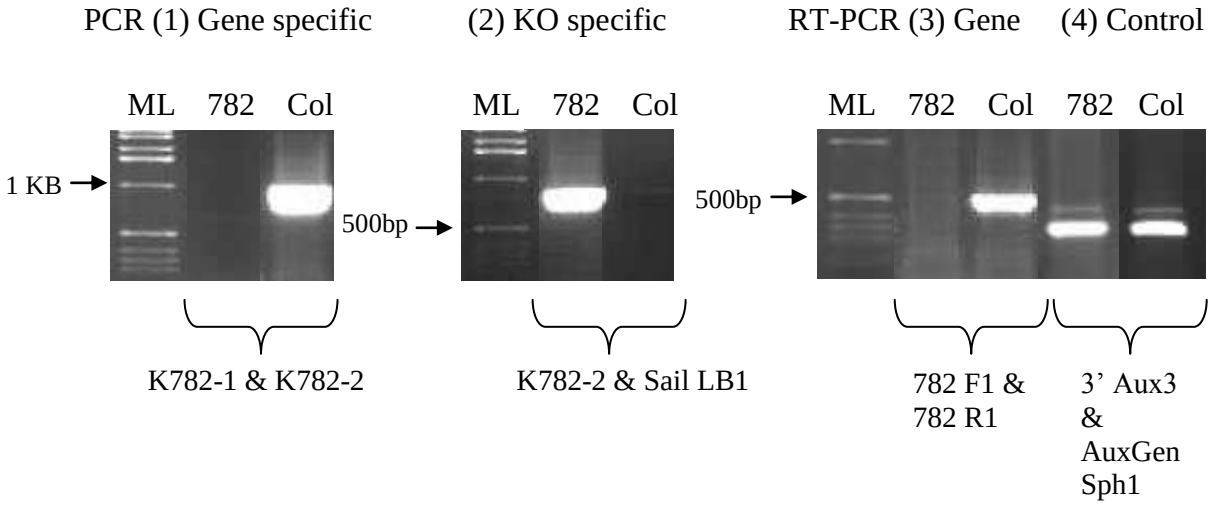

Figure 81: Genotyping and RT-PCR for N822782

N822782 (782) T-DNA insert is a homozygous KO line with complete loss of mRNA expression.

9.5.3. At1g70770 – TDNA insert N665550

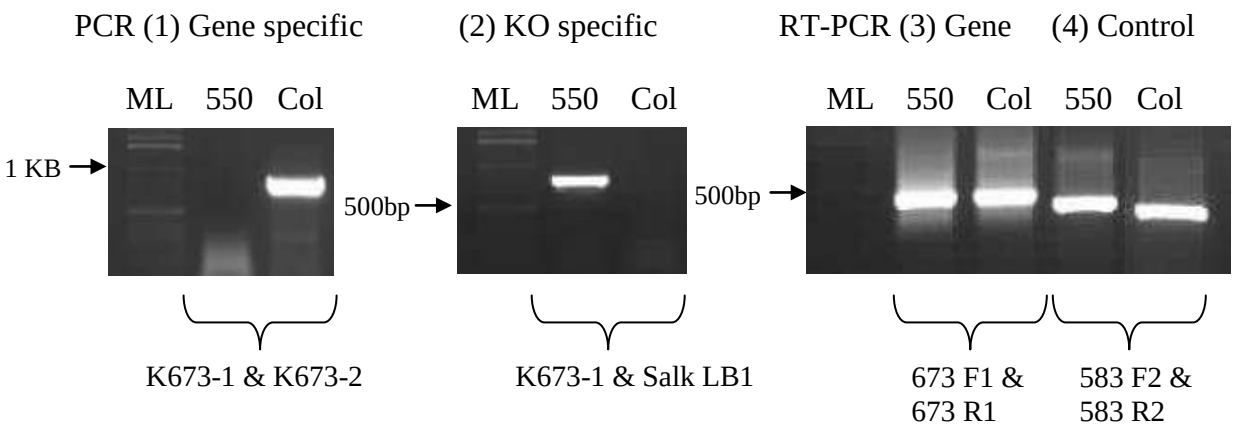

Figure 82: Genotyping and RT-PCR for N665550

N665550 (550) T-DNA insert is a homozygous KO line however mRNA is still expressed, this may be due to the fact that the insert is within the intron, suggesting the mRNA is still spliced correctly.

9.5.4. At1g71780 – TDNA insert N614289

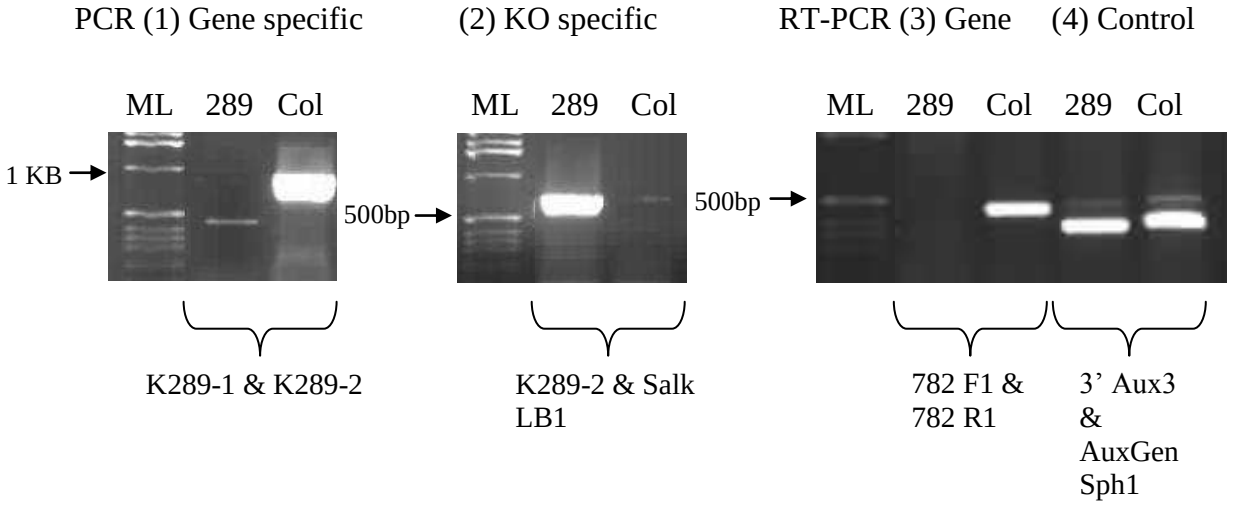

Figure 83: Genotyping and RT-PCR for N614289

N614289 (289) T-DNA insert is a homozygous KO line with complete loss of mRNA expression.

9.5.5. At2g16760 - TDNA insert N663810

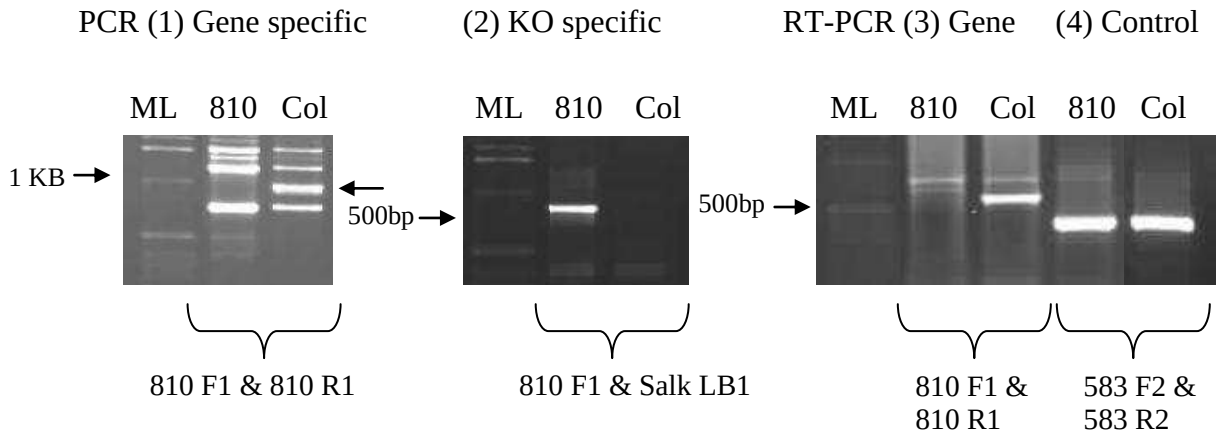

Figure 84: Genotyping and RT-PCR for N663810

N663810 (810) T-DNA insert is a homozygous KO line with complete loss of mRNA expression.

9.5.6. At2g36290 – TDNA insert N525841

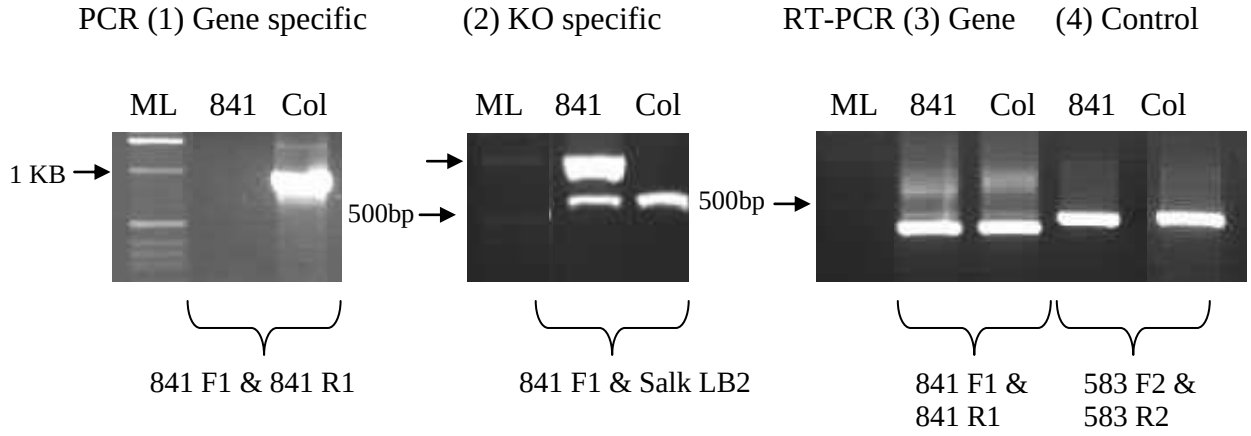

Figure 85: Genotyping and RT-PCR for N525841

N525841 (841) T-DNA insert is a homozygous KO line however mRNA is still expressed, this may be due to the fact that the insert is within the intron, suggesting the mRNA is still spliced correctly.

9.5.7. At3g07190 – TDNA insert N661700

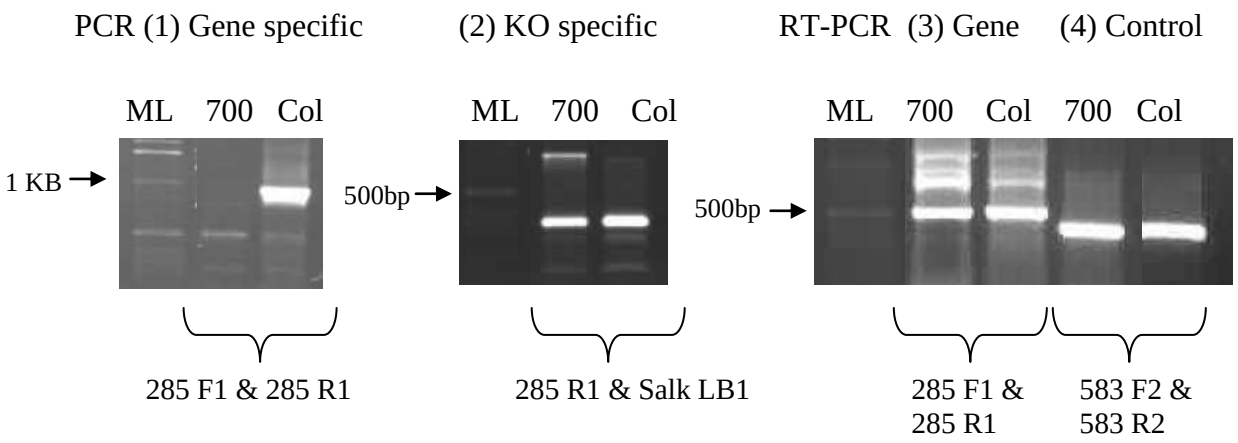

Figure 86: Genotyping and RT-PCR for N661700

N661700 (700) T-DNA insert is a homozygous KO line however mRNA is still expressed, this may be due to the fact that the insert is within the intron, suggesting the mRNA is still spliced correctly.

9.5.8. At4g16170 – TDNA insert N829287

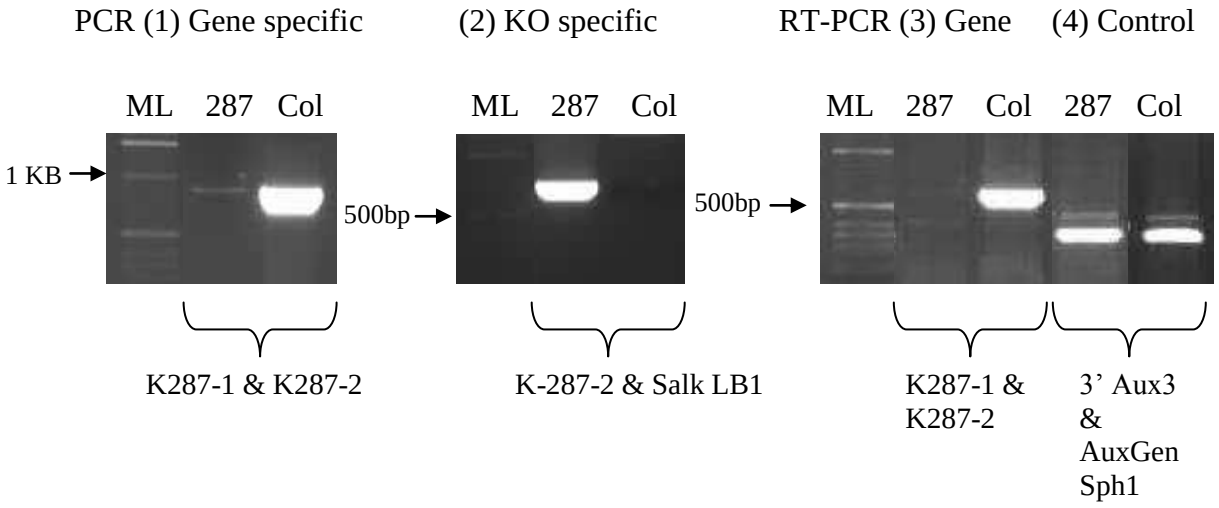

Figure 87: Genotyping and RT-PCR for N829287

N829287 (287) T-DNA insert is a homozygous KO line with complete loss of mRNA expression.

9.5.9. At4g29520 – TDNA insert N665520

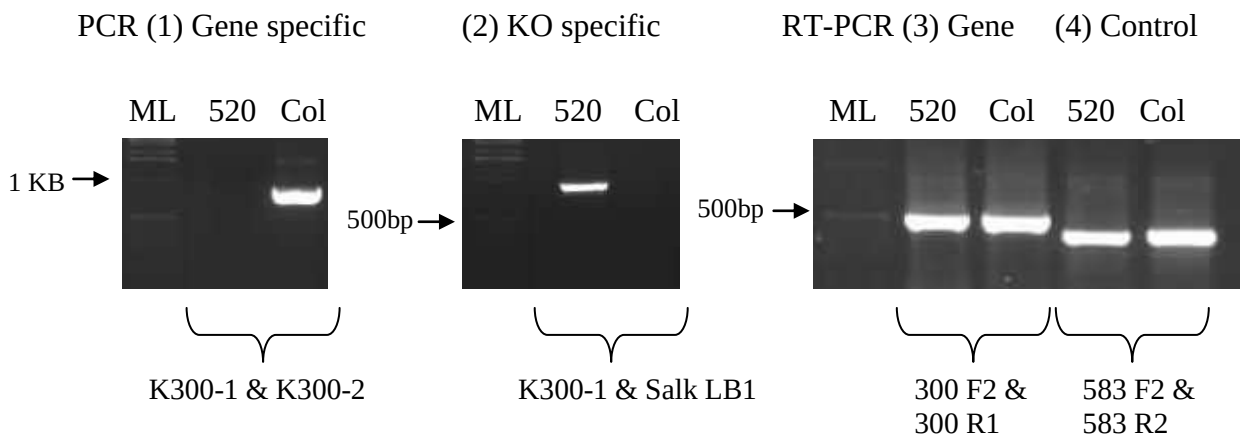

Figure 88: Genotyping and RT-PCR for N665520

N665520 (520) T-DNA insert is a homozygous KO line however mRNA is still expressed, insert is only in the last 80 bp of the gene, therefore may cause a truncated protein is this case, as there is no sign of T-DNA within the mRNA.

9.5.10. At4g32130 – TDNA insert N663464

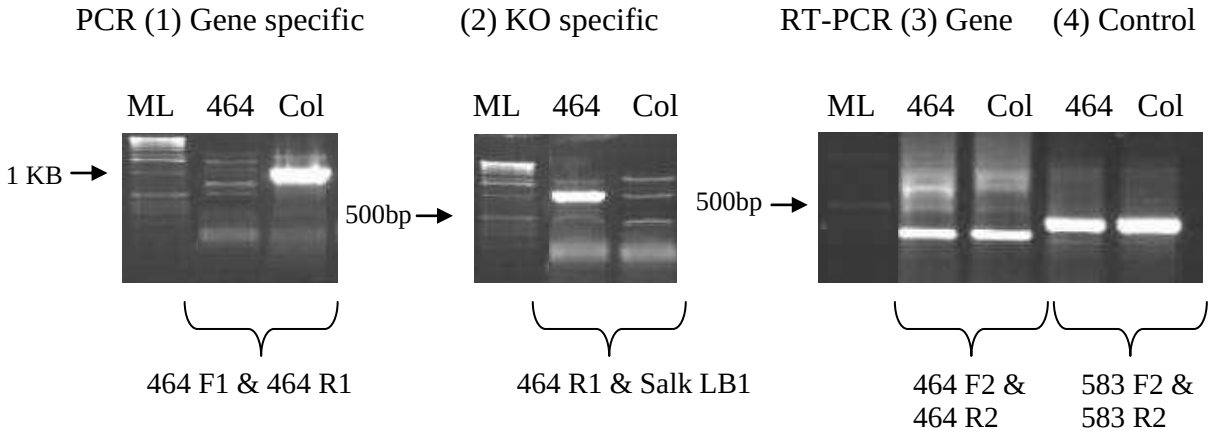

Figure 89: Genotyping and RT-PCR for N663464

N663464 (464) T-DNA insert is a homozygous KO line however mRNA is still expressed, this may be due to the fact that the insert is within the intron, suggesting the mRNA is still spliced correctly.

9.5.11. At5g42570 – TDNA insert 482

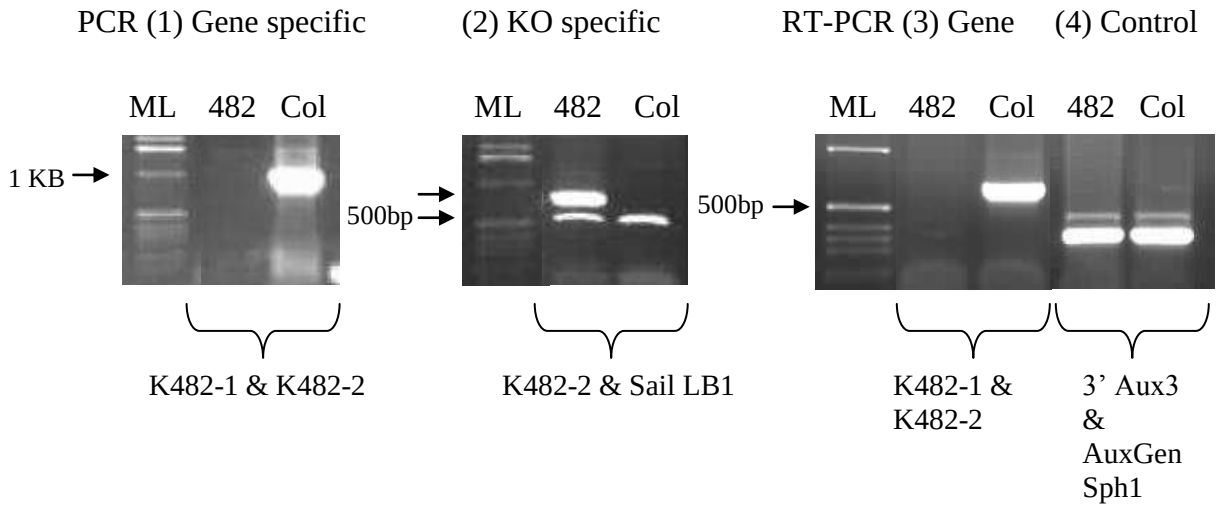

Figure 90: Genotyping and RT-PCR for N822482

N822482 (482) T-DNA insert is a homozygous KO line with complete loss of mRNA expression.

9.5.12. At5g42570 – TDNA insert N642314

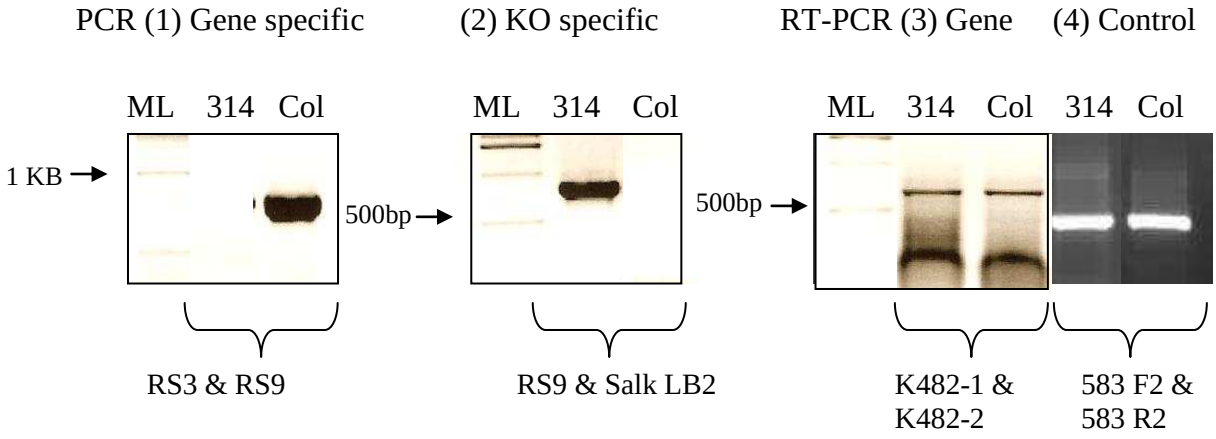

Figure 91: Genotyping and RT-PCR for N642314

N642314 (314) T-DNA insert is a homozygous KO line however mRNA is still expressed, this may be due to the fact that the insert is within the 5' UTR and the T-DNA itself may drive the expression of At5g42570.

9.5.13. At5g48660 – TDNA insert N600808

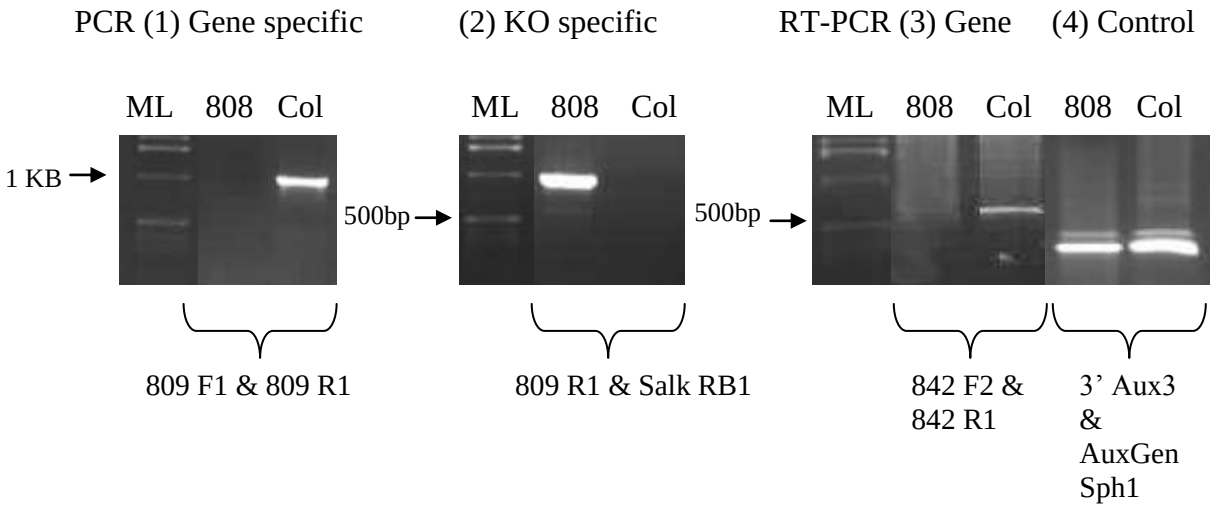

Figure 92: Genotyping and RT-PCR for N600808

N600808 (808) T-DNA insert is a homozygous KO line with complete loss of mRNA expression.

9.6. MULTIPLE SEQUENCE ALIGNMENT OF PLANT AXR4-LIKE SEQUENCES

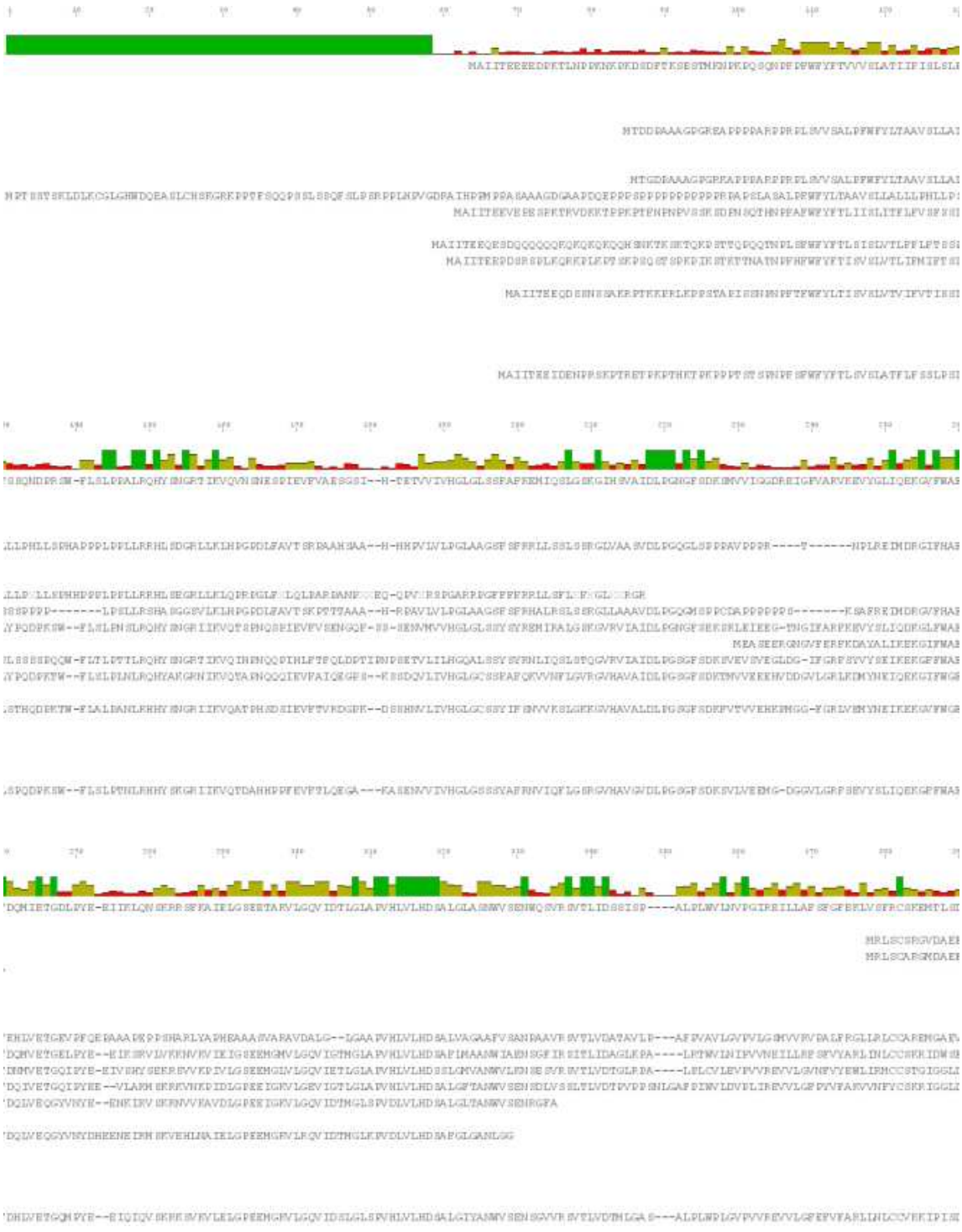

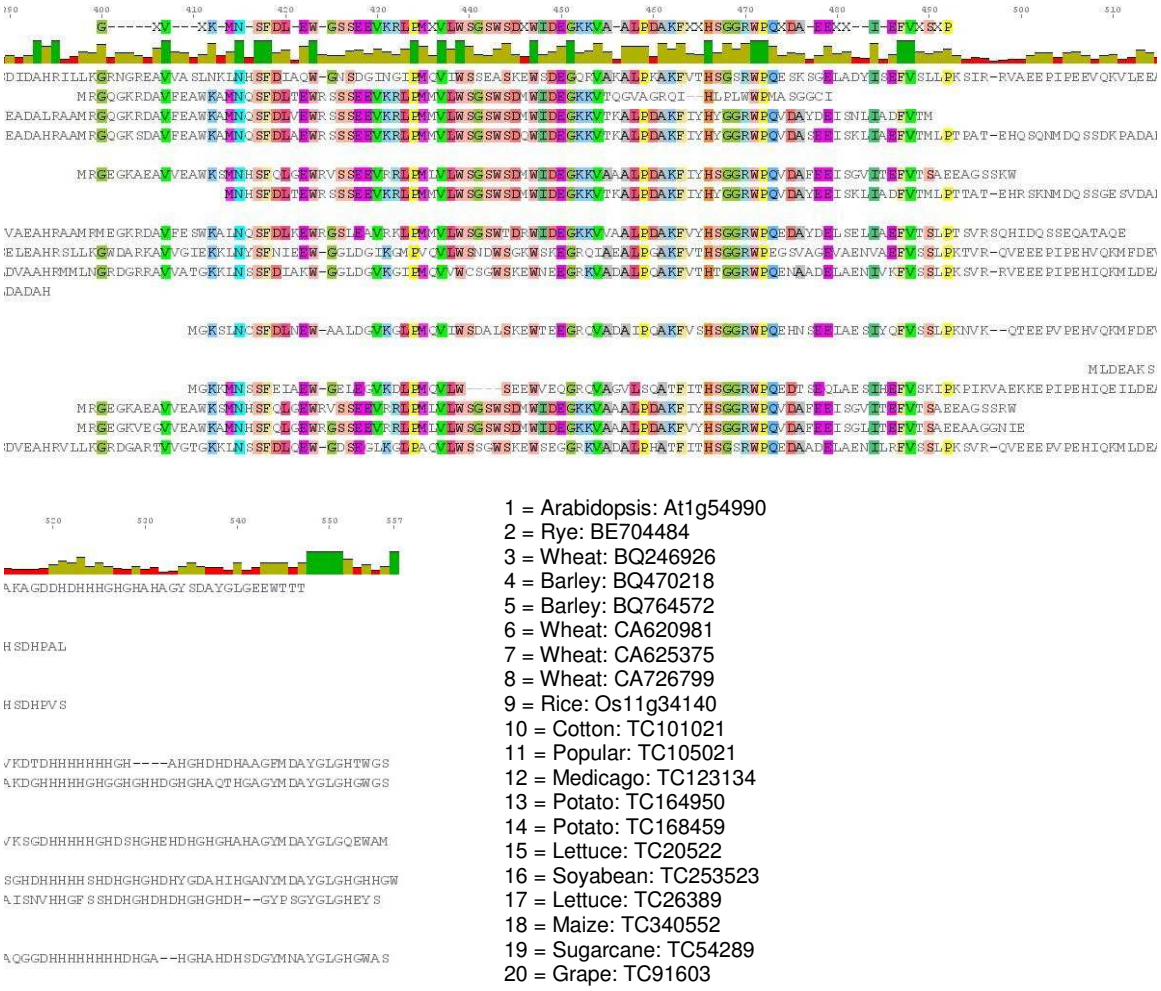

Figure 93: Multiple sequence alignment of 20 plant AXR4 like sequences.

9.7. SITE DIRECTED MUTAGENESIS

Site Directed Mutage-nesis	Amino Acid Targeted	Nucleo-tide change	Predicted nucleotides	Predicted amino acids	Primers & Predicted sizes
Gly^{113}	GGT	NNT	GGT, GCT, GAT, GTT, CGT, CCT, CAT, CTT, AGT, ACT, AAT, ATT, TGT, TCT, TAT, TTT	Gly, Asp, Val, Ala, Ser, Asn, Ile, Thr, Cys, Tyr, Phe, Ser, Arg, His, Leu, Pro	PCR 1 = AxS 113 R1 & Ax4 (415 bp) PCR 2 = AxS 113 F1 & GFP 4 (2,400 bp) PCR 3 = Ax4 & Ax2 (2 kb)
Leu^{140}	CTT	NNT	GGT, GCT, GAT, GTT, CGT, CCT, CAT, CTT, AGT, ACT, AAT, ATT, TGT, TCT, TAT, TTT	Gly, Asp, Val, Ala, Ser, Asn, Ile, Thr, Cys, Tyr, Phe, Ser, Arg, His, Leu, Pro	PCR 1 = AxS 140 R1 & Ax4 (490 bp) PCR 2 = AxS 140 F1 & GFP 4 (2,300 bp) PCR 3 = Ax4 & Ax2 (2 kb)
Asp^{151}	GAT	NNT	GGT, GCT, GAT, GTT, CGT, CCT, CAT, CTT, AGT, ACT, AAT, ATT, TGT, TCT, TAT, TTT	Gly, Asp, Val, Ala, Ser, Asn, Ile, Thr, Cys, Tyr, Phe, Ser, Arg, His, Leu, Pro	PCR 1 = AxS 151 R1 & Ax4 (515 bp) PCR 2 = AxS 151 F1 & Ax2 (1,500 bp) PCR 3 = Ax4 & Ax2 (2 kb)
Gly^{154}	GGA	NNA	GGA, GCA, GTA, GAA,	Gly, Ala, Val, Gly, Arg, Pro, Leu, Gln, Stop	PCR 1 = AxS 154 R1 & Ax4 (530 bp) PCR 2 = AxS 154

			CGA, CCA, CTA, CAA, TGA, TCA, TTA, TAA, AGA, ACA, ATA, AAA	codon, Ser, Leu, Arg, Thr, Ile, Lys	F1 & GFP 4 (2,280 bp) PCR 3 = Ax4 & Ax2 (2 kb)
Asp^{201}	GAT	NNT	GGT, GCT, GAT, GTT, CGT, CCT, CAT, CTT, AGT, ACT, AAT, ATT, TGT, TCT, TAT, TTT	Gly, Asp, Val, Ala, Ser, Asn, Ile, Thr, Cys, Tyr, Phe, Ser, Arg, His, Leu, Pro	PCR 1 = AxS 201 R1 & Ax4 (680 bp) PCR 2 = AxS 201 F1 & GFP 4 (2,100 bp) PCR 3 = Ax4 & Ax2 (2 kb)
Leu^{246}	TTG	NNG	TTG, TGG, TCG, TAG, GGG, GCG, GTG, GAG, CGG, CCG, CTG, CAG, AGG, ACG, ATG, AAG	Leu, Trp, Ser, Stop codon, Gly, Ala, Val, Glu, Arg, Pro, Leu, Gln, Arg, Thr, Met, Asn	PCR 1 = AxS 246 R1 & Ax4 (820 bp) PCR 2 = AxS 246 F1 & GFP 4 (1,970 bp) PCR 3 = Ax4 & Ax2 (2 kb)
Asp^{250}	GAT	NNT	GGT, GCT, GAT, GTT, CGT, CCT, CAT, CTT, AGT, ACT, AAT, ATT, TGT, TCT, TAT, TTT	Gly, Asp, Val, Ala, Ser, Asn, Ile, Thr, Cys, Tyr, Phe, Ser, Arg, His, Leu, Pro	PCR 1 = AxS 250 R1 & Ax4 (810 bp) PCR 2 = AxS 250 F1 & Ax2 (1,200 bp) PCR 3 = Ax4 & Ax2 (2 kb)

Asp^{320}	GAT	NNT	GGT, GCT, GAT, GTT, CGT, CCT, CAT, CTT, AGT, ACT, AAT, ATT, TGT, TCT, TAT, TTT	Gly, Asp, Val, Ala, Ser, Asn, Ile, Thr, Cys, Tyr, Phe, Ser, Arg, His, Leu, Pro	PCR 1 = AxS 320 R1 & Ax4 (1015 bp) PCR 2 = AxS 320 F1 & Ax2 (970 bp) PCR 3 = Ax4 & Ax2 (2 kb)
Pro^{361}	CCG	NNG	TTG, TGG, TCG, TAG, GGG, GCG, GTG, GAG, CGG, CCG, CTG, CAG, AGG, ACG, ATG, AAG	Leu, Trp, Ser, Stop codon, Gly, Ala, Val, Glu, Arg, Pro, Leu, Gln, Arg, Thr, Met, Asn	PCR 1 = AxS 361 R1 & Ax4 (1180 bp) PCR 2 = AxS 361 F1 & GFP 4 (1630 bp) PCR 3 = Ax4 & Ax2 (2 kb)

Table 38: AxS site directed mutagenesis summary

Amino acids targeted and their predicted nucleotides and amino acids from the mutagenesised PCR. Last column shows primers used to for each site, as well predicted sizes.